

**Role of secondary metabolites
in antiphage defense
in *Streptomyces***

Inaugural Dissertation

for the attainment of the title of doctor in the Faculty of
Mathematics and Natural Sciences at the Heinrich-Heine-University
Düsseldorf

presented by

Aël Hardy

From Nouméa (New Caledonia)

Jülich, February 2022

The thesis has been conducted at the Institute of Bio- and Geosciences, IBG-1: Biotechnology, Forschungszentrum Jülich, from October 2018 until February 2022 under the supervision of Prof. Dr. Julia Frunzke.

Published by permission of the Faculty of Mathematics and Natural Sciences at Heinrich Heine University Düsseldorf.

Supervisor:

Prof. Dr. Julia Frunzke
Institute of Bio- and Geosciences
IBG-1: Biotechnology
Forschungszentrum Jülich, Jülich

Mentor:

Prof. Dr. Georg Groth
Institute of Biochemical Plant Physiology
Heinrich-Heine-University Düsseldorf, Düsseldorf

Date of oral examination: April 29th 2022

Publications

The work presented in this dissertation has been published in the following articles:

Hardy, A.; Sharma, V.; Kever, L.; Frunzke, J. Genome Sequence and Characterization of Five Bacteriophages Infecting *Streptomyces coelicolor* and *Streptomyces venezuelae*: Alderaan, Coruscant, Dagobah, Endor1 and Endor2 (2020). *Viruses*, 12, 1065.

Kever, L.[#]; **Hardy, A.**[#]; Luthe, L.; Hünnefeld M.; Gätgens, C.; Milke, L; Wiechert, J.; Wittmann, J.; Moraru, C.; Marienhagen, J.; and Frunzke, J. Aminoglycoside antibiotics inhibit phage infection by blocking an early step of the infection cycle (2022). *mBio*. 2022 May 4:e0078322. doi: 10.1128/mbio.00783-22.

[#] Authors contributed equally to this work.

Hardy, A.; Kever, L.; Frunzke, J. Antiphage molecules produced by bacteria – beyond protein-mediated defenses. (*Submitted*)

Additionally, we would like to acknowledge the following papers, although they were not included in this dissertation:

Sharma, V.; **Hardy, A.**; Luthe; T. & Frunzke, J. Phylogenetic Distribution of WhiB- and Lsr2-Type Regulators in Actinobacteriophage Genomes (2021). *Microbiol Spectr* 9, e0072721.

Hünnefeld, M.; Viets, U.; Sharma, V.; Wirtz, A.; **Hardy, A.**; Frunzke, J. Genome Sequence of the Bacteriophage CL31 and Interaction with the Host Strain *Corynebacterium glutamicum* ATCC 13032 (2021). *Viruses*, 13, 495.

Abbreviations

AAC	Aminoglycoside acetyltransferase	HGT	Horizontal gene transfer
ATCC	American Type Culture Collection	LC-MS	Liquid chromatography – mass spectrometry
AG	Aminoglycoside	MALDI	Matrix-assisted laser desorption ionization
AME	Aminoglycoside-modifying enzyme	OD _x	Optical density at x nm
BGC	Biosynthetic gene cluster	PCR	Polymerase chain reaction
CRISPR	Clustered regularly interspaced short palindromic repeats	RNA	Ribonucleic acid
DNA	Deoxyribonucleic acid	rRNA	Ribosomal RNA
dsDNA	Double-stranded DNA	RM	Restriction modification
e.g.	<i>exempli gratia</i>	RMTases	16S ribosomal RNA methyltransferases
<i>et al.</i>	<i>et alii</i>	SM	Spent medium
etc.	<i>et cetera</i>	TA	Toxin-antitoxin
FISH	Fluorescence <i>in situ</i> hybridization	UV	Ultraviolet
GYM	Glucose yeast extract medium	WT	Wild-type
		XS	Xenogeneic silencing
		YEME	Yeast extract malt extract

Further abbreviations not included in this section are according to international standards, as, for example, listed in the author guidelines of the Journal of Cell Biology (<http://jcb.rupress.org/content/standard-abbreviations>).

Table of contents

1 Summary	1
2 Scientific context and key results of this thesis	2
2.1 Bacteriophages	2
2.1.1 Bacteriophages and phage lifestyles	2
2.1.2 Protein-based antiphage defense strategies	5
2.2 Chemical defense against phage infection in <i>Streptomyces</i>	9
2.2.1 Secondary metabolism in bacteria	10
2.2.2 <i>Streptomyces</i> , a gifted secondary metabolite producer	11
2.2.3 Phages of <i>Streptomyces</i>	14
2.2.4 Phage-induced natural product synthesis in <i>Streptomyces</i>	20
2.2.5 Aminoglycosides, antibacterial but also antiviral molecules	27
2.2.6 Antiphage defense at the community level mediated by small molecules	37
2.3 Conclusions and future perspectives	40
2.4 References	41
3 Publications and manuscripts	52
3.1 Genome Sequence and Characterization of Five Bacteriophages Infecting <i>Streptomyces coelicolor</i> and <i>Streptomyces venezuelae</i> : Alderaan, Coruscant, Dagobah, Endor1 and Endor2	53
3.2 Aminoglycoside antibiotics inhibit phage infection by blocking an early step of the phage infection cycle	69
3.3 Antiphage molecules produced by bacteria – beyond protein-mediated defenses	86
3.4 Phage-triggered synthesis of actinorhodin and undecylprodigiosin in <i>Streptomyces coelicolor</i>	113
4 Appendix	131
4.1 Supplementary Information to “2.2.4 Phage-induced natural product synthesis in <i>Streptomyces</i> ”	131
4.2 Supplementary information to “Genome Sequence and Characterization of Five Bacteriophages Infecting <i>Streptomyces coelicolor</i> and <i>Streptomyces venezuelae</i> : Alderaan, Coruscant, Dagobah, Endor1 and Endor2”	145
4.3 Supplementary information to “Aminoglycoside antibiotics inhibit phage infection by blocking an early step of the phage infection cycle”	150
4.4 Supplementary information to "Antiphage molecules produced by bacteria – beyond protein-mediated defenses"	172
4.5 Supplementary information to “Phage-triggered synthesis of actinorhodin and undecylprodigiosin in <i>Streptomyces coelicolor</i> ”	183
5 Acknowledgments	192

1 Summary

Bacteriophages (phages) are viruses preying on bacteria and as such pose a major and ubiquitous threat to bacterial communities. To cope with viral challenges, bacteria have evolved a diversified arsenal of defense systems. However, this repertoire is known to rely predominantly on protein or RNA effectors. On the other hand, bacteria produce an extraordinary diversity of secondary metabolites, whose physiological function is often unknown. In this thesis, we explore the role of bacterial secondary metabolites in the defense against phage predation. To this end, we used as a model system *Streptomyces*, a prolific producer of secondary metabolites.

First, we isolated and characterized both experimentally and bioinformatically a set of novel *Streptomyces* phages. Interestingly, phage infection in *S. coelicolor* triggered a phenotypic response in the form of coloured halos surrounding phage lysis zones. This observation triggered our interest in the study of these halos, which showed the release of the well-known secondary metabolites actinorhodin and undecylprodigiosin in reaction to phage infection. However, we could not demonstrate a protective effect of these compounds against phage predation, suggesting that actinorhodin and undecylprodigiosin are not direct inhibitors of phage infection.

Lastly, we investigated the antiphage properties of aminoglycosides, a major antibiotics class naturally produced by *Streptomyces*. We showed that aminoglycosides—and in particular apramycin—provide strong protection against phages infecting widely divergent bacterial hosts. Furthermore, protection from phage infection could also be achieved using supernatants from a natural apramycin producer, highlighting the physiological significance of this inhibition. Testing the antiphage effect of supernatants of apramycin mutants further supported the key role of apramycin in this inhibitory effect on phage infection. These results suggest that aminoglycosides may offer protection against phage infection at the community level and shape bacterial communities in ways which were until now not appreciated. Remarkably, using acetylation of apramycin as a model, we could show that chemical decoration of apramycin leads to a loss of its antibacterial activity, but did not affect its antiphage action. These findings indicate a possible decoupling between the antibacterial and antiviral properties of aminoglycosides and underline the existence of different molecular targets responsible for this dual effect.

Overall, this thesis provides insights into the connections between phage infection and secondary metabolism in bacteria. Further, it suggests that secondary metabolites may be important players of the antiviral immunity in bacteria, this role having been overlooked until now.

2 Scientific context and key results of this thesis

2.1 Bacteriophages

2.1.1 Bacteriophages and phage lifestyles

Bacteriophages (or phages for short) are viruses that predate bacteria, bacteriophage meaning 'bacteria-eater' in Greek. In most environments, direct counts typically show 10-times more phages than bacteria, which highlights their abundance (Hendrix, 2002). It is estimated that 10^{31} phage particles are found on Earth, making them the most abundant biological entities on our planet (Hendrix et al., 1999; Mushegian, 2020; Wommack and Colwell, 2000).

Discovered independently by Frederick Twort and Félix d'Hérelle one century ago (D'Hérelle, 1917; Twort, 1915), phages were used in the 1920s and 1930s for their potential against bacterial infections. However, lacking evidence for their efficacy combined with the then unrivalled success of antibiotics led to a decline in the interest in phage therapy in Western countries (Salmond and Fineran, 2015). At the same time, fundamental research on phages focused on a few model phages infecting *E. coli* such as the T-series phages and phage λ , leading to a false impression that the intricacies of these viruses were mostly elucidated by the start of the 1970s (Keen, 2015). In contrast, the 2000s have seen a worldwide resurgence of interest in the study of phages, carried by the genomic era and fuller appreciation of the phage diversity (Ofir and Sorek, 2018; Salmond and Fineran, 2015).

Phage classification was originally mainly based on virion morphology (tailed, polyhedral, filamentous or pleomorphic) and nucleic acid composition (either double- or single-stranded DNA or RNA) (**Figure 1**). More than 95% of the described phages belong to the *Caudovirales* order, comprising tailed and double-stranded DNA phages. Members of the *Caudovirales* order are further classified into three main families depending on their tail's morphology: *Myoviridae* (contractile tail), *Siphoviridae* (long, flexible tail) and *Podoviridae* (short, stubby tail) (Ackermann, 2009). The advent of fast genome sequencing technologies has challenged this decades-old classification as it revealed substantial levels of horizontal gene transfer between phage genomes characterized by a striking mosaic structure (Tolstoy et al., 2018). The transition to a genome-based classification system has been initiated in the last years to fully appreciate diversity characterizing viral communities. Integration of molecular- and genomic-based approaches has led to an improved classification of phages into subfamilies and genera, and may lead to the classification of metagenome-based virus isolates in the future (De Smet et al., 2017; Turner et al., 2021).

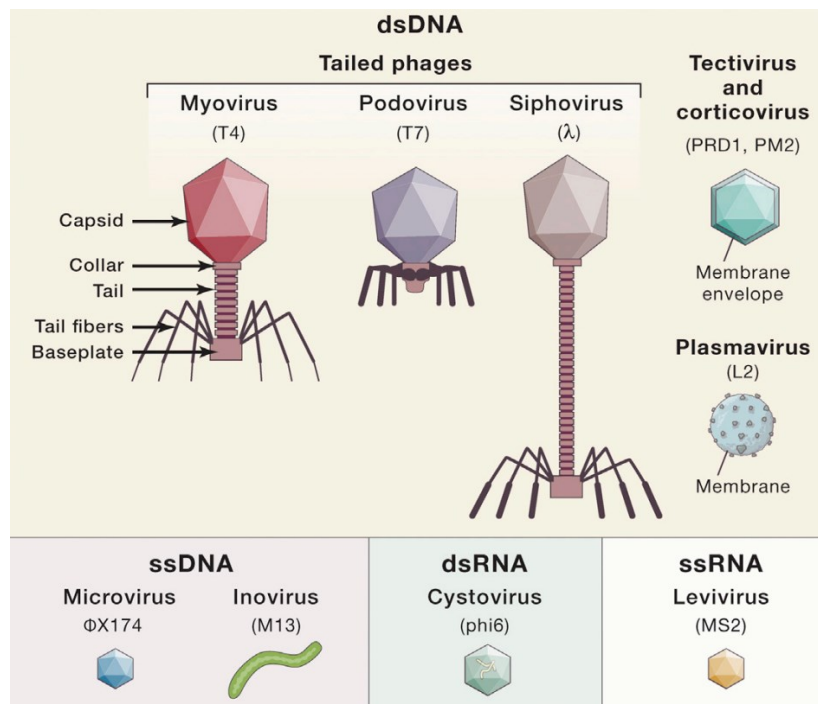


Figure 1 | **Phage taxonomy based on morphology and genome composition.** For each taxonomical group, a representative type phage is shown in brackets (adapted from Ofir and Sorek, 2018).

Like other viruses, phages are obligate intracellular parasites of the cells they infect and have diverse lifestyles, comprising the lytic and lysogenic cycles (**Figure 2**) as well as chronic infection. For lytic phages, production of viral progeny is carried out at the expense of the host bacterium, as the release of virions typically comes with the death of the infected cell. On the other hand, temperate phages are capable of a lytic cycle but can also form a stable association with their host, termed lysogeny. During lysogeny, the phage genome, termed prophage, is either integrated into the bacterial chromosome or stays in a free, plasmid-like (episomal) state. The prophage then replicates in concert with the host DNA, hence spreading in the bacterial population by vertical transmission, until the phage re-enters its lytic cycle at some point - a process named induction (Salmond and Fineran, 2015). Induction is usually due to DNA damage caused by extrinsic (UV radiation, DNA replication-targeting antibiotics, etc.) or intrinsic (stalled replication forks, etc.) factors. Induction can also happen in the absence of an external trigger, a phenomenon called spontaneous prophage induction. The complex switch from lysogeny to the lytic state has been thoroughly studied using the infection of *Escherichia coli* by model phage λ . Entry into either lytic or lysogenic cycle depends on the relative concentrations of mutually antagonistic proteins. Briefly, phage repressor proteins silence most of the phage genome, thus allowing establishment of lysogeny. Direct and indirect inactivation of these proteins then alleviates repression of the lytic promoters, resulting in the transition from lysogenic to lytic phase (Oppenheim et al., 2005). Importantly, sequencing of thousands of bacterial genomes has revealed a

high prevalence of prophage sequences; genomes harbouring more than a half-dozen prophages are not rare and prophages can amount to a staggering 20% of a bacterium's genome (Casjens, 2003).

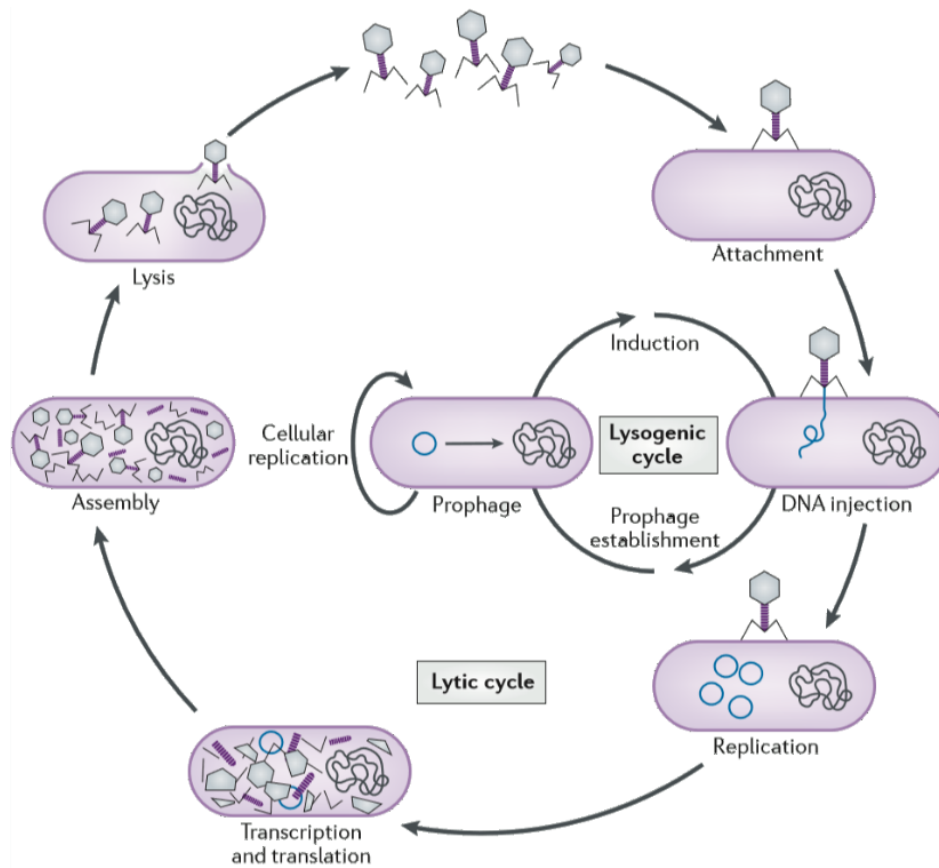


Figure 2 | **The virulent and lysogenic replication cycles of phages.** Most phages are classified as lytic or temperate, depending on their lifestyle. A successful infection by lytic phage typically leads to cell death, whereas infection by a temperate phage can lead either to lysis or lysogeny, i.e., integration of the phage nucleic acid into the host bacterium's genome or formation of a circular replicon in the bacterial cytoplasm (adapted from Salmond and Fineran, 2015).

In contrast to virulent and temperate phages described above, filamentous phages belonging to the class of inoviruses (Figure 1) cause chronic infections and are continuously secreted from the bacterium typically without causing host death (Clokie et al., 2011). Furthermore, alternative lifestyles have received increasing attention over recent years, which contributed to bring more complexity and nuance into our conception of phage replication strategies (Correa et al., 2021; Mäntynen et al., 2021). Next to the classical lytic-lysogenic dichotomy and chronic infection, other lifestyles have emerged as important features of phage biology. These include pseudolysogeny, where an unintegrated phage genome is arrested during its replication cycle and asymmetrically passed on to daughter cells, and carrier-state life cycle – a population-level phenomenon describing the coexistence of phage resistant and sensitive hosts in the same population (Mäntynen et al., 2021).

An important consequence of the lysogenic cycle is the following: as prophages are vertically passed on to daughter cells as they replicate, the residing phages temporarily deviate from a purely parasitic relationship with their hosts to a symbiotic one. Indeed, any improvement of bacterial fitness caused by the prophage, a process called lysogenic conversion, would favour the prophage dispersion as well (Bondy-Denomy and Davidson, 2014). Infamous instances of increased bacterial virulence caused by lysogenic conversion include the production of the diphtheria, cholera and shigellosis toxins from prophages (Parajuli et al., 2017; Wagner and Waldor, 2002; Waldor and Mekalanos, 1996). Of particular importance from an epidemiological point of view: the mobility of phage-borne toxin genes makes them particularly concerning as it facilitates the emergence of novel pathogens. The beneficial effects of prophages on bacterial fitness are not limited to increased pathogenesis and comprise for example the inhibition of infection by closely related phages (superinfection exclusion) and the supply of prophage-encoded CRISPR-Cas systems (Bondy-Denomy and Davidson, 2014).

2.1.2 Protein-based antiphage defense strategies

In response to the constant predation threat exerted by bacteriophages, bacteria have evolved a wide range of defense mechanisms. The majority of currently known prokaryotic defense systems relies on a wide range of molecular mechanisms, but is mainly mediated by protein or RNA complexes acting at the cellular level (Hampton et al., 2020; Rostøl and Marraffini, 2019). Here, we aim at presenting the main protein-based antiphage defense strategies and highlight some of the most recent discoveries in this blooming field.

Not surprisingly, bacterial immune systems hamper the different stages of the life cycle that phages need to complete in order to produce new progeny particles (**Figure 3A**). In response, phages have evolved a myriad of ways to overcome these protective mechanisms. In combination with considerable phage diversity, this molecular arms race has further fostered the diversification of bacterial antiviral strategies.

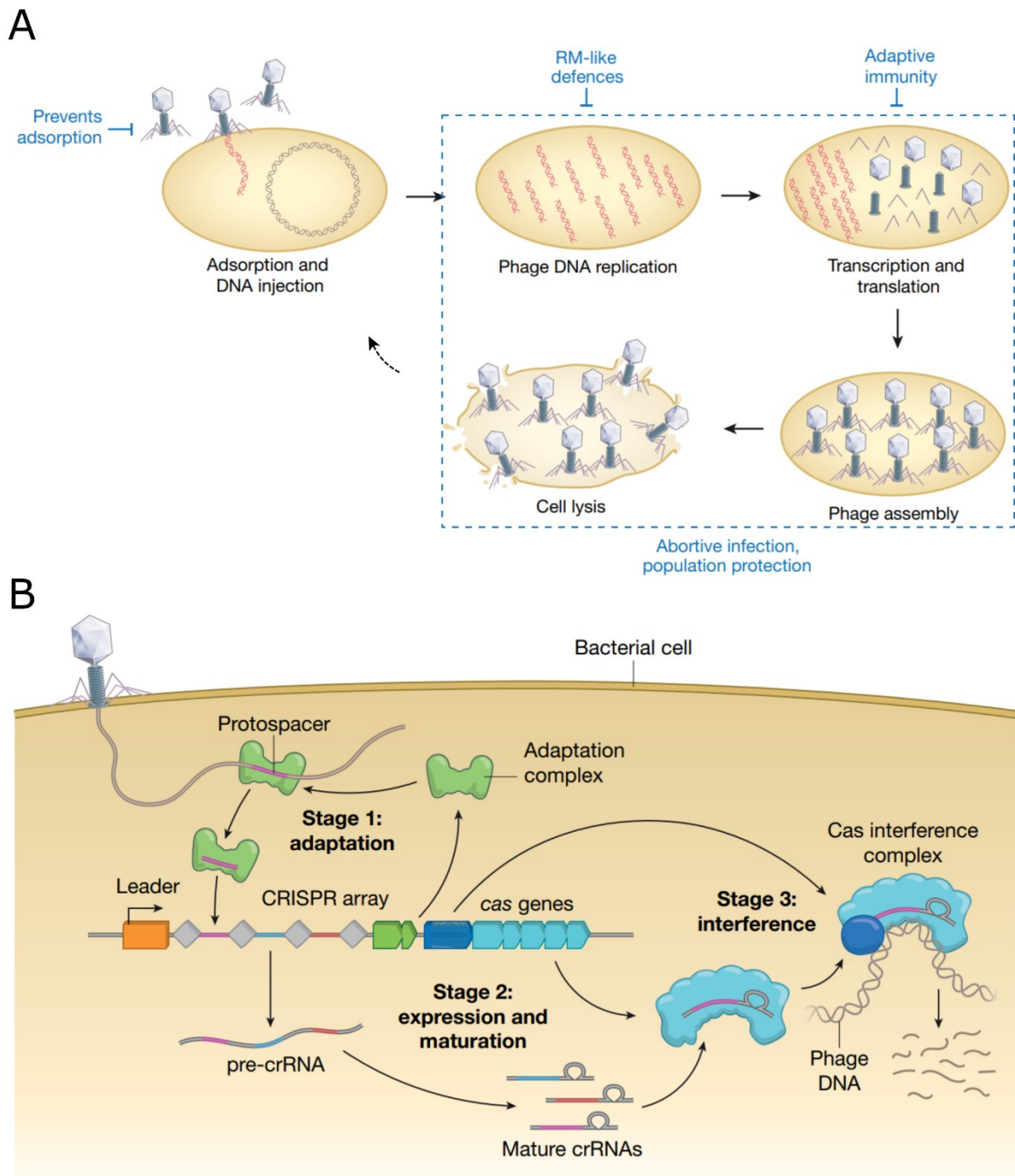


Figure 3 | **Bacterial antiphage defense mechanisms.** (A) The antiphage defense systems deployed by bacteria act at different steps of the phage lifecycle to disrupt productive infection. Defense systems referred to as abortive infection arrest the phage life cycle at various steps. Their action is shown by the dashed blue line. (B) Schematic of the three main steps of CRISPR–Cas immunity, comprising adaptation (stage 1), expression and maturation of crRNAs (stage 2), and interference (stage 3). crRNA: CRISPR RNA. (adapted and modified from Hampton et al., 2020)

2.1.2.1 Preventing phage adsorption and entry

To infect their host, phages first have to recognize the bacterial cell and adsorb to the cell surface. This step represents a prime barrier against phage infection and the instances of ways used by bacteria to prevent phage binding and adsorption are plentiful. They include for example modifications, masking or loss of phage receptors and production of extracellular matrix that shield the receptors (Labrie et al., 2010).

Importantly, alterations of the bacterial surface can lead to high fitness costs, which are sometimes not observable in a simple ‘one bacterium-one phage’ laboratory set-up. This notion was greatly exemplified by the finding that CRISPR-mediated phage resistance is favored over modifications of the phage receptor in complex microbial communities (Alseth et al., 2019). Indeed, using *Pseudomonas aeruginosa* as a model, authors showed that, while monocultures typically gained resistance through surface modifications, co-cultivation with other bacterial species amplified the fitness costs of surface resistance and tipped the balance in favour of the evolution of CRISPR-based resistance.

2.1.2.2 Targeting phage nucleic acids: restriction-modification systems and CRISPR-Cas immunity

In case the infecting phage could successfully attach to its host cell and inject its genome, two additional defense systems can enter into play to destruct phage nucleic acids: restriction modification systems (RM systems) and CRISPR-Cas immunity (Hampton et al., 2020; Rostøl and Marraffini, 2019). They both rely on the sequence-specific detection and subsequent cleavage of the invading genetic material, but fundamentally differ in their underlying molecular mechanisms. As a so-called ‘innate immune system’, RM systems rely on the discrimination between host and foreign DNA based on different methylation patterns (Loenen et al., 2014). In contrast, CRISPR-Cas systems provide ‘adaptive’ immunity through the generation of a ‘genomic record’ of past infections, which later serves as a basis for the elimination of a phage possessing the same or similar genome (**Figure 3B**) (Barrangou et al., 2007; Hille et al., 2018; Sorek et al., 2013).

Although RM and CRISPR-Cas systems provide effective protection against phage-mediated lysis, they come with a substantial disadvantage, namely that the bacterial host cannot benefit from potentially valuable genes encoded by the invading phage. Conversely, xenogeneic silencing (XS) allows the integration of foreign genetic elements into the host regulatory networks, by using silencing proteins which repress the expression of alien DNA based on their lower GC-content (Gordon et al., 2010; Pfeifer et al., 2019; Singh et al., 2016). Although no direct involvement of XS in antiphage defense has

been demonstrated yet, XS could represent a valuable yet underestimated element in the bacterial antiphage arsenal (Pfeifer et al., 2016, 2019).

2.1.2.3 ‘Dying for the greater good’: Abortive infection systems and toxin-antitoxin systems

Unlike systems mentioned earlier, abortive infection (Abi) systems act primarily at the population level by triggering the death of phage-infected cells to prevent virion release and thus protect the rest of the bacterial community.

Abi is defined based on a phenotype (‘altruistic’ programmed-cell death in reaction to phage infection) rather than genotypic criteria, which explains that a large diversity of mechanisms of action are gathered under this term (Lopatina et al., 2020). The precise cues triggering growth arrest or death are often poorly known, but comprise for example the formation of specific DNA-protein complexes, which, in the case of the *E. coli* model phage T4 activates an ion channel depolarizing the membrane (Parma et al., 1992; Wong et al., 2021, 2021).

In contrast, toxin-antitoxin (TA) systems rely on a genetically well-identified TA pair, where the toxin activity is prevented by the corresponding cognate antitoxin module. Upon phage infection, expression levels of the antitoxin are lowered, releasing the catalytic activity of the toxin and leading to bacterial dormancy or death (Harms et al., 2018). The mechanisms of action mediating phage defense have been recently expanded, with for example ADP-ribosylation of phage DNA by the TarTG TA system preventing both replication and transcription of the phage genome (LeRoux et al., 2021). Similarly to other abortive infection mechanisms, the key information often missing is the way by which phage infection is sensed.

2.1.2.4 A new world of antiphage mechanisms

A feature shared among phages is that most of their genomes encodes genes of unknown function, so-called ‘dark viral matter’ (Hatfull, 2015; Krishnamurthy and Wang, 2017). Our limited knowledge about viral genomes has limited our understanding of the warfare between phages and their hosts.

However, the recent years have seen a considerable expansion of the known antiphage arsenal, carried by large-scale bioinformatics screening combined with experimental validation (Doron et al., 2018; Gao et al., 2020). These screenings were built upon the “guilty-by-association” approach, which hypothesizes that genes markedly enriched in the vicinity of known defense genes are probably also involved in antiphage defense. This discovery strategy confirmed the existence of genomic “defense islands”, where defense systems clustered in combinatorial arrangements which differed at the strain

level. Yet, the antiviral arsenal of a given strain should be seen as a dynamic and fluctuating ensemble, as bacteria are permanently engaged in the exchange of genes through horizontal gene transfer (HGT) with closely related strains. This view is summed up by the recently proposed notion of ‘pan-immune’ system of bacteria, making defense systems a community resource shared between closely related bacteria (Bernheim and Sorek, 2020).

The discovery of new defense systems expanded the mechanisms known to be at play to protect bacteria against phage infection. For example, cyclic nucleotides emerged as a widespread signaling molecules that activate immune effectors leading to cell suicide (Cohen et al., 2019; Tal et al., 2021). Depletion of the essential molecule nicotinamide adenine dinucleotide NAD⁺ pools was also shown to be the endpoint of numerous new defense systems (Bernheim et al., 2021; Cohen et al., 2019; Ofir et al., 2021; Tal et al., 2021). Retrons are genetic elements composed of a non-coding RNA and reverse transcriptase, but their function remained mysterious since their discovery 40 years ago (Yee et al., 1984). They were recently shown to protect from phage infection via abortive infection, by ‘guarding’ the antiphage RecBCD complex under standard conditions – this inhibition being lifted upon phage infection (Millman et al., 2020).

Interestingly, the study of this new members of the prokaryotic antiviral repertoire revealed striking similarities with eukaryotic antiviral immune systems. Notable instances include the production of the same chain terminators by human viperins and their prokaryotic homologs (Bernheim et al., 2021), and the involvement of Toll/interleukin-1 receptor (TIR) domain into the Thoeris defense system (Doron et al., 2018; Ofir et al., 2021). TIR domains are a canonical component of animal and plant immune systems and, paralleling their action in eukaryotes, TIR domains determined the specificity of the immune response against phages too. These observations suggest that a previously underappreciated fraction of eukaryotic immunity evolved from prokaryotic antiphage defenses.

2.2 Chemical defense against phage infection in *Streptomyces*

Although defense systems presented above (cf. part 2.1.2) greatly differ in their molecular mechanisms, they all rely on protein or RNA complexes to provide protection against phage infection. On the other hand, small molecules produced by bacteria represent a facet of prokaryotic antiviral immunity which was until recently underappreciated. In this part, we present current knowledge about small molecule-based antiviral strategies in bacteria, with a focus on the genus *Streptomyces*.

2.2.1 Secondary metabolism in bacteria

Metabolism is traditionally divided between primary and secondary metabolism. Primary metabolism gathers the synthesis of molecules required for normal growth and reproduction. Conversely, secondary metabolism (also called specialized metabolism) refers to the production of metabolites that are dispensable for growth and instead confer producer cells a specific fitness advantage in competitive, cooperative, or predatory interactions (Tyc et al., 2017; Williams et al., 1989). Secondary metabolites¹ fulfil a wide range of functions, such as signalling or growth inhibition of bacterial competitors (**Figure 4**).

Another important feature of secondary metabolites is their limited taxonomical distribution. While similar secondary metabolites can be produced by distantly related bacteria, a patchy distribution between closely related species is typical. At the genomic level, the biosynthetic gene clusters (BGCs) responsible for the synthesis of secondary metabolites are mainly found in the accessory genome, prone to be exchanged through horizontal gene transfer (HGT) (Kim et al., 2015; McDonald and Currie, 2017; Wyka et al., 2020; Zhang et al., 2020a).

¹ There is ongoing debate about whether ‘natural product’ can be used as interchangeable synonym of ‘secondary metabolite’ or if this term should rather refer to all chemical compounds that are isolated from a living organism. In the following, we will consider natural products and secondary metabolites as equivalent and will not make a distinction between the two terms.

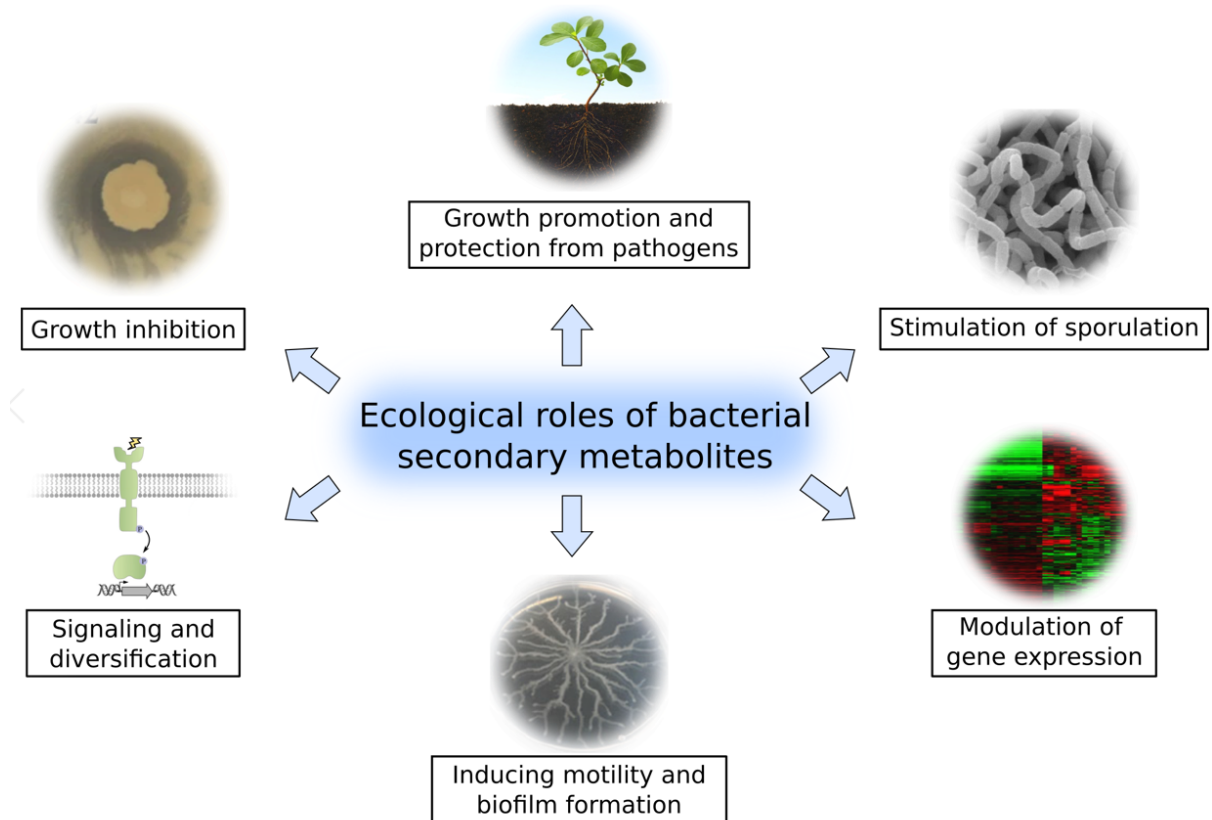


Figure 4 | **Bacterial secondary metabolites play key ecological roles** (modified from Tyc et al., 2017).

Sustained advances in chemical analysis, genome sequencing and bioinformatic detection of BGCs continue to further advance our appreciation of the biochemical diversity characterizing secondary metabolites. Our understanding of the ecological roles of this metabolic wealth is comparatively lagging behind quite dramatically (Tyc et al., 2017). Elucidating the triggers for metabolite synthesis and their physiological function requires extensive screenings and in-depth study, explaining why this knowledge is often missing.

2.2.2 *Streptomyces*, a gifted secondary metabolite producer

The genus *Streptomyces* constitutes with more than 500 species the largest genus of known actinobacteria (Anderson and Wellington, 2001). *Streptomyces* are aerobic, Gram-positive bacteria, that typically thrive in soil and decaying vegetation but can be also found in marine environments and insect digestive tracts (Behie et al., 2017). At the genome level, *Streptomyces* possess large (between 6 and 12 Mbp) and linear genomes that exhibit a high GC-content (on average about 72 mol% G + C)(Lee et al., 2020a).

More precisely, the origin of replication is usually situated at the center of the linear chromosome and terminal inverted repeat (TIR) sequences are located at each end. The “core” region of the chromosome contains essential genes involved in cell maintenance, including transcription, translation, and DNA replication (Bentley et al., 2002). In contrast, conditionally adaptive genes, that are not essential for vegetative growth, are typically located within the “arm” regions of the chromosome. Corroborating the non-essentiality of chromosome arms, these frequently undergo spontaneous deletions and rearrangements which can be massive (loss of up to 2.3 Mb in *Streptomyces ambofaciens* for example (Fischer et al., 1997)). This phenomenon was long known to happen under laboratory conditions, but the physiological relevance of this high degree of chromosomal instability remained unclear. Recently, Zhang and colleagues showed that, in *Streptomyces coelicolor*, genomic heterogeneity drives an increase in antibiotic production and diversity (Zhang et al., 2020b). Importantly, although deleterious mutations caused a loss of fitness of single cells, the fitness of colonies containing mixtures of mutants and their parents was unchanged. These mixed colonies showed stronger growth inhibition of bacterial competitors, due to the higher antibiotic production of mutants (Zhang et al., 2020b). This example illustrates how bacterial populations can benefit from a division of labour, with subpopulations of the same colony specializing to carry out complementary tasks (here, reproduction and antibiotic production).

One prominent feature of *Streptomyces* is their diversified secondary metabolism. In some cases, the chemical diversity is even visible with the naked eye, with pigmented metabolites diffusing around colonies or forming coloured droplets at their surface (Thompson et al., 2002) (**Figure 5**). The advent of large-scale and affordable sequencing technologies confirmed these observations by revealing that *Streptomyces* typically encode between 20 and 30 BGCs per genome (Lee et al., 2020a).

This extensive chemical repertoire has been harnessed for use in agricultural and therapeutical settings, as secondary metabolites produced by *Streptomyces* have demonstrated anticancer, antifungal, and antibacterial activities (Hopwood, 2007). In fact, two thirds of clinically used antibiotics of microbiological origin are derived from *Streptomyces*, highlighting the significant impact that this genus has on human health (Bibb, 2013; Keiser et al., 2000).

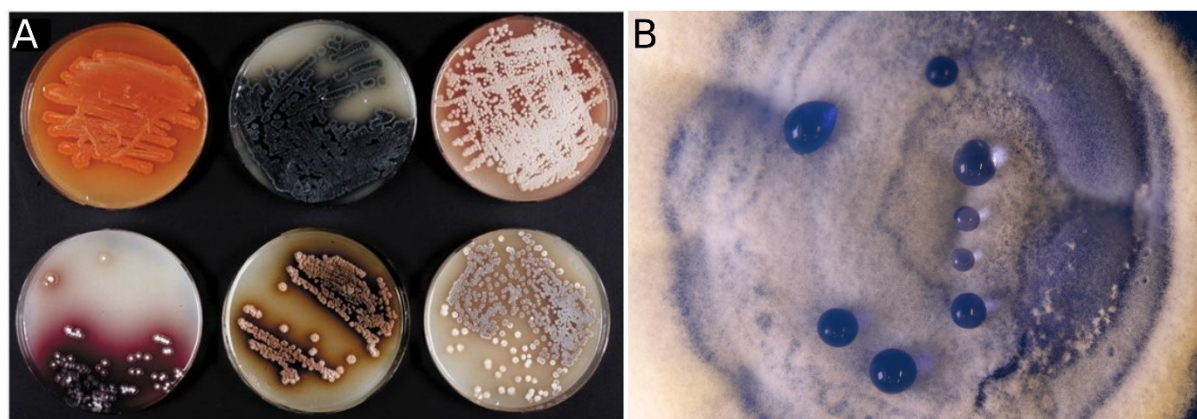


Figure 5 | **Production of pigmented secondary metabolites by *Streptomyces*.** (A) Typical colony morphologies of *Streptomyces* species isolated from the soil. Colonies often secrete coloured pigments, which provides a visual illustration of secondary metabolite biosynthesis (adapted from Thompson et al., 2018). (B) Stereomicroscopic image of a colony of *Streptomyces coelicolor* showing droplets of actinorhodin (unpublished, picture taken by Max Hünnefeld and Larissa Keuer, 2020).

One major limitation to fully harness the chemical potential of *Streptomyces* is the cryptic nature of most of these BGCs, as these clusters are generally not expressed under standard laboratory conditions. A focus of the recent years has been to develop ways to activate these cryptic clusters. Genetic engineering and in-depth chemical analysis represent the two pillars of this approach. The genetic toolbox used to awaken *Streptomyces* silent BGCs is diverse but relies traditionally on the heterologous expression of candidate clusters and the overexpression or deletion of transcription factors (Manteca and Yagüe, 2019; Nguyen et al., 2020). More recently, use of CRISPR interference (Ameruoso et al., 2021) or truncated xenogeneic silencers (Gehrke et al., 2019) emerged as promising ways to turn on cryptic pathways. Besides genetic engineering, microbial interactions have been increasingly recognized as a powerful strategy to stimulate BGCs (Netzker et al., 2018), but viral predation by phages was until now not recognized as an elicitor of secondary metabolism in bacteria.

The second key feature of *Streptomyces* is their development cycle. Contrary to most studied bacteria, which divide by binary fission, *Streptomyces* follow instead a complex life cycle organized around spore formation (**Figure 6**) (Elliot et al., 2008; McCormick and Flärdh, 2012). Spores first germinate and form a network of multinucleated cells, called vegetative mycelium. Upon certain cues such as nutrient depletion, the vegetative mycelium serves as a basis for the coordinated erection of the so-called aerial mycelium. Finally, aerial filaments differentiate into chains of unigenomic spores, which, once released, can start a new cycle.

Importantly, morphological and chemical differentiation are tightly connected in time and space in streptomycetes, the release of secondary metabolites typically coinciding with a specific developmental stage (Keiser et al., 2000). For instance, geosmins are volatile compounds conserved

across *Streptomyces* which are released during sporulation and attract springtails, which would in turn increase dissemination of *Streptomyces* spores (Becher et al., 2020).

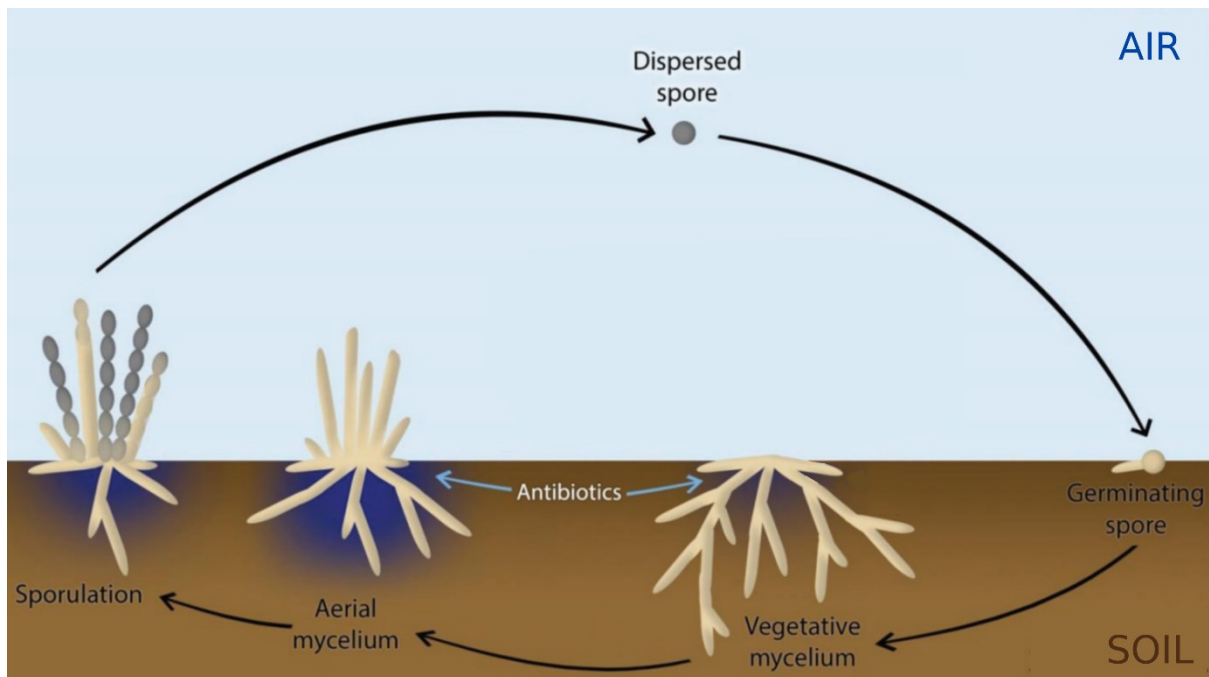


Figure 6 | **Classical life cycle of *Streptomyces*.** *Streptomyces* typically follows a fungus-like growth developmental cycle divided in the four following main steps: germination of a spore, growth of a vegetative mycelium, formation of aerial mycelium and finally sporulation (adapted and modified from Urem et al., 2016).

The canonical life cycle described above has been known for more than 70 years and was thought to be the only mode of development accessible to *Streptomyces*. Recently, Jones and colleagues challenged this view and described an alternative life cycle, termed exploration (Jones et al., 2017). Explorer cells grow as non-branching vegetative hyphae and rapidly traverse both biotic and abiotic surfaces. Entry into exploration mode is triggered by low glucose levels or nearby growth of fungi. Remarkably, the exploratory behaviour can be communicated by exploring cells to other physically separated streptomycetes via the release of volatile organic compounds (Jones and Elliot, 2017; Jones et al., 2017).

2.2.3 Phages of *Streptomyces*

Phages represent a constant and ubiquitous threat to bacterial populations, and *Streptomyces* make no exception to this rule. Historically, the study of *Streptomyces* phages was first motivated to prevent viral outbreaks within industrial-scale cultures of *Streptomyces griseus*, the natural producer of the first antitubercular antibiotic streptomycin (Alexander and McCoy, 1956; Gilmour et al., 1959). The

1970–1980s saw an acceleration of the description of *Streptomyces* phages but most of them were not sequenced later (Anne et al., 1984; Donadio et al., 1986; Dowding, 1973). The phage phiC31 represents a notable exception to this trend. PhiC31's integration system served to establish crucial genetic tools for *Streptomyces* before its complete genome was sequenced in 1999 (Lomovskaya et al., 1972; Smith et al., 1999, 2013). More generally, the intense research on *Streptomyces* phages in the last quarter of the twentieth century focused on deriving genetic tools (primarily cloning vectors) for the study of *Streptomyces* and dedicated surprisingly little attention to the interactions between these phages and their hosts (Bibb et al., 1983; Hopwood et al., 1973; Piret and Chater, 1985). Likewise, the phages R4, SV1, VP5 were the subject of numerous studies mostly in the light of their transduction abilities, but the latter was not sequenced (Burke et al., 2001; Lomovskaya et al., 1980). In recent years, isolation and sequencing of *Streptomyces* phages have undergone sustained acceleration, carried notably by the Science Education Alliance-Phage Hunters Advancing Genomics and Evolutionary Science (SEA-PHAGES) program in the USA (Jordan et al., 2014). However, these phages are in their majority not comprehensively characterized and not readily available for the community.

Facing the lack of *Streptomyces* phages being both experimentally and genomically well-characterized, we isolated and described five novel *Streptomyces* phages (named Alderaan, Coruscant, Dagobah, Endor1 and Endor2) (Hardy et al., 2020).

The first step in the characterization process consists in describing the morphology of the plaques formed on a bacterial lawn by these five phages as well as the morphology of the phage particles themselves. Infection assays on plates revealed different plaques morphologies, with plaques formed by Coruscant and Dagobah being smaller than the ones of Alderaan, Endor1 and Endor2 (**Figure 7A**). More interestingly, we noticed that coloured halos appeared around plaques formed by the three *S. coelicolor* phages (**Figure 7B**). This observation suggested that pigmented metabolites were released in reaction to phage infection and could be involved in chemical defense against phages (cf. part 2.2.4).

Concerning the particle morphology, transmission electron microscopy revealed that all five phages have long tails and icosahedral capsids and were hence classified as siphophages.

Another important part of the experimental characterization consisted in determining the infection dynamics in liquid cultures. Alderaan displayed strong lysing abilities with correspondingly strong phage amplification, while infection was moderate for the other phages. Effective and robust phage amplification in liquid medium facilitates the monitoring of infection, making Alderaan an interesting candidate for future studies.

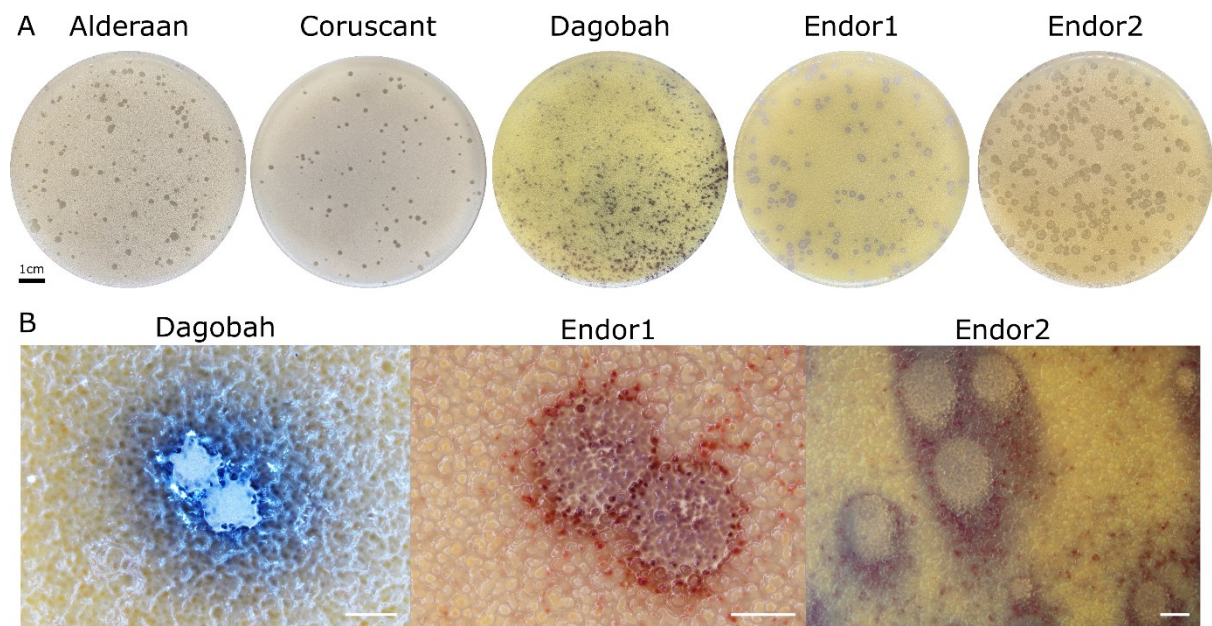


Figure 7 | **Plaque morphology of five newly described *Streptomyces* phages.** (A) Plaque morphologies of the five phages obtained from a standard double agar overlay. *Streptomyces venezuelae* ATCC10712 was infected with the phages Alderaan and Coruscant, while *S. coelicolor* M145 was the host used for the phages Dagobah, Endor1 and Endor2. (B) Stereomicroscopic close-ups of the plaques formed by the three *S. coelicolor* phages (adapted and modified from Hardy et al., 2020).

The second half of the characterization, which is at least as important as the *in vitro* part, involves the *in silico* description of the newly isolated phages. The main parts of the bioinformatical workflow are the following: genome sequencing (using short-read technology), genome assembly and annotation, followed by phylogenetic analyses.

The five phages showed diverse genomic features, with genome sizes and GC content ranging from 39 to 133kb and from 48 to 69%, respectively (**Table 1**). Likewise, the type of genomic ends and predicted lifestyle differed between the phages. Determination of whole-genome sequence relationship showed that four of them proved to be closely related to already known phages and fell in the clusters defined by the Actinobacteriophage Database (PhagesDB; <https://phagesdb.org>), namely the clusters BC, BE and BD for Alderaan, Coruscant and the Endor1/Endor2 pair, respectively. In contrast, the phage Dagobah had no known homologs, which highlights the still largely untapped nature of viral diversity. Although the phage Coruscant showed close relatedness to already known *Streptomyces* phages, this phage presents peculiar and interesting genomic features. While phages typically have lower GC contents than their host, Coruscant's GC content is markedly lower than the one of its host *Streptomyces venezuelae* (72.1%), suggesting that it infected lower-GC hosts in its recent evolutionary past (Pope et al., 2014). Additionally, Coruscant also encodes 41 copies of tRNA genes, covering 19 of the 20 standard amino acids. The rationale for this broad tRNA gene repertoire is unclear, but it could

Scientific context and key results of this thesis

be used to optimize gene expression in hosts that have differing codon usage patterns or counteract the degradation of phage tRNAs by the host (Pope et al., 2014).

The long direct terminal repeats (DTR) of Coruscant and its closely related phages represent another intriguing peculiarity. With their size of 12kb, they are the longest found in actinobacteriophages to date (Hughes et al., 2018). The higher GC content of these regions (54.4%) compared to the rest of the genome (47.0%) suggests that they were acquired from a phage or bacteria that possessed a distinctively GC-rich genome (Sharma et al., 2021). Alternatively, the elevated GC content of DTRs could play a role in the selective recombination of these regions, necessary for the circularization of the injected phage genome.

Table 1 | **Basic genome features of the five newly described *Streptomyces* phages.** DTR: direct terminal repeats (adapted and modified from Hardy et al., 2020).

Phage name	Reference host	Genome size (kb)	GC content (%)	Genome termini class	Lifestyle prediction
Alderaan	<i>Streptomyces venezuelae</i>	39	72.1	Headful (<i>pac</i>)	Virulent
Coruscant	<i>Streptomyces venezuelae</i>	133 (12kb DTR)	48.4	DTR (long)	Virulent
Dagobah	<i>Streptomyces coelicolor</i>	47 kb (1kb DTR)	68.9	DTR (short)	Temperate
Endor1	<i>Streptomyces coelicolor</i>	49	65.8	Headful (<i>pac</i>)	Temperate
Endor2	<i>Streptomyces coelicolor</i>	48	65.1	Headful (<i>pac</i>)	Temperate

This set of well-characterized five phages can serve in the future as a basis to address questions concerning the biology of *Streptomyces* phages, which is a prospect perhaps more important than the initial characterization itself. In particular, an area worthy of investigation is the study of the interconnections between development and phage infection.

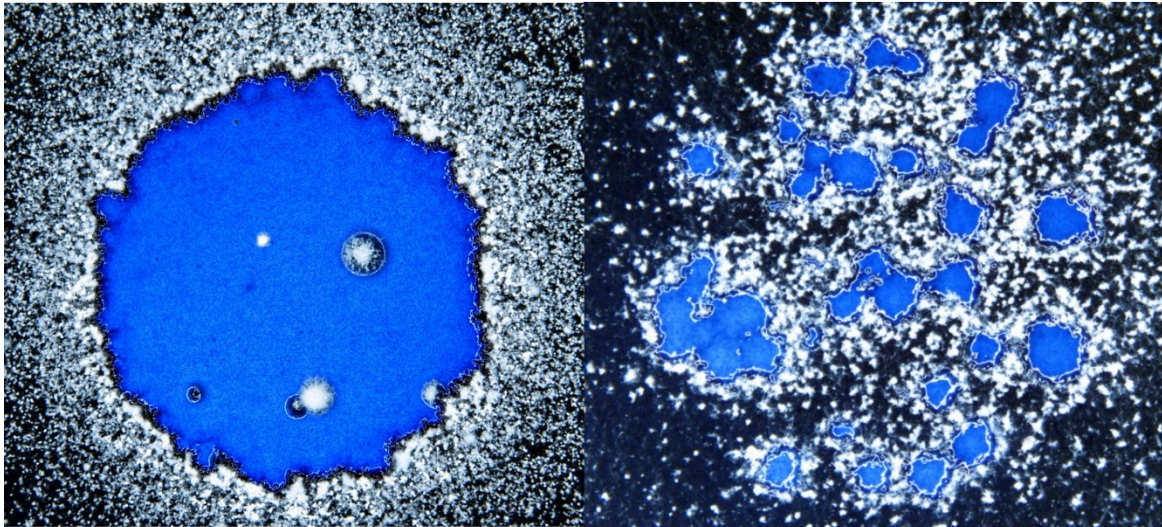
The first outstanding question which has not been properly answered yet is how does the developmental stage of *Streptomyces* influence phage infection. It is commonly stated that production of new phage progeny requires actively growing cells (Marsh and Wellington, 1994; Wang et al., 1996), but this principle was built based on the study of bacteria dividing by binary fission and does not necessarily apply to bacteria with atypical developmental cycles like *Streptomyces*. Investigating one phage of *Streptomyces albus*, phage adsorption was shown to differ depending on the stage of development of *Streptomyces* (Rosner and Gustin, 1980). In this instance, phage adsorption was found to be maximal with mature mycelium, yet more work is needed to refine these observations and extend these investigations to more phages and hosts.

Another understudied aspect of phage infection, which is especially interesting with *Streptomyces*, concerns the late time points. When describing the five novel *Streptomyces* phages we isolated, we observed that, after an initial increase, phage titers declined strongly (Hardy et al., 2020). This infection kinetics differ from prototypical infections in liquid medium, which show a progressive collapse of the bacterial culture with antiparallel increase in phage titers. Cells randomly resistant to the phages can then emerge and are usually responsible for the late regrowth of the infected cultures, but phage titers are generally not determined at these later time points. The fact that the titer drop we observed was found with all five phages indicated a rather conserved phenomenon. At this point, we can only speculate as to the underlying molecular mechanisms at play. Yet, one reasonable hypothesis could be that *Streptomyces* traps phage particles in cellular structures not permissive to phage amplification, e.g. cellular debris resulting from the previous rounds of infection. This would cause a drop in infective phages present extracellularly and in turn allow *Streptomyces* regrowth.

The third and last element of the connections between phage infection and development concerns the use of sporulation as antiphage strategy. We observed that, in particular for the phages Alderaan and Dagobah, a whitish ring formed around plaques and lysis zones after several days of incubation (**Figure 8**). These rings correspond to the formation of aerial hyphae followed by sporulation, suggesting that phage infection triggered premature sporulation of the surrounding mycelium. Further work conducted by Tom Luthe confirmed that sporulation at the infection interface seemed a strategy employed by *Streptomyces* to contain viral outbreaks (Luthe and Frunzke, unpublished work). It is not clear yet how sporulation could help protect from phage infection. However, considering that spores show decreased sensitivity to phages, the formation of a 'wall' of spores at the infection front could deprive phages from permissive hosts required for propagation.

Interestingly, increased sporulation in reaction to phage infection was also seen in explorer cells of *S. venezuelae* infected with Alderaan, suggesting that this response is an important feature of the antiphage response in *Streptomyces* (Figure 8).

A



B

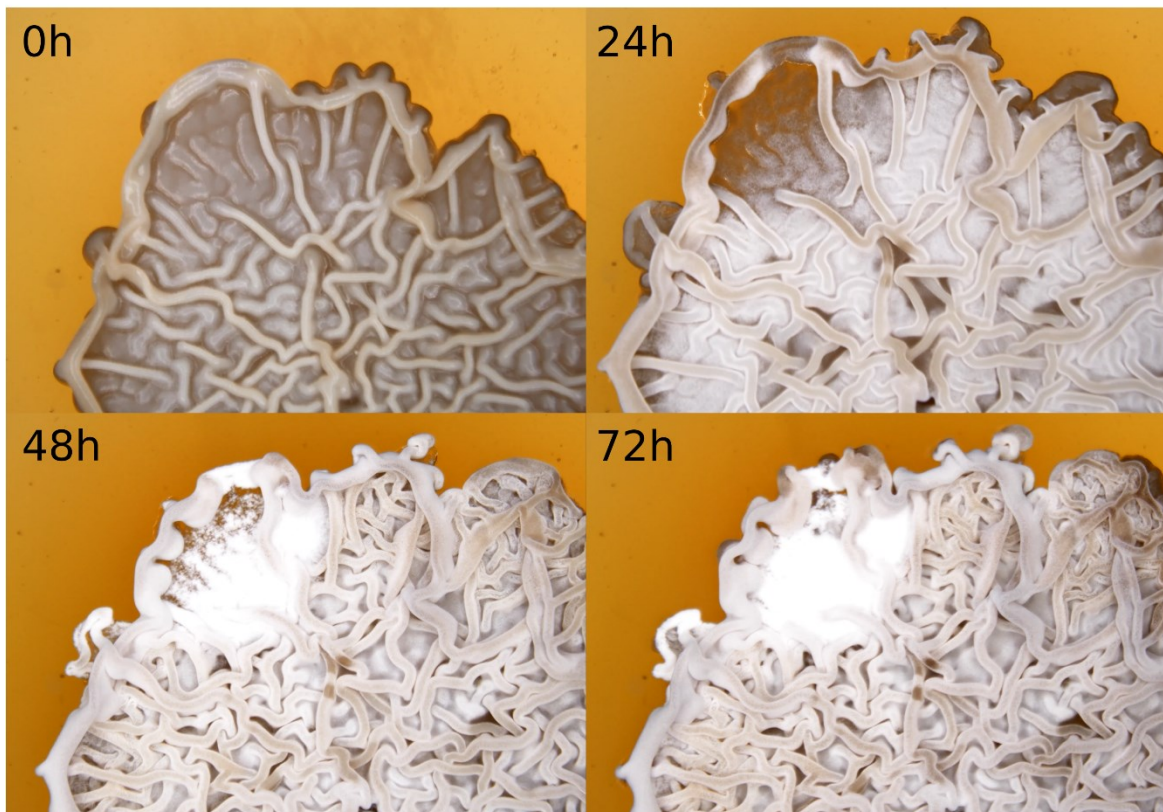


Figure 8 | **Phage infection triggers sporulation in *Streptomyces*.** (A) Lysis zone and single plaques formed by the phage Dagobah on *S. coelicolor* M145. (B) Impact of phage infection on explorer cells. *S. venezuelae* ATCC10712 was grown for 3 days on medium lacking glucose to trigger exploration. At timepoint $t=0$, the phage Alderaan was deposited on the upper left part of the agglomerate of exploring cells, which was further imaged for 72 hours by stereomicroscopy.

Ultimately, we hope that this set of five phages may serve as a basis for future studies to better understand phage-host interactions in *Streptomyces*. We made the five phages available to the community by depositing them in the German Collection of Microorganisms and Cell Cultures (DSMZ).

The isolation and characterization efforts continued (Table 1 in the Appendix 4.1) to increase diversity of our phage collection, allowing for exciting questions to be tackled with increased power in the future.

2.2.4 Phage-induced natural product synthesis in *Streptomyces*

Our observation of pigmented halos around *S. coelicolor* plaques (cf. 2.2.3 Phages of *Streptomyces* and Figure 7) suggested that *Streptomyces* releases secondary metabolites in reaction to phage infection. We were interested to identify these molecules and the role they play in relation to phage predation. To address these questions, we focused on *S. coelicolor* and the three phages infecting this species that we described earlier (Hardy et al., 2020).

Streptomyces coelicolor is amongst the best-studied representatives of the genus *Streptomyces*. Since its first description in the 1950s, it has become a workhorse for genetical studies and a model system for development and antibiotic synthesis (Hoskisson and van Wezel, 2019). Its genome was the first *Streptomyces* genome to be sequenced at the dawn of the 2000s (Bentley et al., 2002). Combined with later genome mining and BGC prediction, it unravelled a rich chemical repertoire, with almost 30 chromosomally-encoded BGCs (Craney et al., 2013) (**Figure 9**). However, *S. coelicolor* is said to produce only four secondary metabolites under standard laboratory conditions (Bednarz et al., 2019; Mast and Stegmann, 2019): coelimycin, a calcium-dependent antibiotic, actinorhodin and undecylprodigiosin. Actinorhodin and undecylprodigiosin are in fact responsible for the name of this species: '*coelicolor*' means in Latin 'colours of the sky', actinorhodin and undecylprodigiosin being traditionally described as 'blue' and 'red' compounds, respectively (Hopwood, 2006). The ease of gauging the production of actinorhodin and undecylprodigiosin by visual inspection significantly contributed to establish this species as model *Streptomyces* species, as it facilitated genetic studies of the clusters encoding these two molecules (Chater, 1999). As for their chemical nature, actinorhodin is a benzoisochromanquinone dimer belonging to the polyketide class, while undecylprodigiosin is a tripyrrole alkaloid pertaining to the broader family of prodiginines. One prominent chemical feature of actinorhodin is the pH-responsiveness of its pigmentation (it is red at acidic pH and blue at basic pH) (Bystrykh et al., 1996).

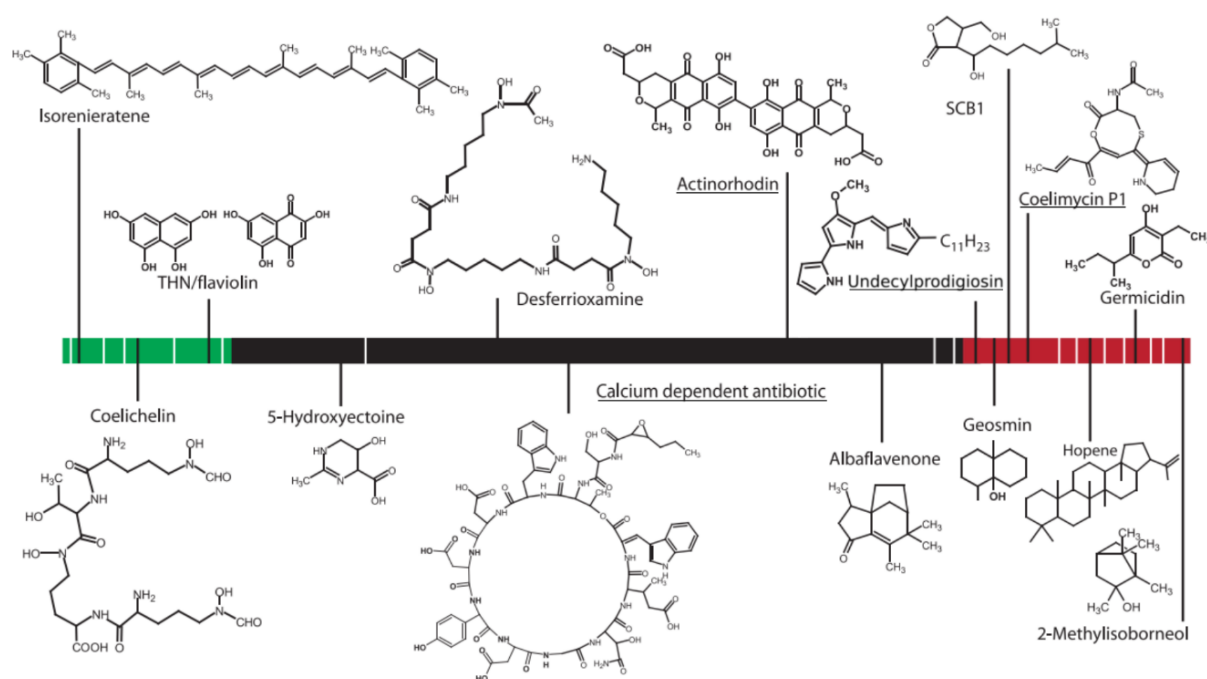


Figure 9 | **Secondary metabolites encoded by *Streptomyces coelicolor* M145.** Secondary metabolites are presented in relation to their chromosomal location. The left and right arms are highlighted in green and red, respectively. The core chromosome region is shown in black. Secondary metabolites without structures are depicted as white ticks on the genome while those with structures are in black. Secondary metabolites produced under standard laboratory conditions are underlined (adapted and modified from Craney et al., 2013).

Despite being well-studied secondary metabolites of *S. coelicolor*, the physiological role of actinorhodin and undecylprodigiosin remains unclear. Actinorhodin was shown to have pH-sensitive bacteriostatic activity against several Gram positive bacteria (Mak and Nodwell, 2017). In *Staphylococcus aureus*, actinorhodin causes oxidative damage of multiple cellular targets, including components of the DNA, proteins and cell envelope (Mak and Nodwell, 2017). Co-cultivation of *S. coelicolor* with the predatory bacterium *Myxococcus xanthus* further revealed that iron competition triggered actinorhodin biosynthesis (Lee et al., 2020b). Taken together with the chemical potential displayed by actinorhodin to bind iron with its close ketone and hydroxyl groups, this suggests that actinorhodin could act as an iron chelator. However, the biological significance of these potential chelating functions remains ambiguous.

In a similar fashion, the biosynthesis and regulation of undecylprodigiosin in *S. coelicolor* was the subject of numerous studies, but the actual role of this molecule in *S. coelicolor*'s physiology received attention only recently. Interestingly, Tenconi and colleagues revealed the involvement of undecylprodigiosin in the programmed cell death process of *S. coelicolor* (Tenconi et al., 2018, 2020). Undecylprodigiosin is synthesized before the onset of aerial hyphae formation and through its toxic

Scientific context and key results of this thesis

effect amplifies cell death in the vegetative mycelium, releasing nutrients necessary for the erection of aerial hyphae. Strong autotoxicity and coordinated regulation are features reminiscent of abortive infection systems (cf. 2.1.2.3), which hence raises interest for the study of undecylprodigiosin production upon phage infection. Outside the prokaryotic world, a number of prodiginines have shown potential antitumor drugs and have entered clinical trials (Williamson et al., 2007). The lead molecule prodigiosin possesses topoisomerase-inhibiting activity by intercalating in the minor groove of the DNA double helix (Montaner et al., 2005), and can cause cleavage of double-stranded DNA (dsDNA) in the presence of copper (Williamson et al., 2007).

The halos surrounding Dagobah's plaques were typically blue while those formed around plaques of Endor1 and Endor2 were reddish, suggesting actinorhodin and undecylprodigiosin as prime suspects (Figure 7). To further confirm this phenotypic reaction to phage infection, we performed 'soft-agar free assays' where bacteria and phages are spotted together on solid medium (Figure 10). Here too, phage infection caused a diffusible dark blue pigment to appear, which was not visible with the uninfected bacteria.

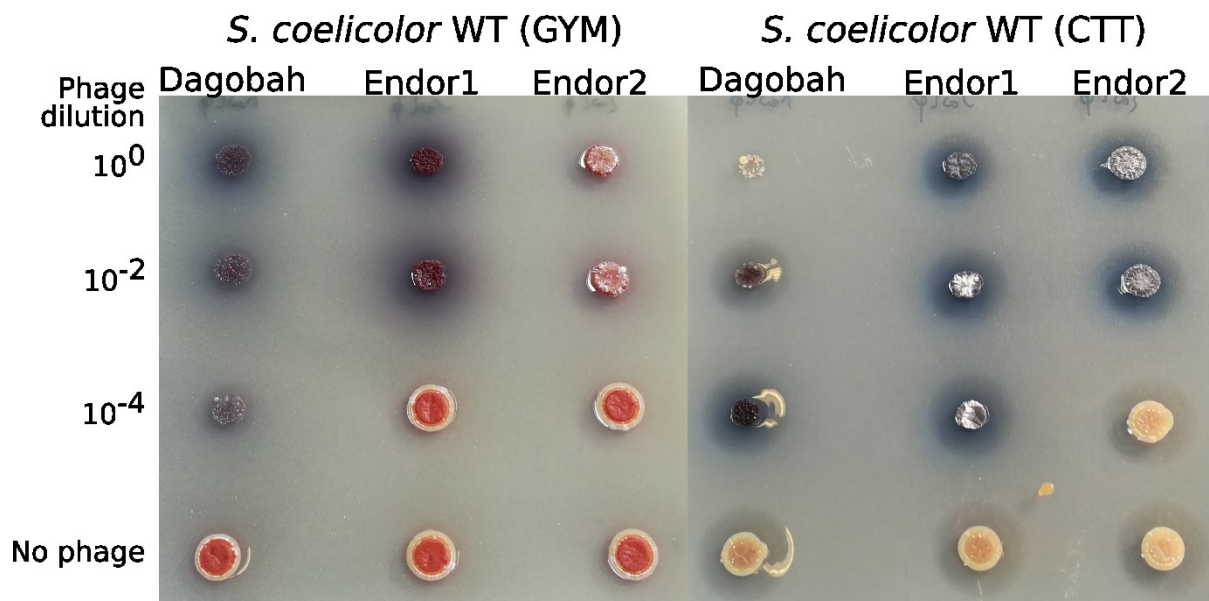


Figure 10 | **Phenotypic response to phage infection in *S. coelicolor***. Overnight cultures of *S. coelicolor* WT (M145) were spotted together with a dilution series of phages so that droplets fused with each other. The plates used were either of GYM (left) or CTT (right) medium. Plates were imaged after 4 days of incubation.

To identify and evaluate quantitatively the metabolites released in reaction to phage infection, we analyzed by LC-MS pieces of agar taken at the border of lysis zones. Actinorhodin itself was not

detected—which is not uncommon with the extraction protocol and LC-MS device that we used—but actinorhodin-related compounds could be measured. Surprisingly, most actinorhodin derivatives were found to be more abundant in the uninfected controls than in the phage-infected samples (Appendix 4.1, Table 2), with the exception of deshydroxy-actinorhodic acid which was enriched in the Dagobah and Endor2 samples. The phage-infected samples contain a substantial zone where cells were lysed by phage infection and hence could not produce actinorhodin (and other secondary metabolites). This fact could explain why absolute amounts of actinorhodin derivatives are higher in the uninfected lawn than in the zones centred on the border of phage lysis zones. Alternatively, issues at the extraction or measurement stages could also explain this unexpected lower abundance of actinorhodin-related pigments in the phage samples compared to the controls.

Next, we examined the relative abundance of undecylprodigiosin. We could not detect undecylprodigiosin and related molecules (streptarubin) in any of the M145 samples, possibly because of the sampling time (3 days post-infection). In contrast, when applying the same procedure to an actinorhodin mutant (Gomez-Escribano and Bibb, 2011), one of the most enriched metabolite in the phage-infected samples compared to the control was undecylprodigiosin, with a 25-fold change (Appendix 4.1, Table 3). These data show an increased release of undecylprodigiosin in reaction to phage infection in a *S. coelicolor* mutant deficient for the production of actinorhodin.

Owing to the limitations of LC-MS performed with plate samples, we performed LC-MS this time on liquid cultures and focused on the phage Endor2. Comparison of the phage-infected culture supernatants with the control ones showed precocious and more intense production of undecylprodigiosin, and to a lesser extent of actinorhodin (**Figure 11**).

Scientific context and key results of this thesis

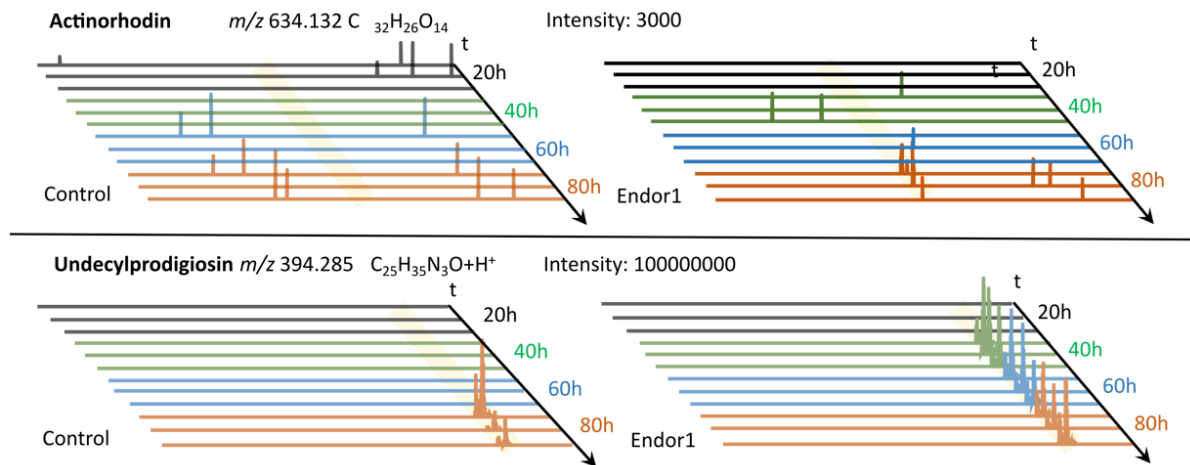


Figure 11 | **Phage infection enhances release of actinorhodin and undecylprodigiosin.** Extracted ion chromatograms of actinorhodin (top) and undecylprodigiosin (bottom), after analysis with liquid chromatography-mass spectrometry (LC-MS) of cultures of *S. coelicolor* M145 either uninfected or infected with Endor2. The expected retention time of the respective ions is shown as an orange band (courtesy of Silke Probst (ETH Zürich, Switzerland) and Larissa Kever).

Given that actinorhodin and undecylprodigiosin are released in reaction to phage infection, we sought to determine whether these two molecules would protect *S. coelicolor* against phage infection. To test this hypothesis, we assessed the sensitivity to phage infection of single deletion mutants as well of a double mutant for both BGCs (Gomez-Escribano and Bibb, 2011; Tenconi et al., 2018). However, mutants showed no difference in sensitivity and course of phage infection, both on plates and in liquid infection assays.

We then reasoned that the difference in chronology of the release of secondary metabolites and phage infection could explain this observation. Indeed, one can imagine that the release of actinorhodin and undecylprodigiosin occurs with a significant delay, after phages have already completed several replication cycles and lysed a significant fraction of the culture. To account for this difference in timelines, we grew wild-type *S. coelicolor*, actinorhodin and undecylprodigiosin deletion mutants and harvested the filtered culture supernatants (hereafter called 'spent medium'). We challenged *S. coelicolor* with phages in presence of varying amounts of spent medium, but, here too, we did not observe differences in infection between cultures supplemented with the spent medium of the wild type and of the mutants. Altogether, these data suggest that actinorhodin and undecylprodigiosin do not provide direct protection against phage infection.

To assess whether cell death in general and not phage infection per se would trigger production of actinorhodin and undecylprodigiosin, we checked the effect of different antibiotics on *S. coelicolor*. Out of the antibiotics tested, only the aminoglycoside kanamycin caused growth inhibition of *S. coelicolor*, and the surrounding bacterial lawn showed reddish halos. Ammonia fume assays

supported the presence of actinorhodin in these halos, indicating that actinorhodin may be a stress-induced molecule rather than an antiphage agent. In accordance with this hypothesis, secretion of actinorhodin was also observed in reaction to predation by myxococcus (Lee et al., 2020b; Pérez et al., 2011). Actinorhodin could therefore act as a signalling molecule to warn neighbours of incoming danger, on top of serving as an antibiotic against certain Gram-positive competitors (Mak and Nodwell, 2017).

Future investigations about this topic will include two main experiments. The first experiment consists in using reporter strains to better appreciate the spatiotemporal release of actinorhodin and undecylprodigiosin in reaction to phage infection. It relies on the plasmid-based expression of fluorescent proteins placed under the control of the promoters of central transcriptional activators of the actinorhodin and undecylprodigiosin pathways ActII-ORF4 and RedZ, respectively. This approach was already used recently with pure cultures of *S. coelicolor* and cultures grown next to the soil-dwelling actinomycete *Amycolatopsis* (Zacharia et al., 2021). Use of such reporter system would provide us with more precise insights in the orchestration of the activation of the biosynthetic clusters in response to phage infection.

The second experiment is a competition assay between the wildtype and actinorhodin or undecylprodigiosin mutants under phage pressure. Indeed, the fitness disadvantage of the mutants when challenged with phages – if there is any—may not manifest in pure cultures but may be observed under co-culture conditions. Tracking of the wild type and the mutants will be possible by tagging the different strains with constitutively expressed fluorescent proteins. These competition experiments could be performed in a mixed, liquid environment, but the results would be even more interesting when performed in a spatially structured environment, e.g. plates. If actinorhodin or undecylprodigiosin help in any way to respond to and contain phage infection, we can expect an enrichment of wild-type cells at the border of plaques.

Phage-induced natural product synthesis in *Streptomyces* is presumably not limited to actinorhodin and undecylprodigiosin. As a result, we expanded our inquiry to other secondary metabolites, the results of these investigations being reported in greater detail in the Appendix (4.1 Supplementary Information to “2.2.4 Phage-induced natural product synthesis in *Streptomyces*”).

Under low-iron conditions, *S. coelicolor* synthesizes various desferrioxamines, which are hydroxamate siderophores used to gather iron (Barona-Gómez et al., 2004; Schupp et al., 1988). The main desferrioxamines produced by *S. coelicolor* are desferrioxamines B and E, whose synthesis is directed by the *desA-D* operon. Exploiting the LC-MS dataset generated to assess production of actinorhodin and undecylprodigiosin in phage-infected plates (cf. above), we examined desferrioxamine abundance

in the different samples. While no major difference was found between the control and the phage-infected samples concerning the abundance of desferrioxamine B and E, the Dagobah samples showed strongly elevated (20- to 50-fold increase in comparison to the control) levels of metabolites identified as desferrioxamine derivatives. Interestingly, these desferrioxamine versions were not found or found at much lower intensity in the samples infected by the phages Endor1 and Endor2, suggesting a specificity of the bacterial response to phage infection.

To further our investigations about the relationship between phage infection and desferrioxamines, we used a *S. coelicolor* mutant carrying a defective *desD* gene and hence deficient for the production of desferrioxamine B and E (Barona-Gómez et al., 2004). Interestingly, when using standard medium (GYM medium), the phage Dagobah did not form plaques on the desferrioxamine-deficient mutant (Appendix 4.1, Figure 1A). The plaques formed by Endor1 and Endor2, although comparable in numbers, were more turbid and substantially smaller. When plated on a different medium (CTT medium), the plaque counts of Dagobah obtained with the desferrioxamine mutant were however comparable to those of the WT, which indicates some medium specificity (Appendix 4.1, Figure 1B).

Next, we examined the effect of supplementation with exogenous desferrioxamine B on phage infection of the desferrioxamine mutant. Addition of increasing amounts of desferrioxamine B did not impact the plaque count and phenotype (Appendix 4.1, Figure 1C). Similarly, supplementation of either ferric or ferrous iron showed only minor effects on plaque morphology and counts (Appendix 4.1, Figure 2). These results could be explained by the fact the concentrations reached of desferrioxamine B or iron were not sufficient, or that other desferrioxamine derivatives are needed to rescue the phenotype. Increased release of desferrioxamines following phage infection could also be a strategy for *Streptomyces* to scavenge iron released from neighbouring lysed cells.

We also performed some preliminary and exploratory work about phage-triggered natural product synthesis in *S. venezuelae*. In 'soft-agar free assays' performed with our two *S. venezuelae* phages, brown halos diffused from phage-infected colonies, suggesting the release of melanin in reaction to phage infection (Appendix 4.1, Figure 3). Furthermore, MALDI-Imaging was applied to colonies of phage-infected *S. venezuelae*. MALDI-Imaging consists in the use of matrix-assisted laser desorption ionization (MALDI) on a solid sample while conserving the spatial structure of the sample. So far, use of this technique revealed metabolites which were strongly enriched in the phage-infected colonies compared to the controls (Appendix 4.1, Figure 4). Although the step of metabolite identification represents the major bottleneck of this approach, MALDI-Imaging is a promising strategy which could illuminate the response to phage infection at the metabolite level.

2.2.5 Aminoglycosides, antibacterial but also antiviral molecules

2.2.5.1 Introduction

Aminoglycosides are a class of bactericidal antibiotics with a broad spectrum of activity and active especially against Gram-negative bacteria (Krause et al., 2016). When using aminoglycoside resistant strains, we noticed that addition of apramycin caused a strong reduction in phage propagation. Prompted by this initial serendipitous observation, we sought to investigate the antiphage properties of aminoglycosides using the modern tools at our disposal. We were particularly interested in examining them through the prism of bacterial communities in nature.

As their name suggests, aminoglycosides are pseudosaccharides decorated with ammonium groups, and most of them share a 2-deoxystreptamine ring (Busscher et al., 2005). They can be subdivided in different subclasses depending on the presence of such 2-deoxystreptamine ring and the moieties attached to it (**Figure 12**). Most aminoglycosides are naturally occurring substances and are readily obtained from actinomycetes of the genus *Streptomyces* (named with the suffix “-mycin”) and to a lesser extent *Micromonospora* (named with the suffix “-micin”)(Busscher et al., 2005). From a historical perspective, the first aminoglycoside to be isolated was streptomycin in 1944. This represented a major breakthrough in the history of medicine, since it was the first antibiotic active against *Mycobacterium tuberculosis* (Kresge et al., 2004; Serio et al., 2018; Woodruff, 2014).

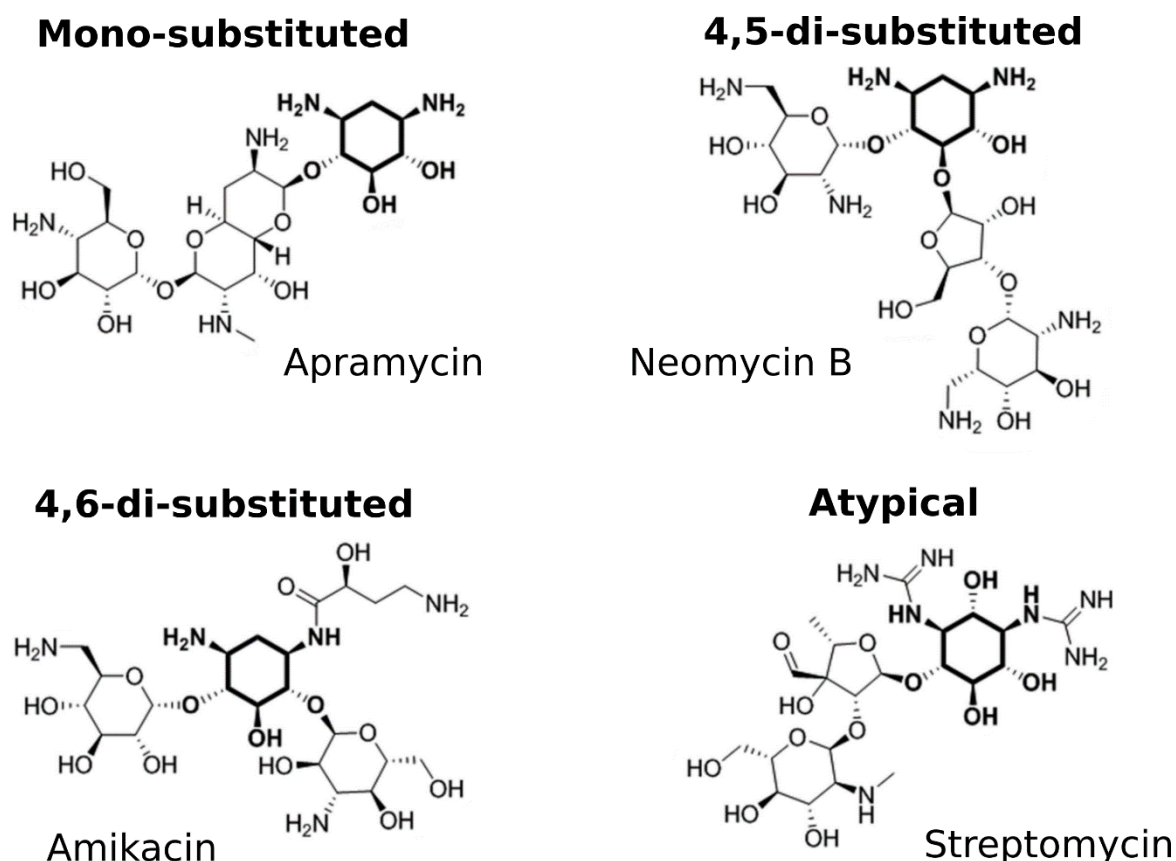


Figure 12 | **Chemical structures of exemplary members of the four aminoglycoside subclasses.** Aminoglycosides are classified in four groups depending on the presence of a 2-deoxystreptamine ring (highlighted in bold) and the number and the position of the substitutions. In the case of streptomycin, the highlighted ring is not 2-deoxystreptamine, but instead a streptidine ring (adapted and modified from Serio et al., 2021).

Despite variations of mechanism of action between individual aminoglycosides, the antibacterial activity of aminoglycosides overall relies on the targeting of the 30S subunit of ribosomes, and the resulting interference with translation (Mingeot-Leclercq et al., 1999). More precisely, aminoglycosides bind the 16S rRNA at the level of the A-site of the ribosome. The altered conformation of the 16S rRNA can in turn block the initiation of protein synthesis, prevent further elongation and cause premature termination, or trigger the incorporation of incorrect amino acids (Krause et al., 2016). The mistranslated proteins may be inserted into the cell membrane, leading to altered permeability, disruption of the membrane potential and ultimately, cell death (Bruni and Kralj, 2020).

Widespread clinical use of aminoglycosides was quickly followed by the emergence of resistance. Similarly to other antibiotics, the main aminoglycoside resistance strategies are the following: decreased intracellular concentrations through reduced uptake or expression of efflux pumps, modification of the target (mutations of the rRNA or ribosomal proteins) and enzymatic inactivation

of the antibiotic itself by so-called aminoglycoside modifying enzymes (AMEs) (**Figure 13**). This last resistance mechanism is the most widespread, and AMEs are subdivided in three subclasses, depending on the chemical modification they apply to their aminoglycoside substrate: aminoglycoside N-acetyltransferases (AACs), aminoglycoside O-nucleotidyltransferases (ANTs) and aminoglycoside O-phosphotransferases (APHs)(Garneau-Tsodikova and Labby, 2016). The chemically modified aminoglycosides have reduced binding affinity to ribosomes, explaining the high-level of resistance conferred by AMEs. AMEs are typically plasmid-encoded and are highly mobile between members of the same species but also among a large variety of bacterial species. The dissemination of resistance phenotypes enabled by AMEs is especially problematic in pathogenic bacteria, as it contributes to the emergence of multidrug resistant bacteria (Mingeot-Leclercq et al., 1999). Alteration of the ribosomal binding sites represents another major mechanism of resistance to aminoglycosides. Mutations in the genes encoding the 16S rRNA are relatively rare, as modifications in this vital cellular machinery often have lethal consequences. In contrast, modification of the aminoglycoside binding site by 16S rRNA methyltransferases (RMTases) is commonly found in actinomycetes naturally producing aminoglycosides. Contrary to AMEs which usually show high substrate specificity, RMTases protect aminoglycoside producers against the various aminoglycosides and their intermediates they produce (Garneau-Tsodikova and Labby, 2016). Here again, RMTases can be mobilized to other bacterial species, most commonly by uptake of a plasmid containing the RMTase gene.

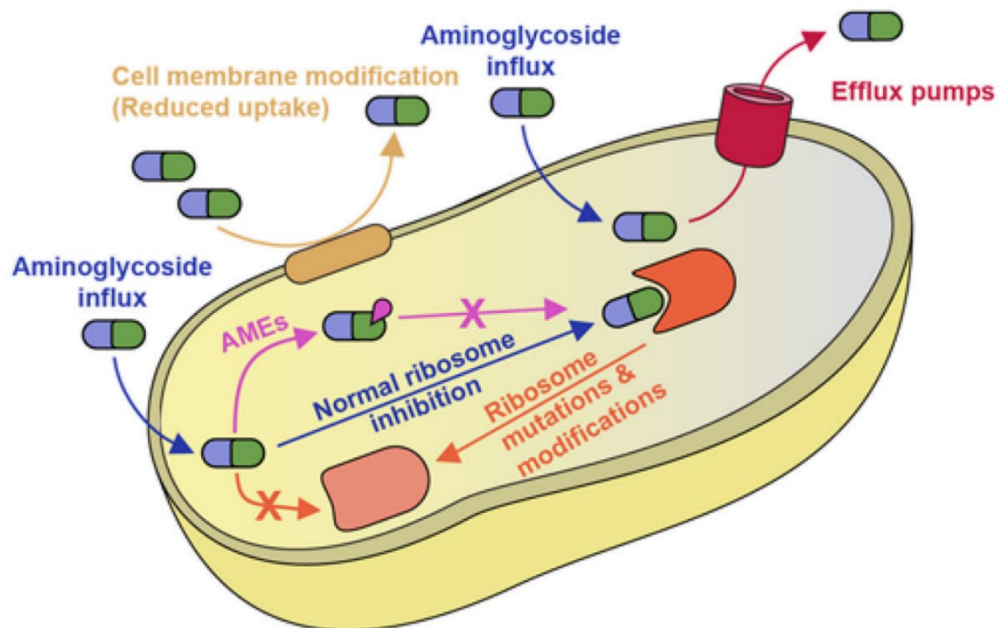


Figure 13 | **Resistance mechanisms to aminoglycosides in bacteria.** AMEs: aminoglycoside-modifying enzymes (adapted and modified from Garneau-Tsodikovaa and Labby, 2016)

Soon after industrial scale-cultures of *Streptomyces griseus* were set to produce large amounts of streptomycin, phage outbreaks occurred and caused major concern for the production of streptomycin. These hurdles spurred efforts to look for ways to prevent phage infection, and large screening efforts were undertaken to find compounds able to block phage infection in actinomycetes (Asheshov et al., 1954; Schatz and Jones, 1947). Ironically, streptomycin itself proved to effectively inhibit infection by diverse phages—dsDNA phages as well as a RNA phage (Brock, 1962; Brock et al., 1963). However, the high concentrations of streptomycin used in these studies may have precipitated the viral particles. The mechanism of action also remains disputed, with different models proposed to explain the blockage of phage infection imposed by streptomycin (Brock and Wooley, 1963; Brock et al., 1963, 1965). Since the 1970s, study of the antiphage properties of aminoglycosides have fallen into oblivion, with the notable exception of a recent report of the inhibition of *Mycobacterium tuberculosis* phages by kanamycin and hygromycin (Jiang et al., 2020).

2.2.5.2 Aminoglycosides are potent inhibitors of phage infection in diverse hosts

The first step of our study consisted in constructing bacterial resistant hosts carrying plasmid-borne AMEs (Kever et al., 2021). While wild-type hosts sensitive to aminoglycosides suffice for exploratory screenings, in-depth analysis of the impact of aminoglycosides on phage infection is greatly facilitated by the use of resistant hosts. Indeed, the broad antibacterial activity of aminoglycosides would cause strong growth defect of wild-type hosts, interfering with the investigation of their antiviral effect. Unless otherwise stated, all bacterial hosts we used in the following experiments carried genomically-integrated resistance cassettes for the corresponding aminoglycosides.

The bacterial hosts included in the screening comprise three actinobacterial species (*S. venezuelae*, *S. coelicolor* and *Corynebacterium glutamicum*) and the Gram-negative model *Escherichia coli*. All the actinophages we used belong to the siphophage type, but the *E. coli* phages showed greater diversity, with siphophages, podophages, myophages as well as filamentous and RNA phages. The aminoglycosides tested were the following: hygromycin, apramycin, spectinomycin, streptomycin and kanamycin. In this screening, only siphophages showed inhibition by aminoglycosides, and this inhibition revealed aminoglycoside-, phage- and host-specificity, with for example all three phages infecting *S. coelicolor* showing no sensitivity to any aminoglycosides (**Figure 14A**). The two phage-host pairs showing the strongest inhibition were Alderaan and *S. venezuelae* as well as λ infecting *E. coli*. Both pairs showed a strong inhibition of plaque formation by apramycin (**Figure 14B**), and this effect was the most consistent among the tested aminoglycosides. As a result, we chose to focus on apramycin for future studies.

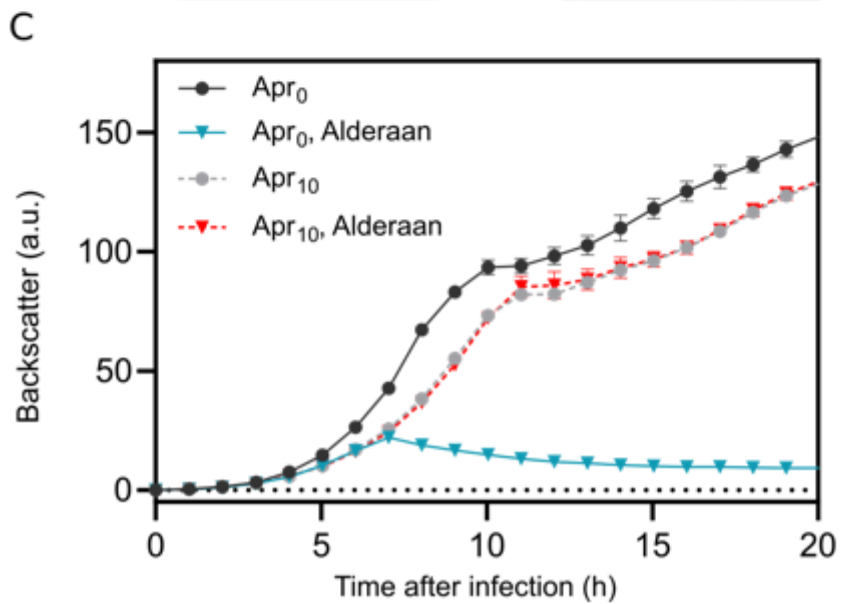
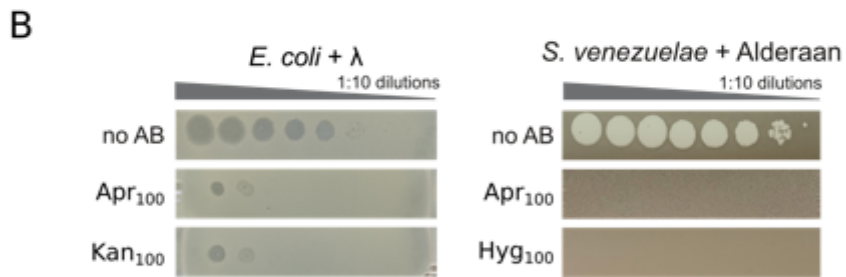
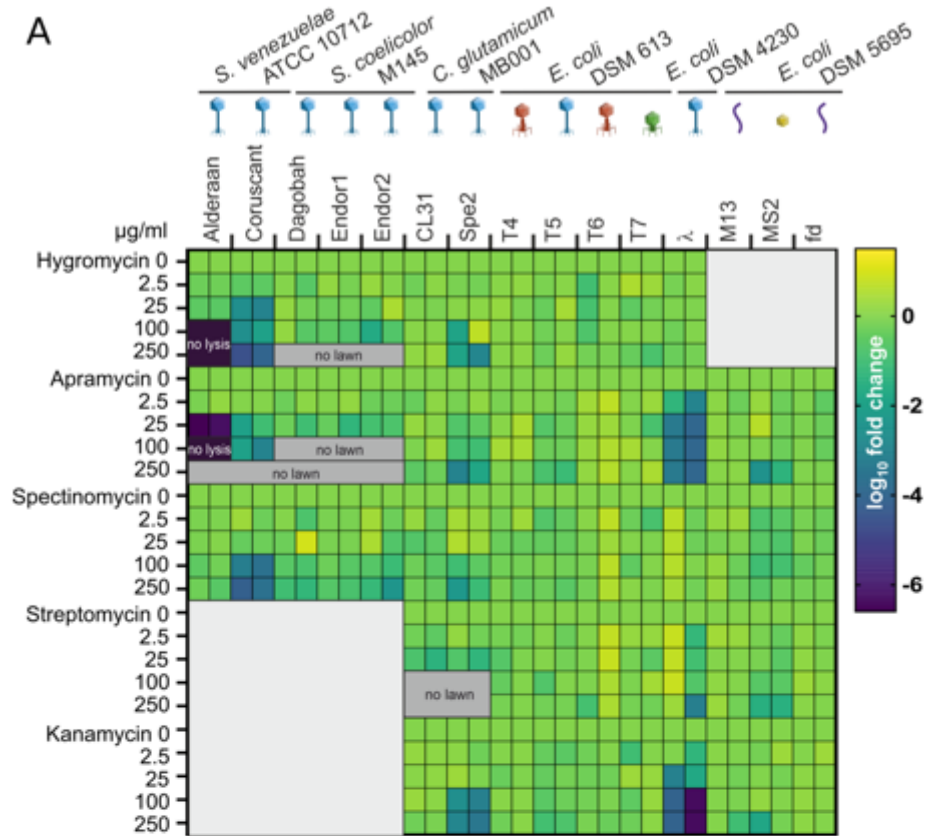


Figure 14 | **Aminoglycosides inhibit phages infecting widely divergent bacterial hosts.** (A) Results of the screening, showing the log₁₀-fold change in plaque counts compared to the aminoglycoside-free control. 'no lysis' and 'no lawn' refer to the absence of plaques and lysis zones caused by aminoglycosides, and to the very poor growth of bacterial lawn, respectively. (B) Exemplary pictures of infection assays performed with the phages λ and Alderaan. no AB: no antibiotic. (C) Infection curves of *Streptomyces venezuelae* infected with the phage Alderaan in the absence and presence of apramycin.

Next, we assessed if apramycin would inhibit phage infection in liquid medium too. Infection performed in microtiter plates showed that apramycin concentration as low as 10 µg/ml was sufficient to completely inhibit the propagation of the phage Alderaan (**Figure 14C**), and comparable results were obtained with the phage λ. Performing infection of *S. venezuelae* with Alderaan in a microfluidic system allowed the visualisation of the protective effect of apramycin: in absence of apramycin the mycelium was quickly lysed whereas the mycelium cultivated in presence of apramycin grew unaffected by the phages. Interestingly, magnesium chloride was found to counteract the inhibition of phage infection exerted by aminoglycosides. The explanation of this phenomenon is not clear, but may involve decreased uptake of aminoglycosides because of competition of the magnesium ions with aminoglycosides for their binding sites at the cell surface (Hancock et al., 1981). The removal of inhibition of phage infection caused by magnesium was already observed with streptomycin (Brock and Wooley, 1963).

2.2.5.3 Aminoglycosides block an early step of the phage lifecycle, between genome injection and replication

After showing the strong antiphage properties of apramycin, we sought to determine the underlying mechanism of action, in other words which step of the phage lifecycle is inhibited by apramycin.

The first step of the phage lifecycle is the adsorption of phage particles and subsequent injection of the phage genome inside the cytoplasm. In *S. venezuelae*, adsorption assays showed no difference in the evolution of adsorbed phages over time when performed in absence or presence of apramycin. Further infection assays including a washing step performed 15 min after phage addition indicated that apramycin does not prevent irreversible adsorption of phage particles but rather a later stage of the phage lifecycle. In Gram-negative bacteria, so-called potassium efflux assays use the increase of extracellular potassium concentrations following phage addition as a proxy for successful genome injection. When performing such potassium efflux assays with *E. coli* and λ, we did not observe an impact of apramycin, suggesting that in *E. coli* the injection step of the λ genome is not significantly affected by aminoglycosides.

To gain further insights in the influence of apramycin on the phage lifecycle, we followed intracellular amounts of Alderaan DNA over several infection cycles by quantitative PCR (qPCR). In absence of apramycin, amounts of intracellular phage DNA increased exponentially over time. In contrast, the apramycin-treated cultures showed a very weak increase in phage intracellular phage DNA followed by a progressive decline, the ratios phage/bacterial DNA quickly passing below the detection limit.

Next, we employed phage targeting direct-geneFISH to visualize intracellular phage DNA during infection. This technique is derived from fluorescence *in situ* hybridization (FISH) and relies on fluorescently labelled oligonucleotides designed to specifically anneal to the phage genome. In *E. coli*, phage targeting direct-geneFISH showed that infection with λ performed in presence of apramycin led to the apparition of foci in cells, but these foci did not progress to the intense and diffuse intracellular signals associated to genome replication and instead disappeared over time. When infecting *S. venezuelae* with Alderaan, very weak intracellular phage signal was visible in the apramycin-treated samples throughout the course of infection. This diverging result with λ can be due to a sensitivity not allowing the detection of single phage genomes or to degradation of the injected phage genome before the first sampling point in the case of *Streptomyces*. Alternatively, we cannot exclude that in *S. venezuelae* apramycin interferes with the injection process of Alderaan. Altogether, these experiments indicate that the blockage imposed by apramycin occurs at an early step of the phage lifecycle, between injection and replication of the phage genome. The mechanism of action of aminoglycosides could differ between bacterial hosts. It is possible that in the case of *S. venezuelae*, some additional interference exists at the injection step.

As a last part of the investigation about the mechanism of action, we checked the impact of apramycin on transcription of phage DNA. To this end, we sequenced intracellular RNAs at 2 time-points post-infection of *S. venezuelae* with Alderaan. While phage transcripts showed a strong build-up in the controls indicating ongoing transcription, barely any phage transcript could be detected in the infected cultures supplemented with apramycin. These data suggest a blockage of the phage lifecycle prior to phage DNA replication and transcription.

2.2.5.4 Spent medium from an apramycin natural producer prevents phage infection

In all experiments presented until this point, the inhibition of phage replication we observed was obtained using pure aminoglycosides purchased from chemical suppliers. We asked ourselves whether we could achieve a comparable inhibition using this time culture supernatants from natural aminoglycoside producers, which would support the physiological significance of the antiviral properties of aminoglycosides. In nature, apramycin is readily produced by *Streptoalloteichus*

Scientific context and key results of this thesis

tenebrarius (formerly known as *Streptomyces tenebrarius*) (Tamura et al., 2008). We cultivated *S. tenebrarius* and harvested the filtered supernatants of the cultures—referred to as ‘spent medium’. When supplemented to cultures of *S. venezuelae*, spent medium from *S. tenebrarius* prevented the lysis of the cultures caused by Alderaan (Figure 15A and 15B). Analysis of the spent medium by LC-MS confirmed the presence of significant amounts of apramycin (>10 µg/ml) (Figure 15C). It further established a temporal correlation between the presence of apramycin and protective effect of the supernatant, i.e., the spent medium harvested before the onset of apramycin production did not prevent phage amplification, while older spent medium containing apramycin did.

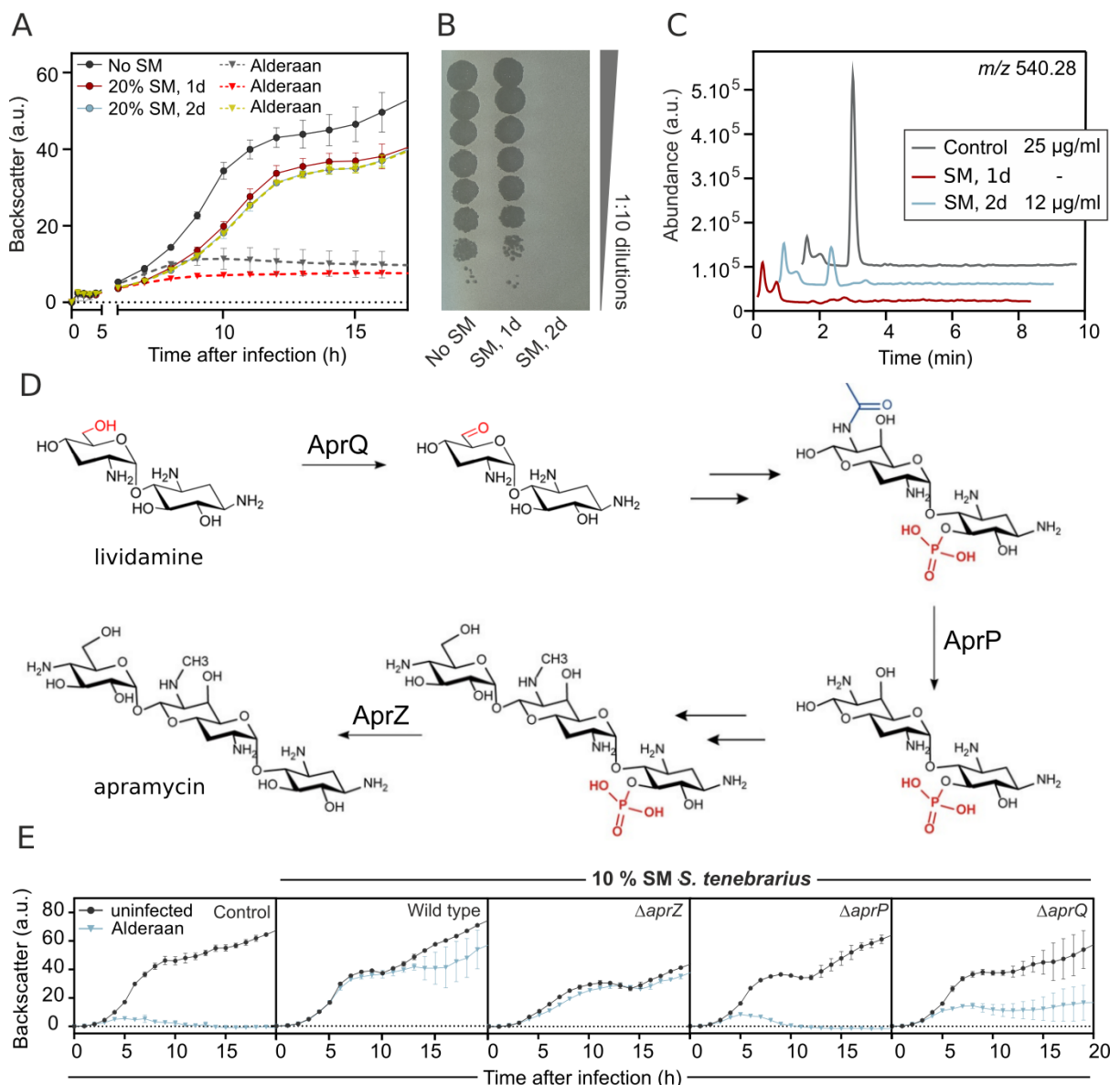


Figure 15 | Spent medium from a natural apramycin producer inhibits phage infection. (A) Infection curves for *S. venezuelae* ATCC10712 infected with the phage Alderaan, supplemented with 20% of spent medium (SM) of *Streptoalloteichus tenebrarius* (B) Determination of the final phage titers of the infected cultures shown in (A). (C) Extracted ion chromatogram of the spent medium (SM) of *S. tenebrarius* assessing by LC-MS the concentration of apramycin (m/z 540.28). (D) Simplified

biosynthetic pathway showing the synthesis of apramycin from lividamine (adapted from Lv et al., 2016 and Zhang et al., 2021). (E) Infection curves obtained by infecting *S. venezuelae* with the phage Alderaan in presence of 10% spent medium (SM) of different *S. tenebrarius* mutants defective for apramycin biosynthesis.

To further ascertain the role of apramycin as main antiphage molecule of the *S. tenebrarius* spent medium, we took advantage of *S. tenebrarius* mutants having deletions in different enzymes of the apramycin biosynthetic pathway (**Figure 15D**). Out of the three mutants tested, two ($\Delta aprQ$ and $\Delta aprP$) had the apramycin biosynthesis blocked at the pseudo- and trisaccharide stage, respectively (Lv et al., 2016; Zhang et al., 2021). In the last mutant ($\Delta aprZ$), the very last step leading to the formation of mature apramycin was lacking, leading to the extracellular accumulation of 5-O-phosphorylated apramycin (Zhang et al., 2021). Interestingly, the supernatants from the $\Delta aprQ$ and $\Delta aprP$ mutants did not protect *S. venezuelae* anymore against phage infection, suggesting that apramycin gained its antiviral properties after these biosynthesis stages (**Figure 15E**). In contrast, the supernatants from the $\Delta aprZ$ mutant caused an inhibition of phage infection which was comparable to the one obtained with wild-type *S. tenebrarius*. These data hint that the phosphoryl group carried by 5-O-phosphorylated apramycin does not interfere with its antiviral properties, despite being used by *S. tenebrarius* to temporarily inactivates apramycin's antibacterial activity and hence avoid auto-toxicity (Zhang et al., 2021). *S. tenebrarius* produces several aminoglycosides, including the well-known tobramycin (Kharel et al., 2004), and the biosynthesis pathways share common portions. Yet, to our knowledge, the deletion of *aprP* should have not affected the biosynthesis of other related aminoglycosides. These experiments performed with the *S. tenebrarius* apramycin mutants bring therefore further support in favour of apramycin being the main molecule responsible for the antiphage effect of the *S. tenebrarius* supernatants.

One outstanding question which remains at the moment mostly unanswered concerns the stage of the apramycin biosynthesis at which the antiviral activity emerges. To this end, additional apramycin mutants should be included and in-depth analysis via LC-MS of the culture supernatant should be performed to confirm the expected consequences of the mutations (i.e., missing product and accumulating substrate) and rule out pleiotropic effects. Such investigations could allow to trace the antiviral properties of the supernatants down to one or few molecules. Ideally, the different apramycin intermediates could be purified before testing their individual impact on phage infection.

2.2.5.5 Acetylated apramycin strongly inhibits phage infection, despite the loss of its antibacterial properties

As described earlier, chemical decoration of aminoglycoside by AMEs causes the loss of their antibacterial activity. We were interested in determining the impact of such modifications on the antiviral properties of aminoglycosides. To this end, we used AAC(3)IV, a well-known AME inactivating apramycin by adding an acetyl moiety to the 3-amino group of apramycin's 2-deoxystreptamine ring (Magalhaes and Blanchard, 2005). Using purified AAC(3)IV enzyme, we generated *in vitro* acetylated apramycin. After checking the efficiency of the reaction by LC-MS, we tested the impact of this acetylated apramycin on phage infection, this time using *S. venezuelae* wild-type (not carrying any resistance gene to aminoglycosides). Not surprisingly, addition of acetylated apramycin did not alter growth of *S. venezuelae* wild type, since the acetylation of apramycin prevented its binding to bacterial ribosomes. In contrast, acetylated apramycin still fully inhibited phage amplification, to levels similar with those of unacetylated apramycin in apramycin-resistant *S. venezuelae*. These findings suggest that acetylation of apramycin abolish its antibacterial, but not antiphage activity. Further, they support the assumption that this dual effect of apramycin is rooted in the existence of distinct molecular targets. As a consequence, we can envision a possible decoupling between the antiviral and antibacterial action of aminoglycosides, the loss of one of them not impacting the other one.

AMEs are prime resistance mechanisms to aminoglycosides, but are by far not the only means used by bacteria to withstand the action of aminoglycosides. An exciting research direction concerns the impact of the bacterial resistance mechanism to aminoglycosides on the inhibition of phage infection by these molecules. Here, the resistant hosts we used were all constructed using AMEs for the respective aminoglycosides. Resistance conferred by 16S rRNA methyltransferases is especially interesting as it leaves untouched the aminoglycosides and enables the study of the antiphage effect of the original, unmodified aminoglycoside.

Assuming that aminoglycosides exert their antiphage action intracellularly, we can speculate that use of efflux pumps as resistance to aminoglycosides would not lead to inhibition of phage infection by aminoglycosides. Accordingly, this resistance strategy potentially comes with a trade-off, as resistance to aminoglycosides would come at the cost of the loss of their protective effect against phages. Interestingly, very few pumps have been reported to confer complete resistance to aminoglycosides (Krause et al., 2016), which is not surprising considering the disruption of cell membrane caused by aminoglycosides (Bruni and Kralj, 2020).

Further, studying the effect of aminoglycosides on phages infecting aminoglycoside producers themselves would significantly advance our understanding of the antiviral role of aminoglycosides in

natural environments. In the work reported here, phage inhibition by aminoglycosides was demonstrated only in non-aminoglycoside producers, and the question of the physiological relevance of this inhibition has to be kept in mind. Until now, our repeated phage isolation efforts using *S. tenebrarius* as an isolation host proved unsuccessful. The two most probably explanations include the actual inhibition of phage infection by the aminoglycosides produced by *S. tenebrarius* during cultivation and a low abundance of *S. tenebrarius*-infecting phages in our samples. Phage isolation was not significantly facilitated by the use of apramycin mutants instead of the wild-type *S. tenebrarius*, which supports the second hypothesis. Once phages infecting *S. tenebrarius* are obtained, a particularly interesting question would be whether phage infection triggers the synthesis of aminoglycosides with antiviral properties, which could be verified by analysing phage-infected cultures over time with LC-MS.

2.2.6 Antiphage defense at the community level mediated by small molecules

Aminoglycosides are secreted by producer cells and can be taken up by neighbouring bacteria, which raises the question of antiphage defense at the community level. In this context, aminoglycosides could act as ‘public goods’ not only keeping bacterial competitors at bay but also conferring protection against phages to the community (**Figure 16**). Aminoglycosides being able to block phage infection in both Gram-negative and Gram-positive hosts, this broad spectrum of antiviral activity could create a local antiviral milieu favouring growth of aminoglycoside producers and other resistant bacteria. The dual antibacterial and antiviral activities of aminoglycosides make the acquisition of resistance by neighbouring bacteria —e.g. through HGT of AMEs from producers— even more profitable. Indeed, recipient cells would not be affected by the antibacterial effect of aminoglycosides and at the same time benefit from their antiviral properties. Contemplating these questions highlights the importance of local concentrations and community architecture. In soil environments, bacteria are typically organized in complex and spatially structured biofilms, allowing the build-up of metabolites and signalling molecules concentrations locally (Flemming and Wingender, 2010). Given that most natural biofilms are formed by diverse bacterial species (Yang et al., 2011), the dual properties of aminoglycosides probably shape significantly bacterial communities comprising aminoglycoside producers, in ways we can only speculate about at the moment.

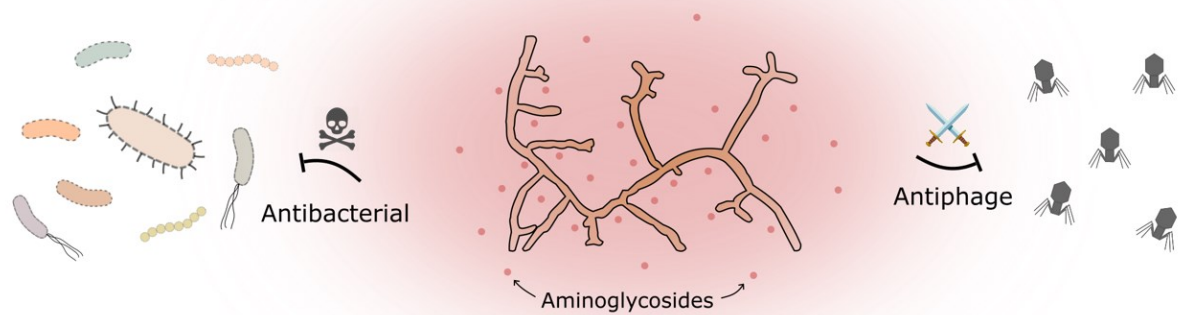


Figure 16 | **Schematical illustration of the dual properties of aminoglycosides.** Aminoglycosides are secreted by *Streptomyces* in the environment and can kill sensitive bacteria in the vicinity as well as protect resistant cells from phage infection.

In this work, we used hosts engineered for resistance to aminoglycosides in order to study the antiviral properties of aminoglycosides. However, how the combination of different stresses can influence evolutionary strategies of resistance towards phages and aminoglycosides is currently unknown. Considering a bacterium initially sensitive to aminoglycosides and a phage which is sensitive to aminoglycosides, we can imagine different scenarios, that could be tested in an adaptive laboratory evolution experiment followed by sequencing of resistant clones (**Figure 17**). In presence of aminoglycosides alone, bacterial cells could develop resistance by limiting the intracellular concentrations of the antibiotic through decrease uptake or active efflux. Challenge with phages would probably select for cells whose receptor for this phage is either modified or lost, as this is the most commonly found mechanism of resistance to phage infection *in vitro*. Lastly, we speculate that simultaneous pressure from aminoglycosides and phages could favour resistance strategies that abolish the antibacterial effect of aminoglycosides but still exploit their antiphage properties. Modification by AMEs fulfils these two criteria, assuming that modification of aminoglycosides does not interfere with their antiphage properties, as we observed with acetylation of apramycin by AAC(3)IV (cf. section 2.2.5.4). In this experimental set-up, monoculture does not allow acquisition of AMEs from other bacteria via HGT and aminoglycoside modification thus requires an adaption of existing enzymes to modify the target aminoglycoside. As a result, the likelihood of this evolutionary strategy is probably significantly lower in this setting than in a multispecies, physiological environment where HGT is pervasive.

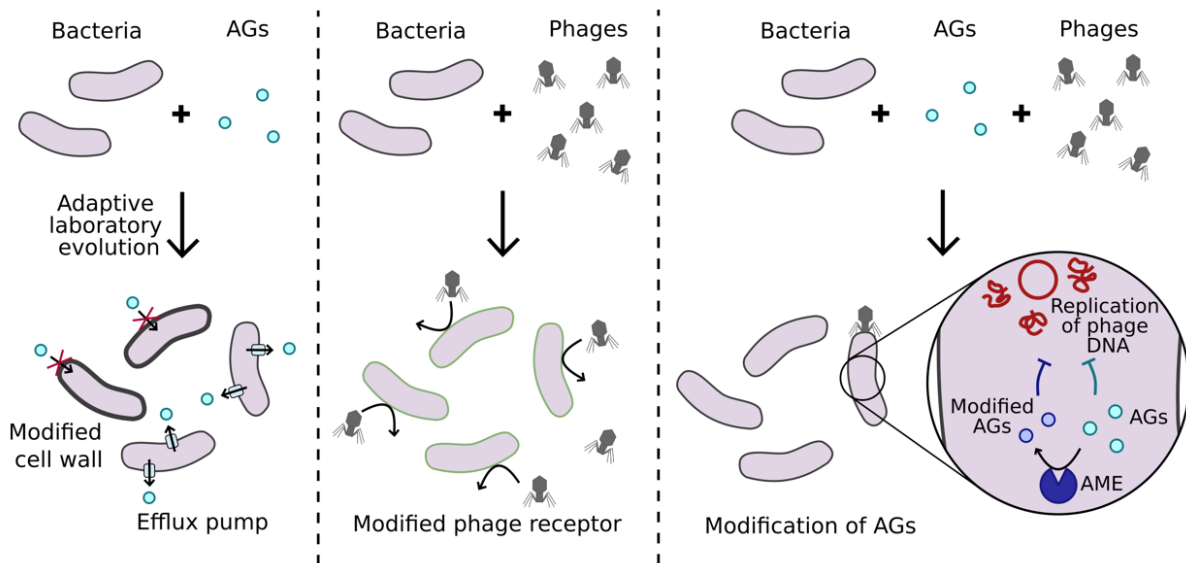


Figure 17 | **Predicted evolutionary strategies in response to challenge by phages and aminoglycosides.** Starting from a bacterial host sensitive to both aminoglycosides and a given phage, we outline potential routes of resistance depending on whether cells are subjected to aminoglycoside or phage pressure, or both at the same time. AGs: aminoglycosides; AME: aminoglycoside-modifying enzyme.

We focused thus far on the ecological implications of aminoglycosides' antiviral properties, but they are not the only class of natural products showing antiphage activity. Anthracyclines are another class of secondary metabolites naturally produced by *Streptomyces*, but in contrast to aminoglycosides they do not show antibacterial abilities (Achmatowicz et al., 2008). Since their discovery in the 1960s, they have been used against a variety of cancers and are still considered to be among the most effective anticancer treatments ever developed (Minotti et al., 2004; Peng et al., 2005; Weiss, 1992).

Recently, anthracyclines were shown to be potent inhibitors of phage infection (Kronheim et al., 2018). Similarly to aminoglycosides, anthracyclines exhibited a broad spectrum of activity, as they inhibited the replication of dsDNA phages infecting hosts as diverse as *S. coelicolor*, *E. coli* and *P. aeruginosa*. Another shared feature with aminoglycosides is the stage of the phage lifecycle they target, namely an early phase between the injection and replication steps. This raises the possibility that just injected phage genome is a prime target for phage defense mediated by small molecules. In contrast to the bacterial genome, the phage genome is transiently linear, not coated by proteins and in a relaxed state (Casjens and Gilcrease, 2009), and hence potentially highly sensitive to DNA-binding small molecules like aminoglycosides and anthracyclines.

Small metabolites can be involved in antiphage defense not only through a direct inhibitory role, but also as signalling or regulatory molecules. In bacteria, quorum-sensing is a communication system

based on secreted extracellular molecules which modulates gene expression in response to cell density (Mukherjee and Bassler, 2019). Highly dense bacterial populations are particularly vulnerable to phage predation, hence a quorum-sensing-mediated activation of phage defense systems at increasing cell densities is advantageous. Quorum-sensing was shown to coordinate the antiviral response at the community level, for example by reducing the level of phage λ receptors in *E. coli* (Høyland-Kroghsbo et al., 2013) or activating the expression of CRISPR-Cas systems (Høyland-Kroghsbo et al., 2017; Patterson et al., 2016). As is often the case, phages have evolved ways to counteract these defense strategies. For instance, a phage of *P. aeruginosa* encodes a so-called quorum-sensing anti-activator protein which inhibits the master regulator of quorum sensing, thereby dampening multiple defense systems (Shah et al., 2021).

2.3 Conclusions and future perspectives

The present thesis provides insights about the relationships between secondary metabolism and antiphage defense in *Streptomyces*. First, we isolated and characterized five novel phages infecting the model *Streptomyces* species *S. venezuelae* and *S. coelicolor* (Hardy et al., 2020). The number of *Streptomyces* phages which are both sequenced and thoroughly characterized is surprisingly low, and these phages can serve as a basis for subsequent studies.

During the characterization process, we noticed pigmented halos around plaques formed on *S. coelicolor*, suggesting the release of actinorhodin and undecylprodigiosin in reaction to phage infection (Hardy et al., 2020). This observation prompted us to examine their role as antiphage molecules, but we could not demonstrate any protection against phage predation conferred by these molecules. The role of actinorhodin and undecylprodigiosin in the response to phage infection is probably complex, and these major secondary metabolites of *S. coelicolor* seem to be involved in more global stress responses (Lee et al., 2020b; Mak and Nodwell, 2017).

Next, we investigated the antiviral properties of a major class of antibiotics: aminoglycosides. Inhibition of phage infection by aminoglycosides was already reported, but the mechanism of action underlying their antiviral activity is still subject to debate and the physiological significance of this inhibition was not appreciated. We showed that aminoglycosides are potent inhibitors of phages infecting widely divergent bacteria, both Gram-negative and Gram-positive bacteria (Kever et al., under review). Using bacterial hosts resistant to aminoglycosides, we interrogated the mechanism of action behind aminoglycosides' antiviral action. The blockage exerted by aminoglycosides occurs early in the phage lifecycle, between genome injection and replication. Yet, there could be significant differences depending on the bacterial host considered, injection being a step potentially also

impaired in *Streptomyces*. Remarkably, inhibition of phage infection was achieved not only with pure aminoglycosides, but also with supernatants from natural aminoglycoside producers. These results suggest that the antiviral action of aminoglycosides could be relevant in a natural setting, conferring protection against phages at the community level. We elaborated on chemical defense against phages in a broader sense in a review. In this piece, we aimed at integrating the wealth of research done in this field with exciting directions for the future of this research area.

Chemical defense against phages mediated by small molecules is only one facet of the broader arsenal deployed by bacteria against their viral predators. Integration of chemical defense with other, protein-based defense systems remains a major blind spot in our current knowledge and clearly deserves some consideration in the future. Visualization by microscopy of the activation of different defense systems at the cellular level could for instance shed light on the spatio-temporal coordination of antiviral responses.

Understanding better the use of small molecules in antiphage defense is a fascinating prospect from a fundamental point of view but also has potential therapeutical implications. In fact, the two main antiphage molecule classes known today—anthracyclines and aminoglycosides—are already used in the clinic, as anticancer drugs and antibiotics, respectively. Discovering novel antiphage molecules and deciphering their mechanism of action could provide us with innovative means to interfere with biological processes of interest. The most obvious field of application concerns treatments against viral eukaryotic infections. Unexpectedly strong conservation between prokaryotic and eukaryotic antiviral immunity is a concept gaining more and more traction (Bernheim et al., 2021; Morehouse et al., 2020; Ofir et al., 2021). Therefore, it would stand to reason that some metabolites targeting core features of the phage infection cycle could interfere with eukaryotic viruses too, as this was already shown with the modified ribonucleotides produced by viperins (Bernheim et al., 2021).

In this thesis, we focused on the genus *Streptomyces*, yet there are many more interesting candidate clades worthy of investigation. The chemical potential of phyla like planctomycetes or myxobacteria has been recognized comparatively much later and the knowledge of the ecological roles played by secondary metabolite produced by these bacteria is scarce. We envision that the repertoire of antiphage metabolites will be further expanded in the future and look forward to the progress which will be made in this direction.

2.4 References

Achmatowicz, O., Alloatti, D., Fotso, S., Fujioka, H., Giannini, G., Gryniewicz, G., Kita, Y., Laatsch, H., Mäntsälä, P., Metsä-Ketelä, M., et al. (2008). *Anthracycline Chemistry and Biology I* (Berlin, Heidelberg: Springer Berlin Heidelberg).

Ackermann, H.-W. (2009). Phage Classification and Characterization. In *Bacteriophages*, (Humana Press), pp. 127–140.

Alexander, R.R., and McCoy, E. (1956). Characterization of *Streptomyces griseus* bacteriophages. *Journal of Bacteriology* 72, 378–386.

Alseth, E.O., Pursey, E., Luján, A.M., McLeod, I., Rollie, C., and Westra, E.R. (2019). Bacterial biodiversity drives the evolution of CRISPR-based phage resistance. *Nature* 574, 549–552.

Ameruoso, A., Kcam, M.C.V., Cohen, K.P., and Chappell, J. (2021). Activating natural product synthesis using CRISPR interference and activation systems in *Streptomyces*.

Anderson, A.S., and Wellington, E. (2001). The taxonomy of *Streptomyces* and related genera. *INTERNATIONAL JOURNAL OF SYSTEMATIC AND EVOLUTIONARY MICROBIOLOGY* 51, 797–814.

Anne, J., Wohlleben, W., Burkardt, H.J., Springer, R., and Pohler, A. (1984). Morphological and Molecular Characterization of Several Actinophages Isolated from Soil Which Lyse *Streptomyces cattleya* or *S. venezuelae*. *Microbiology* 130, 2639–2649.

Asheshov, I.N., Strelitz, F., Hall, E., and Flon, H. (1954). A Survey of Actinomycetes for Antiphage Activity. *Antibiotics & Chemotherapy* 4, 380–394.

Barona-Gómez, F., Wong, U., Giannakopoulos, A.E., Derrick, P.J., and Challis, G.L. (2004). Identification of a Cluster of Genes that Directs Desferrioxamine Biosynthesis in *Streptomyces coelicolor* M145. *J. Am. Chem. Soc.* 126, 16282–16283.

Barrangou, R., Fremaux, C., Deveau, H., Richards, M., Boyaval, P., Moineau, S., Romero, D.A., and Horvath, P. (2007). CRISPR Provides Acquired Resistance Against Viruses in Prokaryotes. *Science* 315, 1709–1712.

Becher, P.G., Verschut, V., Bibb, M.J., Bush, M.J., Molnár, B.P., Barane, E., Al-Bassam, M.M., Chandra, G., Song, L., Challis, G.L., et al. (2020). Developmentally regulated volatiles geosmin and 2-methylisoborneol attract a soil arthropod to *Streptomyces* bacteria promoting spore dispersal. *Nat Microbiol* 5, 821–829.

Bednarz, B., Kotowska, M., and Pawlik, K.J. (2019). Multi-level regulation of coelimycin synthesis in *Streptomyces coelicolor* A3(2). *Appl Microbiol Biotechnol* 103, 6423–6434.

Behie, S.W., Bonet, B., Zacharia, V.M., McClung, D.J., and Traxler, M.F. (2017). Molecules to Ecosystems: Actinomycete Natural Products In situ. *Front. Microbiol.* 7.

Bentley, S.D., Chater, K.F., Cerdeño-Tárraga, A.-M., Challis, G.L., Thomson, N.R., James, K.D., Harris, D.E., Quail, M.A., Kieser, H., Harper, D., et al. (2002). Complete genome sequence of the model actinomycete *Streptomyces coelicolor* A3(2). *Nature* 417, 141–147.

Bernheim, A., and Sorek, R. (2020). The pan-immune system of bacteria: antiviral defence as a community resource. *Nature Reviews Microbiology* 18, 113–119.

- Bernheim, A., Millman, A., Ofir, G., Meitav, G., Avraham, C., Shomar, H., Rosenberg, M.M., Tal, N., Melamed, S., Amitai, G., et al. (2021). Prokaryotic viperins produce diverse antiviral molecules. *Nature* *589*, 120–124.
- Bibb, M.J. (2013). Understanding and manipulating antibiotic production in actinomycetes. *Biochem Soc Trans* *41*, 1355–1364.
- Bibb, M.J., Chater, K.F., and Hopwood, D.A. (1983). CHAPTER 4 - Developments in *Streptomyces* Cloning. In *Experimental Manipulation of Gene Expression*, M. Inouye, ed. (Academic Press), pp. 53–82.
- Bondy-Denomy, J., and Davidson, A.R. (2014). When a virus is not a parasite: the beneficial effects of prophages on bacterial fitness. *Journal of Microbiology* *52*, 235–242.
- Brock, T.D. (1962). The inhibition of an RNA bacteriophage by streptomycin, using host bacteria resistant to the antibiotic. *Biochem. Biophys. Res. Commun.* *9*, 184–187.
- Brock, T.D., and Wooley, S.O. (1963). Streptomycin as an Antiviral Agent: Mode of Action. *Science* *141*, 1065–1067.
- Brock, T.D., Mosser, J., and Peacher, B. (1963). The inhibition by streptomycin of certain *streptococcus* bacteriophages, using host bacteria resistant to the antibiotic. *J. Gen. Microbiol.* *33*, 9–22.
- Brock, T.D., Johnson, R.M., and DeVille, W.B. (1965). Physical and chemical properties of a bacterial virus as related to its inhibition by streptomycin. *Virology* *25*, 439–453.
- Bruni, G.N., and Kralj, J.M. (2020). Membrane voltage dysregulation driven by metabolic dysfunction underlies bactericidal activity of aminoglycosides. *ELife* *9*, e58706.
- Burke, J., Schneider, D., and Westpheling, J. (2001). Generalized transduction in *Streptomyces coelicolor*. *PNAS* *98*, 6289–6294.
- Busscher, G.F., Rutjes, F.P.J.T., and van Delft, F.L. (2005). 2-Deoxystreptamine: Central Scaffold of Aminoglycoside Antibiotics. *Chem. Rev.* *105*, 775–792.
- Bystrykh, L.V., Fernández-Moreno, M.A., Herrema, J.K., Malpartida, F., Hopwood, D.A., and Dijkhuizen, L. (1996). Production of actinorhodin-related “blue pigments” by *Streptomyces coelicolor* A3(2). *J. Bacteriol.* *178*, 2238–2244.
- Casjens, S. (2003). Prophages and bacterial genomics: what have we learned so far? *Mol. Microbiol.* *49*, 277–300.
- Casjens, S.R., and Gilcrease, E.B. (2009). Determining DNA Packaging Strategy by Analysis of the Termini of the Chromosomes in Tailed-Bacteriophage Virions. *Methods Mol Biol* *502*, 91–111.
- Chater, K. (1999). David Hopwood and the emergence of *Streptomyces* genetics. *Int. Microbiol.* *2*, 61–68.
- Clokier, M.R., Millard, A.D., Letarov, A.V., and Heaphy, S. (2011). Phages in nature. *Bacteriophage* *1*, 31–45.

Cohen, D., Melamed, S., Millman, A., Shulman, G., Oppenheimer-Shaanan, Y., Kacen, A., Doron, S., Amitai, G., and Sorek, R. (2019). Cyclic GMP–AMP signalling protects bacteria against viral infection. *Nature* *574*, 691–695.

Correa, A., Howard-Varona, C., Coy, S., Buchan, A., Sullivan, M., and Weitz, J. (2021). Revisiting the rules of life for viruses of microorganisms. *Nature Reviews Microbiology* *19*.

Craney, A., Ahmed, S., and Nodwell, J. (2013). Towards a new science of secondary metabolism. *J Antibiot* *66*, 387–400.

De Smet, J., Hendrix, H., Blasdel, B.G., Danis-Wlodarczyk, K., and Lavigne, R. (2017). *Pseudomonas* predators: understanding and exploiting phage–host interactions. *Nature Reviews Microbiology* *15*, 517–530.

D’Hérelle, F. (1917). Sur un microbe invisible antagoniste des bacilles dysentériques. *C.R. Acad. Sci. Paris* *165*, 373–375.

Donadio, S., Paladino, R., Costanzi, I., Sparapani, P., Schreil, W., and Iaccarino, M. (1986). Characterization of bacteriophages infecting *Streptomyces erythreus* and properties of phage-resistant mutants. *J Bacteriol* *166*, 1055–1060.

Doron, S., Melamed, S., Ofir, G., Leavitt, A., Lopatina, A., Keren, M., Amitai, G., and Sorek, R. (2018). Systematic discovery of antiphage defense systems in the microbial pangenome. *Science* *359*.

Dowding, J.E. (1973). Characterization of a Bacteriophage Virulent for *Streptomyces coelicolor* A3 (2) | Microbiology Society. *Journal of General Microbiology* *76*, 163–176.

Elliot, M.A., Buttner, M.J., and Nodwell, J.R. (2008). 24 Multicellular Development in *Streptomyces*. *Myxobacteria* 419–438.

Fischer, G., Decaris, B., and Leblond, P. (1997). Occurrence of deletions, associated with genetic instability in *Streptomyces ambofaciens*, is independent of the linearity of the chromosomal DNA. *J Bacteriol* *179*, 4553–4558.

Flemming, H.-C., and Wingender, J. (2010). The biofilm matrix. *Nat Rev Microbiol* *8*, 623–633.

Gao, L., Altae-Tran, H., Böhning, F., Makarova, K.S., Segel, M., Schmid-Burgk, J.L., Koob, J., Wolf, Y.I., Koonin, E.V., and Zhang, F. (2020). Diverse enzymatic activities mediate antiviral immunity in prokaryotes. *Science* *369*, 1077–1084.

Garneau-Tsodikova, S., and Labby, K.J. (2016). Mechanisms of Resistance to Aminoglycoside Antibiotics: Overview and Perspectives. *Medchemcomm* *7*, 11–27.

Gehrke, E.J., Zhang, X., Pimentel-Elardo, S.M., Johnson, A.R., Rees, C.A., Jones, S.E., Hindra, Gehrke, S.S., Turvey, S., Boursalie, S., et al. (2019). Silencing cryptic specialized metabolism in *Streptomyces* by the nucleoid-associated protein Lsr2. *ELife* *8*, e47691.

Gilmour, C.M., Noller, E.C., and Watkins, B. (1959). Studies on *Streptomyces* phage: I. Growth Characteristics of the *Streptomyces griseus* Host-Phage System. *Journal of Bacteriology* *78*, 186–192.

Gomez-Escribano, J.P., and Bibb, M.J. (2011). Engineering *Streptomyces coelicolor* for heterologous expression of secondary metabolite gene clusters. *Microb Biotechnol* *4*, 207–215.

Scientific context and key results of this thesis

Gordon, B.R.G., Li, Y., Wang, L., Sintsova, A., Bakel, H. van, Tian, S., Navarre, W.W., Xia, B., and Liu, J. (2010). Lsr2 is a nucleoid-associated protein that targets AT-rich sequences and virulence genes in *Mycobacterium tuberculosis*. *PNAS* *107*, 5154–5159.

Hampton, H.G., Watson, B.N.J., and Fineran, P.C. (2020). The arms race between bacteria and their phage foes. *Nature* *577*, 327–336.

Hancock, R.E., Raffle, V.J., and Nicas, T.I. (1981). Involvement of the outer membrane in gentamicin and streptomycin uptake and killing in *Pseudomonas aeruginosa*. *Antimicrob Agents Chemother* *19*, 777–785.

Hardy, A., Sharma, V., Kever, L., and Frunzke, J. (2020). Genome Sequence and Characterization of Five Bacteriophages Infecting *Streptomyces coelicolor* and *Streptomyces venezuelae*: Alderaan, Coruscant, Dagobah, Endor1 and Endor2. *Viruses* *12*, 1065.

Harms, A., Brodersen, D.E., Mitarai, N., and Gerdes, K. (2018). Toxins, Targets, and Triggers: An Overview of Toxin-Antitoxin Biology. *Molecular Cell* *70*, 768–784.

Hatfull, G.F. (2015). Dark Matter of the Biosphere: the Amazing World of Bacteriophage Diversity. *Journal of Virology*.

Hendrix, R.W. (2002). Bacteriophages: evolution of the majority. *Theor Popul Biol* *61*, 471–480.

Hendrix, R.W., Smith, M.C.M., Burns, R.N., Ford, M.E., and Hatfull, G.F. (1999). Evolutionary relationships among diverse bacteriophages and prophages: All the world's a phage. *PNAS* *96*, 2192–2197.

Hille, F., Richter, H., Wong, S.P., Bratovič, M., Ressel, S., and Charpentier, E. (2018). The Biology of CRISPR-Cas: Backward and Forward. *Cell* *172*, 1239–1259.

Hopwood, D.A. (2006). Soil To Genomics: The *Streptomyces* Chromosome. *Annual Review of Genetics* *40*, 1–23.

Hopwood, D.A. (2007). *Streptomyces* in Nature and Medicine: The Antibiotic Makers (Oxford, New York: Oxford University Press).

Hopwood, D.A., Chater, K.F., Dowding, J.E., and Vivian, A. (1973). Advances in *Streptomyces coelicolor* genetics. *BACTERIOL. REV.* *37*, 35.

Hoskisson, P.A., and van Wezel, G.P. (2019). *Streptomyces coelicolor*. *Trends Microbiol* *27*, 468–469.

Høyland-Krogsho, N.M., Maerkedahl, R.B., and Svenningsen, S.L. (2013). A quorum-sensing-induced bacteriophage defense mechanism. *MBio* *4*, e00362-00312.

Høyland-Krogsho, N.M., Paczkowski, J., Mukherjee, S., Broniewski, J., Westra, E., Bondy-Denomy, J., and Bassler, B.L. (2017). Quorum sensing controls the *Pseudomonas aeruginosa* CRISPR-Cas adaptive immune system. *Proc Natl Acad Sci U S A* *114*, 131–135.

Hughes, L.E., Shaffer, C.D., Ware, V.C., Aguayo, I., Aziz, R.M., Bhuiyan, S., Bindert, I.S., Calovich-Benne, C.K., Chapman, J., Donegan-Quick, R., et al. (2018). Eight Genome Sequences of Cluster BE1 Phages That Infect *Streptomyces* Species. *Genome Announc* *6*.

- Jiang, Z., Wei, J., Liang, Y., Peng, N., and Li, Y. (2020). Aminoglycoside Antibiotics Inhibit Mycobacteriophage Infection. *Antibiotics* 9, 714.
- Jones, S.E., and Elliot, M.A. (2017). *Streptomyces* Exploration: Competition, Volatile Communication and New Bacterial Behaviours. *Trends in Microbiology* 25, 522–531.
- Jones, S.E., Ho, L., Rees, C.A., Hill, J.E., Nodwell, J.R., and Elliot, M.A. (2017). *Streptomyces* exploration is triggered by fungal interactions and volatile signals. *ELife* 6, e21738.
- Jordan, T.C., Burnett, S.H., Carson, S., Caruso, S.M., Clase, K., DeJong, R.J., Dennehy, J.J., Denver, D.R., Dunbar, D., Elgin, S.C.R., et al. (2014). A Broadly Implementable Research Course in Phage Discovery and Genomics for First-Year Undergraduate Students. *MBio* 5.
- Keen, E.C. (2015). A century of phage research: Bacteriophages and the shaping of modern biology. *Bioessays* 37, 6–9.
- Keiser, T., Bibb, M.J., Buttner, M.J., Chater, K.F., and Hopwood, D.A. (2000). *Practical Streptomyces Genetics* (Norwich: The John Innes Foundation).
- Kever, L., Hardy, A., Luthe, T., Hünnefeld, M., Gätgens, C., Milke, L., Wiechert, J., Wittmann, J., Moraru, C., Marienhagen, J., et al. (2021). Aminoglycoside antibiotics inhibit phage infection by blocking an early step of the phage infection cycle.
- Kharel, M.K., Basnet, D.B., Lee, H.C., Liou, K., Woo, J.S., Kim, B.-G., and Sohng, J.K. (2004). Isolation and characterization of the tobramycin biosynthetic gene cluster from *Streptomyces tenebrarius*1. *FEMS Microbiology Letters* 230, 185–190.
- Kim, J.-N., Kim, Y., Jeong, Y., Roe, J.-H., and Cho, B.-G.K. and B.-K. (2015). Comparative Genomics Reveals the Core and Accessory Genomes of *Streptomyces* Species. 25, 1599–1605.
- Krause, K.M., Serio, A.W., Kane, T.R., and Connolly, L.E. (2016). Aminoglycosides: An Overview. *Cold Spring Harb Perspect Med* 6.
- Kresge, N., Simoni, R.D., and Hill, R. (2004). Selman Waksman: the Father of Antibiotics.
- Krishnamurthy, S.R., and Wang, D. (2017). Origins and challenges of viral dark matter. *Virus Research* 239, 136–142.
- Kronheim, S., Daniel-Ivad, M., Duan, Z., Hwang, S., Wong, A.I., Mantel, I., Nodwell, J.R., and Maxwell, K.L. (2018). A chemical defence against phage infection. *Nature* 564, 283.
- Labrie, S.J., Samson, J.E., and Moineau, S. (2010). Bacteriophage resistance mechanisms. *Nat Rev Microbiol* 8, 317–327.
- Lee, N., Hwang, S., Kim, J., Cho, S., Palsson, B., and Cho, B.-K. (2020a). Mini review: Genome mining approaches for the identification of secondary metabolite biosynthetic gene clusters in *Streptomyces*. *Computational and Structural Biotechnology Journal* 18, 1548–1556.
- Lee, N., Kim, W., Chung, J., Lee, Y., Cho, S., Jang, K.-S., Kim, S.C., Palsson, B., and Cho, B.-K. (2020b). Iron competition triggers antibiotic biosynthesis in *Streptomyces coelicolor* during coculture with *Myxococcus xanthus*. *The ISME Journal*.

- LeRoux, M., Srikant, S., Littlehale, M.H., Teodoro, G., Doron, S., Badiie, M., Leung, A.K.L., Sorek, R., and Laub, M.T. (2021). The DarTG toxin-antitoxin system provides phage defense by ADP-ribosylating viral DNA.
- Loenen, W.A.M., Dryden, D.T.F., Raleigh, E.A., Wilson, G.G., and Murray, N.E. (2014). Highlights of the DNA cutters: a short history of the restriction enzymes. *Nucleic Acids Res* 42, 3–19.
- Lomovskaya, N.D., Mkrtumian, N.M., Gostimskaya, N.L., and Danilenko, V.N. (1972). Characterization of Temperate Actinophage oC31 Isolated from *Streptomyces coelicolor* A3(2). *J. VIROL.* 9, 5.
- Lomovskaya, N.D., Chater, K.F., and Mkrtumian, N.M. (1980). Genetics and molecular biology of *Streptomyces* bacteriophages. *Microbiology and Molecular Biology Reviews* 44, 206–229.
- Lopatina, A., Tal, N., and Sorek, R. (2020). Abortive Infection: Bacterial Suicide as an Antiviral Immune Strategy. *Annu. Rev. Virol.* 7, 371–384.
- Lv, M., Ji, X., Zhao, J., Li, Y., Zhang, C., Su, L., Ding, W., Deng, Z., Yu, Y., and Zhang, Q. (2016). Characterization of a C3 Deoxygenation Pathway Reveals a Key Branch Point in Aminoglycoside Biosynthesis. *J. Am. Chem. Soc.* 138, 6427–6435.
- Magalhaes, M.L.B., and Blanchard, J.S. (2005). The Kinetic Mechanism of AAC(3)-IV Aminoglycoside Acetyltransferase from *Escherichia coli*. *Biochemistry* 44, 16275–16283.
- Mak, S., and Nodwell, J.R. (2017). Actinorhodin is a redox-active antibiotic with a complex mode of action against Gram-positive cells: Molecular action of actinorhodin. *Molecular Microbiology* 106, 597–613.
- Manteca, Á., and Yagüe, P. (2019). *Streptomyces* as a Source of Antimicrobials: Novel Approaches to Activate Cryptic Secondary Metabolite Pathways (IntechOpen).
- Mäntynen, S., Laanto, E., Oksanen, H.M., Poranen, M.M., and Díaz-Muñoz, S.L. (2021). Black box of phage–bacterium interactions: exploring alternative phage infection strategies. *Open Biology* 11, 210188.
- Marsh, P., and Wellington, E.M.H. (1994). Phage-host interactions in soil. *FEMS Microbiology Ecology* 15, 99–107.
- Mast, Y., and Stegmann, E. (2019). Actinomycetes: The Antibiotics Producers. *Antibiotics* 8, 105.
- McCormick, J.R., and Flärdh, K. (2012). Signals and regulators that govern *Streptomyces* development. *FEMS Microbiol Rev* 36, 206–231.
- McDonald, B.R., and Currie, C.R. (2017). Lateral Gene Transfer Dynamics in the Ancient Bacterial Genus *Streptomyces*. *MBio*.
- Millman, A., Bernheim, A., Stokar-Avihail, A., Fedorenko, T., Voichek, M., Leavitt, A., Oppenheimer-Shaanan, Y., and Sorek, R. (2020). Bacterial Retrons Function In Anti-Phage Defense. *Cell* 183, 1551-1561.e12.
- Mingeot-Leclercq, M.-P., Glupczynski, Y., and Tulkens, P.M. (1999). Aminoglycosides: Activity and Resistance. *Antimicrob Agents Chemother* 43, 727–737.

- Minotti, G., Menna, P., Salvatorelli, E., Cairo, G., and Gianni, L. (2004). Anthracyclines: Molecular Advances and Pharmacologic Developments in Antitumor Activity and Cardiotoxicity. *Pharmacological Reviews*.
- Montaner, B., Castillo-Avila, W., Martinell, M., Ollinger, R., Aymami, J., Giralt, E., and Pérez-Tomás, R. (2005). DNA interaction and dual topoisomerase I and II inhibition properties of the anti-tumor drug prodigiosin. *Toxicol Sci* 85, 870–879.
- Morehouse, B.R., Govande, A.A., Millman, A., Keszei, A.F.A., Lowey, B., Ofir, G., Shao, S., Sorek, R., and Kranzusch, P.J. (2020). STING cyclic dinucleotide sensing originated in bacteria. *Nature* 586, 429–433.
- Mukherjee, S., and Bassler, B.L. (2019). Bacterial quorum sensing in complex and dynamically changing environments. *Nat Rev Microbiol* 17, 371–382.
- Mushegian, A.R. (2020). Are There 1031 Virus Particles on Earth, or More, or Fewer? *J Bacteriol* 202, e00052-20.
- Netzker, T., Flak, M., Krespach, M.K., Stroe, M.C., Weber, J., Schroeckh, V., and Brakhage, A.A. (2018). Microbial interactions trigger the production of antibiotics. *Curr Opin Microbiol* 45, 117–123.
- Nguyen, C.T., Dhakal, D., Pham, V.T.T., Nguyen, H.T., and Sohng, J.-K. (2020). Recent Advances in Strategies for Activation and Discovery/Characterization of Cryptic Biosynthetic Gene Clusters in *Streptomyces*. *Microorganisms* 8, 616.
- Ofir, G., and Sorek, R. (2018). Contemporary Phage Biology: From Classic Models to New Insights. *Cell* 172, 1260–1270.
- Ofir, G., Herbst, E., Baroz, M., Cohen, D., Millman, A., Doron, S., Tal, N., Malheiro, D.B.A., Malitsky, S., Amitai, G., et al. (2021). Antiviral activity of bacterial TIR domains via immune signalling molecules. *Nature* 600, 116–120.
- Oppenheim, A.B., Kobilier, O., Stavans, J., Court, D.L., and Adhya, S. (2005). Switches in bacteriophage lambda development. *Annu. Rev. Genet.* 39, 409–429.
- Parajuli, P., Adamski, M., and Verma, N.K. (2017). Bacteriophages are the major drivers of *Shigella flexneri* serotype 1c genome plasticity: a complete genome analysis. *BMC Genomics* 18, 722.
- Parma, D.H., Snyder, M., Sobolevski, S., Nawroz, M., Brody, E., and Gold, L. (1992). The Rex system of bacteriophage lambda: tolerance and altruistic cell death. *Genes Dev* 6, 497–510.
- Patterson, A.G., Jackson, S.A., Taylor, C., Evans, G.B., Salmond, G.P.C., Przybilski, R., Staals, R.H.J., and Fineran, P.C. (2016). Quorum Sensing Controls Adaptive Immunity through the Regulation of Multiple CRISPR-Cas Systems. *Mol Cell* 64, 1102–1108.
- Peng, X., Chen, B., Lim, C.C., and Sawyer, D.B. (2005). The cardiotoxicology of anthracycline chemotherapeutics: translating molecular mechanism into preventative medicine. *Mol Interv* 5, 163–171.
- Pérez, J., Muñoz-Dorado, J., Braña, A.F., Shimkets, L.J., Sevillano, L., and Santamaría, R.I. (2011). *Mycococcus xanthus* induces actinorhodin overproduction and aerial mycelium formation by *Streptomyces coelicolor*. *Microbial Biotechnology* 4, 175–183.

Scientific context and key results of this thesis

Pfeifer, E., Hünnefeld, M., Popa, O., Polen, T., Kohlheyer, D., Baumgart, M., and Frunzke, J. (2016). Silencing of cryptic prophages in *Corynebacterium glutamicum*. *Nucleic Acids Res* 44, 10117–10131.

Pfeifer, E., Hünnefeld, M., Popa, O., and Frunzke, J. (2019). Impact of Xenogeneic Silencing on Phage–Host Interactions. *Journal of Molecular Biology*.

Piret, J.M., and Chater, K.F. (1985). Phage-mediated cloning of *bldA*, a region involved in *Streptomyces coelicolor* morphological development, and its analysis by genetic complementation. *Journal of Bacteriology*.

Pope, W.H., Jacobs-Sera, D., Russell, D.A., Rubin, D.H.F., Kajee, A., Msibi, Z.N.P., Larsen, M.H., Jacobs Jr, W.R., Lawrence, J.G., Hendrix, R.W., et al. (2014). Genomics and Proteomics of Mycobacteriophage Patience, an Accidental Tourist in the *Mycobacterium* Neighborhood. *MBio*.

Rosner, A., and Gustin, R. (1980). Adsorption of actinophage Pal 6 to developing mycelium of *Streptomyces*.

Rostøl, J.T., and Marraffini, L. (2019). (Ph)ighting Phages: How Bacteria Resist Their Parasites. *Cell Host & Microbe* 25, 184–194.

Salmond, G.P.C., and Fineran, P.C. (2015). A century of the phage: past, present and future. *Nature Reviews Microbiology* 13, 777.

Schatz, A., and Jones, D. (1947). The Production of Antiphage Agents by Actinomycetes. *Bulletin of the Torrey Botanical Club* 74, 9.

Schupp, T., Toupet, C., and Divers, M. (1988). Cloning and expression of two genes of *Streptomyces pilosus* involved in the biosynthesis of the siderophore desferrioxamine B. *Gene* 64, 179–188.

Serio, A.W., Keepers, T., Andrews, L., and Krause, K.M. (2018). Aminoglycoside Revival: Review of a Historically Important Class of Antimicrobials Undergoing Rejuvenation. *EcoSal Plus* 8.

Shah, M., Taylor, V.L., Bona, D., Tsao, Y., Stanley, S.Y., Pimentel-Elardo, S.M., McCallum, M., Bondy-Denomy, J., Howell, P.L., Nodwell, J.R., et al. (2021). A phage-encoded anti-activator inhibits quorum sensing in *Pseudomonas aeruginosa*. *Mol Cell* 81, 571-583.e6.

Sharma, V., Hardy, A., Luthe, T., and Frunzke, J. (2021). Phylogenetic Distribution of WhiB- and Lsr2-Type Regulators in Actinobacteriophage Genomes. *Microbiol Spectr* 9, e0072721.

Singh, K., Milstein, J.N., and Navarre, W.W. (2016). Xenogeneic Silencing and Its Impact on Bacterial Genomes. *Annu. Rev. Microbiol.* 70, 199–213.

Smith, M.C.M., Burns, R.N., Wilson, S.E., and Gregory, M.A. (1999). The complete genome sequence of the *Streptomyces* temperate phage ϕ C31: evolutionary relationships to other viruses. *Nucleic Acids Res* 27, 2145–2155.

Smith, M.C.M., Hendrix, R.W., Dedrick, R., Mitchell, K., Ko, C.-C., Russell, D., Bell, E., Gregory, M., Bibb, M.J., Pethick, F., et al. (2013). Evolutionary Relationships among Actinophages and a Putative Adaptation for Growth in *Streptomyces* spp. *Journal of Bacteriology* 195, 4924–4935.

Sorek, R., Lawrence, C.M., and Wiedenheft, B. (2013). CRISPR-Mediated Adaptive Immune Systems in Bacteria and Archaea. *Annu. Rev. Biochem.* 82, 237–266.

- Tal, N., Morehouse, B.R., Millman, A., Stokar-Avihail, A., Avraham, C., Fedorenko, T., Yirmiya, E., Herbst, E., Brandis, A., Mehlman, T., et al. (2021). Cyclic CMP and cyclic UMP mediate bacterial immunity against phages. *Cell* *184*, 5728-5739.e16.
- Tamura, T., Ishida, Y., Otoguro, M., Hatano, K., and Suzuki, K. (2008). Classification of '*Streptomyces tenebrarius*' Higgins and Kastner as *Streptoalloteichus tenebrarius* nom. rev., comb. nov., and emended description of the genus *Streptoalloteichus*. *International Journal of Systematic and Evolutionary Microbiology* *58*, 688–691.
- Tenconi, E., Traxler, M.F., Hoebreck, C., van Wezel, G.P., and Rigali, S. (2018). Production of Prodiginines Is Part of a Programmed Cell Death Process in *Streptomyces coelicolor*. *Front. Microbiol.* *9*.
- Tenconi, E., Traxler, M., Tellatin, D., van Wezel, G.P., and Rigali, S. (2020). Prodiginines Postpone the Onset of Sporulation in *Streptomyces coelicolor*. *Antibiotics* *9*, 847.
- Thompson, C.J., Fink, D., and Nguyen, L.D. (2002). Principles of microbial alchemy: insights from the *Streptomyces coelicolor* genome sequence. *Genome Biology* *3*, reviews1020.1.
- Tolstoy, I., Kropinski, A.M., and Brister, J.R. (2018). Bacteriophage Taxonomy: An Evolving Discipline. In *Bacteriophage Therapy: From Lab to Clinical Practice*, J. Azeredo, and S. Sillankorva, eds. (New York, NY: Springer), pp. 57–71.
- Turner, D., Kropinski, A.M., and Adriaenssens, E.M. (2021). A Roadmap for Genome-Based Phage Taxonomy. *Viruses* *13*, 506.
- Twort, F.W. (1915). An investigation on the nature of ultra-microscopic viruses. *Lancet* *186*, 1241–1243.
- Tyc, Olaf, Song, C., Dickschat, J.S., Vos, M., and Garbeva, P. (2017). The Ecological Role of Volatile and Soluble Secondary Metabolites Produced by Soil Bacteria. *Trends in Microbiology* *25*, 280–292.
- Urem, M., Rossum, T. van, Bucca, G., Moolenaar, G.F., Laing, E., Świątek-Połatyńska, M.A., Willemse, J., Tenconi, E., Rigali, S., Goosen, N., et al. (2016). OsdR of *Streptomyces coelicolor* and the Dormancy Regulator DevR of *Mycobacterium tuberculosis* Control Overlapping Regulons. *MSystems*.
- Wagner, P.L., and Waldor, M.K. (2002). Bacteriophage Control of Bacterial Virulence. *Infection and Immunity* *70*, 3985–3993.
- Waldor, M.K., and Mekalanos, J.J. (1996). Lysogenic conversion by a filamentous phage encoding cholera toxin. *Science* *272*, 1910–1914.
- Wang, I.-N., Dykhuizen, D.E., and Slobodkin, L.B. (1996). The evolution of phage lysis timing. *Evol Ecol* *10*, 545–558.
- Weiss, R.B. (1992). The anthracyclines: will we ever find a better doxorubicin? *Semin Oncol* *19*, 670–686.
- Williams, D.H., Stone, M.J., Hauck, P.R., and Rahman, S.K. (1989). Why are secondary metabolites (natural products) biosynthesized? *J Nat Prod* *52*, 1189–1208.

- Williamson, N.R., Fineran, P.C., Gristwood, T., Chawrai, S.R., Leeper, F.J., and Salmond, G.P. (2007). Anticancer and immunosuppressive properties of bacterial prodiginines. *Future Microbiology* 2, 605–618.
- Wommack, K.E., and Colwell, R.R. (2000). Virioplankton: Viruses in Aquatic Ecosystems. *Microbiol Mol Biol Rev* 64, 69–114.
- Wong, S., Alattas, H., and Slavcev, R.A. (2021). A snapshot of the λ T4rII exclusion (Rex) phenotype in *Escherichia coli*. *Curr Genet* 67, 739–745.
- Woodruff, H.B. (2014). Selman A. Waksman, winner of the 1952 Nobel Prize for physiology or medicine. *Appl Environ Microbiol* 80, 2–8.
- Wyka, S.A., Mondo, S.J., Liu, M., Nalam, V., and Broders, K.D. (2020). A large accessory genome, high recombination rates, and selection of secondary metabolite genes help maintain global distribution and broad host range of the fungal plant pathogen *Claviceps purpurea*.
- Yang, L., Liu, Y., Wu, H., Høiby, N., Molin, S., and Song, Z. (2011). Current understanding of multi-species biofilms. *Int J Oral Sci* 3, 74–81.
- Yee, T., Furuichi, T., Inouye, S., and Inouye, M. (1984). Multicopy single-stranded DNA isolated from a gram-negative bacterium, *Myxococcus xanthus*. *Cell* 38, 203–209.
- Zacharia, V.M., Ra, Y., Sue, C., Alcalá, E., Reaso, J.N., Ruzin, S.E., and Traxler, M.F. (2021). Genetic Network Architecture and Environmental Cues Drive Spatial Organization of Phenotypic Division of Labor in *Streptomyces coelicolor*. *MBio* 12, e00794-21, /mbio/12/3/mBio.00794-21.atom.
- Zhang, Q., Chi, H.-T., Wu, L., Deng, Z., and Yu, Y. (2021). Two Cryptic Self-Resistance Mechanisms in *Streptomyces tenebrarius* Reveal Insights into the Biosynthesis of Apramycin. *Angewandte Chemie International Edition* 60, 8990–8996.
- Zhang, Y., Wang, J., Yajun, C., Zhou, M., Wang, W., Geng, M., Xu, D., and Xu, Z. (2020a). Comparative Genomics Uncovers the Genetic Diversity and Synthetic Biology of Secondary Metabolite Production of *Trametes*. *Mycobiology* 48, 104–114.
- Zhang, Z., Du, C., Barys, F. de, Liem, M., Liakopoulos, A., Wezel, G.P. van, Choi, Y.H., Claessen, D., and Rozen, D.E. (2020b). Antibiotic production in *Streptomyces* is organized by a division of labor through terminal genomic differentiation. *Science Advances* 6, eaay5781.

3 Publications and manuscripts

The “Contributor Roles Taxonomy (CRediT)” is a description of the respective contributions of authors of scientific publications (McNutt et al., 2018). The following table, which was extracted from the publication of McNutt and colleagues, was used to describe the role of the authors of the manuscripts gathered in this dissertation:

#	ROLE	DEFINITION
1	Conceptualization	Ideas; formulation or evolution of overarching research goals and aims.
2	Data curation	Management activities to annotate (produce metadata), scrub data and maintain research data (including software code, where it is necessary for interpreting the data itself) for initial use and later re-use.
3	Formal analysis	Application of statistical, mathematical, computational, or other formal techniques to analyse or synthesize study data.
4	Funding acquisition	Acquisition of the financial support for the project leading to this publication.
5	Investigation	Conducting a research and investigation process, specifically performing the experiments, or data/evidence collection.
6	Methodology	Development or design of methodology; creation of models.
7	Project administration	Management and coordination responsibility for the research activity planning and execution.
8	Resources	Provision of study materials, reagents, materials, patients, laboratory samples, animals, instrumentation, computing resources, or other analysis tools.
9	Software	Programming, software development; designing computer programs; implementation of the computer code and supporting algorithms; testing of existing code components.
10	Supervision	Oversight and leadership responsibility for the research activity planning and execution, including mentorship external to the core team.
11	Validation	Verification, whether as a part of the activity or separate, of the overall replication/reproducibility of results/experiments and other research outputs.
12	Visualization	Preparation, creation and/or presentation of the published work, specifically visualization/data presentation.
13	Writing – original draft	Preparation, creation and/or presentation of the published work, specifically writing the initial draft (including substantive translation).
14	Writing – review & editing	Preparation, creation and/or presentation of the published work by those from the original research group, specifically critical review, commentary or revision – including pre- or post-publication stages.

3.1 Genome Sequence and Characterization of Five Bacteriophages Infecting *Streptomyces coelicolor* and *Streptomyces venezuelae*: Alderaan, Coruscant, Dagobah, Endor1 and Endor2

5 **Hardy A.**, Sharma V., Kever L., and Frunzke J.

Published in *Viruses*, 2020

CONTRIBUTOR ROLE	CONTRIBUTOR
Conceptualization	AH (50%), JF (30%), VS (10%), LK (10%)
Data curation	VS (55%), AH (30%), LK (10%), JF (5%)
Formal analysis	VS (80%), AH (15%), LK (5%)
Funding acquisition	JF (100%)
Investigation	AH (85%), LK (10%), VS (5%)
Methodology	AH (55%), VK (25%), JF (10%), LK (10%)
Project administration	JF (60%), AH (40%)
Resources	-
Software	VS (95%), AH (5%)
Supervision	JF (60%), AH (40%)
Validation	AH (35%), LK (35%), VS (30%)
Visualization	AH (55%), VS (40%), LK (5%)
Writing – original draft	AH (70%), VS (15%), JF (10%), LK (5%)
Writing – review & editing	AH (40%), JF (40%), LK (10%), VS (10%)

10 **Overall contribution AH: 60%**



Article

Genome Sequence and Characterization of Five Bacteriophages Infecting *Streptomyces coelicolor* and *Streptomyces venezuelae*: Alderaan, Coruscant, Dagobah, Endor1 and Endor2

Aël Hardy , Vikas Sharma, Larissa Kever and Julia Frunzke * 

Institute of Bio- and Geosciences, IBG-1: Biotechnology, Forschungszentrum Jülich, 52425 Jülich, Germany; a.hardy@fz-juelich.de (A.H.); v.sharma@fz-juelich.de (V.S.); l.kever@fz-juelich.de (L.K.)

* Correspondence: j.frunzke@fz-juelich.de; Tel.: +49-2461-615430

Received: 17 August 2020; Accepted: 21 September 2020; Published: 23 September 2020



Abstract: *Streptomyces* are well-known antibiotic producers, also characterized by a complex morphological differentiation. *Streptomyces*, like all bacteria, are confronted with the constant threat of phage predation, which in turn shapes bacterial evolution. However, despite significant sequencing efforts recently, relatively few phages infecting *Streptomyces* have been characterized compared to other genera. Here, we present the isolation and characterization of five novel *Streptomyces* phages. All five phages belong to the *Siphoviridae* family, based on their morphology as determined by transmission electron microscopy. Genome sequencing and life style predictions suggested that four of them were temperate phages, while one had a lytic lifestyle. Moreover, one of the newly sequenced phages shows very little homology to already described phages, highlighting the still largely untapped viral diversity. Altogether, this study expands the number of characterized phages of *Streptomyces* and sheds light on phage evolution and phage-host dynamics in *Streptomyces*.

Keywords: phage isolation; phage genomics; *Streptomyces*; *Siphoviridae*; actinobacteriophages; actinorhodin

1. Introduction

Streptomyces is a genus of Gram-positive bacteria belonging to the order of Actinobacteria that exhibit a high GC-content (on average about 73 mol% G + C). *Streptomyces* are prolific producers of natural products with a wide range of biological activities. This repertoire of bioactive molecules has been harnessed for medical and agricultural purposes, as for example 2/3 of known antibiotics of microbial origin are produced by *Streptomyces* [1–3].

Another distinctive feature of *Streptomyces* is their complex developmental cycle. Unlike most bacteria—that divide by binary fission, *Streptomyces* development is instead centered on the formation of spores. Germinating spores first form a network of interconnected cells, called vegetative mycelium. The vegetative mycelium later serves as a basis for the coordinated erection of an aerial mycelium. This is followed by the segmentation of these aerial filaments into spores, which can then start a new cycle [3–5].

Phages infecting *Streptomyces* were described at a quick pace in the 1970–1980s, but most of them were not sequenced later [6–8]. The phage phiC31 represents a notable exception to this trend, as it was used to develop crucial genetic tools for *Streptomyces* before being sequenced in 1999 [9–11]. Phages R4, SV1, VP5 were also the subject of numerous studies, but the latter was not sequenced [12,13].

Streptomyces peculiarities were studied in the context of phage infection. For example, adsorption to mycelium of phage Pal6 was shown to differ depending on the stage of development of

Streptomyces albus [14]. In this instance, phage adsorption was found to be maximal for germinating spores. Combined with the observation that germinating spores showed an intense average metabolic activity, this suggests that spore germination represents the most sensitive development stage for phage infection.

Conversely, the recent years have seen a sustained effort into the isolation and sequencing of *Streptomyces* phages, notably by the Science Education Alliance-Phage Hunters Advancing Genomics and Evolutionary Science (SEA-PHAGES; <https://seaphages.org/>) program in the USA [15]. However, few of these phages were extensively characterized.

Here, we report the isolation, characterization and genome analysis of five novel *Streptomyces* phages. Two of them (Alderaan and Coruscant) were isolated using *S. venezuelae*, the remaining three (Dagobah, Endor1 and Endor2) were isolated using *S. coelicolor*. Observation with transmission electron microscopy showed that all five phages belong to the *Siphoviridae* family. Lifestyle prediction with the complete nucleotide sequences revealed that four (Alderaan, Dagobah, Endor1 and Endor2) are probably temperate, while Coruscant was predicted to be a virulent phage. Alderaan, Coruscant, Endor1 and Endor2 show close relatedness to already described *Streptomyces* phages—Endor1 and Endor2 being highly homologous to each other. In contrast, Dagobah showed very little relatedness to any sequenced phage, highlighting the still massively untapped viral diversity.

2. Materials and Methods

2.1. Bacterial Strains and Growth Conditions

Streptomyces venezuelae ATCC 10712 [16] and *Streptomyces coelicolor* M600 [17] and strain M145 [18] were used as main host strains in this study. Cultures were started by inoculating spores from spore stocks stored in 20% glycerol at $-20\text{ }^{\circ}\text{C}$ [19]. *S. venezuelae* was grown in liquid Glucose Yeast Malt extract (GYM) medium, while *S. coelicolor* was grown in liquid Yeast Extract Malt Extract (YEME) medium. Unless otherwise stated, cultivation was carried out at $30\text{ }^{\circ}\text{C}$. For double agar overlays, GYM agar was used for both species, with 0.5% and 1.5% agar for the top and bottom layers, respectively.

2.2. Phage Isolation and Propagation

Phages were isolated from soil samples taken near the Forschungszentrum Jülich (Jülich, Germany). Phages contained in soil samples were resuspended by incubation in sodium chloride/magnesium sulfate (SM) buffer (10 mM Tris-HCl pH 7.3, 100 mM NaCl, 10 mM MgSO_4 , 2mM CaCl_2) for 2 h. The samples were centrifuged at $5000\times g$ for 10 min to remove solid impurities. The supernatants were filtered through a 0.22- μm pore-size membrane filter to remove bacteria. For each sample, 1 mL of filtered supernatant was mixed with 3 mL of liquid medium inoculated with 10^7 *Streptomyces* spores.

After overnight incubation, the culture supernatant was collected by centrifugation at $5000\times g$ for 10 min and filtered through a 0.22- μm pore-size membrane filter. Serial dilutions of the filtrate were then spotted on a bacterial lawn propagated by mixing 200 μL of *Streptomyces* overnight culture with 4 mL top agar, according to a modified version of the double agar overlay method [20]. Plaques were visualized after overnight incubation at $30\text{ }^{\circ}\text{C}$.

Purification of the phage samples was carried out by restreaking single plaques twice [20]. Phage amplification was achieved by mixing 100 μL of the purified phage lysate into top agar to obtain confluent lysis on the plate. After overnight incubation, 5 mL of SM buffer were used to soak the plates and resuspend phages. The resulting phage lysate was centrifuged, and the supernatant was filtered to obtain the high-titer phage solution used for downstream processes.

To assess presence of actinorhodin, the plates were inverted and exposed to ammonia fumes for 15 min by placing 5 mL of 20% ammonium hydroxide solution on the inner surface of the lid.

2.3. Electron Microscopy Observation of Phage Virions

For electron microscopy, 5 μ L of purified phage suspension were deposited on a glow-discharged formvar carbon-coated nickel grids (200 mesh; Maxtaform; Plano, Wetzlar, Germany) and stained with 0.5% (*w/v*) uranyl acetate. After air drying, the sample was observed with a TEM LEO 906 (Carl Zeiss, Oberkochen, Germany) at an acceleration voltage of 60 kV.

2.4. Phage Infection Curves

Growth experiments were performed in the BioLector[®] microcultivation system of m2p-labs (Aachen, Germany). Cultivation was performed as biological triplicates in 48-well FlowerPlates (m2plabs) at 30 °C and a shaking frequency of 1200 rpm [21]. Backscatter was measured by scattered light with an excitation wavelength of 620 nm (filter module: $\lambda_{Ex}/\lambda_{Em}$: 620 nm/620 nm, gain: 25) every 15 min. Each well contained 1 mL YEME or GYM medium and was inoculated using an overnight culture of *S. coelicolor* or *S. venezuelae*, respectively, to an initial OD₄₅₀ of 0.1. Phages were directly added to an initial titer of 10⁵, 10⁶ or 10⁷ PFU/mL, and sampling was performed at the indicated time points. Subsequently, 2 μ L of the supernatants were spotted on a lawn of *S. coelicolor* or *S. venezuelae* propagated on a double overlay of GYM agar inoculated at an initial OD₄₅₀ = 0.5.

2.5. Host Range Determination

The host range of our phages was determined for the following *Streptomyces* species: *S. rimosus* (DSM 40260), *S. scabiei* (DSM 41658), *S. griseus* (DSM 40236), *S. platensis* (DSM 40041), *S. xanthochromogenes* (DSM 40111), *S. mirabilis* (DSM 40553), *S. lividans* TK24 [22], *S. olivaceus* (DSM 41536) and *S. cyaneofuscatus* (DSM 40148). The different *Streptomyces* species were grown in GYM medium, to which glass beads were added to favor dispersed growth.

The host range was determined by spotting serial dilutions of phage solution on lawns of the different *Streptomyces* species, in duplicates. A species was considered sensitive to a given phage only if single plaques could be detected; we further indicated if the phages are able to lyse a species (Table 1).

2.6. DNA Isolation

For isolation of phage DNA, 1 μ L of 20 mg/mL RNase A and 1 U/ μ L DNase (Invitrogen, Carlsbad, CA, USA) were added to 1 mL of the filtered lysates to limit contamination by host nucleic acids. The suspension was incubated at 37 °C for 30 min. Then, EDTA, proteinase K and SDS were added to the mixture at final concentrations of 50 μ g/mL (EDTA and proteinase K) and 1% SDS (*w/v*), respectively. The digestion mixture was incubated for 1 h at 56 °C, before adding 250 μ L of phenol:chloroform:isopropanol. The content was thoroughly mixed before centrifugation at 16,000 \times g for 4 min.

The upper phase containing the DNA was carefully transferred to a clean microcentrifuge tube and 2 volumes of 100% ethanol were added as well as sodium acetate to a final concentration of 0.3 M. After centrifugation at 16,000 \times g for 10 min, the supernatant was discarded, and the pellet washed with 1 mL 70% ethanol. Finally, the dried pellet was resuspended in 30 μ L DNase-free water and stored at 4 °C until analyzed.

2.7. DNA Sequencing and Genome Assembly

The DNA library was prepared using the NEBNext Ultra II DNA Library Prep Kit for Illumina according to the manufacturer's instructions and shotgun-sequenced using the Illumina MiSeq platform with a read length of 2 \times 150 bp (Illumina). In total, 100,000 reads were subsampled for each phage sample, and de novo assembly was performed with Newbler (GS De novo assembler; 454 Life Sciences, Branford, CT, USA). Finally, contigs were manually curated with Consed version 29.0 [23].

2.8. Gene Prediction and Functional Annotation

Open reading frames (ORFs) in the phage genomes were identified with Prodigal v2.6.3 [24] and functionally annotated using an automatic pipeline using Prokka 1.11 [25]. The functional annotation was automatically improved and curated with hidden Markov models (HMMs), and Blastp [26] searches against different databases (Prokaryotic Virus Orthologous Groups (pVOGs) [27], viral proteins and Conserved Domain Database CDD [28]), with the *e*-value cutoff 10^{-10} .

The annotated genomes were deposited in GenBank under the following accession numbers: MT711975 (Alderaan), MT711976 (Coruscant), MT711977 (Dagobah), MT711978 (Endor1) and MT711979 (Endor2). The ends of the phage genomes were determined with PhageTerm [29] using default parameters. Phage lifecycle was predicted with PhageAI [30] using default parameters.

2.9. Genome Comparison and Classification

To classify the unknown phage genomes at the nucleotide level, 31 complete reference actinophage genomes belonging to different known clusters were downloaded from the Actinobacteriophage Database [31]. Pairwise average nucleotide identities (ANI) were calculated with the five unknown *Streptomyces* phages and the 31 reference genomes using the python program pyani 0.2.9 [32] with ANIb method. The output average percentage identity matrix file generated from pyani was used for clustering and displayed using the ComplexHeatmap package in R [33]. Phage genome map with functional annotation was displayed using the gggenes package in R.

2.10. Protein Domain-Based Classification

An alternative approach was used to classify newly sequenced phages based on conserved protein domains [28]. RPS-BLAST (Reverse PSI-BLAST) searches were performed with *e*-value cutoff 0.001 against the Conserved Domain Database [28] using the 2486 complete reference actinophages [31], including the newly sequenced phage genomes. Identified Pfam protein domains output files from each phage genome were merged and converted into a numerical presence-absence matrix. The hierarchical clustering dendrogram was constructed with the help of the ward.2 method using the R platform. The resulting dendrogram was visualized using ggtree [34].

3. Results

3.1. Phage Isolation and Virion Morphology

Five novel phages infecting *Streptomyces* were isolated from soil samples close to the Forschungszentrum Jülich in Germany. The phages Alderaan and Coruscant were isolated using *Streptomyces venezuelae* ATCC 10712. Alderaan formed small, transparent, and round plaques of approximately 2 mm of diameter, while the plaques formed Coruscant were very small (<1 mm) and were fully visible only after 2 days of incubation (Figure 1A).

The phages Dagobah, Endor1 and Endor2 were isolated using *Streptomyces coelicolor* M600 as a host strain. Dagobah's plaques were very small (<1 mm) and were completely formed only after 2 days of incubation. Endor1 and Endor2 formed plaques of 2 mm in diameter with a distinct turbid zone in the center. Additionally, colored halos circling the plaques appeared after 3 days of incubation (Figure 1B). These halos were mostly brownish in the case of Dagobah, and reddish for Endor1 and Endor2. Exposure to ammonia fume resulted in a pronounced blue coloration around plaques, confirming that the halos surrounding plaques contained actinorhodin (Figure S1) [35].

TEM observation of the phage particles revealed that all five phages exhibit an icosahedral capsid and a non-contractile tail (Figure 1C). Based on the morphology, the phages were classified as members of the *Siphoviridae* family.

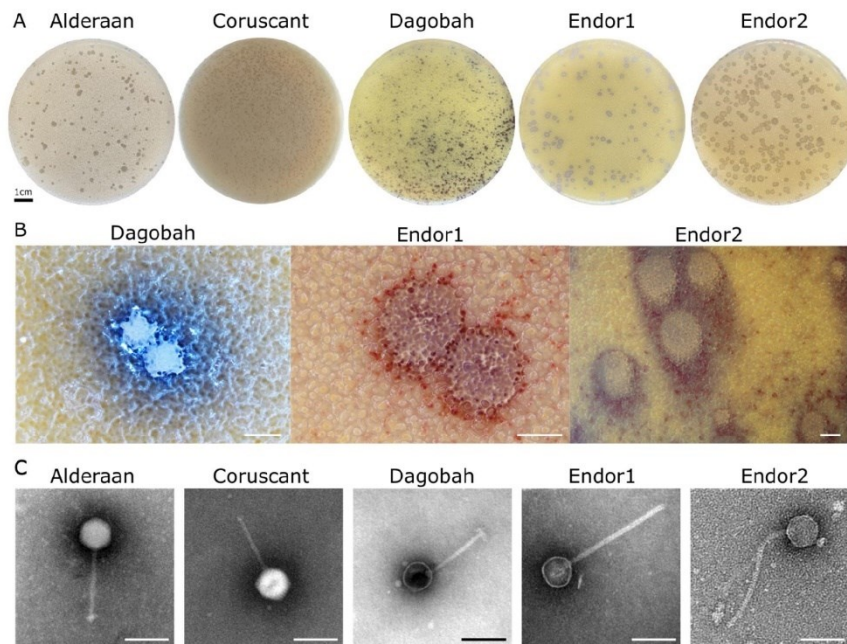


Figure 1. Morphology observation of five novel *Streptomyces* phages. (A) Plaque morphologies of the five phages. Double agar overlays were performed to infect *S. venezuelae* ATCC 10712 with the phages Alderaan and Coruscant, and *S. coelicolor* M600 with the phages Dagobah, Endor1, and Endor2. Plates were incubated overnight at 30 °C and another day (3 days in the case of Dagobah) at room temperature to reach full maturity of the bacterial lawn. (B) Close-ups of phage plaques imaged using a stereomicroscope Nikon SMZ18. *S. coelicolor* M145 was infected by phages using GYM double agar overlays. The plates were incubated at 30 °C overnight and then kept at room temperature for two (Endor1 and Endor2) or three days (Dagobah). Scale bar: 1 mm. (C) Transmission electron microscopy (TEM) of phage isolates. The phage virions were stained with uranyl acetate. Scale bar: 150 nm.

3.2. Infection Curves and Host-Range Determination

Phage infection in liquid cultures was performed to assess infection dynamics. Due to the complex developmental cycle of *Streptomyces*, standard one-step growth curves could not be performed. Instead, we cultivated *S. coelicolor* and *S. venezuelae* in microtiter plates in presence of phage challenge, and cell growth was monitored over a 24 h time period using continuous backscatter measurements. In both cases, phage titer was measured over time to estimate the production of phage progeny.

Infection of *S. venezuelae* with Alderaan showed a marked culture collapse at the highest initial phage load (10^7 PFU/mL), and a plateauing of cell biomass at a significantly reduced level for the intermediate phage challenge (10^6 PFU/mL). In contrast, addition of Coruscant causes only a mild but initial titer-dependent growth delay of the cultures (Figure 2A). For both phages, phage titers peaked at 6 h at the higher initial phage titer (10^7 PFU/mL), and at the intermediate phage challenge, phage amplification was delayed or very weak for Alderaan and Coruscant, respectively.

As for the *S. coelicolor* phages (Figure 2B), infection with Dagobah caused a mild growth delay, visible especially when 10^7 PFU/mL was initially added. In parallel, the phage titers either declined over time or grew moderately (10-fold increase between 0 and 8 h) for initially intermediate (10^6 PFU/mL) or high (10^7 PFU/mL) phage challenge, respectively. Infection with Endor1 and Endor2 showed a similar behavior and caused a stronger growth delay than Dagobah, even for the intermediate initial

phage burden (10^6 PFU/mL). The phage titers showed concordant behavior, with a strong increase in titers for both Endor1 and Endor2 until 10 h, followed by a marked decline up to 24 h.

Altogether, infection curves revealed that all five phages can successfully propagate in liquid cultures at the expense of their host. Surprisingly, the titers of all phages dropped after an initial increase, which needs further investigation.

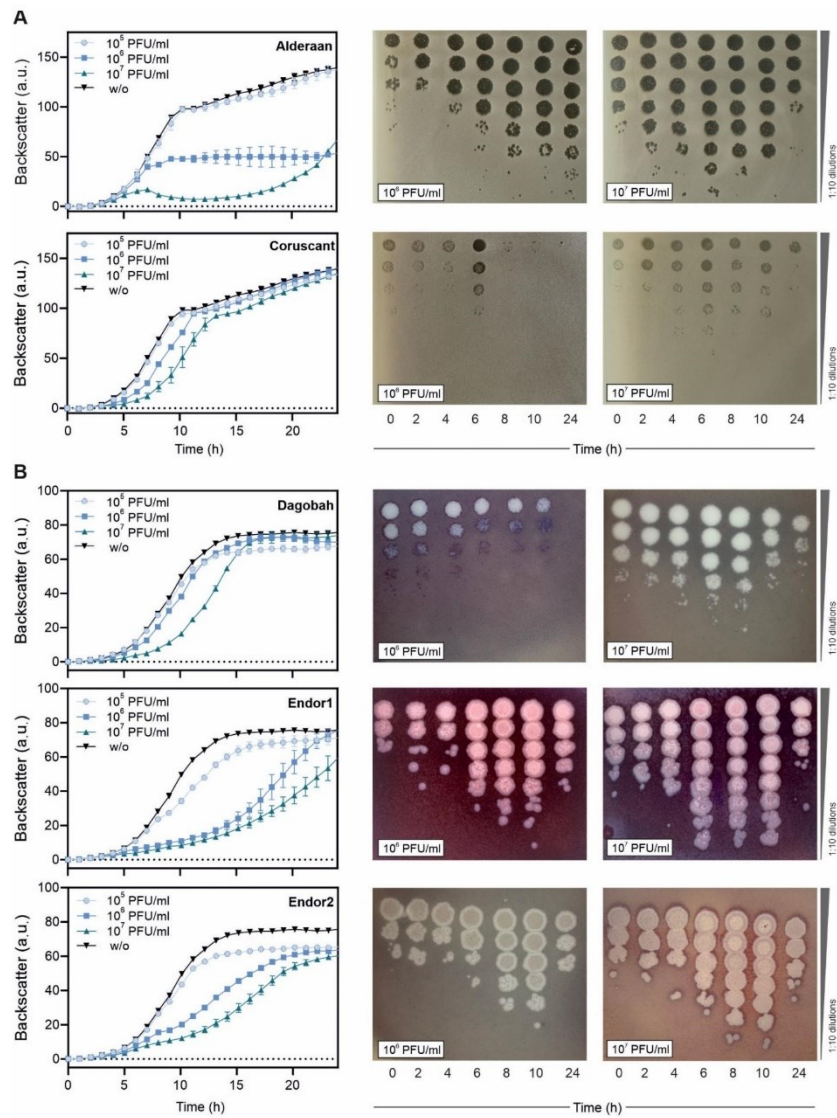


Figure 2. Infection curves of the five phages infecting *S. venezuelae* (A) and *S. coelicolor* (B). *S. venezuelae* or *S. coelicolor* were inoculated to GYM or YEME medium, respectively, and grown in microtiter plates, to which phages were added at the indicated initial phage titers. Backscatter was measured over time (left panels), in parallel to phage titers (right panels).

While phages usually have a relatively narrow host range, some phages can sometimes infect many strains of the same species and even distinct species. We assessed the host-range of our phages by spotting them on lawns of different *Streptomyces* species (Table 1).

Table 1. The host range of the five phages was assessed by spotting serial dilutions of these phages on lawns of different *Streptomyces* species propagated on GYM medium. The outcome of the spot assays is reported as follows: plaque formation (green), clearance of the bacterial lawn without visible plaques (yellow), no plaque or lysis visible (no color). The efficiency of plating (EOP) of a phage on a given strain relative to the host used for isolation is indicated, when plaques are countable.

	Alderaan	Coruscant	Dagobah	Endor1	Endor2
<i>S. venezuelae</i>	Green	Green			
<i>S. coelicolor</i> M600	Green	Green			
<i>S. coelicolor</i> M145			1	1	1
<i>S. rimosus</i> subsp. <i>rimosus</i>					
<i>S. scabiei</i>				Yellow	
<i>S. griseus</i>					
<i>S. platensis</i>				Yellow	
<i>S. xanthochromogenes</i>				Yellow	
<i>S. lividans</i>	Yellow		0.2		
<i>S. olivaceus</i>					4
<i>S. cyaneofuscatus</i>				0.08	0.4

S. coelicolor M145 showed the same sensitivity pattern than the M600 strain. M145 and M600 are both plasmid-free derivatives of A3(2) and mainly differ from each other in the length of their direct terminal repeats [17].

Beside *S. venezuelae* and *S. coelicolor*, *S. lividans* showed plaque formation by phage Dagobah. Endor1 and Endor2 also formed plaques on *S. olivaceus* and *S. cyaneofuscatus*. Alderaan, Endor1 and Endor2 caused indefinite clearance of the bacterial lawn of several species, but higher dilutions did not reveal distinct, single plaques. For these species, the phage lysates could have inhibitory effects on growth or cause non-productive infection [36,37].

In summary, Endor1 and Endor2 showed the broadest host range, but overall, the five phages we isolated feature a relatively modest host range, as they are only able to infect few other *Streptomyces* species.

3.3. Genome Sequencing and Genome Features

All phages were sequenced using short-read technology (Illumina Mi-Seq). Each genome could be assembled to a single contig, to which >80% of the reads could be mapped confirming the purity of the samples.

The genome features of the five phages are summed up in Table 2. Briefly, they show diverse genome sizes (39 to 133 kb), GC-contents (48 to 72%) and ORFs numbers (51 to 290). The phage Coruscant differed from other phages, in that its genome is significantly larger than the other phages and exhibits a markedly low GC content (48%), in comparison to the one of its host (72%). The genomic ends were predicted using PhageTerm, which detects biases in the number of reads to determine DNA termini and phage packaging mechanisms [29]. Alderaan, Endor1 and Endor2 showed a headful packaging mechanism where the phage genomes have a fixed start at the *pac* site, but the end of the genome is variable. In contrast, phages Coruscant and Dagobah have direct terminal repeats (DTR). These DTR were identified in the initial assembly by an approximately 2-fold increase in

coverage clearly delimited at single base positions. Phage lifecycle was predicted using PhageAI, which developed a lifecycle classifier based on machine learning and natural language processing [30].

Table 2. Basic genome features of the five phages. Open reading frames (ORFs) were predicted using Prokka [25] and were later manually curated. Protein domains encoded in ORFs were identified using RPS-BLAST against the Conserved Domain Database (CDD). The type of genome ends was determined using Phage Term [29]. The lifestyle of each phage was predicted by the machine-learning based program PhageAI [30].

Phage Name	Accession Number	Reference Host	Genome Size (kb)	GC Content (%)	ORF Number	Genome Termini Class	Lifestyle Prediction
Alderaan	MT711975	<i>Streptomyces venezuelae</i> ATCC 10712	39	72.1	51	Headful (<i>pac</i>)	Temperate
Coruscant	MT711976	<i>Streptomyces venezuelae</i> ATCC 10712	133 (12 kb DTR)	48.4	290	DTR (long)	Virulent
Dagobah	MT711977	<i>Streptomyces coelicolor</i> M600	47 kb (1 kb DTR)	68.9	93	DTR (short)	Temperate
Endor1	MT711978	<i>Streptomyces coelicolor</i> M600	49	65.8	75	Headful (<i>pac</i>)	Temperate
Endor2	MT711979	<i>Streptomyces coelicolor</i> M600	48	65.1	75	Headful (<i>pac</i>)	Temperate

Phage genes involved in the same function are usually clustered together, forming functional modules (Figure 3) [38,39]. These modules fulfil the basic functions necessary for production of progeny phages, including DNA/RNA metabolism, DNA replication and repair, DNA packaging, virion structure and assembly (tail and capsid), regulation, lysogeny (in the case of temperate phages) and lysis.

Interestingly, Coruscant's large genomes is paralleled by a high genome complexity. It contains no less than 41 copies of tRNAs, covering 19 different amino acids—all standard amino acids except valine. Coruscant has also a relatively high fraction of coding sequences for which no function could be predicted (155 hypothetical proteins out 290 CDS compared to 16/51 for Alderaan).

The phages were also found to encode homologs of bacterial regulators that are typically used by *Streptomyces* to control sporulation and overall development. For example, *whiB* (found in Alderaan, and Coruscant) and *ssgA* (found in Dagobah) are both essential for sporulation of *Streptomyces* [40,41]. Three phages (Coruscant, Endor1 and Endor2) also encode Lsr2-like proteins, which are nucleoid-associated proteins functioning as xenogeneic silencing proteins and are conserved throughout Actinobacteria [42].

Additionally, despite overall high synteny and homology, the phages Endor1 and Endor2 showed sequence variations in the tail fiber proteins, tapemeasure and endolysin. In particular, the region encoding distal elements of the tail (ORF_00022 to ORF_00025 in Endor1, ORF_00023 to ORF_00026 in Endor2) displays reduced similarity at the nucleotide level (Supplementary Table S1). The resulting differences at the protein level could potentially account for the differences in host range between these two phages, e.g., infectivity on *S. olivaceus* (Table 1).

3.4. Average Nucleotide Identity (ANI) Analysis

We established the sequence relationship between the newly sequenced *Streptomyces* phages and the selected genomes from the representative group members of actinophages.

The Average nucleotide identity (ANI) based clustering dendrogram analysis showed that four (Endor1, Endor2, Alderaan, and Coruscant) out of five phage genomes clustered confidently with the members of already known clusters (Endor1/Endor2: BD, Coruscant: BE, and Alderaan: BC) (Figure 4). However, one of the phage genomes (Dagobah) does not share sufficient similarity and was therefore clustered as an unresolved group. Calculation of virus intergenomic similarities using VIRIDIC [43] showed congruent results to the ANI-based clustering (Figure S2), providing further support to the clustering shown in Figure 4. Altogether, the overall analysis showed that except Dagobah, all four phages show close relatedness to *Streptomyces* phages.

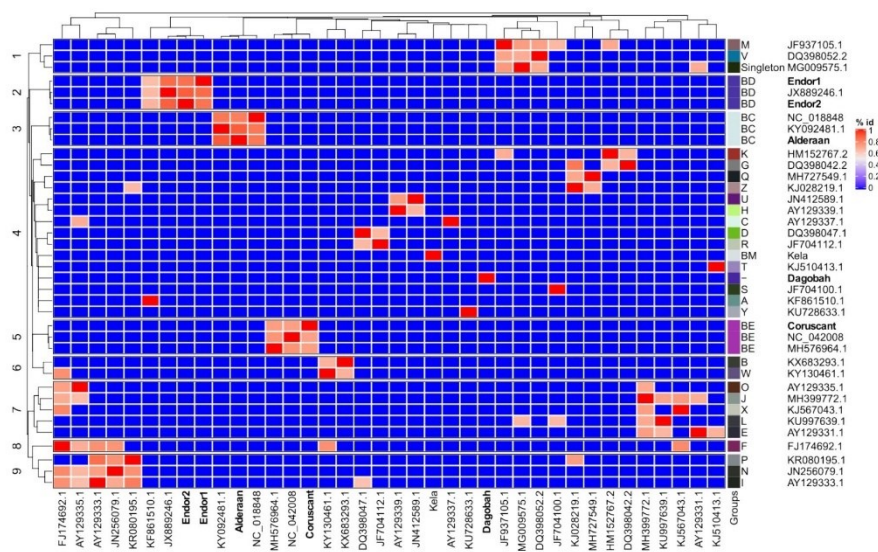


Figure 4. Average nucleotide-based dendrogram analysis using 38 actinophage genomes. These 38 genomes include 31 genomes downloaded from the Actinophage Database (<https://phagesdb.org/>), two genomes from NCBI based on close relatedness, and the five newly sequenced phages. The group of each phage, as defined by the Actinophage Database, is indicated.

3.5. Protein Domain-Based Analysis

Sequence relationship between the phage genomes is most commonly determined with the help of genome-wide similarity or average nucleotide identity-based analysis. However, a traditional method such as phylogeny with single genes is challenging because of the high variability and lack of universal genes across the phage genomes. Thus, we used additional phyletic-based analysis to establish a sequence relationship between the phage genomes. The hierarchical clustering dendrogram based on the identified 703 Pfam domains presence-absence matrix confidently clusters newly sequenced phages with known actinophages (Figure 5).

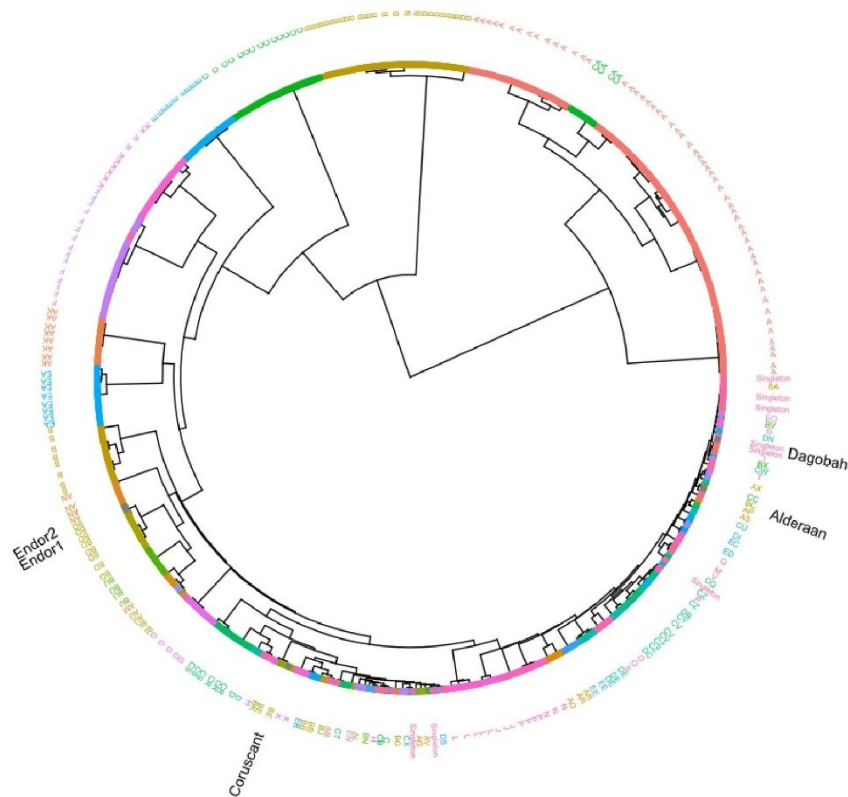


Figure 5. Protein domain-based hierarchical clustering. The dendrogram was constructed based on the presence-absence matrix of the >700 Pfam protein domains identified from 2486 actinophage genomes. Phages are color-coded according to known groups from the Actinobacteriophage Database (<https://phagesdb.org/>) [31]. The overlapping labels of the outer ring were merged to improve the figure's readability. The position of the five new phage genomes is indicated as black text.

In comparison to ANI-based analysis, hierarchical clustering showed congruent topology for the four newly sequenced *Streptomyces* phage genomes (Endor1 and Endor2: BD cluster, Alderaan: BC cluster, and Coruscant: BE cluster) (Supplementary Figures S3–S6). It also resolved polytomy between the unresolved groups and showed that Dagobah comes under the singleton group, consisting of highly divergent phages. Moreover, a high level of congruence was observed between already known groups and the groups identified by our hierarchical clustering. Thus, our results strongly suggest domain-based phyletic or hierarchical clustering analysis as an alternate way of classification of newly sequenced phage genomes.

4. Discussion

In this study, we report the isolation and characterization of five novel *Streptomyces* phages. Alderaan and Coruscant were isolated using *S. venezueale*, while *S. coelicolor* was the host used for isolation of Dagobah, Endor1 and Endor2.

The machine-learning based lifestyle prediction tool PhageAI suggested a temperate lifestyle for four of the phages (Alderaan, Dagobah, Endor1 and Endor2) and a virulent lifestyle for Coruscant.

These results were congruent with the lifestyle indicated by PhagesDB of phages belonging to the same cluster, as shown by the protein domain-based hierarchical clustering (Supplementary Figures S3–S6). However, unlike the other members of the BC cluster, Alderaan does not seem to have any integrase domain or gene. Together with the clear plaques it forms, this suggests that this phage potentially lost its integrase and therefore adopted a lytic lifestyle. Such events alter only slightly the overall genome landscape, be it at the nucleotide or protein level, and could thereby explain why whole-genome based predictions like PhageAI or protein domain-based clustering still predict Alderaan as temperate. These incongruencies, however, highlight the requirement of further experimental validation.

In contrast to the other four phages, Coruscant exhibits a large genome (superior to 130 kb) with massive direct terminal repeats (12 kb) and a low GC content (48%), in comparison to the 72% of its *Streptomyces* host. Coruscant also encodes 41 copies of tRNA genes, spanning 19 of the 20 standard amino acids. This large tRNA gene repertoire could be used to optimize gene expression in hosts that have differing codon usage patterns or to counteract potential tRNA-based degradation defense systems [44]. Altogether, the combination of a low GC content and a substantial tRNA equipment suggests a recent adaptation of the phage Coruscant to *Streptomyces*.

ANI and hierarchical clustering analysis revealed that Alderaan, Coruscant and Endor1/Endor2 belong to clusters BC, BE and BD defined by PhagesDB [31], respectively. In contrast, Dagobah showed very little homology with described phages, and was thus considered as a singleton. This finding highlights the largely untapped phage diversity, making the isolation of entirely “novel” phages still possible.

Streptomyces are characterized by their complex lifestyle and cellular differentiation. Interestingly, the isolated actinophages also encode homologs of SsgA, WhiB and Lsr2 proteins—regulatory proteins typically encoded by their hosts. The *ssgA* gene product was previously shown to be necessary for proper sporulation of *Streptomyces coelicolor* [41]; *whiB* is also essential for sporulation of *Streptomyces* and was already reported to be found in several actinophages [45–47]. Interestingly, the WhiB-like protein of mycobacteriophage TM4, WhiB_{TM4}, was shown to inhibit the transcription of *Mycobacterium whiB2*. Expression of WhiB_{TM4} in *M. smegmatis* led to hindered septation resembling a WhiB2 knockout phenotype, highlighting how phage can interfere with their host’s development [46].

Lsr2-like proteins are nucleoproteins conserved in Actinobacteria. In *Streptomyces*, they were recently shown to silence cryptic specialized metabolic clusters [48]. The first example of a phage-encoded Lsr2-like protein is the prophage-encoded Lsr2-like protein CgpS in *Corynebacterium glutamicum* [49]. CgpS was shown to maintain the lysogenic state of the prophage on which it resides. Further bioinformatic searches revealed that Lsr2-like proteins are abundant in actinophages, with almost 20% of *Streptomyces* phages encoding such proteins [42]. However, their role in the coordination of the phage life cycle still remains unclear. Altogether, these observations suggest that phages manipulate their host development, by interfering with central processes such as sporulation and antibiotic production.

More generally, the specificities of *Streptomyces*—especially its morphological complexity—impact the phage isolation and characterization process. For example, the mycelial nature of streptomycetes complicates quantitative studies. The notion of MOI loses a lot of its significance once mycelium has formed, as the network structure originating from one spore has greatly increased phage adsorption but would still be counted as one CFU [14,50]. Furthermore, the formation of clumps, although mitigated by the addition of glass beads or increase of osmotic pressure [51], makes accurate monitoring of cell growth (based on optical density or backscatter) difficult.

S. coelicolor was established as a model system for the *Streptomyces* genus partly because of its prolific pigment production [52]. Interestingly, we observed colored halos around the plaques formed by the *S. coelicolor* phages. Exposure to ammonia fume confirmed that these colored halos contain actinorhodin. This observation suggests that *Streptomyces* release metabolites in reaction to phage predation, some of which may potentially have anti-phage properties as it was shown recently with anthracyclines in *Streptomyces peucetius* [53].

Understanding the processes governing phage infection has the potential to illuminate the basic physiology of their hosts. Therefore, phages can serve as a basis to study *Streptomyces*' specific traits—its complex reproduction cycle and abundant production of secondary metabolites—in the context of phage infection.

Supplementary Materials: The following are available online at <http://www.mdpi.com/1999-4915/12/10/1065/s1>, Figure S1: Close-ups of phage plaques imaged using a Nikon SMZ18 stereomicroscope, before (upper row) and after (lower row) exposure to ammonia fumes. Figure S2: VIRIDIC generated heatmap showing the intergenomic similarities of the newly sequenced phages with reference phages. Figure S3: Subclade dendrogram with *Streptomyces* phage Alderaan and its closely related actinophages. Figure S4: Subclade dendrogram with *Streptomyces* phage Coruscant and its closely related actinophages. Figure S5: Subclade dendrogram with *Streptomyces* phage Dagobah and its closely related actinophages. Figure S6: Subclade dendrogram with *Streptomyces* phages Endor1 and Endor2 and their closely related actinophages. Supplementary Table S1: List of the functional annotation of proteins ORFs within phage genomes.

Author Contributions: Conceptualization, A.H., and J.F.; methodology, All; validation, All; formal analysis, All; investigation, A.H. and L.K.; resources, V.S. and J.F.; data curation, A.H. and V.S.; writing—original draft preparation, A.H. and V.S.; writing—review and editing, All; visualization, A.H., V.S. and L.K.; supervision, J.F.; project administration, J.F.; funding acquisition, J.F. All authors have read and agreed to the published version of the manuscript.

Funding: We thank the European Research Council (ERC Starting Grant, grant number 757563) for financial support. A.H. was supported by a fellowship from the Ecole Normale Supérieure (Paris, France).

Acknowledgments: We thank David Brandt (Center for Biotechnology, University of Bielefeld) for his help with genome assembly and Julio Ortiz (Forschungszentrum Jülich) for his assistance during electron microscopy. The *S. cyaneofuscatus* and *S. olivaceus* strains were kindly provided by the German Collection of Microorganisms and Cell Cultures (DSMZ). We are also grateful to the entire Frunzke lab for fruitful discussions.

Conflicts of Interest: The authors declare no conflict of interest.

References

1. Bibb, M.J. Understanding and manipulating antibiotic production in actinomycetes. *Biochem. Soc. Trans.* **2013**, *41*, 1355–1364. [[CrossRef](#)] [[PubMed](#)]
2. Hopwood, D.A. *Streptomyces in Nature and Medicine: The Antibiotic Makers*; Oxford University Press: Oxford, NY, USA, 2007; ISBN 978-0-19-515066-7.
3. Keiser, T.; Bibb, M.J.; Buttner, M.J.; Chater, K.F.; Hopwood, D.A. *Practical Streptomyces Genetics*; The John Innes Foundation: Norwich, UK, 2000; ISBN 0-7084-0623-8.
4. Elliot, M.A.; Buttner, M.J.; Nodwell, J.R. 24 Multicellular Development in *Streptomyces*. *Mycobacteria* **2008**, *419–438*. [[CrossRef](#)]
5. McCormick, J.R.; Flärdh, K. Signals and regulators that govern *Streptomyces* development. *FEMS Microbiol. Rev.* **2012**, *36*, 206–231. [[CrossRef](#)] [[PubMed](#)]
6. Anne, J.; Wohlleben, W.; Burkardt, H.J.; Springer, R.; Pohler, A. Morphological and Molecular Characterization of Several Actinophages Isolated from Soil Which Lyse *Streptomyces cattleya* or *S. venezuelae*. *Microbiology* **1984**, *130*, 2639–2649. [[CrossRef](#)] [[PubMed](#)]
7. Donadio, S.; Paladino, R.; Costanzi, I.; Sparapani, P.; Schreil, W.; Iaccarino, M. Characterization of bacteriophages infecting *Streptomyces erythreus* and properties of phage-resistant mutants. *J. Bacteriol.* **1986**, *166*, 1055–1060. [[CrossRef](#)] [[PubMed](#)]
8. Dowding, J.E. Characterization of a Bacteriophage Virulent for *Streptomyces coelicolor* A3(2) | Microbiology Society. *J. Gen. Microbiol.* **1973**, *76*, 163–176. [[CrossRef](#)]
9. Smith, M.C.M.; Hendrix, R.W.; Dedrick, R.; Mitchell, K.; Ko, C.-C.; Russell, D.; Bell, E.; Gregory, M.; Bibb, M.J.; Pethick, F.; et al. Evolutionary Relationships among Actinophages and a Putative Adaptation for Growth in *Streptomyces* spp. *J. Bacteriol.* **2013**, *195*, 4924–4935. [[CrossRef](#)]
10. Smith, M.C.M.; Burns, R.N.; Wilson, S.E.; Gregory, M.A. The complete genome sequence of the *Streptomyces* temperate phage ϕ C31: Evolutionary relationships to other viruses. *Nucleic Acids Res.* **1999**, *27*, 2145–2155. [[CrossRef](#)]
11. Lomovskaya, N.D.; Mkrtumian, N.M.; Gostimskaya, N.L.; Danilenko, V.N. Characterization of Temperate Actinophage ϕ C31 Isolated from *Streptomyces coelicolor* A3(2). *J. Virol.* **1972**, *9*, 5. [[CrossRef](#)]

12. Lomovskaya, N.D.; Chater, K.F.; Mkrtumian, N.M. Genetics and molecular biology of *Streptomyces* bacteriophages. *Microbiol. Mol. Biol. Rev.* **1980**, *44*, 206–229. [[CrossRef](#)]
13. Burke, J.; Schneider, D.; Westpheling, J. Generalized transduction in *Streptomyces coelicolor*. *Proc. Natl. Acad. Sci. USA* **2001**, *98*, 6289–6294. [[CrossRef](#)] [[PubMed](#)]
14. Rosner, A.; Gustein, R. Adsorption of actinophage Pal 6 to developing mycelium of *Streptomyces*. *Can. J. Microbiol.* **1981**, *27*, 254–257. [[CrossRef](#)] [[PubMed](#)]
15. Jordan, T.C.; Burnett, S.H.; Carson, S.; Caruso, S.M.; Clase, K.; DeJong, R.J.; Dennehy, J.J.; Denver, D.R.; Dunbar, D.; Elgin, S.C.R.; et al. A Broadly Implementable Research Course in Phage Discovery and Genomics for First-Year Undergraduate Students. *mBio* **2014**, *5*. [[CrossRef](#)] [[PubMed](#)]
16. Pullan, S.T.; Chandra, G.; Bibb, M.J.; Merrick, M. Genome-wide analysis of the role of GlnR in *Streptomyces venezuelae* provides new insights into global nitrogen regulation in actinomycetes. *BMC Genom.* **2011**, *12*, 175. [[CrossRef](#)] [[PubMed](#)]
17. Weaver, D.; Karoonuthaisiri, N.; Tsai, H.-H.; Huang, C.-H.; Ho, M.-L.; Gai, S.; Patel, K.G.; Huang, J.; Cohen, S.N.; Hopwood, D.A.; et al. Genome plasticity in *Streptomyces*: Identification of 1 Mb TIRs in the *S. coelicolor* A3(2) chromosome: Identification of 1 Mb TIRs in *S. coelicolor* A3(2). *Mol. Microbiol.* **2004**, *51*, 1535–1550. [[CrossRef](#)]
18. Bentley, S.D.; Chater, K.F.; Cerdeño-Tárraga, A.-M.; Challis, G.L.; Thomson, N.R.; James, K.D.; Harris, D.E.; Quail, M.A.; Kieser, H.; Harper, D.; et al. Complete genome sequence of the model actinomycete *Streptomyces coelicolor* A3(2). *Nature* **2002**, *417*, 141–147. [[CrossRef](#)]
19. Shepherd, M.D.; Kharel, M.K.; Bosserman, M.A.; Rohr, J. Laboratory Maintenance of *Streptomyces* species. *Curr. Protoc. Microbiol.* **2010**, *18*, 10E.1.1–10E.1.8. [[CrossRef](#)]
20. Kauffman, K.M.; Polz, M.F. Streamlining standard bacteriophage methods for higher throughput. *MethodsX* **2018**, *5*, 159–172. [[CrossRef](#)]
21. Kensy, F.; Zang, E.; Faulhammer, C.; Tan, R.-K.; Büchs, J. Validation of a high-throughput fermentation system based on online monitoring of biomass and fluorescence in continuously shaken microtiter plates. *Microb. Cell Fact.* **2009**, *8*, 31. [[CrossRef](#)]
22. Rückert, C.; Albersmeier, A.; Busche, T.; Jaenicke, S.; Winkler, A.; Friðjónsson, Ó.H.; Hreggviðsson, G.Ó.; Lambert, C.; Badcock, D.; Bernaerts, K.; et al. Complete genome sequence of *Streptomyces lividans* TK24. *J. Biotechnol.* **2015**, *199*, 21–22. [[CrossRef](#)]
23. Gordon, D.; Green, P. Consed: A graphical editor for next-generation sequencing. *Bioinformatics* **2013**, *29*, 2936–2937. [[CrossRef](#)] [[PubMed](#)]
24. Hyatt, D.; Chen, G.-L.; LoCasio, P.F.; Land, M.L.; Larimer, F.W.; Hauser, L.J. Prodigal: Prokaryotic gene recognition and translation initiation site identification. *BMC Bioinform.* **2010**, *11*, 119. [[CrossRef](#)] [[PubMed](#)]
25. Seemann, T. Prokka: Rapid prokaryotic genome annotation. *Bioinformatics* **2014**, *30*, 2068–2069. [[CrossRef](#)] [[PubMed](#)]
26. Altschul, S.F.; Gish, W.; Miller, W.; Myers, E.W.; Lipman, D.J. Basic local alignment search tool. *J. Mol. Biol.* **1990**, *215*, 403–410. [[CrossRef](#)]
27. Grazziotin, A.L.; Koonin, E.V.; Kristensen, D.M. Prokaryotic Virus Orthologous Groups (pVOGs): A resource for comparative genomics and protein family annotation. *Nucleic Acids Res.* **2017**, *45*, D491–D498. [[CrossRef](#)]
28. Marchler-Bauer, A.; Derbyshire, M.K.; Gonzales, N.R.; Lu, S.; Chitsaz, F.; Geer, L.Y.; Geer, R.C.; He, J.; Gwadz, M.; Hurwitz, D.I.; et al. CDD: NCBI’s conserved domain database. *Nucleic Acids Res.* **2015**, *43*, D222–D226. [[CrossRef](#)]
29. Garneau, J.R.; Depardieu, F.; Fortier, L.-C.; Bikard, D.; Monot, M. PhageTerm: A tool for fast and accurate determination of phage termini and packaging mechanism using next-generation sequencing data. *Sci. Rep.* **2017**, *7*, 8292. [[CrossRef](#)]
30. Tynecki, P.; Guziński, A.; Kazimierczak, J.; Jadczyk, M.; Dastyk, J.; Onisko, A. PhageAI—Bacteriophage Life Cycle Recognition with Machine Learning and Natural Language Processing. *Bioinformatics* **2020**. [[CrossRef](#)]
31. Russell, D.A.; Hatfull, G.F. PhagesDB: The actinobacteriophage database. *Bioinformatics* **2017**, *33*, 784–786. [[CrossRef](#)]
32. Pritchard, L. Widdowquinn/pyani. 2020. Available online: <https://github.com/widdowquinn> (accessed on 21 September 2020).
33. Gu, Z.; Eils, R.; Schlesner, M. Complex heatmaps reveal patterns and correlations in multidimensional genomic data. *Bioinformatics* **2016**, *32*, 2847–2849. [[CrossRef](#)]

34. Yu, G.; Smith, D.K.; Zhu, H.; Guan, Y.; Lam, T.T.-Y. Ggtree: An R package for visualization and annotation of phylogenetic trees with their covariates and other associated data. *Methods Ecol. Evol.* **2017**, *8*, 28–36. [[CrossRef](#)]
35. Rudd, B.A.M.; Hopwood, D.A. Genetics of Actinorhodin Biosynthesis by *Streptomyces coelicolor* A3(2). *Microbiology* **1979**, *114*, 35–43. [[CrossRef](#)]
36. Abedon, S.T. Lysis from without. *Bacteriophage* **2011**, *1*, 46–49. [[CrossRef](#)]
37. Abedon, S.T. Detection of Bacteriophages: Phage Plaques. In *Bacteriophages: Biology, Technology, Therapy*; Harper, D.R., Abedon, S.T., Burrowes, B.H., McConville, M.L., Eds.; Springer International Publishing: Cham, Switzerland, 2018; pp. 1–32. ISBN 978-3-319-40598-8.
38. Botstein, D. A Theory of Modular Evolution for Bacteriophages. *Ann. N. Y. Acad. Sci.* **1980**, *354*, 484–491. [[CrossRef](#)] [[PubMed](#)]
39. Brüßow, H.; Desiere, F. Comparative phage genomics and the evolution of *Siphoviridae*: Insights from dairy phages. *Mol. Microbiol.* **2001**, *39*, 213–223. [[CrossRef](#)] [[PubMed](#)]
40. Molle, V.; Palframan, W.J.; Findlay, K.C.; Buttner, M.J. WhiD and WhiB, homologous proteins required for different stages of sporulation in *Streptomyces coelicolor* A3(2). *J. Bacteriol.* **2000**, *182*, 1286–1295. [[CrossRef](#)]
41. van Wezel, G.P.; van der Meulen, J.; Kawamoto, S.; Luiten, R.G.M.; Koerten, H.K.; Kraal, B. *ssgA* Is Essential for Sporulation of *Streptomyces coelicolor* A3(2) and Affects Hyphal Development by Stimulating Septum Formation. *J. Bacteriol.* **2000**, *182*, 5653–5662. [[CrossRef](#)]
42. Pfeifer, E.; Hünnefeld, M.; Popa, O.; Frunzke, J. Impact of Xenogeneic Silencing on Phage–Host Interactions. *J. Mol. Biol.* **2019**. [[CrossRef](#)] [[PubMed](#)]
43. Moraru, C.; Varsani, A.; Kropinski, A.M. VIRIDIC—A novel tool to calculate the intergenomic similarities of prokaryote-infecting viruses. *bioRxiv* **2020**. [[CrossRef](#)]
44. Hyman, P.; Abedon, S.T. Chapter 7—Bacteriophage Host Range and Bacterial Resistance. In *Advances in Applied Microbiology*; Academic Press: Cambridge, MA, USA, 2010; Volume 70, pp. 217–248.
45. Morris, P.; Marinelli, L.J.; Jacobs-Sera, D.; Hendrix, R.W.; Hatfull, G.F. Genomic Characterization of Mycobacteriophage Giles: Evidence for Phage Acquisition of Host DNA by Illegitimate Recombination. *J. Bacteriol.* **2008**, *190*, 2172–2182. [[CrossRef](#)]
46. Rybniker, J.; Nowag, A.; van Gumpel, E.; Nissen, N.; Robinson, N.; Plum, G.; Hartmann, P. Insights into the function of the WhiB-like protein of mycobacteriophage TM4—A transcriptional inhibitor of WhiB2. *Mol. Microbiol.* **2010**, *77*, 642–657. [[CrossRef](#)]
47. Van Dessel, W.; Van Mellaert, L.; Liesegang, H.; Raasch, C.; DeKeersmaeker, S.; Geukens, N.; Lammertyn, E.; Streit, W.; Anné, J. Complete genomic nucleotide sequence and analysis of the temperate bacteriophage VWB. *Virology* **2005**, *331*, 325–337. [[CrossRef](#)] [[PubMed](#)]
48. Gehrke, E.J.; Zhang, X.; Pimentel-Elardo, S.M.; Johnson, A.R.; Rees, C.A.; Jones, S.E.; Gehrke, S.S.; Turvey, S.; Boursalie, S.; Hill, J.E.; et al. Silencing cryptic specialized metabolism in *Streptomyces* by the nucleoid-associated protein Lsr2. *eLife* **2019**, *8*, e47691. [[CrossRef](#)]
49. Pfeifer, E.; Hünnefeld, M.; Popa, O.; Polen, T.; Kohlheyer, D.; Baumgart, M.; Frunzke, J. Silencing of cryptic prophages in *Corynebacterium glutamicum*. *Nucleic Acids Res.* **2016**, *44*, 10117–10131. [[CrossRef](#)] [[PubMed](#)]
50. Gilmour, C.M.; Noller, E.C.; Watkins, B. Studies on Streptomyces Phage: I. Growth Characteristics of the *Streptomyces griseus* Host-Phage System. *J. Bacteriol.* **1959**, *78*, 186–192. [[CrossRef](#)] [[PubMed](#)]
51. Nguyen, L.D.; Kalachová, L.; Novotná, J.; Holub, M.; Kofroňová, O.; Benada, O.; Thompson, C.J.; Weiser, J. Cultivation System Using Glass Beads Immersed in Liquid Medium Facilitates Studies of *Streptomyces* Differentiation. *Appl. Environ. Microbiol.* **2005**, *71*, 2848–2852. [[CrossRef](#)] [[PubMed](#)]
52. Chater, K. David Hopwood and the emergence of *Streptomyces* genetics. *Int. Microbiol.* **1999**, *2*, 61–68.
53. Kronheim, S.; Daniel-Ivad, M.; Duan, Z.; Hwang, S.; Wong, A.I.; Mantel, I.; Nodwell, J.R.; Maxwell, K.L. A chemical defence against phage infection. *Nature* **2018**, *564*, 283. [[CrossRef](#)]



© 2020 by the authors. Licensee MDPI, Basel, Switzerland. This article is an open access article distributed under the terms and conditions of the Creative Commons Attribution (CC BY) license (<http://creativecommons.org/licenses/by/4.0/>).

3.2 Aminoglycoside antibiotics inhibit phage infection by blocking an early step of the phage infection cycle

5 Kever L.#, **Hardy A.#**, Luthe L., Hünnefeld M., Gätgens C., Milke L, Wiechert J., Wittmann J., Moraru C., Marienhagen J. and Frunzke J.

Authors contributed equally to this work.

Research article, accepted at mBio

CONTRIBUTOR ROLE	CONTRIBUTOR
Conceptualization	LK (30%), AH (30%), JF (25%), TL (10%), MH (5%)
Data curation	LK (50%), AH (30%), TL (10%), LM (5%), JWie (5%)
Formal analysis	LK (60%), MH (20%), AH (10%), LM (10%)
Funding acquisition	JF (95%), JM (5%)
Investigation	LK (40%), AH (30%), TL (12.5%), MH (7.5%), CG (5%), LM (2.5%), JWie (2.5%)
Methodology	LK (40%), AH (25%), TL (15%), MH (10%), LM (5%), CM (5%)
Project administration	LK (40%), AH (30%), JF (20%), CG (10%)
Resources	JWit (60%), CM (40%)
Software	MH (60%), LM (20%), TL (20%)
Supervision	JF (50%), LK (25) AH (20%), MH (2.5%), JM (2.5%)
Validation	LK (65%), AH (25%), JF (10%)
Visualization	LK (55%), AH (25%), TL (10%), MH (5%), LM (5%)
Writing – original draft	AH (45%), LK (40%), JF (7.5%), MH (2.5%), TL (2.5%) LM (2.5%)
Writing – review & editing	JF (40%), AH (30%), LK (15%), TL (5%), JM (5%), JWie (2.5%), MH (2.5%)

10

Overall contribution AH: 35%



Aminoglycoside Antibiotics Inhibit Phage Infection by Blocking an Early Step of the Infection Cycle

Larissa Kever,^a Aël Hardy,^a Tom Luthe,^a Max Hünnefeld,^a Cornelia Gätgens,^a Lars Milke,^a Johanna Wiechert,^a Johannes Wittmann,^b Cristina Moraru,^c Jan Marienhagen,^{a,d}  Julia Frunzke^a

^aInstitute of Bio- und Geosciences, IBG-1: Biotechnology, Forschungszentrum Jülich, Jülich, Germany

^bLeibniz Institute DSMZ—German Collection of Microorganisms and Cell Cultures, Braunschweig, Germany

^cInstitute for Chemistry and Biology of the Marine Environment, Carl von Ossietzky University Oldenburg, Oldenburg, Germany

^dInstitute of Biotechnology, RWTH Aachen University, Aachen, Germany

Larissa Kever and Aël Hardy contributed equally to this work. To determine the order of the two co-first authors, we flipped a coin.

ABSTRACT In response to viral predation, bacteria have evolved a wide range of defense mechanisms, which rely mostly on proteins acting at the cellular level. Here, we show that aminoglycosides, a well-known class of antibiotics produced by *Streptomyces*, are potent inhibitors of phage infection in widely divergent bacterial hosts. We demonstrate that aminoglycosides block an early step of the viral life cycle, prior to genome replication. Phage inhibition was also achieved using supernatants from natural aminoglycoside producers, indicating a broad physiological significance of the antiviral properties of aminoglycosides. Strikingly, we show that acetylation of the aminoglycoside antibiotic apramycin abolishes its antibacterial effect but retains its antiviral properties. Altogether, our study expands the knowledge of aminoglycoside functions, suggesting that aminoglycosides not only are used by their producers as toxic molecules against their bacterial competitors but also could provide protection against the threat of phage predation at the community level.

IMPORTANCE Predation by phages is a major driver of bacterial evolution. As a result, elucidating antiphage strategies is crucial from both fundamental and therapeutic standpoints. While protein-mediated defense mechanisms, like restriction-modification systems or CRISPR/Cas, have been extensively studied, much less is known about the potential antiphage activity of small molecules. Focusing on the model bacteria *Escherichia coli* and *Streptomyces venezuelae*, our findings revealed significant antiphage properties of aminoglycosides, a major class of translation-targeting antibiotics produced by *Streptomyces*. Further, we demonstrate that supernatants from natural aminoglycoside producers protect bacteria from phage propagation, highlighting the physiological relevance of this inhibition. Suppression of phage infection by aminoglycosides did not result from the indirect inhibition of bacterial translation, suggesting a direct interaction between aminoglycosides and phage components. This work highlights the molecular versatility of aminoglycosides, which have evolved to efficiently block protein synthesis in bacterial competitors and provide protection against phages.

KEYWORDS *Streptomyces*, aminoglycosides, antibiotics, bacteriophages, phage defense, phage-host interaction

Bacteriophages are viruses that prey upon bacteria. Facing the existential threat posed by phage predation, prokaryotes have developed numerous lines of defense, which together form the prokaryotic “immune system” (1). In response, phages have evolved a multitude of ways to circumvent these barriers, thereby fostering the diversification of

Editor Gisela Storz, National Institute of Child Health and Human Development

Copyright © 2022 Kever et al. This is an open-access article distributed under the terms of the Creative Commons Attribution 4.0 International license.

Address correspondence to Julia Frunzke, j.frunzke@fz-juelich.de.

The authors declare no conflict of interest.

Received 18 March 2022

Accepted 1 April 2022

bacterial antiviral strategies. Recent bioinformatics-guided screenings revealed a large number of previously unknown antiviral defense systems (2, 3). However, the majority of currently known prokaryotic defense systems rely on a wide range of molecular mechanisms but are mediated mainly by protein or RNA complexes (4).

Environmental bacteria produce a wide range of small molecules, conferring producer cells a specific fitness advantage in competitive or predatory interactions. However, the potential antiphage role of this extensive chemical repertoire remains largely unexplored. Recently, new types of defense systems that rely on small molecules rather than on proteins or RNA have been discovered (5, 6). Anthracyclines are secondary metabolites naturally produced by *Streptomyces* species and were shown to inhibit infection by double-stranded-DNA (dsDNA) phages (5). These molecules act as DNA-intercalating agents and block the replication of phage—but not bacterial—DNA. Since these secondary metabolites are excreted by *Streptomyces* cells and are diffusible molecules, their production may provide broad protection against dsDNA phages at the community level.

In nature, producers of secondary metabolites are generally resistant to the molecules they synthesize (7, 8). This feature is of special importance when screening small molecules for antiviral properties, as toxic effects on bacterial growth would prevent the appreciation of any inhibition of phage infection. In this study, we leveraged this principle to look for phage inhibition by secondary metabolites, using bacterial hosts resistant to the compounds tested.

Aminoglycosides are antibiotics well known for their bactericidal effect by targeting the 30S subunit of the ribosome and thereby either directly inhibiting protein synthesis or, for most aminoglycosides, promoting mistranslation. The aminoglycoside streptomycin, discovered in 1943, was the first antibiotic active against *Mycobacterium tuberculosis* (9). Strikingly, we observed strong phage inhibition in the presence of aminoglycosides when using strains resistant to the antibiotic. In agreement with this observation, decades-old reports described the inhibition of various phages by streptomycin (10–12). However, the biological significance of these observations was not explored, and the underlying mechanism of action remains unclear. For these reasons, we focused our efforts on aminoglycosides and set out to investigate their potential antiphage properties.

In this study, we show that aminoglycoside antibiotics inhibit phages infecting the actinobacterial model species *Streptomyces venezuelae* and *Corynebacterium glutamicum* as well as the λ phage infecting *Escherichia coli*. Investigations of the mechanism of action point toward a blockage of phage infection occurring after DNA injection but before genome replication. Furthermore, the antiphage activity observed with the purified aminoglycoside apramycin could be reproduced with supernatants from the natural producer *Streptoalloteichus tenebrarius*, suggesting a broad physiological significance of the antiphage properties of aminoglycosides.

RESULTS

Aminoglycosides inhibit a broad range of phages. To investigate a potential antiviral activity of aminoglycosides, we first constructed resistant strains carrying a plasmid-borne resistance cassette encoding an aminoglycoside-modifying enzyme (Table S1 and S2A). With respect to the aminoglycosides selected for this study, we focused on antibiotics produced by *Streptomyces* species and included the atypical aminoglycoside streptomycin, aminoglycosides containing a monosubstituted deoxystreptamine ring (apramycin and hygromycin), kanamycin (4,6-di-substituted deoxystreptamine ring), and the aminocyclitol spectinomycin (13, 14). We challenged the aminoglycoside-resistant strains with a set of different phages using double-agar overlays with increasing aminoglycoside concentrations as screening platform (Fig. 1a). In the screening, we included phages from three different viral realms (15): dsDNA viruses from the order *Caudovirales* in *Duplodnaviria* (families *Sipho-*, *Myo-*, and *Podoviridae*), single-stranded DNA (ssDNA) viruses from the family *Inoviridae* in *Monodnaviria*, and

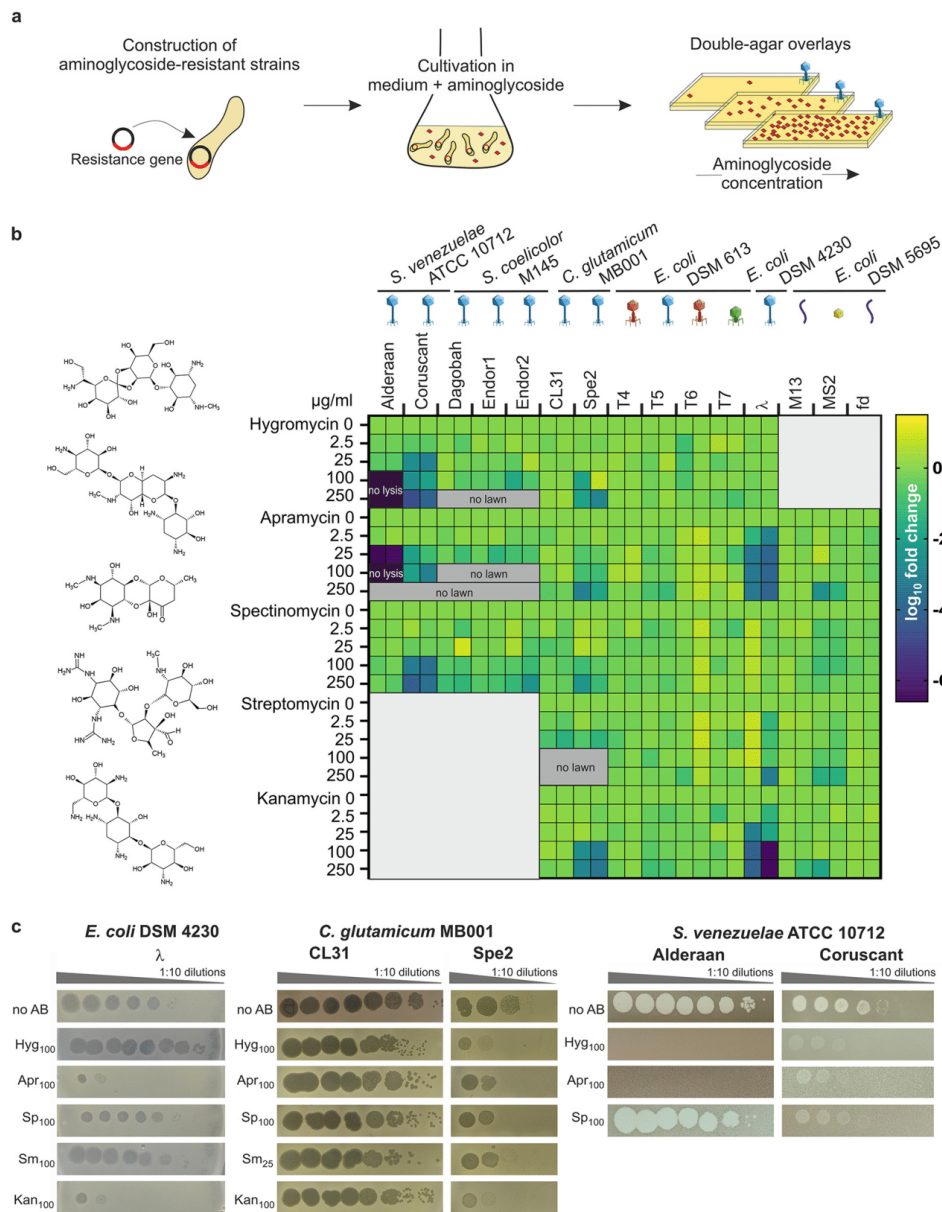


FIG 1 Aminoglycosides inhibit a wide range of phages. (a) Schematic representation of the screening for the antiphage effect of different aminoglycosides. Strains resistant to the aminoglycosides were constructed using plasmid-borne resistance cassettes and subsequently challenged by phages in the presence of increasing aminoglycoside concentrations. (b) Overview of the screening results, showing the log₁₀ fold change in plaque formation by tested phages relative to the aminoglycoside-free control. Molecular structures of the aminoglycosides tested are indicated on the left. High concentrations of aminoglycosides prevented in some cases either the formation of plaque or lysis zone by the spotted phages ("no lysis") or bacterial growth ("no lawn"). *n* = 2 independent biological replicates. The different phage morphologies are depicted with icons according to the following color scheme: blue, *Siphoviridae*; red, *Myoviridae*; green, *Podoviridae*; purple, *Inoviridae*; yellow, *Leviviridae*. (c) Exemplary pictures from propagation assays performed in the presence of the indicated aminoglycoside concentration. Results are representative of two biological replicates.

ssRNA viruses from the family *Leviviridae* in *Riboviria* (Table S2B). The efficiency of plating comparing plaque formation under aminoglycoside pressure with aminoglycoside-free conditions was calculated for phages infecting either the actinobacterial model species *Streptomyces venezuelae*, *Streptomyces coelicolor*, and *Corynebacterium glutamicum* or the Gram-negative species *Escherichia coli* (Fig. 1b).

The extent of inhibition showed clear differences between the individual phages and aminoglycosides. Remarkably, infection with some phages, namely, the virulent phages Alderaan, Coruscant, and Spe2 as well as the temperate *E. coli* phage λ , was significantly impaired with increasing aminoglycoside concentrations. In contrast, all phages infecting *S. coelicolor*, CL31 infecting *C. glutamicum* MB001, and the T phages, RNA phage MS2, and filamentous phages M13 and fd infecting *E. coli* displayed no susceptibility to the tested aminoglycosides. The phages susceptible to aminoglycosides infect widely divergent hosts and possess different lifestyles and types of genome ends (Table S2B). However, they are all dsDNA phages belonging to the family *Siphoviridae*, suggesting a specificity of aminoglycosides for this phage family.

In the case of *S. venezuelae* phages, we observed the strongest inhibition with the aminocyclitol antibiotic apramycin. The *S. venezuelae* phage Alderaan showed the highest susceptibility among all tested phages, leading to $\sim 10^6$ -fold reduction in numbers of PFU for 25 $\mu\text{g}/\text{mL}$ apramycin and a complete inhibition of cell lysis at 100 $\mu\text{g}/\text{mL}$ hygromycin or apramycin (Fig. 1b and c). This observation was in line with results from infection assays in liquid culture revealing no more culture collapse when supplementing the respective aminoglycosides (Fig. 2a). The antiviral activity was further demonstrated to be dose dependent, showing already an inhibition of infection at 1 $\mu\text{g}/\text{mL}$ apramycin (Fig. S1). In contrast, no antiviral activity was detected for spectinomycin (Fig. 2a).

To visualize the effect of apramycin on infection dynamics using live-cell imaging, *S. venezuelae* mycelium was grown from spores in a microfluidic device and infected with the phage Alderaan. Addition of apramycin almost completely inhibited phage-mediated lysis of *Streptomyces* mycelium, confirming the protective effect of apramycin against phage infection (Fig. 2b and Video S1).

Infection of *E. coli* with the model phage λ was also strongly impaired in the presence of aminoglycosides. Here, apramycin and kanamycin at concentrations as low as 25 $\mu\text{g}/\text{mL}$ showed a protective effect in liquid cultures (Fig. 2c and Fig. S2a) as well as an up to 1,000-fold reduction in numbers of PFU (Fig. 1b and c). Furthermore, this effect was shown to be independent of the host strain used (Fig. S2b).

In the case of temperate phages such as λ , an increased entry into the lysogenic cycle could explain the absence of phage amplification in the presence of aminoglycosides. To test this hypothesis, we conducted a reinfection experiment, in which cells surviving the first round of infection were washed and exposed to the same phage again. In the first infection round, cultures without apramycin showed a strongly increasing phage titer associated with extensive lysis of the culture. In contrast, infection in the presence of apramycin was completely inhibited, showing no phage amplification during λ infection and even an ~ 100 -fold decrease in phage titers over time for Alderaan (Fig. 2d and Fig. S2c).

Interestingly, removal of the antibiotic and reinfection of cells from apramycin-treated cultures resulted in similar amplification kinetics of Alderaan and λ compared to an untreated control. Hence, these results do not support the selection of genetically encoded resistance traits or, in the case of λ , an increased formation of lysogens but rather indicate a reversible antiphage effect of apramycin.

Since elevated Mg^{2+} levels were previously shown to interfere with aminoglycoside uptake (16) and streptomycin-mediated inhibition of phage infection (12), we examined whether the antiviral effect of apramycin is alleviated in the presence of MgCl_2 . As shown in Fig. 2e, phage infection was completely restored by the addition of 5 mM MgCl_2 , as evidenced by the strong growth defect and the increasing phage titer during infection. Comparable results regarding the antagonistic effects of MgCl_2 were also

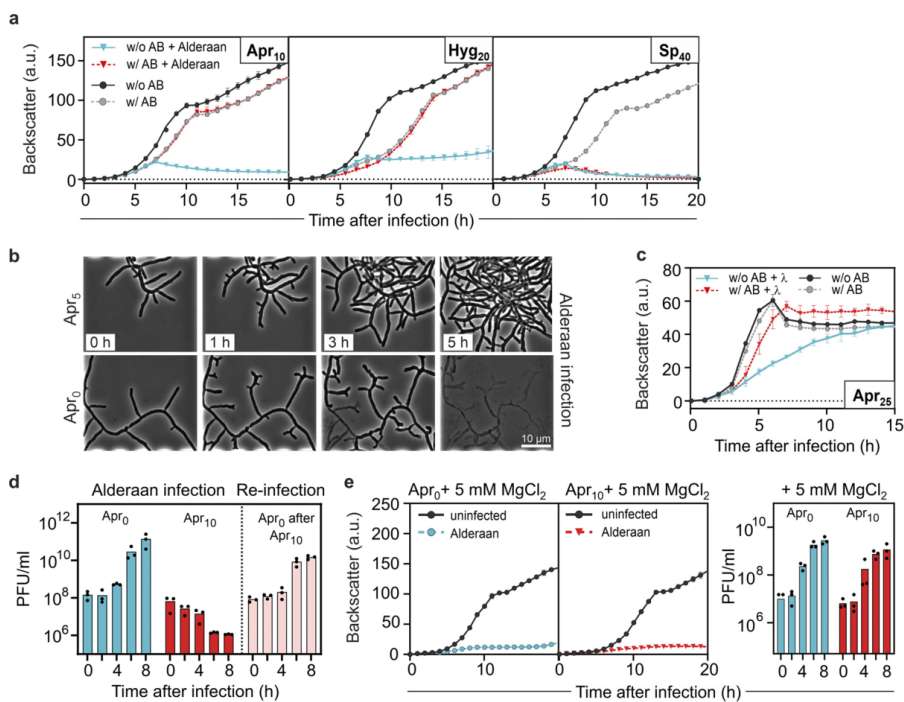


FIG 2 Aminoglycosides strongly inhibit phage amplification in liquid cultures. (a) Infection curves for *Streptomyces venezuelae* infected by phage Alderaan in the presence of different aminoglycosides (concentrations, in $\mu\text{g/mL}$, are indicated with subscripts; AB, antibiotic). (b) Time-lapse micrographs of *S. venezuelae* cultivated in a microfluidics system and challenged with Alderaan (insets show time after infection). (c) Infection curves for *E. coli* DSM 4230 infected by λ in the presence of $25 \mu\text{g/mL}$ apramycin. (d) Phage titers determined over two successive rounds of infection. A first infection round of *S. venezuelae* by Alderaan was performed in the presence or absence of apramycin. At the end of the cultivation, surviving cells from the apramycin-treated cultures were collected and exposed to phage Alderaan again, this time in the absence of apramycin. (e) Effect of MgCl_2 on infection of *S. venezuelae* by Alderaan, assessed by infection curves and determination of the corresponding phage titers over time. (a, d, and e) Alderaan was added to an initial titer of 10^7 PFU/mL; (c) λ was added to an initial titer of 10^8 PFU/mL. For growth curves and phage titers in panels a, c, d, and e, data are averages for three independent biological replicates ($n = 3$).

obtained for λ (Fig. S2d). Overall, these results suggest that the antiviral effect of aminoglycosides is based on an interference with phage infection at the intracellular level, probably during or shortly after phage DNA injection.

Spent medium of a natural aminoglycoside producer provides protection against phage predation. As *Streptomyces* are the natural producers of aminoglycosides, we examined whether infection of *S. venezuelae* in spent medium of the apramycin producer *Streptoalloteichus tenebrarius* (formerly known as *Streptomyces tenebrarius* [17]) provides protection against phage predation. Alderaan infection was not impaired by spent medium of *S. tenebrarius* harvested after 1 day of cultivation. In contrast, cultivation in spent medium taken after 2 days completely reproduced the antiviral effect observed during experiments with supplemented purified apramycin, showing equivalent growth of infected and uninfected cultures (Fig. 3a). Endpoint quantification of extracellular phage titers confirmed this inhibition of infection, as no more infective extracellular phages were detectable in the supernatants of the infected cultures (Fig. 3b). Importantly, this protective effect of *S. tenebrarius* spent medium coincided with the presence of apramycin in cultures, as determined by liquid chromatography-mass spectrometry (LC-MS) (Fig. 3c). While the phage-inhibitory effect of the supernatants is very likely to be caused by the native levels of apramycin, we cannot exclude the possibility that this strain may produce other compounds with antiphage

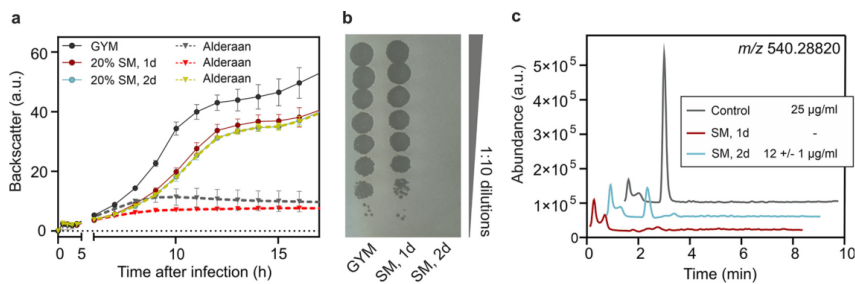


FIG 3 Secondary metabolites produced by *Streptoalloteichus tenebrarius* inhibit phage infection. (a) Influence of spent medium from *S. tenebrarius* on infection of *S. venezuelae* by Alderaan. Data are averages for three independent biological replicates; error bars represent standard deviations. (b) Determination of the final phage titers of infected cultures shown in panel a. Results are representative of two biological replicates. (c) Extracted ion chromatogram of samples analyzed by LC-MS assessing the presence of apramycin (molecular weight, 539.58 g/mol) in spent medium (SM) of *S. tenebrarius*. The indicated concentrations of apramycin are close to the detection limit under these measuring conditions. GYM, glucose-yeast extract-malt extract medium.

properties. Taken together, these data suggest that production of aminoglycoside antibiotics in natural environments might serve as a chemical defense providing protection against phage infection on a community level.

Aminoglycosides block an early step of phage infection. To decipher the mechanism underlying the antiviral activity of aminoglycosides, we investigated the influence of apramycin on the different steps of the phage infection cycle (Fig. 4a).

First, we determined the impact of apramycin on the adsorption step, by following phage titers over time after performing an intense washing 15 min after phage addition to remove Alderaan phages that are only reversibly adsorbed to *Streptomyces mycelium* (Fig. S3). We confirmed that this 15-min preincubation time was sufficient to reach the stage of irreversible adsorption of phage particles, as the control without apramycin showed strongly increasing titers following washing. Importantly, the outcome of phage amplification was determined only in the presence of apramycin in the main culture, as preincubation with apramycin had no influence on later phage titers. Taken together with the adsorption assay performed in the presence of apramycin (Fig. S4a), these data suggest that apramycin does not inhibit irreversible adsorption but rather a later stage of the phage life cycle. In accordance with these findings, preincubation of phage particles with apramycin showed no impact on phage infectivity at physiologically relevant levels of 10 or 50 $\mu\text{g}/\text{mL}$ apramycin (Fig. S5). In contrast, higher concentrations ($>500 \mu\text{g}/\text{mL}$) strongly impacted phage infectivity, showing a ~ 100 -fold reduction in PFU/mL after 24 h of incubation.

Next, we assessed phage DNA delivery and amplification by determining the level of intracellular Alderaan DNA during infection via quantitative real-time PCR (qPCR). In the absence of apramycin, the phage DNA levels increased exponentially until 360 min post-infection, indicating active genome replication across several rounds of infection (Fig. 4b). Simultaneous measurement of extracellular phage titers showed stable titers until 120 min, followed by a strong rise indicative of the release of new phage progeny after cells lysis (Fig. 4c). Conversely, only a slight increase in intracellular DNA was obtained for infection under apramycin pressure (Fig. 4b; note that measurement in the presence of apramycin is close to the detection limit). Relative phage concentrations then declined starting at 45 min and were even similar to those measured in the uninfected controls at 360 and 450 min, hinting at degradation of intracellular phage DNA. In the meantime, extracellular phage titers of apramycin-treated cultures declined from 120 min (Fig. 4c). Overall, these results suggest an inhibition of phage genome replication but do not exclude an interference with the injection process in *S. venezuelae*.

Assuming that apramycin blocks an early step of phage infection prior to genome replication, addition of the antibiotic after the replication phase would not interfere

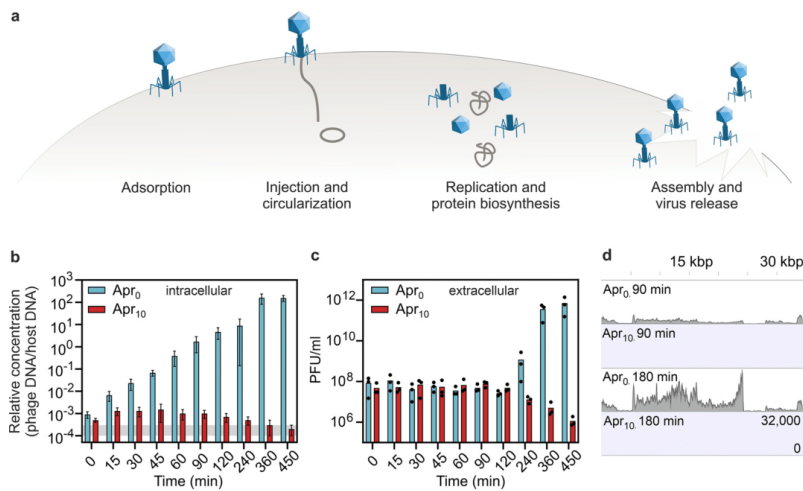


FIG 4 Apramycin blocks the phage life cycle at an early stage—before replication and transcription of phage DNA. (a) Scheme of the phage lytic life cycle, highlighting the different steps which could be inhibited by antiphage metabolites. (b) Infection of *S. venezuelae* by Alderaan; time-resolved quantification of phage DNA by qPCR in the intracellular fraction. To quantify the relative concentration of phage DNA per host DNA, a gene coding for the minor tail protein of Alderaan (HQ601_00028) and the housekeeping gene *atpD* of *S. venezuelae* were used. The corresponding oligonucleotide sequences are provided in Table S2D. Data are means for three independent biological replicates measured as technical duplicates. The range of relative concentrations measured for the uninfected controls (measured 120 min postinfection) is marked in gray. Note that the values measured for apramycin-treated samples are close to or even below the detection limit. (c) Time-resolved determination of Alderaan titers in the extracellular medium via double-agar overlays. $n = 3$ independent replicates. (d) RNA-seq coverage of the Alderaan genome (39 kbp) during infection in the presence and absence of apramycin.

with the infection. This hypothesis was indeed confirmed by supplementation of the aminoglycoside at different time points post infection (Fig. S4b). Corresponding infection assays indicated that apramycin addition 30 min after infection was sufficient to prevent a reproductive Alderaan infection. The observed decrease in extracellular phage titers is probably the result of adsorption and subsequent DNA injection of a fraction of phages without release of new infective viral particles.

In contrast, no decrease in extracellular phage titers was observed when apramycin was added 1 to 2 h after infection, indicating that the first phages were able to complete their infection cycle before apramycin was added. Comparison of these results with the quantification of intracellular phage DNA (Fig. 4b) further showed that this period corresponds to the replication phase, indicating that replication is a sensitive time point for the antiviral activity of aminoglycosides. In the case of the *E. coli* system, the measurement of potassium efflux is an established approach to probe the successful delivery of phage DNA into the bacterial cell (18). Applying this method to infection of *E. coli* with phage λ confirmed that the injection process was not impaired by apramycin (Fig. S2e).

Next, we examined the influence of apramycin on phage DNA transcription. RNA sequencing revealed an increasing transcription of Alderaan DNA during phage infection under normal infection conditions, whereas addition of apramycin drastically hindered phage gene expression (Fig. 4d and Fig. S4c). In accordance with the previous results, these data suggest a blockage of phage infection prior to phage DNA replication and transcription, which is congruent with a recent report of inhibition of two mycobacteriophages by streptomycin, kanamycin, and hygromycin (19).

To visualize intracellular phage infections in the presence and absence of apramycin, we performed fluorescence *in situ* hybridization of phage DNA (phage-targeting direct-geneFISH) using Alexa Fluor 647-labeled probes specific for the phage genome. In this

assay, the formation of bright and distinct fluorescent foci is indicative of advanced viral infections (20). When infecting *E. coli* with λ , comparable amounts of injected phage DNA were detected for both infection conditions after 30 min. This result is in line with the potassium efflux assay described above, which showed similar injection kinetics in the presence of apramycin for *E. coli* (Fig. S2e). As the infection progressed, only samples without apramycin exhibited a strong increase in fluorescence intensity 90 min and 180 min post-infection, further hinting at an inhibited replication in the presence of apramycin (Fig. 5a). For Alderaan, an increase in red fluorescence and thus intracellular phage DNA could be observed 4 h after infection and was even more pronounced at 6 h, reflecting phage DNA replication. In contrast, apramycin-treated samples showed only a very weak and more diffuse red fluorescent signal in the 6-h samples (Fig. 5c), which is overall consistent with the quantification of intracellular phage DNA by qPCR (Fig. 4b). Plotting the distribution of fluorescence intensity per pixel confirmed that the massive increase in fluorescence at the last time point (180 min for λ and 6 h for Alderaan, respectively) was inhibited in the presence of apramycin, supporting the blockage of replication exerted by apramycin (Fig. 5b and d; Fig. S6a and c). Interestingly, determination of the percentage of λ -infected *E. coli* cells over time showed a peak at 30 min in apramycin-treated samples followed by a decline down to almost no infected cell at 180 min (Fig. S6b). This observation suggests that intracellular phage DNA was degraded following the halt of the phage life cycle caused by apramycin.

Acetylation of apramycin abolishes its antibacterial, but not antiphage properties.

Enzymatic modification of aminoglycosides is a major mechanism of bacterial resistance to these antibiotics. Aminoglycoside-modifying enzymes are categorized in three major classes: aminoglycoside *N*-acetyltransferases (AACs), aminoglycoside *O*-nucleotidyltransferases (ANTs), and aminoglycoside *O*-phosphotransferases (APHs) (13). Addition of an acetyl, adenylyl, or phosphoryl group at various positions of the aminoglycoside core scaffold decreases the binding affinity of the drug for its primary ribosomal target, leading to the loss of the antibacterial potency, with the modified aminoglycosides being described as “inactivated.”

However, the impact of these modifications on the antiphage activity of aminoglycosides is unknown. We set out to answer this question using apramycin and the acetyltransferase AAC(3)IV (21), also referred to as “Apr” in the literature. In the presence of apramycin, AAC(3)IV catalyzes the acetylation of the 3-amino group of the deoxystreptamine ring, using acetyl coenzyme A (acetyl-CoA) as a cosubstrate (Fig. 6a).

Using purified AAC(3)IV enzyme, we performed an *in vitro* acetylation reaction of apramycin. LC-MS analysis of the reaction mixtures revealed complete acetylation of apramycin, as the peak of apramycin (m/z 540) disappeared in favor of the one corresponding to acetylated apramycin (m/z 582) (Fig. 6b).

The efficiency of the acetylation reaction being confirmed, we tested the effect of acetylated apramycin on phage infection in liquid medium, using wild-type *S. venezuelae* (not carrying a plasmid-borne acetyltransferase gene) and its phage Alderaan. As expected, apramycin fully prevented growth of *S. venezuelae*, while acetylated apramycin did not show any toxicity effect. Strikingly, phage infection was completely inhibited in the presence of acetylated apramycin, suggesting that acetylation of apramycin does not interfere with its antiphage properties (Fig. 6c). Plate assays showed a comparable pattern: acetylation of apramycin suppressed its antibacterial effect but did not disrupt its ability to inhibit phage infection (Fig. 6d). Altogether, these results suggest a decoupling of the antibacterial and antiphage properties of apramycin and further highlight the distinct molecular target accounting for apramycin’s antiphage properties.

DISCUSSION

We have shown that aminoglycosides inhibit phage infection in a diverse set of bacterial hosts by blocking an early step of the phage life cycle prior to DNA replication. These findings highlight the multifunctionality of this class of antibiotics, as they possess both antibacterial and antiviral properties. The dual properties of aminoglycosides

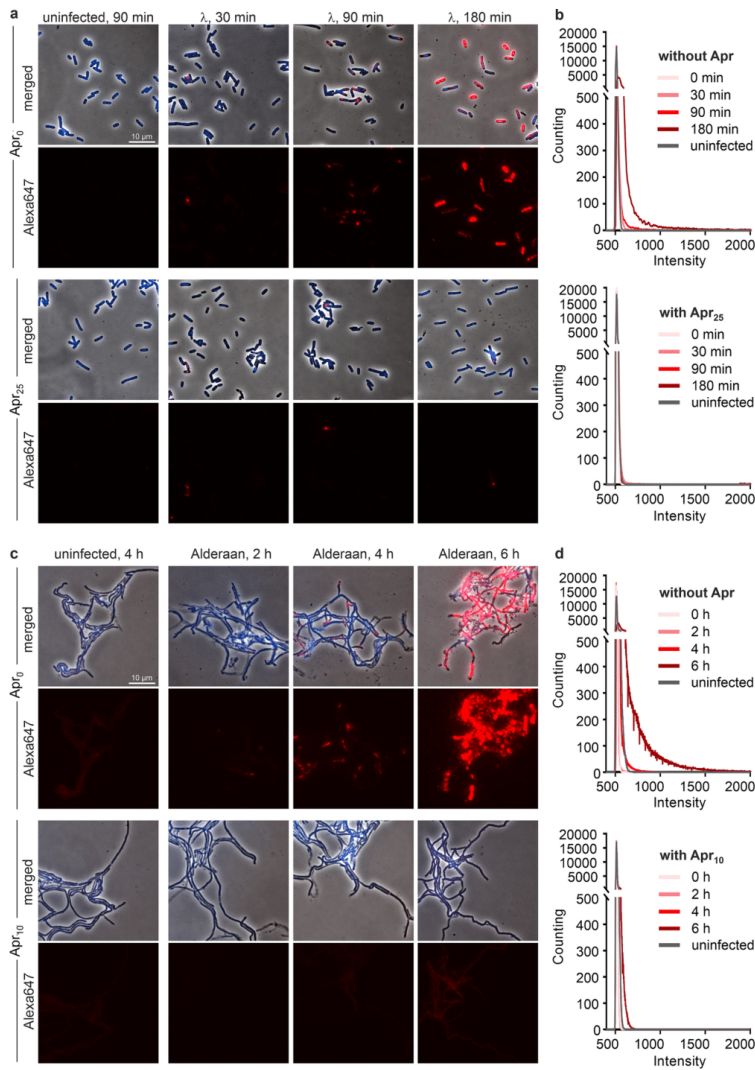


FIG 5 Visualization of intracellular phage DNA by phage targeting direct-geneFISH. (a and c) Phage-targeting direct-geneFISH micrographs of (a) *E. coli* DSM4230 infected with λ and (c) *S. venezuelae* infected with Alderaan in the presence and absence of 25 $\mu\text{g/mL}$ and 10 $\mu\text{g/mL}$ apramycin, respectively. (First and third rows) Phase-contrast pictures merged with fluorescence signal from bacterial DNA (DAPI, blue) and phage DNA (Alexa647, red). (Second and fourth rows) Fluorescence signal from phage DNA only (Alexa647, red). Bar, 10 μm . (b and d) Quantification of Alexa647 fluorescence in (b) *E. coli* cells infected with λ and (d) *S. venezuelae* cells infected with Alderaan, shown as density plots of pixel counts relative to their fluorescence intensity. Data are averages for biological three independent biological replicates ($n = 3$); the data for all replicates are shown in Fig. S6a and b.

were first recognized in the 1950s and 1960s (10–12, 22), but mechanistic studies about their impact on phage infection differed in their conclusions. Brock and colleagues proposed a 2-fold inhibition of streptomycin on *Enterococcus faecium*, where streptomycin would be able to inhibit both genome injection and replication (12). In the same year, it was proposed that streptomycin inhibits the process of injection of

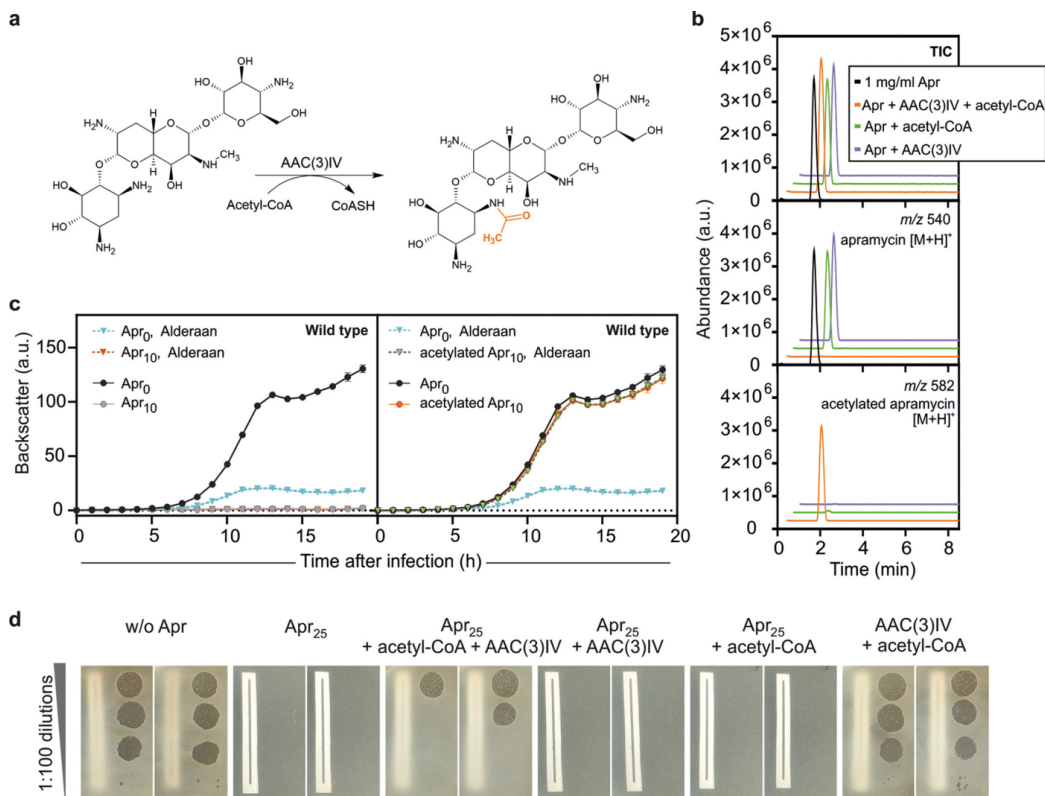


FIG 6 Acetylated apramycin strongly inhibits phage infection, despite the loss of its antibacterial properties. (a) Acetylation reaction of apramycin catalyzed by the AAC(3)IV acetyltransferase. (b) Total ion chromatogram and extracted ion chromatograms of samples analyzed by LC-MS assessing the presence of apramycin (molecular weight, 539.58 g/mol; m/z 540) and acetylated apramycin (molecular weight, 581.62 g/mol; m/z 582) after *in vitro* acetylation of apramycin. (c and d) Effect of acetylated apramycin on infection of wild-type *S. venezuelae* with Alderaan, performed in liquid (c) and solid (d) media. For panel d, the reaction mixtures of the *in vitro* acetylation assays containing apramycin, acetyl-CoA, the AAC(3)IV acetyltransferase, or different combinations of these were used to supplement the plates. A piece of paper was placed below plates to facilitate assessment of bacterial growth.

these phages by preventing proper unfolding of the phage genome through cross-linking of the phage DNA (23). Recently, Jiang and colleagues reported the inhibition of two *M. tuberculosis* phages by streptomycin, kanamycin, and hygromycin (19). Following adsorption and quantifying of viral DNA, the authors proposed that the blockage caused by aminoglycosides occurs between genome circularization and replication. Our results put forward different pictures depending on the bacterial host. Infection with λ and Alderaan phages seems to be blocked at the genome replication stage by apramycin in both cases. However, we cannot exclude some additional interference with the injection step of phage Alderaan. This disparity presumably has its roots in the major differences in cell wall architectures between Gram-positive and -negative bacteria. Moreover, it opens the possibility that aminoglycosides exert a multilayered inhibition of phage infection in their natural producers.

More recently, sublethal aminoglycoside concentrations of aminoglycosides were shown to inhibit phage infection in *E. coli* and *Bacillus cereus* (24). Interestingly, tetracycline, another translation-inhibiting antibiotic binding to the 30S ribosome, was much less effective at suppressing phage proliferation. This difference suggests a direct

antiphage action of aminoglycosides and indicates that inhibition of phage replication is not a common trait of antibiotics blocking protein synthesis.

One crucial question is that of which structural features or chemical groups of aminoglycosides are responsible for their antiphage properties. Our screening revealed that aminoglycosides belonging to 3 of 4 subclasses showed antiphage activity, suggesting that these properties are widespread among aminoglycosides and not limited to one particular subclass. Furthermore, a potential antiviral activity is probably also strongly influenced by the uptake and cell envelope structure of a particular host species. However, thorough structure-function relationship studies are needed to address this topic.

The versatility of aminoglycosides can be attributed to their ability to bind a wide variety of molecules, including nucleic acids—DNA or RNA, biologically or nonbiologically derived. The most prominent target of aminoglycosides is the 16S rRNA, accounting for the disruption of protein translation and hence their bactericidal properties (13). Aminoglycosides have also been shown to bind to seemingly unrelated families of RNA molecules such as group I introns (25), a hammerhead ribozyme (26), the *trans*-activating response element (TAR) (27) and the Rev response element (RRE) of the human immunodeficiency virus (HIV) (28–30). Interestingly, this effect on HIV is the only report of a direct inhibition of eukaryotic viruses by aminoglycosides. Evidence of indirect influence on infection by eukaryotic viruses comprises the activation of interferon-based antiviral response following topical application of aminoglycosides (31), and the enhancement of plaque formation by coxsackieviruses via increased diffusion of virions in the extracellular matrix (32). Furthermore, *in vitro* studies showed condensation of purified phage λ DNA by aminoglycosides. It was proposed that the clamp formed by aminoglycosides around the DNA double helix causes a bend responsible for the formation of toroids and other structural deformations (33, 34).

Injected phage DNA is linear, in a relaxed state, and not protected by DNA-binding proteins, and it is therefore probably highly sensitive to DNA-binding molecules. Interestingly, anthracyclines—another class of secondary metabolites produced by *Streptomyces* strains with antiphage properties—inhibit phage infection at a similar stage (5). While the exact mechanism of action underlying phage inhibition by anthracyclines and aminoglycosides remains elusive, these recent results suggest that already injected but not yet replicating phage DNA is preferentially targeted by antiviral molecules. Repeated efforts to isolate Alderaan clones that developed resistance to apramycin were not successful, suggesting that phage inhibition by apramycin relies on structural properties of phage DNA that cannot be readily overcome by single-base mutations or small structural variants.

Therapeutical use of phages—known as phage therapy—is often combined with an antibiotic treatment due to the potentially synergistic effect between these two antimicrobial agents. In contrast, we describe here an antagonistic impact of a common antibiotic class on phages, which has important implications for phage-aminoglycoside combination treatment. We propose that sensitivity of the phage to aminoglycosides be assessed *in vitro* before administration of such combination therapy.

From a more fundamental perspective, these findings also shed new light on the role of aminoglycosides in natural bacterial communities. While their use as antibiotics for medical applications has been extensively documented, until now, relatively little was known about their function in the natural setting. We posit that aminoglycosides not only are used by their producers as a powerful weapon against bacterial competitors but also protect them against phage predation at the community level. In streptomycetes, antibiotic production happens mainly at later stages of development, typically during the formation of aerial hyphae (35–37), while phages preferentially attack young mycelium (38). This clear difference in chronology may make secondary-metabolite-mediated antiphage defense seem irrelevant when studied in a laboratory setting. However, this defense strategy takes its full meaning in the light of community

ecology, where older fractions of an established microbial community could ensure a protective “antiviral milieu” for their descendants.

Another key consideration to appreciate aminoglycoside antiviral properties in an ecological context concerns the importance of the resistance mechanism to these antibiotics. Using *Streptomyces venezuelae* and its phage Alderaan, we showed that acetylation of apramycin led to a loss of its antibacterial properties, while leaving its ability to block phage infection untouched. Assuming that this observation can be extended to more phages and aminoglycoside-modifying enzymes, it raises the question of whether deflecting the antibacterial effect of aminoglycosides while benefiting from their intracellular protective effect against phages would be a strategy favored over antibiotic resistance by efflux. Interestingly, unlike many antibiotic classes (39), efflux proteins reported to pump out aminoglycosides are relatively rare and conferred only partial resistance to aminoglycosides (13). In contrast, aminoglycoside-modifying enzymes are widespread and found in natural producers and clinical isolates alike (13, 40). Natural aminoglycoside producers often encode a second line of resistance represented by 16S rRNA methyltransferases, whose action makes their ribosomes insensitive to aminoglycosides without interfering with the action of the latter on phages (40).

Considering the colossal number of molecules produced by environmental bacteria whose physiological role is still unclear, we postulate that additional prokaryotic anti-phage metabolites are to be discovered in the future, further underlining the extraordinary diversity of strategies employed by bacteria against their viral predators.

MATERIALS AND METHODS

Bacterial strains and growth conditions. All bacterial strains, phages, and plasmids used in this study are listed in Table S2A, B, and C, respectively. For growth studies and double-agar overlay assays, *Streptomyces* sp. cultures were inoculated from spore stocks and cultivated at 30°C and 120 rpm using glucose-yeast extract-malt extract (GYM) medium for *S. venezuelae* and *Streptoalloteichus tenebrarius* and yeast extract-malt extract (YEME) medium for *S. coelicolor* (35). *E. coli* was cultivated in lysogeny broth (LB) medium at 37°C and 170 rpm, while *C. glutamicum* was grown in brain heart infusion (BHI) medium at 30°C and 120 rpm.

For double-agar overlays, BHI agar for *C. glutamicum*, LB agar for *E. coli*, and GYM agar (pH 7.3) for all *Streptomyces* species were used, with 0.4% and 1.5% agar for the top and bottom layers, respectively. For quantification of extracellular phages, 2 μ L of the culture supernatants was spotted on a bacterial lawn propagated on a double-agar overlay inoculated at an initial optical density at 450 nm (OD_{450}) of 0.4 for *Streptomyces* spp., an OD_{600} of 0.1 for *E. coli*, and an OD_{600} of 0.7 for *C. glutamicum*. Both agar layers were supplemented with antibiotics at the indicated concentrations.

For standard cloning applications, *E. coli* DH5 α was cultivated in LB medium containing the appropriate antibiotic at 37°C and 120 rpm. For conjugation between *Streptomyces* spp. and *E. coli*, the conjugative *E. coli* strain ET12567/pUZ8002 was used (41).

Recombinant DNA work and cloning. All plasmids and oligonucleotides used in this study are listed in Table S2C and D, respectively. Standard cloning techniques such as PCR and restriction digestion were performed according to standard protocols (42). In all cases, Gibson assembly was used for plasmid construction (43). DNA regions of interest were amplified via PCR using the indicated plasmid DNA as the template. The plasmid backbone was cut using the listed restriction enzymes. DNA sequencing and synthesis of oligonucleotides was performed by Eurofins Genomics (Ebersberg, Germany).

Phage infection curves. For phage infection curves, the BioLector microcultivation system of m2p-labs (Baesweiler, Germany) was used (44). Cultivations were performed as biological triplicates in FlowerPlates (m2p-labs, Germany) at 30°C and a shaking frequency of 1,200 rpm. During cultivation, biomass was measured as a function of backscattered light intensity with an excitation wavelength (λ_{ex}) of 620 nm (filter module: $\lambda_{ex}/\lambda_{em}$, 620 nm/620 nm; gain, 25 or 20 in Fig. 3a) every 15 min. All growth curves are baseline corrected. Main cultures of *Streptomyces* spp. in 1 mL GYM medium containing the indicated supplements were inoculated with overnight cultures in the same medium to an initial OD_{450} of 0.15. Infection was performed by adding phages to an initial titer of 10^7 PFU/mL. Supernatants were collected in 2-h intervals to determine the time course of phage titer via double-agar overlays. Phage infection curves in *E. coli* were done in the same way at 37°C and 1,200 rpm using an initial OD_{600} of 0.1 in 1 mL LB medium and an initial phage titer of 10^8 PFU/mL, resulting in a multiplicity of infection (MOI) of 1.

Phage infection curves in shaking flasks were performed analogously to the cultivation in microbio-reactors using a shaking frequency of 120 rpm. To study phage infection and the influence of aminoglycosides in *Streptomyces*, we draw attention to the importance of ion content, e.g., of water used for medium preparation.

Cultivation and perfusion in microfluidic devices. Single-cell analysis of *S. venezuelae* cells infected with phage Alderaan in presence and absence of apramycin was performed using an in-house-developed microfluidic platform (45–47). Cultivation and time-lapse imaging were performed in three steps. First, cultivation chambers in the microfluidic chip were inoculated with GYM medium containing an

initial spore titer of 10^8 PFU/mL. During the following precultivation phase, cells in all chambers were cultivated under continuous GYM medium supply supplemented with 2.5 μ g/mL apramycin (flow rate, 300 nL/min) to allow comparable growth conditions. After 6 h of precultivation, cells were cultivated for 3 h in GYM medium containing one of the final apramycin concentrations (0, 5, or 10 μ g/mL). Subsequently, infection was initiated by a continuous supply of GYM medium containing the final apramycin concentrations and Alderaan phages with a titer of 10^8 PFU/mL (flow rate, 200 nL/min). By using disposable syringes (Omnifix-F tuberculins, 1 mL; B. Braun Melsungen AG, Melsungen, Germany) and a high-precision syringe pump system (neMESYS; Cetoni GmbH, Korbussen, Germany), continuous medium supply and waste removal were achieved. Phase-contrast images were obtained at 5-min intervals (exposure time, 100 ms) by a fully motorized inverted Nikon Eclipse Ti microscope (Nikon Europe B.V., Amsterdam, Netherlands). During the complete cultivation, the temperature was set to 30°C using an incubator system (PeCon GmbH, Erbach, Germany).

Cultivation in spent medium. For preparation of spent medium, cultures of the natural apramycin producer *Streptoaaloteichus tenebrarius* were prepared by inoculating 50 mL of GYM medium to an initial OD_{450} of 0.1 and were cultivated for 4 days. Spent medium of the culture was collected every day by centrifugation and subsequent filtration of the supernatant. After adjustment of the pH to 7.3, GYM medium and spent medium were mixed in a ratio of 4:1, so that spent medium accounted for 20% of the total volume. Ten-times-concentrated GYM was added to keep the concentration of C sources equal to that of fresh GYM medium. Cultivation and infection of the apramycin-resistant *S. venezuelae*/pJLK04 strain in 20% spent medium was conducted in microbioreactors as describe above by using an initial OD_{450} of 0.5 and an initial phage titer of 10^6 PFU/mL.

LC-MS measurements of apramycin. Aminoglycosides were analyzed using an Agilent ultrahigh-performance LC (UHPLC) 1290 Infinity system coupled to a 6130 Quadrupole LC-MS system (Agilent Technologies, Waldbronn, Germany). LC separation was carried out using an InfinityLab Poroshell 120 2.7- μ m EC-C₁₈ column (3.0 by 150 mm; Agilent Technologies, Waldbronn, Germany) at 40°C. For elution, 0.1% acetic acid (solvent A) and acetonitrile supplemented with 0.1% acetic acid (solvent B) were applied as the mobile phases at a flow rate of 0.3 mL/min. A gradient elution was used, where the amount of solvent B was increased stepwise: minutes 0 to 6, 10% to 25%; minutes 6 to 7, 25% to 50%; minutes 7 to 8, 50% to 100%; and minutes 8 to 8.5, 100% to 10%. The mass spectrometer was operated in the positive electrospray ionization (ESI) mode, and data were acquired using the selected-ion-monitoring (SIM) mode. An authentic apramycin standard was obtained from Sigma-Aldrich (Munich, Germany). Area values for $[M+H]^+$ mass signals were linear for metabolite concentrations from 10 to 50 μ g/mL.

Potassium efflux assays. Cultures of *E. coli* DSM 4230/pEKEx2.d were grown in LB medium supplemented with 50 μ g/mL apramycin at 37°C and 170 rpm overnight. Fresh LB medium (50 μ g/mL apramycin if needed) was inoculated 1:100 from the overnight cultures and incubated at 37°C and 120 rpm for 1.5 h. The cultures were centrifuged at $5,000 \times g$ for 20 min, and the pellets were resuspended in SM buffer (0.1 M NaCl, 8 mM MgSO₄, 50 mM Tris-HCl [pH 7.5]). The OD_{600} was measured and adjusted to 2. The cultures were stored at 4°C and incubated at 37°C for 5 min directly before use. The measurements were performed using an Orion potassium ion selective electrode (Thermo Fisher Scientific, Waltham, MA, USA). Five microliters of the prepared cultures was mixed 1:50 with Orion ionic strength adjuster (ISA) (Thermo Fisher Scientific, Waltham, MA, USA), and measurements were started immediately to monitor the electric potential (in millivolts) every 5 s for a total of 60 min at room temperature with constant stirring. If apramycin was needed, it was added in the beginning to a concentration of 100 μ g/mL. After 5.5 min, 100 μ L of a polyethylene glycol (PEG)-precipitated λ phage lysate in SM buffer (10^{11} PFU/mL) was added to the cultures.

Quantitative real-time PCR. Quantification of cell-associated Alderaan phages was performed via quantitative real-time PCR. For this, infection of the apramycin-resistant strain *S. venezuelae* ATCC 10712 pJLK04 with Alderaan was performed as described in "Phage infection curves." At the indicated time points, 3 OD units of cells were harvested via centrifugation at $5,000 \times g$ and 4°C for 10 min and washed twice with phosphate-buffered saline (PBS) before being stored at -20°C. For quantification of intracellular phage DNA in presence and absence of apramycin, cells were resuspended in 500 μ L lysis buffer (10 mM Tris, 50 mM NaCl [pH 7.0]), and cell disruption was performed using a Precellys instrument (Bertin, Montigny Le Bretonneux, France) at 6,000 rpm three times for 40 s each. After centrifugation at $16,000 \times g$ and 4°C for 10 min, DNA concentrations in the supernatants were determined via nanophotometer (Implen, Munich, Germany) and adjusted to 1 ng/ μ L. Finally, 5 μ L of the diluted supernatants as the template DNA was mixed with 10 μ L 2 \times Luna universal qPCR master mix (New England Biolabs, Ipswich, MA, USA) and 1 μ L of each oligonucleotide (Table S2D) (final oligonucleotide concentration, 0.5 μ M) and adjusted to a final volume of 20 μ L with double-distilled water (ddH₂O). Measurements were performed in 96-well plates in the qTOWER 2.2 (Analytik Jena, Jena, Germany). For the determination of the relative concentration of cell-associated phages, the relative expression ratio of the phage target phage gene (HQ601_00028, coding for the minor tail protein of Alderaan; PCR product, 144 bp) to the *S. venezuelae* housekeeping gene *atpD* (coding for the ATP synthase beta subunit; PCR product, 147 bp) was calculated via the "Relative quantification method" function of the qPCRsoft 3.1 software (Analytik Jena, Jena, Germany).

Transcriptomics via RNA sequencing. To compare transcription of phage and host DNA in presence and absence of apramycin, infection of the apramycin-resistant strain *S. venezuelae* ATCC 10712/pJLK04 with Alderaan was conducted as described in "Phage infection curves." Cells were harvested 90 min and 180 min after infection on ice at $5,000 \times g$ and 4°C for 10 min. RNA purification was done using the Monarch total RNA miniprep kit (New England Biolabs, Ipswich, MA, USA) according to the

manufacturer's manual. Depletion of rRNA, library preparation, and sequencing were conducted by Genewiz (Leipzig, Germany).

After sequencing, all subsequent steps were conducted using CLC genomic workbench V. 20.0.4 software (Qiagen, Hilden, Germany). The initial quality check to analyze read quality and sequencing performances was followed by a trimming step. This step was used to remove read-through adapter sequences, leftover adapter sequences, low-quality reads (limit = 0.05), and ambiguous nucleotides. Subsequently, the trimmed reads were mapped against the genomes of *S. venezuelae* (accession no. NC_018750.1) and the phage Alderaan (accession no. MT711975.1). Coverage plots were generated to show the distribution of mapped reads on both genomes. Subsequently, transcripts-per-million (TPM) values were calculated using the RNA-seq analysis tool of CLC genomics workbench (read alignment parameters: mismatch cost, 2; insertion cost, 3; deletion cost, 3; length fraction, 0.8; similarity fraction, 0.8; strand specificity, both; maximum number of hits for a read, 10). A table containing these values and an overview matrix containing all values were exported for each sample.

Phage targeting direct-geneFISH. Visualization and quantification of intracellular phage DNA during the time course of infection were conducted via fluorescence *in situ* hybridization (FISH), following the direct-geneFISH protocol (48), with modifications as described below.

Design of phage gene probes was done using the gene-PROBER (49). Sequences of the 200-bp polynucleotides for Alderaan and 300-bp polynucleotides for λ are provided in Table S3. Phage infection was performed as described in "Phage infection curves" using 10^7 PFU/mL as the initial phage titer for both phages. For infection of *E. coli*, the chemical labeling of polynucleotides with Alexa Fluor 647 dye (Thermo Fisher Scientific, Waltham, MA, USA) as well as the "core" direct-geneFISH protocol for microscopic slides was conducted as described previously using 0.5 mg/mL lysozyme for permeabilization and 35% (vol/vol) formamide during the hybridization step. Imaging of cells was performed with an inverted time-lapse live cell microscope (Nikon Europe B.V., Amsterdam, Netherlands) using a 100 \times oil immersion objective (CFI Plan Apo Lambda DM; 100 \times oil; numerical aperture [NA], 1.45; Nikon Europe B.V., Amsterdam, Netherlands) (45). Fluorescence was recorded using the optical filters DAPI (4',6-diamidino-2-phenylindole) and CY5-4040C (DAPI: excitation, 360/40 nm; dichroic, 400 nm; emission, 460/50 nm; exposure time, 500 ms; CY5: excitation, 628/40 nm; dichroic, 660 nm; emission, 692/40 nm; exposure time, 500 ms [AHF Analysentechnik AG, Tübingen, Germany]). Phase contrast was imaged with an exposure time of 500 ms.

For *S. venezuelae* infection, the protocol was adjusted as follows. Fixation of cells and phages was performed in 50% ethanol overnight at 4°C. After washing and immobilization, permeabilization was performed with 1.5 mg/mL lysozyme for 60 min at 37°C. Due to the high GC content of the phage Alderaan, the formamide concentration in the hybridization buffer and in the humidity chamber was adjusted to 60% (vol/vol) and the NaCl concentration in the washing buffer was reduced to 4 mM. After counterstaining with DAPI, imaging of cells was performed as described for *E. coli* using the optical filters DAPI and CY5-4040C with the indicated exposure times (DAPI: excitation, 360/40 nm; dichroic, 400; emission, 460/50 nm; exposure time, 800 ms; CY5: excitation, 628/40 nm; dichroic, 660; emission, 692/40 nm; exposure time, 500 ms [AHF Analysentechnik AG, Tübingen, Germany]). Phase contrast was imaged with an exposure time of 500 ms. The images for phage signal quantification were taken at the same exposure times to enable comparison; exposure times were adjusted to avoid overexposure of the signals. Preparation of image cut-outs and adjustments of lookup tables (LUTs) were performed using NIS-Elements BR 5.30.03 (64 bit).

As a quantification of the microscopic analyses, plots showing the distribution of Cy5 signal intensities for single microscopy images were generated. To this end, signal intensity of each pixel of the Cy5 channel images was determined using the software Fiji (50), and the frequency of occurrence of each intensity was calculated and plotted using R with the Rstudio interface (51, 52). Fluorescence intensity profiles of single replicates are shown in Fig. S6a and c.

Purification of the AAC(3)IV apramycin acetyltransferase. For heterologous protein overproduction, *E. coli* BL21(DE3) cells containing the pAN6_aac(3)IV_CStrep plasmid were cultivated as described in "Bacterial strains and growth conditions." Precultivation was performed in LB medium supplemented with 50 μ g/mL kanamycin (LB Kan₅₀), which was incubated overnight at 37°C and 120 rpm. The main culture in LB Kan₅₀ medium was inoculated to an OD₆₀₀ of 0.1 using the preculture. At an OD₆₀₀ of 0.6, gene expression was induced using 100 μ M IPTG (isopropyl- β -D-thiogalactopyranoside). Cells were harvested after additional 24 h of incubation at 20°C.

Cell harvesting and disruption were performed as described earlier (53) using buffer A (100 mM Tris-HCl [pH 8.0]) with cComplete protease inhibitor (Roche, Basel, Switzerland) for cell disruption and buffer B (100 mM Tris-HCl, 500 mM NaCl [pH 8.0]) for purification. Purification of the Strep-tagged AAC(3)IV apramycin acetyltransferase was conducted by applying the supernatant to an equilibrated 2-mL Strep-Tactin-Sepharose column (IBA, Göttingen, Germany). After washing with 20 mL buffer B, the protein was eluted with 5 mL buffer B containing 15 mM D-desthiobiotin (Sigma-Aldrich, St. Louis, MO, USA).

After purification, the purity of the elution fractions was checked by SDS-PAGE (54) using a 4 to 20% Mini-Protein gradient gel (Bio-Rad, Munich, Germany). The protein concentration of the elution fraction was determined with the Pierce bicinchoninic acid (BCA) protein assay kit (Thermo Fisher Scientific, Waltham, MA, USA), and the elution fraction with the highest protein concentration was chosen for further use.

In vitro acetylation reaction of apramycin. Protein purification of the AAC(3)IV apramycin acetyltransferase was conducted as described above. Acetylation of apramycin was performed using a modified version of the protocol described by Magalhaes and Blanchard (21). Assay mixtures were composed of 100 μ L 100 mM Tris-HCl-500 mM NaCl (pH 8.0) containing the AAC(3)IV at a concentration of 10 μ g/mL, as well as 10 mM apramycin (approximately 5 mg/mL) and 10 mM acetyl-CoA sodium salt (Sigma-Aldrich, St. Louis, MO, USA). The assay mixtures were incubated at 37°C for 20 min.

Data availability. Raw data as well as processed tables were deposited in the GEO database under the accession number [GSE171784](https://www.ncbi.nlm.nih.gov/geo/query/acc.cgi?acc=GSE171784).

SUPPLEMENTAL MATERIAL

Supplemental material is available online only.

VIDEO S1, MOV file, 2 MB.

FIG S1, PDF file, 1.1 MB.

FIG S2, PDF file, 2.5 MB.

FIG S3, PDF file, 1.1 MB.

FIG S4, PDF file, 1 MB.

FIG S5, PDF file, 1.1 MB.

FIG S6, PDF file, 1.1 MB.

TABLE S1, DOCX file, 0.01 MB.

TABLE S2, DOCX file, 0.05 MB.

TABLE S3, DOCX file, 0.02 MB

ACKNOWLEDGMENTS

We thank the European Research Council (ERC Starting Grant, grant number 757563), the Deutsche Forschungsgemeinschaft (SPP 2330, project 464434020), and the Helmholtz Association (grant number W2/W3-096) for financial support.

We thank Paul Ramp (Forschungszentrum Jülich) and Natalia Tschowri (University of Hannover) for providing strains and plasmids and our bachelor's degree student Lisa Helm for her contribution to this project. We furthermore thank Mark Buttner (John Innes Centre, Norwich, United Kingdom) for introducing us into *Streptomyces* biology and for many fruitful discussions.

We declare no conflict of interest.

REFERENCES

- Hampton HG, Watson BNJ, Fineran PC. 2020. The arms race between bacteria and their phage foes. *Nature* 577:327–336. <https://doi.org/10.1038/s41586-019-1894-8>.
- Doron S, Melamed S, Ofir G, Leavitt A, Lopatina A, Keren M, Amitai G, Sorek R. 2018. Systematic discovery of antiphage defense systems in the microbial pangenome. *Science* 359:eaar4120. <https://doi.org/10.1126/science.aar4120>.
- Gao L, Altae-Tran H, Böhmig F, Makarova KS, Segel M, Schmid-Burgk JL, Koob J, Wolf YI, Koonin EV, Zhang F. 2020. Diverse enzymatic activities mediate antiviral immunity in prokaryotes. *Science* 369:1077–1084. <https://doi.org/10.1126/science.aba0372>.
- Rostøl JT, Marraffini L. 2019. (Ph)ighting phages: how bacteria resist their parasites. *Cell Host Microbe* 25:184–194. <https://doi.org/10.1016/j.chom.2019.01.009>.
- Kronheim S, Daniel-Ivud M, Duan Z, Hwang S, Wong AI, Mantel I, Nodwell JR, Maxwell KL. 2018. A chemical defence against phage infection. *Nature* 564:283–286. <https://doi.org/10.1038/s41586-018-0767-x>.
- Bernheim A, Millman A, Ofir G, Meitav G, Avraham C, Shomar H, Rosenberg MM, Tal N, Melamed S, Amitai G, Sorek R. 2021. Prokaryotic viperins produce diverse antiviral molecules. *Nature* 589:120–124. <https://doi.org/10.1038/s41586-020-2762-2>.
- Hopwood DA. 2007. How do antibiotic-producing bacteria ensure their self-resistance before antibiotic biosynthesis incapacitates them? *Mol Microbiol* 63:937–940. <https://doi.org/10.1111/j.1365-2958.2006.05584.x>.
- Tenconi E, Rigali S. 2018. Self-resistance mechanisms to DNA-damaging antitumor antibiotics in actinobacteria. *Curr Opin Microbiol* 45:100–108. <https://doi.org/10.1016/j.mib.2018.03.003>.
- Schatz A, Bugie E, Waksman SA. 2005. The classic: streptomycin, a substance exhibiting antibiotic activity against gram-positive and gram-negative bacteria. *Clin Orthop Relat Res* 437:3–6. <https://doi.org/10.1097/01.blo.0000175887.98112.fe>.
- Schindler J. 1964. Inhibition of reproduction of the f2 bacteriophage by streptomycin. *Folia Microbiol* 9:269–276. <https://doi.org/10.1007/BF02873305>.
- Bowman BU. 1967. Biological activity of phi-X DNA. I. Inhibition of infectivity by streptomycin. *J Mol Biol* 25:559–561. [https://doi.org/10.1016/0022-2836\(67\)90207-0](https://doi.org/10.1016/0022-2836(67)90207-0).
- Brock TD, Mosser J, Peacher B. 1963. The inhibition by streptomycin of certain *Streptococcus* bacteriophages, using host bacteria resistant to the antibiotic. *J Gen Microbiol* 33:9–22. <https://doi.org/10.1099/00221287-33-1-9>.
- Krause KM, Serio AW, Kane TR, Connolly LE. 2016. Aminoglycosides: an overview. *Cold Spring Harb Perspect Med* 6:a027029. <https://doi.org/10.1101/cshperspect.a027029>.
- Padilla IMG, Burgos L. 2010. Aminoglycoside antibiotics: structure, functions and effects on in vitro plant culture and genetic transformation protocols. *Plant Cell Rep* 29:1203–1213. <https://doi.org/10.1007/s00299-010-0900-2>.
- Koonin EV, Dolja VV, Krupovic M, Varsani A, Wolf YI, Yutin N, Zerbini FM, Kuhn JH. 2020. Global organization and proposed megataxonomy of the virus world. *Microbiol Mol Biol Rev* 84:e00061-19. <https://doi.org/10.1128/MMBR.00061-19>.
- Hancock RE, Raffle VJ, Nicas TI. 1981. Involvement of the outer membrane in gentamicin and streptomycin uptake and killing in *Pseudomonas aeruginosa*. *Antimicrob Agents Chemother* 19:777–785. <https://doi.org/10.1128/AAC.19.5.777>.
- Tamura T, Ishida Y, Otaguro M, Hatano K, Suzuki K. 2008. Classification of *Streptomyces tenebrarius* Higgins and Kastner as *Streptoalloteichus tenebrarius* nom. rev., comb. nov., and emended description of the genus *Streptoalloteichus*. *Int J Syst Evol Microbiol* 58:688–691. <https://doi.org/10.1099/ijs.0.65272-0>.
- Boulanger P, Letellier L. 1992. Ion channels are likely to be involved in the two steps of phage T5 DNA penetration into *Escherichia coli* cells. *J Biol Chem* 267:3168–3172. [https://doi.org/10.1016/S0021-9258\(19\)50710-4](https://doi.org/10.1016/S0021-9258(19)50710-4).
- Jiang Z, Wei J, Liang Y, Peng N, Li Y. 2020. Aminoglycoside antibiotics inhibit mycobacteriophage infection. *Antibiotics (Basel)* 9:714. <https://doi.org/10.3390/antibiotics9100714>.
- Allers E, Moraru C, Duhaime MB, Beneze E, Solonenko N, Barrero-Canosa J, Amann R, Sullivan MB. 2013. Single-cell and population level viral infection dynamics revealed by phageFISH, a method to visualize intracellular and free viruses. *Environ Microbiol* 15:2306–2318. <https://doi.org/10.1111/1462-2920.12100>.
- Magalhaes ML, Blanchard JS. 2005. The kinetic mechanism of AAC3-IV aminoglycoside acetyltransferase from *Escherichia coli*. *Biochemistry* 44:16275–16283. <https://doi.org/10.1021/bi051777d>.

22. Perlman D, Langlykke AF, Rothberg HD, Jr. 1951. Observations on the chemical inhibition of *Streptomyces griseus* bacteriophage multiplication. *J Bacteriol* 61:135–143. <https://doi.org/10.1128/jb.61.2.135-143.1951>.
23. Brock TD, Wooley SO. 1963. Streptomycin as an antiviral agent: mode of action. *Science* 141:1065–1067. <https://doi.org/10.1126/science.141.3585.1065>.
24. Zuo P, Yu P, Alvarez PJJ. 2021. Aminoglycosides antagonize bacteriophage proliferation, attenuating phage suppression of bacterial growth, biofilm formation, and antibiotic resistance. *Appl Environ Microbiol* 87:e0046821. <https://doi.org/10.1128/AEM.00468-21>.
25. Chow CS, Bogdan FM. 1997. A structural basis for RNA–ligand interactions. *Chem Rev* 97:1489–1514. <https://doi.org/10.1021/cr960415w>.
26. Tor Y, Hermann T, Westhof E. 1998. Deciphering RNA recognition: aminoglycoside binding to the hammerhead ribozyme. *Chem Biol* 5:R277–R283. [https://doi.org/10.1016/S1074-5521\(98\)90286-1](https://doi.org/10.1016/S1074-5521(98)90286-1).
27. Zapp ML, Stern S, Green MR. 1993. Small molecules that selectively block RNA binding of HIV-1 Rev protein inhibit Rev function and viral production. *Cell* 74:969–976. [https://doi.org/10.1016/0092-8674\(93\)90720-B](https://doi.org/10.1016/0092-8674(93)90720-B).
28. Litovchick A, Evdokimov AG, Lapidot A. 1999. Arginine-aminoglycoside conjugates that bind to HIV transactivation responsive element RNA in vitro. *FEBS Lett* 445:73–79. [https://doi.org/10.1016/S0014-5793\(99\)00092-7](https://doi.org/10.1016/S0014-5793(99)00092-7).
29. Litovchick A, Evdokimov AG, Lapidot A. 2000. Aminoglycoside–arginine conjugates that bind TAR RNA: synthesis, characterization, and antiviral activity. *Biochemistry* 39:2838–2852. <https://doi.org/10.1021/bi9917885>.
30. Mei H-Y, et al. 1995. Inhibition of an HIV-1 Tat-derived peptide binding to TAR RNA by aminoglycoside antibiotics. *Bioorg Med Chem Lett* 5:2755–2760. [https://doi.org/10.1016/0960-894X\(95\)00467-8](https://doi.org/10.1016/0960-894X(95)00467-8).
31. Gopinath S, Kim MV, Rakib T, Wong PW, van Zandt M, Barry NA, Kaisho T, Goodman AL, Iwasaki A. 2018. Topical application of aminoglycoside antibiotics enhances host resistance to viral infections in a microbiota-independent manner. *Nat Microbiol* 3:611–621. <https://doi.org/10.1038/s41564-018-0138-2>.
32. Acevedo MAW, Erickson AK, Pfeiffer JK, Greber UF. 2019. The antibiotic neomycin enhances coxsackievirus plaque formation. *mSphere* 4:e00632-18. <https://doi.org/10.1128/mSphere.00632-18>.
33. Kopaczynska M, Lauer M, Schulz A, Wang T, Schaefer A, Fuhrhop J-H. 2004. Aminoglycoside antibiotics aggregate to form starch-like fibers on negatively charged surfaces and on phage lambda-DNA. *Langmuir* 20:9270–9275. <https://doi.org/10.1021/la049207m>.
34. Kopaczynska M, Schulz A, Fraczkowska K, Kraszewski S, Podbielska H, Fuhrhop JH. 2016. Selective condensation of DNA by aminoglycoside antibiotics. *Eur Biophys J* 45:287–299. <https://doi.org/10.1007/s00249-015-1095-9>.
35. Kieser T, Bibb MJ, Buttner MJ, Chater KF, Hopwood DA. 2000. Practical streptomycetes genetics: a laboratory manual. John Innes Foundation, Norwich, United Kingdom.
36. Bibb MJ. 2013. Understanding and manipulating antibiotic production in actinomycetes. *Biochem Soc Trans* 41:1355–1364. <https://doi.org/10.1042/BST20130214>.
37. McCormick JR, Flårdh K. 2012. Signals and regulators that govern *Streptomyces* development. *FEMS Microbiol Rev* 36:206–231. <https://doi.org/10.1111/j.1574-6976.2011.00317.x>.
38. Rosner A, Gutstein R. 1981. Adsorption of actinophage Pal 6 to developing mycelium of *Streptomyces albus*. *Can J Microbiol* 27:254–257. <https://doi.org/10.1139/m81-039>.
39. Reygaert WC. 2018. An overview of the antimicrobial resistance mechanisms of bacteria. *AIMS Microbiol* 4:482–501. <https://doi.org/10.3934/microbiol.2018.3.482>.
40. Ogawara H. 2019. Comparison of antibiotic resistance mechanisms in antibiotic-producing and pathogenic bacteria. *Molecules* 24:3430. <https://doi.org/10.3390/molecules24193430>.
41. MacNeil DJ, Gewain KM, Ruby CL, Dezeny G, Gibbons PH, MacNeil T. 1992. Analysis of *Streptomyces avermitilis* genes required for avermectin biosynthesis utilizing a novel integration vector. *Gene* 111:61–68. [https://doi.org/10.1016/0378-1119\(92\)90603-M](https://doi.org/10.1016/0378-1119(92)90603-M).
42. Sambrook J, Russell DW. 2001. Molecular cloning: a laboratory manual, 3rd ed. Cold Spring Harbor Laboratory Press, Cold Spring Harbor, NY.
43. Gibson DG. 2011. Enzymatic assembly of overlapping DNA fragments. *Methods Enzymol* 498:349–361. <https://doi.org/10.1016/B978-0-12-385120-8.00015-2>.
44. Kensy F, Zang E, Faulhammer C, Tan RK, Buchs J. 2009. Validation of a high-throughput fermentation system based on online monitoring of biomass and fluorescence in continuously shaken microtiter plates. *Microb Cell Fact* 8:31. <https://doi.org/10.1186/1475-2859-8-31>.
45. Grünberger A, Probst C, Helfrich S, Nanda A, Stute B, Wiechert W, von Lieres E, Nöh K, Frunzke J, Kohlheyer D. 2015. Spatiotemporal microbial single-cell analysis using a high-throughput microfluidics cultivation platform. *Cytometry A* 87:1101–1115. <https://doi.org/10.1002/cyto.a.22779>.
46. Grünberger A, van Ooyen J, Paczia N, Rohe P, Schiendzielorz G, Eggeling L, Wiechert W, Kohlheyer D, Noack S. 2013. Beyond growth rate 0.6: *Corynebacterium glutamicum* cultivated in highly diluted environments. *Bio-technol Bioeng* 110:220–228. <https://doi.org/10.1002/bit.24616>.
47. Helfrich S, Pfeifer E, Krämer C, Sachs CC, Wiechert W, Kohlheyer D, Nöh K, Frunzke J. 2015. Live cell imaging of SOS and prophage dynamics in isogenic bacterial populations. *Mol Microbiol* 98:636–650. <https://doi.org/10.1111/mmi.13147>.
48. Barrero-Canosa J, Moraru C. 2021. Linking microbes to their genes at single cell level with direct-geneFISH. *Methods Mol Biol* 2246:169–205. https://doi.org/10.1007/978-1-0716-1115-9_12.
49. Moraru C. 2021. Gene-PROBER—a tool to design polynucleotide probes for targeting microbial genes. *Syst Appl Microbiol* 44:126173. <https://doi.org/10.1016/j.syapm.2020.126173>.
50. Schindelin J, Arganda-Carreras I, Frise E, Kaynig V, Longair M, Pietzsch T, Preibisch S, Rueden C, Saalfeld S, Schmid B, Tinevez J-Y, White DJ, Hartenstein V, Eliceiri K, Tomancak P, Cardona A. 2012. Fiji: an open-source platform for biological-image analysis. *Nat Methods* 9:676–682. <https://doi.org/10.1038/nmeth.2019>.
51. Allaire J. 2012. RStudio: integrated development environment for R. RStudio, Boston, MA.
52. R Core Team. 2021. R: a language and environment for statistical computing. R Foundation for Statistical Computing, Vienna, Austria.
53. Pfeifer E, Hünnefeld M, Popa O, Polen T, Kohlheyer D, Baumgart M, Frunzke J. 2016. Silencing of cryptic prophages in *Corynebacterium glutamicum*. *Nucleic Acids Res* 44:10117–10131. <https://doi.org/10.1093/nar/gkw692>.
54. Laemmli UK. 1970. Cleavage of structural proteins during the assembly of the head of bacteriophage T4. *Nature* 227:680–685. <https://doi.org/10.1038/227680a0>.

Acknowledgments

3.3 Antiphage molecules produced by bacteria – beyond protein-mediated defenses

Hardy A., Kever L., and Frunzke J.

Review article part of this thesis; to be submitted

CONTRIBUTOR ROLE	CONTRIBUTOR
Conceptualization	AH (60%), JF (30%), LK (10%)
Data curation	AH (95%), LK (5%)
Formal analysis	-
Funding acquisition	JF (100%)
Investigation	AH (90%), LK (5%), JF (5%)
Methodology	AH (65%), JF (30%), LK (5%)
Project administration	AH (90%), JF (10%)
Resources	-
Software	-
Supervision	AH (60%), JF (40%)
Validation	AH (70%), LK (20%), JF (10%)
Visualization	LK (80%), VS (15%), JF (5%)
Writing – original draft	AH (95%), JF (5%)
Writing – review & editing	JF (60%), AH (30%), LK (10%)

Overall contribution AH: 85%

Antiphage molecules produced by bacteria – beyond protein-mediated defenses

Aël Hardy, Larissa Kever, and Julia Frunzke*

Institute of Bio- und Geosciences, IBG-1: Biotechnology, Forschungszentrum Jülich, 52425 Jülich, Germany

*Corresponding author:

Julia Frunzke; Email: j.frunzke@fz-juelich.de; Phone: +49 2461 615430

Keywords: bacteriophages, natural products, phage defense, chemical defense, phage-host interaction, bacterial immunity

Abstract

Bacterial populations face the constant threat of viral predation exerted by bacteriophages (or phages). In response, bacteria have evolved a wide range of defense mechanisms against phage challenges. Yet the vast majority of antiphage defense systems described until now are mediated by proteins or RNA complexes acting at the cellular level. Here, we review small molecule-based defense strategies against phage infection, with a focus on the antiphage molecules described recently. Importantly, inhibition of phage infection by excreted small molecules has the potential to protect entire bacterial communities, highlighting the ecological significance of these antiphage strategies. Considering the immense repertoire of bacterial metabolites, we envision that the list of antiphage small molecules will be further expanded in the future.

Introduction

Bacteriophages (or phages for short) are viruses preying on bacteria and are considered to be the most abundant biological entities in the biosphere¹. They represent a ubiquitous feature of bacterial existence, as there is virtually no ecosystem where bacteria do not coexist with phages infecting them¹. The strong evolutionary pressure imposed by phage predation has led to a sophisticated arsenal of antiphage strategies, which have been extensively reviewed elsewhere²⁻⁵. The repertoire of known defense systems has been significantly expanded through large-scale bioinformatics screenings followed by experimental validation^{6,7}. In addition to the already known defense systems such as restriction-modification systems, CRISPR-Cas or abortive infection, antiviral strategies now include the use of cyclic nucleotides as signalling molecules (CBASS⁸, Pycsar⁹) and NAD⁺ depletion as a widespread response to viral infection¹⁰⁻¹³. Scrutiny of these novel antiphage defense systems revealed striking similarities to eukaryotic immune systems, suggesting that a previously underappreciated fraction of eukaryotic immunity evolved from prokaryotic antiphage defenses^{8,10,14-16}. With the accelerating pace of discovery of new antiphage systems, keeping an overview of the currently known antiviral prokaryotic arsenal has become increasingly difficult, but has been facilitated by the development of tools aimed at systematic and comprehensive identification of defense systems in prokaryotic genomes^{17,18}. The notion of a bacterial pan-immune system

has been recently proposed to recognize phage defense as a community resource distributed between closely related bacteria via horizontal gene transfer (HGT)¹⁹.

In nature, bacteria live in complex, spatially structured and multispecies communities²⁰, which highlights the need to consider antiphage strategies at the community level. These mechanisms include the release of extracellular vesicles^{21,22}, formation of protective biofilm structures^{23,24} or quorum sensing^{25–27}. Chemical inhibition of phages using small molecules secreted in the extracellular medium represents another effective multicellular strategy against phage infection, which unlike most defense systems described until now does not rely on proteins or RNA.

The direct inhibition of phage infection by bacterial small molecules was an intense research field in the 1950s and 1960s and has recently regained significant attention. Here, we aim at summarizing the extensive but largely overlooked body of research in the field of antiphage molecules and present the latest developments in this emerging research area. Furthermore, we outline future perspectives for the discovery of novel antiphage metabolites and discuss the ecological significance of this defense strategy.

The present review aims at presenting small molecules other than RNAs and proteins that confer protection against phage infection. As a result, antibiotics preventing phage infection by a primary action on the bacterium (e.g. inhibition of bacterial transcription by rifampicin²⁸) are not included.

Chemical defense against phage infection

Overall, the study of antiphage molecules has known two distinct periods of interest – the first one spanning the third quarter of the twentieth century while the second started only a few years ago.

The interest to find new compounds active against phages was very strong in the 1950s^{29–31}, with in some cases heroic screening efforts such as those performed by Schatz and Jones or Asheshov and colleagues—who assessed the antiphage activity of more than 170 and 1000 strains of actinomycetes, respectively^{29,30}. In these screenings, the supernatants of 29% (49/176) and 17% (144/1000) of the tested actinomycete isolates caused an inhibition of

plaque formation, suggesting that the release of antiphage metabolites is not uncommon in actinobacteria.

The primary goal of these screenings was however not to understand how bacteria defend themselves against phages, but rather to find new antiviral drugs usable in a clinical or agricultural setting³¹. An additional focus was put on substances able to specifically prevent phages from infecting *Streptomyces griseus* because of the risk phages posed to industrial production of streptomycin by this important production host³².

Over the decades, a significant number of molecules were described to have antiphage properties. We listed these antiphage compounds in Table 1, which includes the phages inhibited and the proposed mechanism of action. In the following, we focus on the three main classes of antiphage small molecules described to date: anthracyclines, aminoglycosides and modified nucleotides produced by prokaryotic viperins.

Anthracyclines

Anthracyclines are secondary metabolites naturally produced by *Streptomyces*—a common genus of soil-dwelling bacteria. Anthracyclines are DNA-intercalating agents which have been largely used in cancer chemotherapy³³, and are among the most effective anticancer treatments ever developed^{34–36}. The precise mechanism behind their cytotoxic effect in eukaryotic cells is still subject to debate. However, their antitumour activity can be broadly attributed to their ability to intercalate into the DNA helix and/or bind covalently to proteins involved in DNA replication and transcription³⁷.

Multiple reports described the inhibition of phage infection by anthracyclines such as daunorubicin, doxorubicin or cosmomycin (**Table 1**). Parisi and Soller assessed the impact of daunomycin on the steps of the lytic cycle and showed a strong impairment of phage DNA synthesis during phage infection, suggesting a blockage occurring during replication or between injection and replication³⁸.

A major step forward in the understanding of both the mechanism and biological significance of the antiphage properties of anthracyclines was made more than 40 years later by Kronheim and colleagues³⁹. In this study, the authors show that daunorubicin inhibits phage λ in *E. coli*

as well as several double-stranded DNA (dsDNA) phages infecting *E. coli*, *Streptomyces coelicolor* or *Pseudomonas aeruginosa* and encompassing the three main families of tailed phages (*Siphoviridae*, *Podoviridae* and *Myoviridae*). The exact mechanism of action remains unclear, but inhibition by daunorubicin takes place at an early stage of the infection cycle, namely after injection of the phage genome but before phage replication (**Figure 1**). All dsDNA phages tested - whose incoming genome is linear - are inhibited by daunorubicin. In contrast, the filamentous M13 phage, whose ssDNA genome enters as a circular molecule, is not, suggesting that the circularization of incoming linear dsDNA could be the step blocked by daunorubicin. The anthracyclines doxorubicin and cosmomycin D were also shown to have antiphage properties. Importantly, the inhibition of phage infection could be reproduced with supernatants from natural producers of these anthracyclines (*Streptomyces peucetius* for daunorubicin and doxorubicin; strains of the WAC collection⁴⁰ for cosmomycin D, respectively). This observation suggests that phage inhibition by anthracyclines is physiologically relevant in the natural environment.

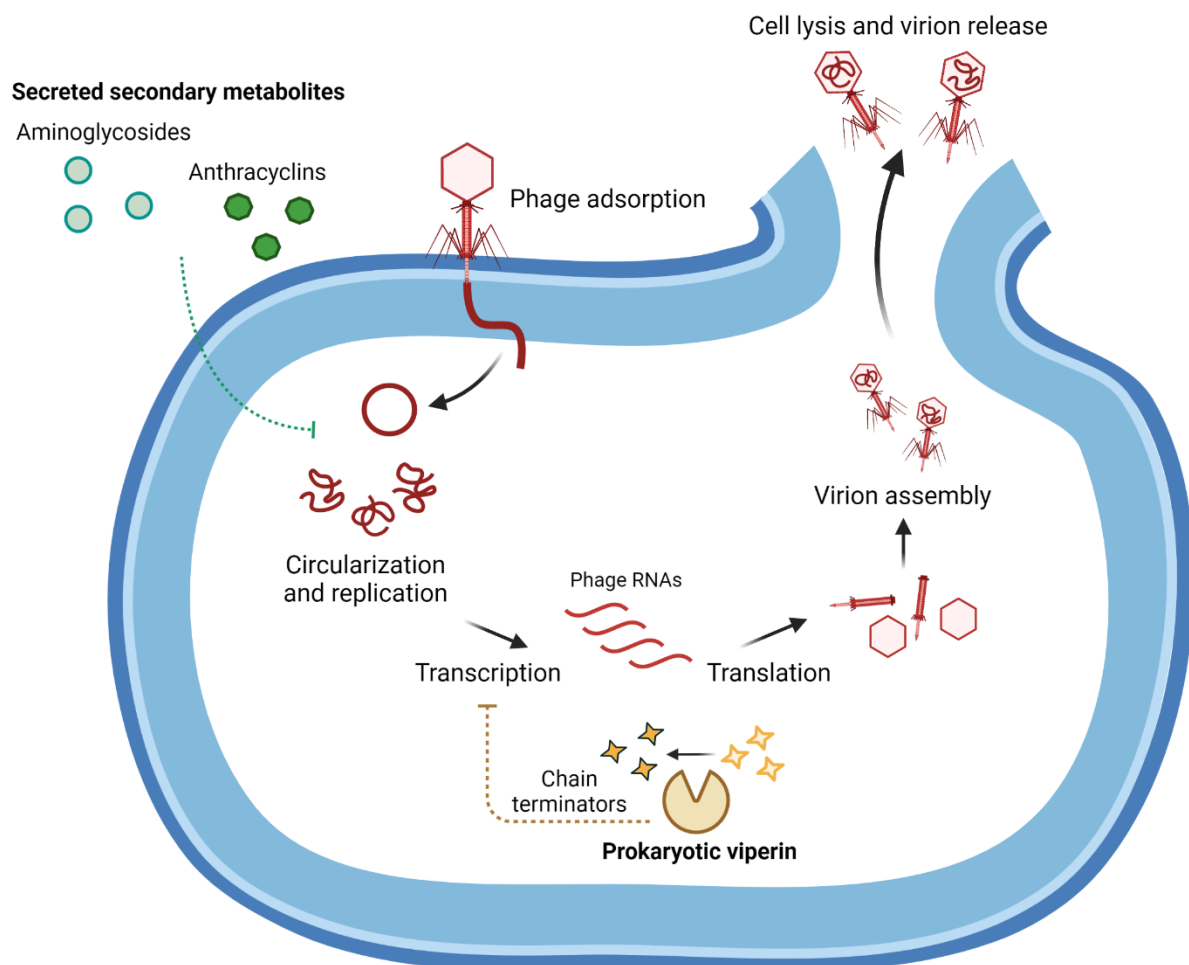


Figure 1 | Mechanism of action of the antiphage molecules anthracyclines, aminoglycosides and modified ribonucleotides produced by prokaryotic viperin homologs (pVips). The phage replication cycle comprises several steps, some of which being targeted by antiphage molecules. Unlike the modified ribonucleotides produced by pVips, anthracyclines and aminoglycosides are secreted by producer cells and can be taken up by neighbouring cells.

Kronheim and colleagues also reported the antiphage properties of synthetic DNA-intercalating agents such as propidium iodide or acridine derivatives³⁹. Further, the inhibition of *E. coli* phage T2 by actinomycin D - another DNA-intercalating agent produced by *Streptomyces* - was already described in 1961⁴¹. Altogether, this suggests that intercalation into phage DNA is probably a widespread antiphage strategy (Table 1).

Aminoglycosides

Aminoglycosides are bactericidal antibiotics that are active against Gram-negative and Gram-positive organisms^{42,43}. They disrupt protein biosynthesis by targeting the 30S subunit of the ribosomes, which in turns leads to complete blockage of translation or promotes mistranslation⁴⁴. Aminoglycosides were originally isolated from actinomycetes belonging to the *Streptomyces* and *Micromonospora* genera⁴⁵. In nature, aminoglycoside producers are resistant to these molecules, which is a feature important to keep in mind when screening aminoglycosides—and small molecules in general—for antiviral properties.

Using bacterial hosts expressing plasmid-borne aminoglycoside resistance cassettes, aminoglycosides were recently shown to inhibit phages infecting the Gram-negative bacteria *E. coli* as well as Gram-positive bacteria such as *Corynebacterium glutamicum* and *Streptomyces venezuelae*⁴⁶. Experiments aiming at shedding light on the molecular mechanism of phage infection inhibition revealed that phage DNA was present inside cells in the presence of aminoglycosides. Together with the observation that amplification of phage DNA was strongly impaired, these results suggest that the blockage exerted by aminoglycosides mostly occurs after DNA injection but before genome replication (Figure 1). These results are in line with those obtained by Jiang and colleagues, who reported the inhibition of the two mycobacteriophages phAE159 and D29 by kanamycin, hygromycin and streptomycin⁴⁷. Following the impact of streptomycin on phage adsorption and amplification

of phage DNA, the authors propose that the blockage caused by aminoglycosides occurs between genome circularization and replication.

One important question is whether this inhibition of phage infection by aminoglycosides is relevant in a physiological context. In the case of apramycin, inhibition of the *Streptomyces* phage Alderaan could be reproduced with supernatants of the natural producer of apramycin, *Streptoalloteichus tenebrarius* (formerly known as *Streptomyces tenebrarius*⁴⁸). Apparition of the antiphage effect of supernatants coincided with the detection of apramycin in the culture supernatants. In combination with the antiphage effect of purified apramycin, these data strongly suggest that the main molecule behind the antiphage properties of the supernatants of *S. tenebrarius* is apramycin⁴⁶. Additionally, it indicates that aminoglycosides are secreted by producers at levels which prevent infection in neighbouring bacteria, opening the door to community-wide protection.

In a natural context, most bacteria do not possess aminoglycoside-resistance genes, and residual concentrations of antibiotics are pervasive across man-shaped and natural environments alike. Zuo and colleagues studied the impact of sublethal concentrations of aminoglycosides on phage infection in aminoglycoside-sensitive hosts⁴⁹. Phage amplification was strongly impeded by concentrations as low as 3 mg/L. Interestingly, tetracycline, another antibiotic blocking protein synthesis by binding to the 30S ribosomal subunit, had a significantly reduced impact on phage proliferation. These results suggest that blockade of translation alone is not sufficient to efficiently prevent phage replication. Alternatively, the mechanism of translation inhibition may be of importance, and the mistranslation caused by tetracycline could participate in the difference of impact observed with aminoglycosides⁴⁹.

Although the action of aminoglycosides on the phage life cycle *in vivo* is not fully understood yet, separate *in vitro* studies provide further hints about the basis of aminoglycosides' antiphage properties. Exposure of purified phage λ DNA to aminoglycosides leads to condensation of DNA, presumably coated by aminoglycoside fibers⁵⁰. The same authors later proposed that aminoglycosides form a clamp around the DNA double helix, causing a bend responsible for the formation of structural deformations such as toroids⁵¹.

In vivo mechanistic studies about the inhibition of phage infection by aminoglycosides are scarce, but Brock and his collaborators contributed work worthy of attention. Using

Streptococcus faecium and its phage P9, Brock and Wooley investigated the inhibition of phage infection by streptomycin⁵². The authors used resistance to shearing forces as an indicator for DNA injection, under the assumption that the formation of a plaque from an initially infected cell subjected to shearing implies a successful delivery of the phage genome. Using this technique, they proposed that streptomycin inhibits phage infection at an early stage of the phage infection cycle, namely the DNA injection step. They further hypothesized that streptomycin exerts its inhibition by binding phage DNA in the capsid, thus preventing its unfolding necessary for infection. It is however important to note that although phage infection could already be inhibited by concentration of 100 µg/ml, high concentrations of streptomycin were used (1 mg/ml) in most experiments. Such high concentration could cause non-specific effects such as phage precipitation potentially not present at lower concentrations. Moreover, the streptomycin-resistant bacterial host was reported to bind very low amounts of streptomycin, which suggests modifications of the cell surface that could in turn influence the antiphage properties of streptomycin. In another study, Brock demonstrated the inhibitory effect of streptomycin on the *E. coli* RNA phage MS-2⁵³. Streptomycin inhibited the formation of phage progeny very early in the replication cycle (5 to 10 minutes after infection), and no impact of streptomycin was noticed when added shortly after injection has occurred.

The fact that aminoglycosides possess both antibacterial and antiviral properties raises the question of the interplay between these two facets. In the case of apramycin, acetylation of one of its amino groups by the well-studied apramycin acetyltransferase AAC(3)IV abolished its impact of bacterial growth, while fully retaining its protective effect against phages⁴⁶. This observation suggests that the antibacterial and antiviral actions of apramycin and potentially further aminoglycosides could be decoupled from one another and that the respective molecular targets are distinct.

Taken together, these studies suggest that aminoglycosides are not only used by their producers as toxic molecules against bacterial competitors but could serve as protection against the threat of phage predation at the community level.

Viperins

Viperins are important players of the innate antiviral response in eukaryotes⁵⁴. They produce ddhCTP, a modified ribonucleoside lacking the 3'-hydroxyl group necessary for elongation of the nascent viral mRNA, hence acting as chain terminators⁵⁵.

Viperin-like genes were known to be present in prokaryotes too, but the function of these prokaryotic viperin homologs (pVips) remained unknown. Recently, they were shown to protect archaea and bacteria from viral infection and displayed a remarkable conservation between the eukaryotic and prokaryotic kingdoms¹⁴. pVips use indeed a similar mode of action to their eukaryotic homologs to inhibit viral transcription (Figure 1)—except that pVips produce a wider range of modified ribonucleotides (ddhCTP but also ddhGTP and ddhUTP)¹⁴. Strikingly, the human viperin, when expressed in *E. coli*, conferred resistance to phage infection, which underlines inhibition of viral transcription as a broad antiviral strategy. Interestingly, inhibition of phage infection was also observed with phages like P1 and λ which do not encode their own RNA polymerases and rely instead on the host polymerase to complete transcription. This raises the possibility that pVips also exert their antiviral activity independently of premature termination of viral transcripts, via mechanisms which remain to be elucidated.

Mirroring the absence of toxic effects caused by human viperin in human cells, expression of pVips in *E. coli* had no effect on host transcription and did not cause toxicity. This observation hints that the bacterial RNA polymerase may be less sensitive than the phage RNA polymerase to ddh-ribonucleotides, as self-resistance to the ddh-ribonucleotides would be favored during co-evolution of bacterial RNA polymerase and pVips. In contrast to anthracyclines and aminoglycosides, the modified nucleotides synthesized by viperins are not secreted but protection is conferred at the cellular level.

Perspectives

Discovery of novel antiphage small molecules

Until now, the antiphage effect of most molecules were either discovered empirically or based on earlier reports describing antiphage properties of the same or closely related

molecules. However, recent progress in the fields of genomics, metabolomics and automation have the potential to greatly accelerate the discovery of new antiviral molecules.

Automated screening allows high-throughput testing of the antiphage properties of molecule libraries (**Figure 2**). To this end, bacteria are cultivated in microtiter plates, either alone, in the presence of phages, or together with both phages and the compounds to be tested. If the addition of a given compound suppresses the phage-mediated lysis of the culture, this hit indicates a probable inhibition of phage infection by this molecule, warranting further investigation. This strategy was successfully used with *E. coli* and phage λ to reveal the antiphage activity of anthracyclines and other DNA-intercalating agents³⁹. One major limitation of this approach is that the compounds tested need to not interfere with the growth of the bacterium, since strong growth defects would prevent the detection of antiphage effects.

Alternatively, spotting the molecules of interest on a phage-infected bacterial lawn represents another screening strategy with potential for automation and upscaling (Figure 2). This technique has been used for decades to assess antibacterial activity of antibiotics and has been harnessed by phage researchers too^{56–58}. It enables the appreciation of antiphage effects (or on the contrary phage antibiotic synergy) despite inhibition of bacterial growth, as shown by rings devoid of plaque formation—or displaying larger plaques, respectively—around the zone of growth inhibition caused by the candidate molecule.

These two strategies are not restricted to pure compounds and can also be used with complex supernatants from bacterial hosts, enabling the exploration of a vaster metabolic landscape as well as of potential synergistic interactions between candidate molecules. In the case where a supernatant inhibits phage infection, bioactivity-guided fractionation followed by liquid chromatography–mass spectrometry (LC-MS) can narrow the antiphage properties of the supernatant down to one or a few compounds³⁹.

These screening approaches are likely to have a low discovery rate due to their untargeted nature. Screening can be narrowed down by testing in priority metabolites released in reaction to phage infection. For example, phage infection in *Streptomyces coelicolor* leads to the formation of coloured halos around phage plaques. The presence of pigmented

compounds at the infection interface suggests that *Streptomyces* reacts to phage infection by releasing these molecules, making them interesting candidates for further analysis⁵⁹.

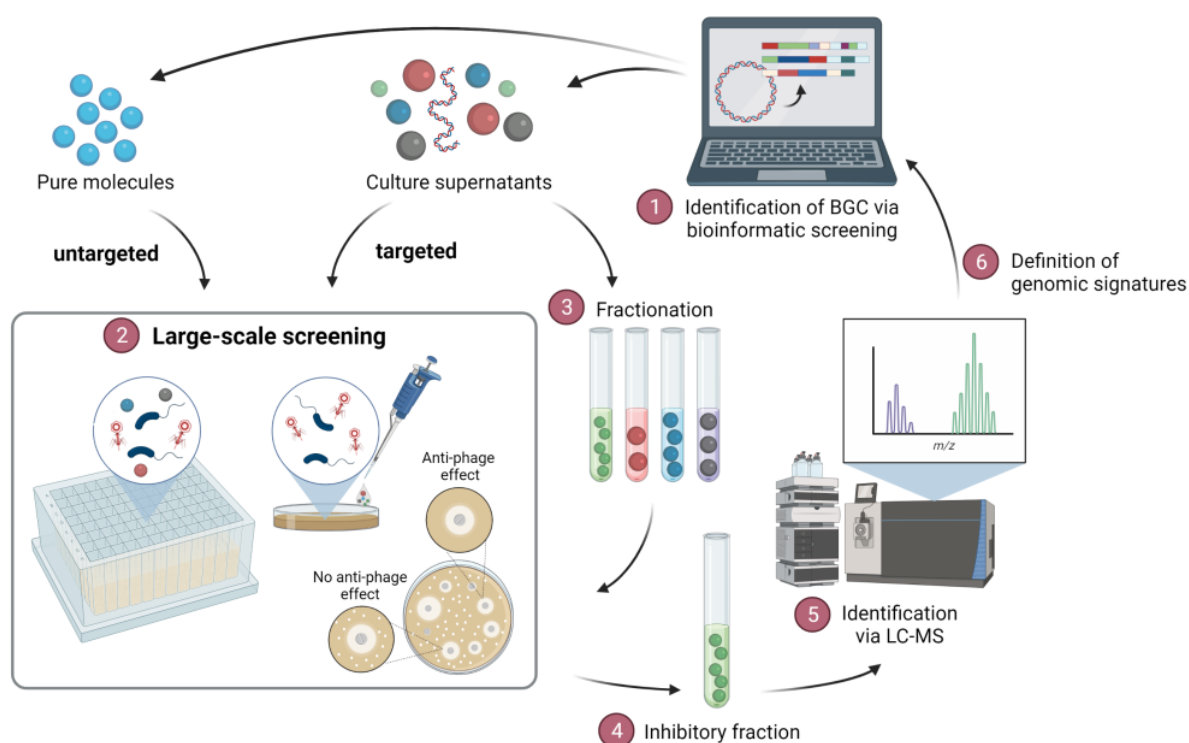


Figure 2 | Discovery strategies for the identification of new antiphage molecules. Bioinformatic prediction of candidate biosynthetic gene clusters (BGCs) whose products may act against phages (1) informs large-scale testing of small molecule libraries as well as complex supernatants (2). The elucidation of the antiphage compounds can be achieved by bioactivity-guided fractionation (3 and 4) followed by analytic techniques such as liquid chromatography–mass spectrometry (LC-MS) (5). Results of the screening efforts can be then fed back to the bioinformatic screening to help define genomic features of antiphage BGCs (6).

In silico prediction of genomic signatures of gene clusters involved in chemical antiphage defense would allow to rationally identify and test candidate molecules. However, antiphage biosynthetic gene clusters (BGCs) such as the ones encoding aminoglycosides and anthracyclines are not detected using the now well-established “guilty-by-association” approach. This discovery strategy is based on the observation that defense systems are clustered in genomic “defense islands”. Genes markedly enriched in the vicinity of known defense genes are therefore assumed to be also involved in antiphage defense⁶. The use of

this concept has led in recent years to a considerable expansion of the known repertoire of antiphage defense systems^{6,7,14}. It is however biased towards small and very well conserved genes, explaining why this approach did not detect large and genus- or sometimes even species-specific BGCs as putative novel antiphage defense systems. Now that tools systematically screening for known defense systems are available^{17,18}, combining detection of phage defense systems and prediction of BGCs could reveal interesting patterns of co-occurrence and help to define genomic features of antiphage BGCs. In the case of antiphage metabolites fulfilling several roles (e.g. antibacterial and antiviral) such as aminoglycosides, these supplementary functions likely impose further genomic and evolutionary constraints, hindering the establishment of genomic signatures for gene clusters encoding multifunctional molecules.

Importantly, empirical approaches and *in silico* screening are not mutually exclusive; uncovering more antiphage secondary metabolites will help to define genomic signatures for antiphage molecules. Although recent and historical efforts focused on molecules produced by actinobacteria, many other bacterial phyla, such as myxobacteria^{60,61} or planctomycetes^{62,63} to name only a few, possess elaborate BGC arsenals which represent promising sources for the discovery of novel antiviral molecules.

Ecological relevance

The ecological significance of antiphage molecules was mostly ignored in the first wave of research focusing on antiphage molecules and has only been recently appreciated. One interesting feature of antiphage molecules described so far is their broad inhibition, as both anthracyclines and aminoglycosides inhibit seemingly very disparate phages infecting diverse bacteria, Gram-positive and negative alike. So far, the rules behind the sensitivity of a given phage to these two classes of compounds remain unclear, the only common feature of the inhibited phages being their double-stranded DNA genome and tailed morphology. This broad range of inhibition has important ecological implications: depending on their local concentrations and diffusion, these antiphage compounds could serve as ‘public goods’ and protect not only producer cells but also neighboring, unrelated cells—provided they are

resistant to these compounds (**Figure 3**). These implications further highlight the key role of spatial structure and biofilms when considering bacterial communities.

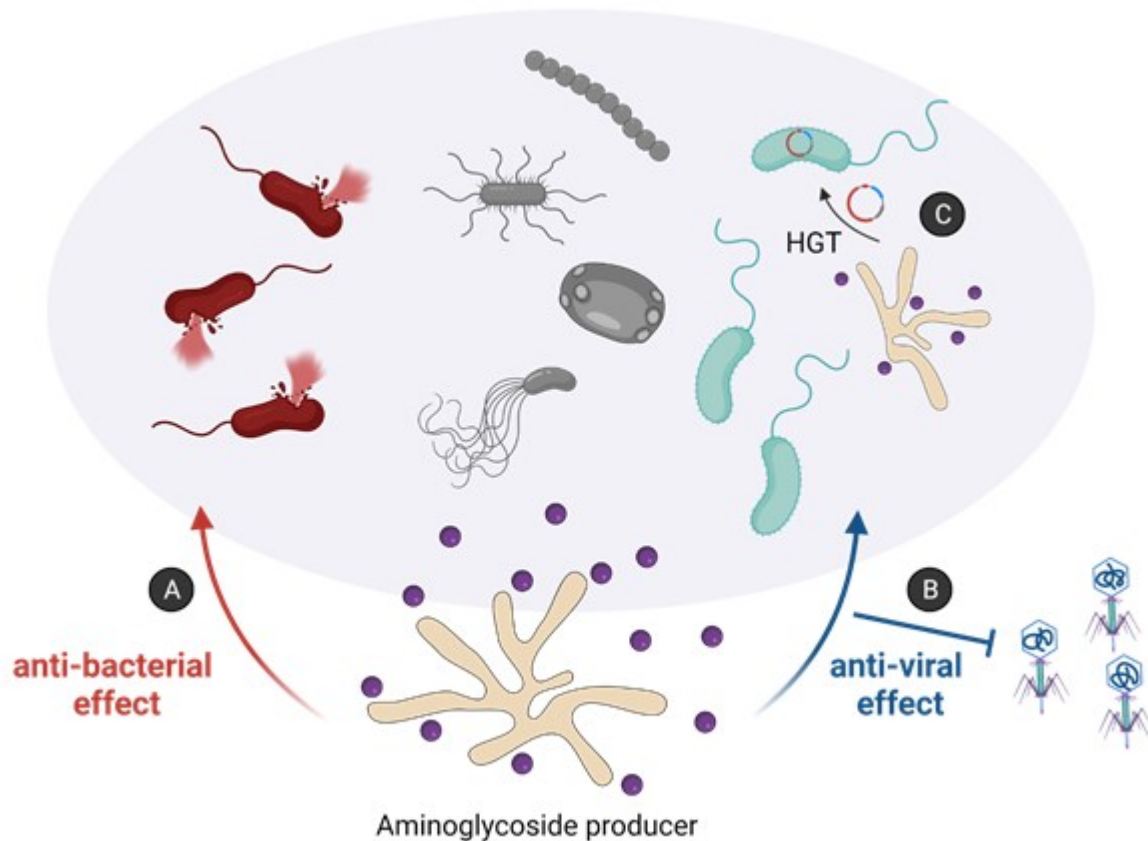


Figure 3 | Ecological significance of the dual properties of aminoglycosides in a bacterial community. Aminoglycoside producers release aminoglycosides (purple) in their environment. Aminoglycosides kill sensitive bacteria (antibacterial effect, A) while they may protect neighbouring bacteria from phage infection (antiviral effect, B), provided they are resistant to these molecules e.g. via prior horizontal gene transfer (HGT) of resistance genes from producer cells (C). Bystander microorganisms not affected by aminoglycosides are shown in grey.

The dual function of certain antiphage molecules adds another layer of complexity. For instance, aminoglycosides represent a remarkable example of molecular multitasking, with the same molecules exerting two seemingly unrelated effects—inhibition of bacterial translation and of phage replication.

Furthermore, acquisition of resistance to aminoglycosides by initially sensitive cells is highly beneficial for two reasons: not suffering from their antibacterial effect anymore while

benefiting from the inhibition of phage infection. Naturally, the mode of resistance to these antibiotics is of particular importance. Considering that aminoglycosides are thought to act intracellularly to block phage infection, resistance mechanisms based on decreased aminoglycoside intracellular concentration—such as decreasing uptake or expressing efflux pumps—would confer resistance to the antibiotic at the expense of the loss of its protective antiphage effect. With the aminoglycoside apramycin, it was shown that acetylation of one of its amino groups suppresses its antibacterial effect while retaining its antiphage properties⁴⁶. Whether this example is a unique case or is a general feature of aminoglycoside modifications remains to be determined. However, this observation could explain the wide distribution of aminoglycoside-modifying enzymes catalyzing, for example, the acetylation, phosphorylation or adenylation of amino or hydroxyl groups at various positions of the aminoglycoside scaffold⁶⁴.

To fully appreciate the ecological significance of chemical defense against phages, moving away from the traditional “one phage – one bacterium” approach represents a key step. Building simplified, synthetic communities by increasing phage and/or bacterial diversity can provide decisive insights into the physiology of antiphage defense strategies, as shown for example with the importance of CRISPR-mediated phage resistance over modifications of the phage receptor in complex microbial communities⁶⁵. Yet, additional mechanistic insights are required to understand the impact of antiphage molecules on community interactions.

Finally, one further direction worthy of investigation is the study of the interplay between the different defense systems—small molecule- and protein-based. Producers of antiphage molecules also encode other defense systems. Our current knowledge about how prokaryotes coordinate these diverse antiphage strategies to mount efficient antiviral responses is still in its infancy and needs to be advanced to provide an integrated view of the prokaryotic immune system.

Concluding Remarks

Phage defense systems are often considered at the level of the individual cell, where it is mechanistically described how they protect a bacterium from being infected by an incoming

phage. By acting at the cellular level, antiphage strategies prevent the spread of the infection and thereby protect the broader bacterial community. However, some mechanisms specifically protect several cells or the entire population simultaneously. One of these consists in the release of small molecules into the extracellular environment. The antiphage metabolites described until now predominantly correspond to anthracyclines and aminoglycosides, both inhibiting the early steps of the phage infection cycle. Interestingly, aminoglycosides are well-known antibacterial agents, but were also shown to be potent inhibitors of phage infection, suggesting that evolutionary constraints allowed the development of two seemingly very distinct functions.

From a therapeutic standpoint, antiviral metabolites in bacteria have the potential to fuel the discovery pipeline for novel antiviral drugs in humans. For example, synthetic nucleoside chain terminators are widely used in conditions such as HIV^{66,67} or infection with herpes viruses⁶⁸ and chain terminators produced by pVips could represent new avenues for treatments of viral infections in humans¹⁴. Knowledge gained about small molecule-mediated inhibition of phage infection is also relevant for phage therapy, e.g. to avoid antagonistic effects when administering phage-antibiotic combination treatments.

The repertoire of bacterial secondary metabolites is extremely large, and the physiological function of many of these compounds remains unclear. We can thus hypothesize that the number of described antiphage molecules will keep growing in the future. For example, molecules triggering death of parts of the bacterial population represent promising candidates, as their release in reaction to phage predation would mimic the effect of protein-mediated abortive infection (Abi) systems.

Phages have developed ways to circumvent most bacterial defense strategies, as part of the arms race in which they are engaged with their bacterial hosts. It is therefore plausible that phages have evolved means to overcome this metabolite-based defense system. Elucidating these adaptations could illuminate phage biology by attributing a function to certain already known phage features and further our understanding of the intricate relationships between phages and their bacterial hosts in the context of chemical defense.

Acknowledgements

Research in the Frunzke Lab is supported by the European Research Council (ERC Starting Grant 757563) and the Deutsche Forschungsgemeinschaft (SPP 2330, project 464434020). We thank Aude Bernheim for critical reading of the manuscript. Figures were created using BioRender.com.

Highlights

- Bacteria are prolific metabolite producers, but the role of this metabolite diversity in protection against phages has been only recently appreciated.
- Anthracyclines, aminoglycosides and chain terminators produced by prokaryotic viperins represent the main classes of antiphage small molecules known to date.
- Aminoglycosides possess both antibacterial and antiphage properties, this dual function making them an interesting example of molecular multitasking.
- Secreted antiphage metabolites have the potential to protect bacterial communities, serving as multicellular defense strategy.

Glossary

Aminoglycosides

Antibacterials naturally produced by *Streptomyces* and *Micromonosporas* species. They target bacterial translation by binding to the 30S ribosomal subunit. Besides their antibacterial action, additional antiphage properties were recently discovered.

Anthracyclines

DNA-intercalating antibiotics produced by *Streptomyces* having antitumor as well as antiphage properties.

Bacteriophages

Viruses that prey on bacteria.

Bioactivity-guided fractionation

Chromatographic separation of extracts aiming at the isolation of a pure biologically active compound.

Chemical defense

Protection against phage infection via bacterial small molecules.

Streptomyces

Genus of Gram-positive bacteria which belongs to the phylum of Actinobacteria. *Streptomyces* species are mainly found in the soil and are characterized by mycelial development as well as by their complex secondary metabolism. *Streptomyces* are one of the most important producers of bioactive molecules.

Viperins

Virus-inhibitory proteins in eukaryotes which convert ribonucleotides into chain terminators, thereby preventing transcription of viral genes. Viperin homologs are found in prokaryotes and are known as prokaryotic viperins (pVips). pVips inhibit phage infection in a similar mode of action than their eukaryotic counterparts.

Outstanding questions

- What is the exact mechanism of action underlying the antiviral activity of anthracyclines and aminoglycosides?

Publications and manuscripts

- How did the dual antibacterial and antiviral functions of aminoglycosides shape the evolution of these molecules?
- To what extent do secreted antiphage molecules confer protection at the community level?
- Can genomic signatures be determined for antiphage biosynthetic gene clusters?
- Is chemical defense against phages a conserved defense strategy across bacteria?

Figures & Tables

Table 1: List of molecules with known antiphage properties, including the phages inhibited and the proposed mechanism of action (when available)

Figure 1: Mechanism of action of antiphage molecules (anthracyclines, aminoglycosides and prokaryotic viperin homologs (pVips)). The phage replication cycle comprises several steps, some of which being targeted by antiphage molecules. Unlike the modified ribonucleotides produced by pVips, anthracyclines and aminoglycosides are secreted by producer cells and can be taken up by neighbouring cells.

Figure 2: Discovery strategies for the identification of new antiphage molecules. Bioinformatic prediction of candidate biosynthetic gene clusters (BGCs) whose products may act against phages (1) inform large-scale testing of small molecule libraries as well as complex supernatants (2). The elucidation of the antiphage compounds can be achieved by bioactivity-guided fractionation (3 and 4) followed by analytic techniques such as liquid chromatography–mass spectrometry (LC-MS) (5). Results of the screening efforts can be then fed back to the bioinformatic screening to help define genomic features of antiphage BGCs (6).

Figure 3: Ecological significance of the dual properties of aminoglycosides in a bacterial community. Aminoglycoside producers release aminoglycosides (purple) in their environment. Aminoglycosides kill sensitive bacteria (antibacterial effect, A) while they may protect neighbouring bacteria from phage infection (antiviral effect, B), provided they are resistant to these molecules e.g. via prior horizontal gene transfer (HGT) of resistance genes from producer cells (C). Bystander microorganisms not affected by aminoglycosides are shown in grey.

References

1. Clokie, M. R., Millard, A. D., Letarov, A. V. & Heaphy, S. Phages in nature. *Bacteriophage* **1**, 31–45 (2011).
2. Rostøl, J. T. & Marraffini, L. (Ph)ighting Phages: How Bacteria Resist Their Parasites. *Cell Host & Microbe* **25**, 184–194 (2019).
3. Stern, A. & Sorek, R. The phage-host arms race: Shaping the evolution of microbes. *BioEssays* **33**, 43–51 (2011).
4. Hampton, H. G., Watson, B. N. J. & Fineran, P. C. The arms race between bacteria and their phage foes. *Nature* **577**, 327–336 (2020).
5. Dy, R. L., Richter, C., Salmond, G. P. C. & Fineran, P. C. Remarkable Mechanisms in Microbes to Resist Phage Infections. *Annu. Rev. Virol.* **1**, 307–331 (2014).
6. Doron, S. *et al.* Systematic discovery of antiphage defense systems in the microbial pangenome. *Science* **359**, (2018).
7. Gao, L. *et al.* Diverse enzymatic activities mediate antiviral immunity in prokaryotes. *Science* **369**, 1077–1084 (2020).
8. Cohen, D. *et al.* Cyclic GMP–AMP signalling protects bacteria against viral infection. *Nature* **574**, 691–695 (2019).
9. Tal, N. *et al.* Cyclic CMP and cyclic UMP mediate bacterial immunity against phages. *Cell* **184**, 5728–5739.e16 (2021).
10. Ofir, G. *et al.* Antiviral activity of bacterial TIR domains via immune signalling molecules. *Nature* **600**, 116–120 (2021).
11. Garb, J. *et al.* Multiple phage resistance systems inhibit infection via SIR2-dependent NAD⁺ depletion. 2021.12.14.472415

- <https://www.biorxiv.org/content/10.1101/2021.12.14.472415v1> (2021)
doi:10.1101/2021.12.14.472415.
12. Zaremba, M. *et al.* *Sir2-domain associated short prokaryotic Argonautes provide defence against invading mobile genetic elements through NAD⁺ depletion.* 2021.12.14.472599
<https://www.biorxiv.org/content/10.1101/2021.12.14.472599v1> (2021)
doi:10.1101/2021.12.14.472599.
13. Tal, N. & Sorek, R. SnapShot: Bacterial immunity. *Cell* **185**, 578-578.e1 (2022).
14. Bernheim, A. *et al.* Prokaryotic viperins produce diverse antiviral molecules. *Nature* **589**, 120–124 (2021).
15. Morehouse, B. R. *et al.* STING cyclic dinucleotide sensing originated in bacteria. *Nature* **586**, 429–433 (2020).
16. Wein, T. & Sorek, R. Bacterial origins of human cell-autonomous innate immune mechanisms. *Nat Rev Immunol* (2022) doi:10.1038/s41577-022-00705-4.
17. Payne, L. J. *et al.* Identification and classification of antiviral defence systems in bacteria and archaea with PADLOC reveals new system types. *Nucleic Acids Research* **49**, 10868–10878 (2021).
18. Tesson, F. *et al.* *Systematic and quantitative view of the antiviral arsenal of prokaryotes.* 2021.09.02.458658 <https://www.biorxiv.org/content/10.1101/2021.09.02.458658v2> (2021) doi:10.1101/2021.09.02.458658.
19. Bernheim, A. & Sorek, R. The pan-immune system of bacteria: antiviral defence as a community resource. *Nature Reviews Microbiology* **18**, 113–119 (2020).
20. Stubbendieck, R. M., Vargas-Bautista, C. & Straight, P. D. Bacterial Communities: Interactions to Scale. *Front. Microbiol.* **7**, (2016).

21. Manning, A. J. & Kuehn, M. J. Contribution of bacterial outer membrane vesicles to innate bacterial defense. *BMC Microbiology* **11**, 258 (2011).
22. Reyes-Robles, T. *et al.* Vibrio cholerae Outer Membrane Vesicles Inhibit Bacteriophage Infection. *Journal of Bacteriology* (2018) doi:10.1128/JB.00792-17.
23. Vidakovic, L., Singh, P. K., Hartmann, R., Nadell, C. D. & Drescher, K. Dynamic biofilm architecture confers individual and collective mechanisms of viral protection. *Nature Microbiology* **3**, 26–31 (2018).
24. Simmons, M., Drescher, K., Nadell, C. D. & Bucci, V. Phage mobility is a core determinant of phage–bacteria coexistence in biofilms. *ISME J* **12**, 531–543 (2018).
25. Høyland-Kroghsbo, N. M., Mærkedahl, R. B. & Svenningsen, S. L. A Quorum-Sensing-Induced Bacteriophage Defense Mechanism. *mBio* **4**, (2013).
26. Silpe, J. E. & Bassler, B. L. A Host-Produced Quorum-Sensing Autoinducer Controls a Phage Lysis-Lysogeny Decision. *Cell* **176**, 268-280.e13 (2019).
27. León-Félix, J. & Villicaña, C. The impact of quorum sensing on the modulation of phage–host interactions. *J Bacteriol* JB.00687-20 (2021) doi:10.1128/JB.00687-20.
28. Abedon, S. T. Phage-Antibiotic Combination Treatments: Antagonistic Impacts of Antibiotics on the Pharmacodynamics of Phage Therapy? *Antibiotics* **8**, 182 (2019).
29. Schatz, A. & Jones, D. The Production of Antiphage Agents by Actinomycetes. *Bulletin of the Torrey Botanical Club* **74**, 9 (1947).
30. Asheshov, I. N., Strelitz, F., Hall, E. & Flon, H. A Survey of Actinomycetes for Antiphage Activity. *Antibiotics & Chemotherapy* **4**, 380–94 (1954).
31. Bydžovský, V. & Šlmeek, A. Antiphage activity of some actinomycetes. *Folia Microbiol* **5**, 46–49 (1960).

32. Perlman, D., Langlykke, A. F. & Rothberg, H. D. Observations on the Chemical Inhibition of *Streptomyces Griseus* Bacteriophage Multiplication. *Journal of Bacteriology* **61**, 135–143 (1951).
33. Fujiwara, A., Hoshino, T. & Westley, J. W. Anthracycline Antibiotics. *Critical Reviews in Biotechnology* **3**, 133–157 (1985).
34. Minotti, G., Menna, P., Salvatorelli, E., Cairo, G. & Gianni, L. Anthracyclines: Molecular Advances and Pharmacologic Developments in Antitumor Activity and Cardiotoxicity. *Pharmacological Reviews* (2004) doi:10.1124/pr.56.2.6.
35. Weiss, R. B. The anthracyclines: will we ever find a better doxorubicin? *Semin Oncol* **19**, 670–686 (1992).
36. Peng, X., Chen, B., Lim, C. C. & Sawyer, D. B. The cardiotoxicology of anthracycline chemotherapeutics: translating molecular mechanism into preventative medicine. *Mol Interv* **5**, 163–171 (2005).
37. Carvalho, C. *et al.* Doxorubicin: The Good, the Bad and the Ugly Effect. *Current Medicinal Chemistry* vol. 16 3267–3285 <https://www.eurekaselect.com/69601/article> (2009).
38. Parisi, B. & Soller, A. Studies on Antiphage Activity of Daunomycin. *Giornale Di Microbiologia* **12**, 183–194 (1964).
39. Kronheim, S. *et al.* A chemical defence against phage infection. *Nature* **564**, 283 (2018).
40. Thaker, M. N. *et al.* Identifying producers of antibacterial compounds by screening for antibiotic resistance. *Nat Biotechnol* **31**, 922–927 (2013).
41. Nakata, A., Sekiguchi, M. & Kawamata, J. Inhibition of Multiplication of Bacteriophage by Actinomycin. *Nature* **189**, 246–247 (1961).
42. Mingeot-Leclercq, M.-P., Glupczynski, Y. & Tulkens, P. M. Aminoglycosides: Activity and Resistance. *Antimicrob Agents Chemother* **43**, 727–737 (1999).

43. Krause, K. M., Serio, A. W., Kane, T. R. & Connolly, L. E. Aminoglycosides: An Overview. *Cold Spring Harb Perspect Med* **6**, (2016).
44. Houghton, J. L., Green, K. D., Chen, W. & Garneau-Tsodikova, S. The Future of Aminoglycosides: The End or Renaissance? *ChemBioChem* **11**, 880–902 (2010).
45. Serio, A. W., Keepers, T., Andrews, L. & Krause, K. M. Aminoglycoside Revival: Review of a Historically Important Class of Antimicrobials Undergoing Rejuvenation. *EcoSal Plus* **8**, (2018).
46. Kever, L. *et al.* Aminoglycoside antibiotics inhibit phage infection by blocking an early step of the phage infection cycle. 2021.05.02.442312
<https://www.biorxiv.org/content/10.1101/2021.05.02.442312v1> (2021)
doi:10.1101/2021.05.02.442312.
47. Jiang, Z., Wei, J., Liang, Y., Peng, N. & Li, Y. Aminoglycoside Antibiotics Inhibit Mycobacteriophage Infection. *Antibiotics* **9**, 714 (2020).
48. Tamura, T., Ishida, Y., Otaguro, M., Hatano, K. & Suzuki, K. 2008. Classification of ‘*Streptomyces tenebrarius*’ Higgins and Kastner as *Streptoalloteichus tenebrarius* nom. rev., comb. nov., and emended description of the genus *Streptoalloteichus*. *International Journal of Systematic and Evolutionary Microbiology* **58**, 688–691.
49. Zuo, P., Yu, P. & Alvarez, P. J. J. Aminoglycosides Antagonize Bacteriophage Proliferation, Attenuating Phage Suppression of Bacterial Growth, Biofilm Formation, and Antibiotic Resistance. *Appl Environ Microbiol* **87**, e0046821 (2021).
50. Kopaczynska, M. *et al.* Aminoglycoside Antibiotics Aggregate To Form Starch-like Fibers on Negatively Charged Surfaces and on Phage λ -DNA. *Langmuir* **20**, 9270–9275 (2004).
51. Kopaczynska, M. *et al.* Selective condensation of DNA by aminoglycoside antibiotics. *Eur Biophys J* **45**, 287–299 (2016).

52. Brock, T. D. & Wooley, S. O. Streptomycin as an Antiviral Agent: Mode of Action. *Science* **141**, 1065–1067 (1963).
53. Brock, T. D. The inhibition of an RNA bacteriophage by streptomycin, using host bacteria resistant to the antibiotic. *Biochem. Biophys. Res. Commun.* **9**, 184–187 (1962).
54. Rivera-Serrano, E. E. *et al.* Viperin Reveals Its True Function. *Annual Review of Virology* **7**, 421–446 (2020).
55. Gizzi, A. S. *et al.* A naturally occurring antiviral ribonucleotide encoded by the human genome. *Nature* **558**, 610–614 (2018).
56. Comeau, A. M., Tétart, F., Trojet, S. N., Prère, M.-F. & Krisch, H. M. Phage-Antibiotic Synergy (PAS): β -Lactam and Quinolone Antibiotics Stimulate Virulent Phage Growth. *PLOS ONE* **2**, e799 (2007).
57. Stachurska, X., Roszak, M., Jabłońska, J., Mizelińska, M. & Nawrotek, P. Double-Layer Agar (DLA) Modifications for the First Step of the Phage-Antibiotic Synergy (PAS) Identification. *Antibiotics* **10**, 1306 (2021).
58. Strelitz, F., Flon, H. & Asheshov, I. N. Nybomycin, a new antibiotic with antiphage and antibacterial properties. *Proc Natl Acad Sci U S A* **41**, 620–624 (1955).
59. Hardy, A., Sharma, V., Kever, L. & Frunzke, J. Genome Sequence and Characterization of Five Bacteriophages Infecting *Streptomyces coelicolor* and *Streptomyces venezuelae*: Alderaan, Coruscant, Dagobah, Endor1 and Endor2. *Viruses* **12**, 1065 (2020).
60. Amiri Moghaddam, J. *et al.* Analysis of the Genome and Metabolome of Marine Myxobacteria Reveals High Potential for Biosynthesis of Novel Specialized Metabolites. *Sci Rep* **8**, 16600 (2018).

61. Gregory, K., Salvador, L. A., Akbar, S., Adaikpoh, B. I. & Stevens, D. C. Survey of Biosynthetic Gene Clusters from Sequenced Myxobacteria Reveals Unexplored Biosynthetic Potential. *Microorganisms* **7**, 181 (2019).
62. Kallscheuer, N. & Jogler, C. The bacterial phylum Planctomycetes as novel source for bioactive small molecules. *Biotechnology Advances* **53**, 107818 (2021).
63. Wiegand, S. *et al.* Cultivation and functional characterization of 79 planctomycetes uncovers their unique biology. *Nat Microbiol* **5**, 126–140 (2020).
64. Ramirez, M. S. & Tolmasky, M. E. Aminoglycoside modifying enzymes. *Drug Resistance Updates* **13**, 151–171 (2010).
65. Alseth, E. O. *et al.* Bacterial biodiversity drives the evolution of CRISPR-based phage resistance. *Nature* **574**, 549–552 (2019).
66. Dionne, B. Key Principles of Antiretroviral Pharmacology. *Infectious Disease Clinics of North America* **33**, 787–805 (2019).
67. Simon, V., Ho, D. D. & Abdool Karim, Q. HIV/AIDS epidemiology, pathogenesis, prevention, and treatment. *Lancet* **368**, 489–504 (2006).
68. Shiraki, K. Antiviral Drugs Against Alphaherpesvirus. *Adv Exp Med Biol* **1045**, 103–122 (2018).

3.4 Phage-triggered synthesis of actinorhodin and undecylprodigiosin in *Streptomyces coelicolor*

Hardy A., Kever L., Widdick D., Truman A., Probst S., Piel J. and Frunzke J.

Research article part of this thesis; to be submitted

CONTRIBUTOR ROLE	CONTRIBUTOR
Conceptualization	AH (50%), JF (40%), LK (10%)
Data curation	AH (70%), LK (20%), DW (5%), SP (5%)
Formal analysis	AH (80%), AT (10%), SP (10%)
Funding acquisition	JF (90%), AT (5%), JP (5%)
Investigation	AH (65%), LK (20%), SP (10%), DW (5%)
Methodology	AH (50%), SP (25%), AT (10%), JF (10%), LK (5%)
Project administration	AH (80%), JF (10%), LK (10%)
Resources	DW (25%), AT (25%), SP (25%), JP (25%)
Software	-
Supervision	JF (50%), AH (40%), AT (5%), JP (5%)
Validation	AH (70%), LK (20%), JF (10%)
Visualization	AH (85%), LK (7.5%), SP (7.5%)
Writing – original draft	AH (95%), JF (5%)
Writing – review & editing	JF (60%), AH (25%), LK (15%)

Overall contribution AH: 70%

Phage-triggered synthesis of actinorhodin and undecylprodigiosin in *Streptomyces coelicolor*

Aël Hardy¹, Larissa Kever¹, David Widdick², Andrew Truman², Silke Probst³, Jörn Piel³ and Julia Frunzke^{1*}

¹Institute of Bio- und Geosciences, IBG-1: Biotechnology, Forschungszentrum Jülich, 52425 Jülich, Germany

²Department of Molecular Microbiology, John Innes Centre, Norwich NR4 7UH, United Kingdom

³Eidgenössische Technische Hochschule (ETH) Zürich, Institute of Microbiology, Vladimir-Prelog-Weg 4, 8093, Zürich, Switzerland

*Corresponding author:

Julia Frunzke; Email: j.frunzke@fz-juelich.de; Phone: +49 2461 615430

Abstract

Actinorhodin and undecylprodigiosin are two major secondary metabolites produced by the model species *Streptomyces coelicolor*. In contrast to their well-dissected biosynthesis pathway, their physiological role remains unclear. Here, we show that phage infection triggers the synthesis of actinorhodin and undecylprodigiosin in *S. coelicolor*. Disruption of the actinorhodin and undecylprodigiosin synthesis did not lead to increased sensitivity towards phage infection, suggesting that these two molecules do not directly inhibit phage infection. More investigations are needed to elucidate the role of actinorhodin and undecylprodigiosin in relation to phage infection. We hypothesize that they may act as signal molecules warning neighbouring cells from an incoming danger.

Introduction

Streptomyces coelicolor is a model species of *Streptomyces* and is amongst the best-studied representatives of the genus. Since its first description in the 1950s, it has become a workhorse for genetical studies and a model system for development and antibiotic production (Hoskisson and van Wezel, 2019). Its genome was the first *Streptomyces* genome to be sequenced at the dawn of the 2000s (Bentley et al., 2002). Combined with later genome mining and biosynthetic gene cluster (BGC) prediction, it unravelled a rich chemical repertoire, with almost 30 chromosomally-encoded BGCs (Craney et al., 2013).

Two of these BGCs have been the focus of extensive studies: those responsible for the biosynthesis of actinorhodin and undecylprodigiosin. These two secondary metabolites are in fact responsible for the name of this species, '*coelicolor*' meaning in Latin 'colours of the sky'. Actinorhodin and undecylprodigiosin are traditionally described as 'blue' and 'red' compounds, respectively (Hopwood, 2006), although actinorhodin's pigmentation is pH-responsive (it is red at acidic pH and blue at basic pH) (Bystrykh et al., 1996). In fact, the ease of visually checking the production of actinorhodin and undecylprodigiosin significantly contributed to establish this species as model *Streptomyces* species, as it facilitated genetic studies of the clusters encoding these two molecules (Chater, 1999).

Despite being well-studied secondary metabolites of *S. coelicolor*, the physiological role of actinorhodin and undecylprodigiosin remains unclear. Actinorhodin was shown to have pH-sensitive bacteriostatic activity against several Gram positive bacteria (Mak and Nodwell, 2017). In *Staphylococcus aureus*, actinorhodin causes oxidative damage of multiple cellular targets, including components of the DNA, proteins and cell envelope (Mak and Nodwell, 2017). Co-cultivation of *S. coelicolor* with the predatory bacterium *Myxococcus xanthus* further revealed that iron competition

triggered actinorhodin biosynthesis (Lee et al., 2020). Taken together with the chemical potential displayed by actinorhodin to bind iron with its close ketone and hydroxyl groups, this suggests that actinorhodin could act as an iron chelator. However, the biological significance of these potential chelating functions remains unclear.

Similarly, the biosynthesis and regulation of undecylprodigiosin in *S. coelicolor* was the subject of numerous studies, but the actual role of this molecule in *S. coelicolor*'s physiology received attention only recently. Interestingly, Tenconi and colleagues revealed the involvement of undecylprodigiosin in the programmed cell death process of *S. coelicolor* (Tenconi et al., 2018, 2020). Undecylprodigiosin is synthesized before the onset of aerial hyphae formation and through its toxic effect amplifies cell death in the vegetative mycelium, releasing nutrients necessary for the erection of aerial hyphae. Strong autotoxicity and coordinated regulation are features reminiscent of abortive infection systems, which hence raises interest for the study of undecylprodigiosin production upon phage infection.

In previous work, we observed that phage plaques formed on *S. coelicolor* were surrounded by pigmented halos (Hardy et al., 2020). Here, we investigate these coloured halos and show that they contain actinorhodin and undecylprodigiosin. Using deletion mutants for actinorhodin and undecylprodigiosin, we could not identify an increased sensitivity of these mutants to phage infection. The role of these secondary metabolites in the response to viral predation may therefore be indirect, rather than directly interfering with phage amplification.

Material and methods

Bacterial strains and growth conditions

All bacterial strains, phages and plasmids used in this study are listed in Supplementary Files 2, 3 and 4, respectively. For growth studies and double-agar overlay assays, *Streptomyces coelicolor* cultures were inoculated from spore stocks and cultivated at 30 °C and 120 rpm using Yeast extract Malt extract (YEME) medium (Keiser et al., 2000).

For double agar overlays, GYM agar (pH 7.3) was used, with 0.4% and 1.5% agar for the top and bottom layers, respectively. For quantification of extracellular phages, 2 µl of the culture supernatants were spotted on a bacterial lawn propagated on a double-agar overlay inoculated at an initial OD₄₅₀=0.5.

Exposure to ammonia fume was performed as follows: the plates were inverted over 5 ml of 20 % ammonium hydroxide solution placed in a Petri dish lid and incubated for at least 30 minutes (Rudd and Hopwood, 1979).

Phage infection curves

For phage infection curves, the BioLector microcultivation system of m2p-labs (Baesweiler, Germany) was used (Kensy et al., 2009). Cultivations were performed as biological triplicates in FlowerPlates (m2p labs, Germany) at 30 °C and a shaking frequency of 1200 rpm. During cultivation, biomass was measured as a function of backscattered light intensity with an excitation wavelength of 620 nm (filter module: $\lambda_{Ex}/\lambda_{Em}$: 620 nm/ 620 nm, gain: 25) every 15 minutes. All growth curves are baseline corrected with respect to the backscatter values at time point 0. The main cultures of *Streptomyces coelicolor* were performed in 1 ml YEME medium and were inoculated with overnight cultures grown in the same medium to an initial OD₄₅₀= 0.1. Unless indicated otherwise, infection was performed by adding phages to an initial phage titer of 10⁷ PFU/ml. Supernatants were collected at the indicated timepoints to determine the evolution of phage titer over time using double agar overlays.

LC-MS on plates

Double agar overlays of *S. coelicolor* were prepared as biological triplicates as described above, and phages were spotted in the middle of the plate, so as to form a central lysis zone. After 3 days of incubation at 30°C, the periphery of the lysis zone was sampled using a cork borer. The resulting pieces of agar were first frozen at 20°C, then metabolite extraction was performed using 50% ethanol and incubation at 60°C for 30 min with shaking. Next, the samples were centrifuged and the supernatants were stored at -20°C before analysis with LC-MS.

The samples were loaded to a HPLC system coupled to a Shimadzu LCMS-IT-TOF™ mass spectrometer, with an injection volume of 10 µl. Samples were supplemented with 0.01% formic acid and washing was performed with an increasing ratio of acetonitrile, up to 95%. Samples were analyzed in positive and negative ionisation mode.

Mass spectrometric data was uploaded to XCMS online (Domingo-Almenara and Siuzdak, 2020; Forsberg et al., 2018). Biological triplicates were pooled and analysed as pairwise job comparing the phage-infected samples with the uninfected controls. The parameters chosen were HPLC / Ion trap.

LC-MS on liquid samples

5 mL of supernatant of *Streptomyces coelicolor* M145 cultures infected and non-infected with the phage Endor2 were normalized by pellet weight and adjusted to pH=6.9. They were next extracted three times with ethyl acetate and dried under vacuum.

The samples were loaded on a Dionex Ultimate 3000 HPLC system coupled to a Thermo Scientific™ Q Exactive™ Hybrid Quadrupole-Orbitrap Mass Spectrometer. Experiments were conducted using

solvents A (H₂O + 0.1 % formic acid) and B (MeCN + 0.1 % formic acid) with a Phenomenex Kinetex column 2.6 µm XB-C18 150 x 4.6 mm.

The settings used were the following: flowrate 0.5 mL/min, 5% to 95% B in 12 min, 95% B for 4 min, 95% to 5% B in 1 min, 5% B for 1 min. MS-settings: Spray Voltage 3.5 kV, capillary temperature 320 °C, sheath gas (52.50), auxiliary gas (13.75), spare gas (2.75), probe heater 437.50 °C, S-Lens RF (50), positive mode, resolution 70.000, AGC target 1e6, microscans 1, maximum IT 100 ms, scan range 135-2000 m/z.

Results

Phage infection triggers the release of actinorhodin and undecylprodigiosin

Our interest in the role of actinorhodin and undecylprodigiosin was initially triggered by the observation of pigmented halos around *S. coelicolor* plaques (Hardy et al., 2020). The halos were typically dark blue in the case of Dagobah and rather reddish in the case of Endor1 and Endor2, suggesting actinorhodin and undecylprodigiosin as prime suspects (**Figure 1A**). We also performed phage infection in solid medium following a different method, using so-called ‘soft-agar free assays’ where droplets of phages and bacteria are mixed together without a top agar layer. In this setup too, we observed colour changes of the phage-infected colonies as well as the production of pigmented halos, which were absent in the controls (**Figure 1B**). A simple test to assess the presence of actinorhodin is the fuming of plates with ammonium hydroxide vapours. Exposure to these vapours causes a shift of the agar to more alkaline pH, which in turn changes the colour of actinorhodin from red to blue and decreases its solubility (Bystrykh et al., 1996). Performing these tests with phage-infected plates further indicated a release of actinorhodin, especially in reaction to infection with Dagobah (**Figure S1**).

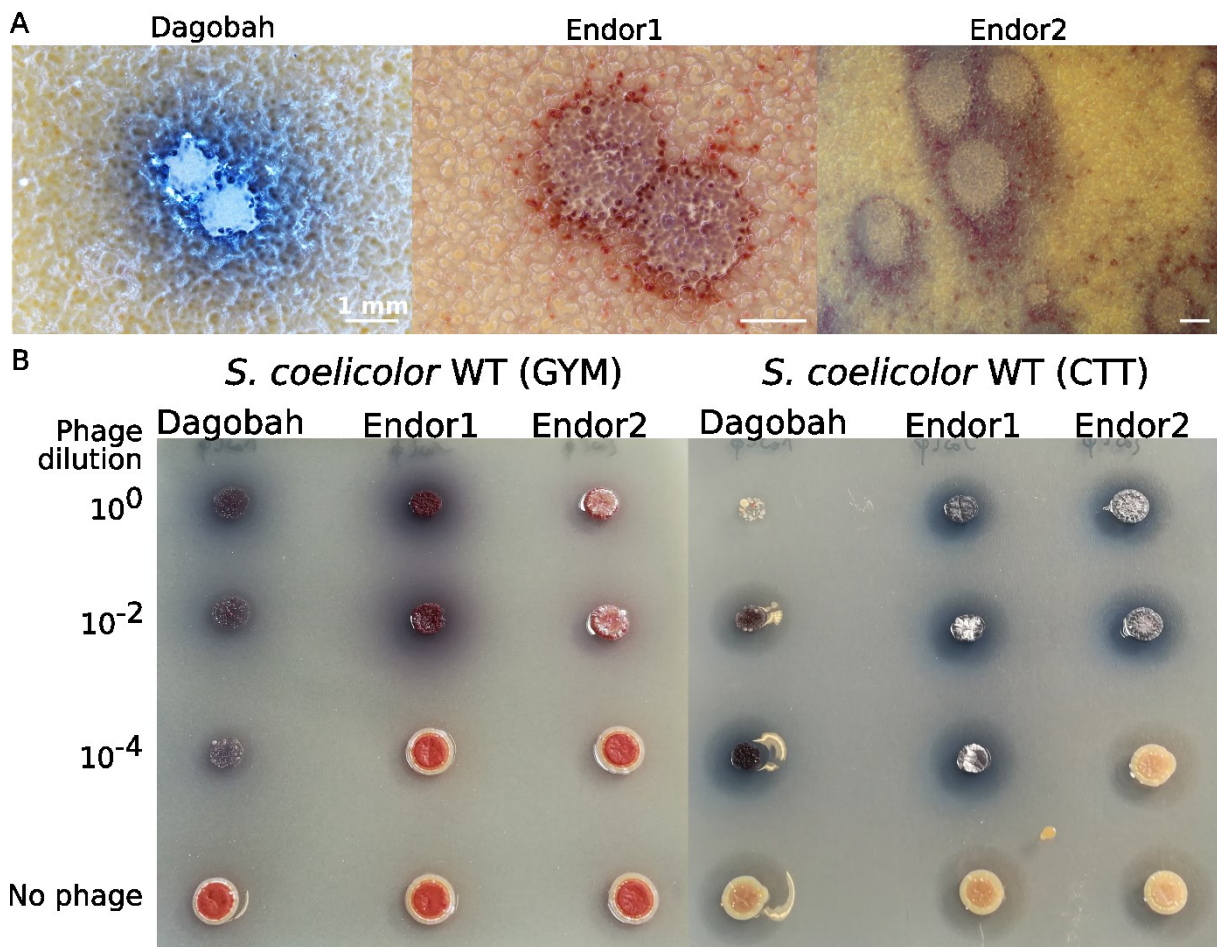


Figure 1 | **Phenotypic response to phage infection in *S. coelicolor*.** (A) Close-up pictures of phage plaques on *S. coelicolor* M145 imaged using a stereomicroscope SMZ18. The plates were imaged after 4 and 2 days for the phages Dagobah and Endor1/Endor2, respectively (reproduced from Hardy et al., 2020). (B) Overnight cultures of *S. coelicolor* M145 were spotted together with a dilution series of phages so that droplets fused with each other. The plates used were either of GYM (left) or CTT (right) medium. Plates were imaged after 4 days of incubation at 30°C.

To ascertain the presence of actinorhodin and undecylprodigiosin, we analysed phage-infected plates using LC-MS, in cooperation with David Widdick (John Innes Centre, UK). The samples probed were pieces of agar taken at the border of lysis zones, where the pigmented halos are the most visible.

Surprisingly, actinorhodin itself was not detected in the samples—which is not unusual with the extraction protocol and the LC-MS equipment that we used—but actinorhodin-related compounds could be quantified. Except deshydroxy-actinorhodic acid, most actinorhodin derivatives showed insignificantly decreased abundance in the phage-infected samples compared to the controls (**Table 1**, see chemical structures in **Figure S2**). This finding, which is in contradiction with our phenotypic observations (Figure 1 and S1), could be explained by the sheer reduction of living cells in the phage-infected samples. Indeed, actinorhodin is constitutively produced also in the absence of phage infection, and massive phage-mediated lysis of cells could mask locally increased production of actinorhodin at the periphery of lysis zones.

Publications and manuscripts

Table 1 | **Comparison of the abundance of actinorhodin derivatives in phage-infected samples compared to uninfected controls in *S. coelicolor* M145.** 'Up' ('down') refer to increased (decreased, respectively) abundance of the considered metabolite in the phage-infected sample in comparison to the control. The p-value was calculated for a t-test performed between the phage-infected samples and the uninfected controls.

Compounds	Exact masses	Dagobah		Endor1		Endor2	
		fold-change	p-value	fold-change	p-value	fold-change	p-value
Actinorhodin	633.125	-	-	-	-	-	-
Kalafungin	315.051	-	-	-	-	-	-
γ -Actinorhodin	629.0937	1.5 DOWN	0.50	1.1 DOWN	0.87	1.4 DOWN	0.51
Actinorhodic acid	665.1148	1.9 DOWN	0.40	2.0 DOWN	0.41	-	-
ϵ -Actinorhodin	647.1042	1.1 DOWN	0.94	8.7 DOWN	0.11	1.2 DOWN	0.78
Deshydroxy-actinorhodic acid	649.1199	4.9 UP	0.23	-	-	2.7 UP	0.36

Next, we evaluated the presence of undecylprodigiosin in the phage-infected samples and in the controls. For unclear reasons, we could not detect undecylprodigiosin and the related streptarubin in any of the WT samples. We then checked the presence of undecylprodigiosin in a *S. coelicolor* Δact strain defective for actinorhodin production (Gomez-Escribano and Bibb, 2011), which was infected with phages and analyzed in the same way the *S. coelicolor* WT (M145). In contrast, undecylprodigiosin was detected in high amounts in phage-infected samples and was found to be strongly enriched in these samples compared to the controls, with a 25-fold higher abundance (**Table 2** and **Figure S3**). The fact undecylprodigiosin was only detected in the actinorhodin mutant could be explained by a higher production of undecylprodigiosin in absence of actinorhodin as well as a potential compensating effect, assuming that actinorhodin and undecylprodigiosin fulfil similar roles in response to phage infection.

Table 2 | **Comparison of the abundance of undecylprodigiosin in phage-infected samples compared to uninfected controls in *S. coelicolor* Δact .** 'Up' ('down') refer to increased (decreased, respectively) abundance of the considered metabolite in the phage-infected sample in comparison to the control. The p-value was calculated for a t-test performed between the phage-infected samples and the uninfected control.

Compound	Exact mass	Dagobah		Endor1		Endor2	
		fold-change	p-value	fold-change	p-value	fold-change	p-value
Undecylprodigiosin	394.2853	27.4 UP	0.09	29.9 UP	0.11	22.9 UP	0.11

We complemented the metabolic analyses presented above by performing LC-MS this time on phage-infected cultures. Focusing on the phage Endor2, phage-infected culture supernatants showed earlier and more intense production of undecylprodigiosin in comparison to the controls (**Figure 2**). A similar trend was observed with actinorhodin, although to a lesser extent.

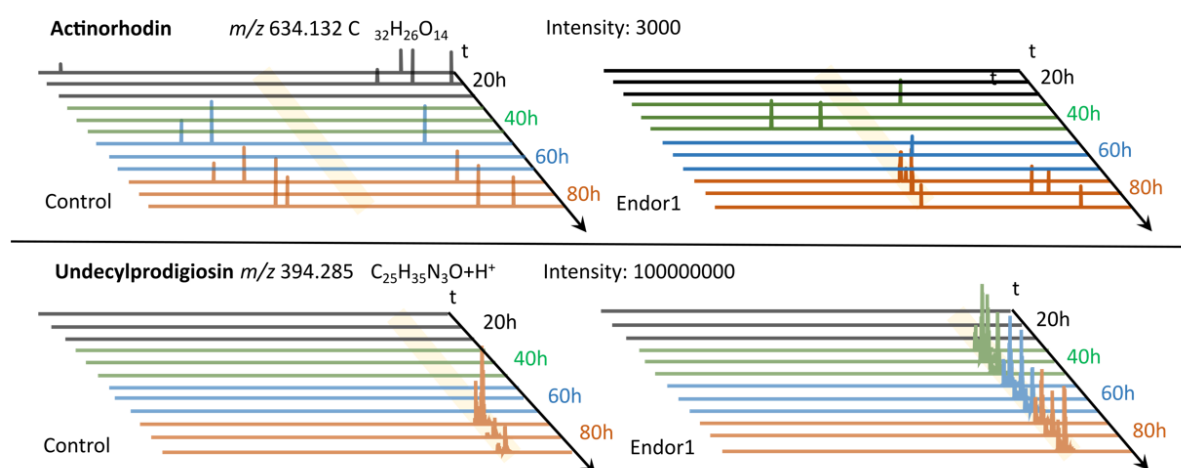


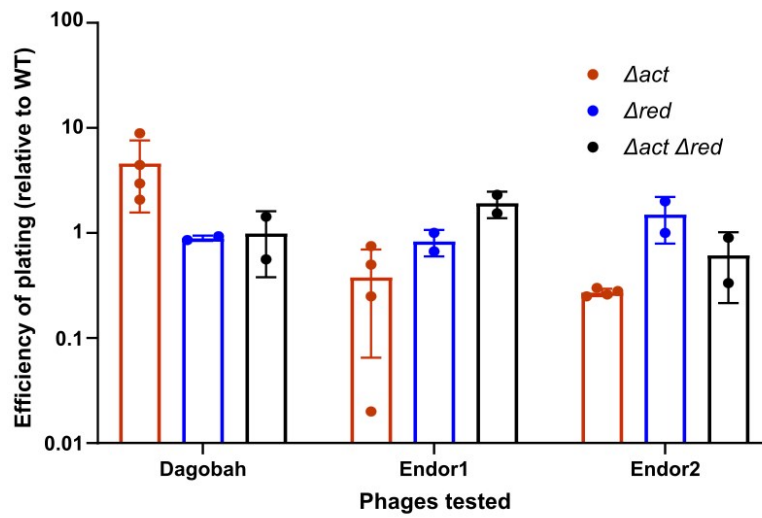
Figure 2 | Phage infection amplifies synthesis of actinorhodin and undecylprodigiosin. Extracted ion chromatograms of actinorhodin (top) and undecylprodigiosin (bottom), after analysis with liquid chromatography-mass spectrometry (LC-MS) of uninfected cultures of *S. coelicolor* and cultures of *S. coelicolor* infected with Endor2. The expected retention time of the respective ions is shown as an orange band.

Undecylprodigiosin and actinorhodin mutants do not show increased sensitivity to phage infection

Because actinorhodin and undecylprodigiosin are released in reaction to phage infection, we sought to determine whether these two molecules would confer protection *S. coelicolor* against phage infection. To test this hypothesis, we assessed the sensitivity to phage infection of single deletion mutants as well of a double mutant for both BGCs (**Figure 3**). Plaque counts on the single mutants and the double mutant were comparable to those obtained with the WT (**Figure 3A**). Plaque phenotype of the mutants was also similar to the one observed with the WT, with the difference that in the actinorhodin mutant the halos surrounding the plaques are orange (**Figure S4**). Infection in liquid

cultures with the WT showed a very modest amplification of Dagobah and a more pronounced infection with Endor1 (**Figure 3B**). Infection curves obtained with the actinorhodin-defective mutant showed patterns very similar to the control, suggesting that the absence of actinorhodin does not stimulate phage propagation.

A



B

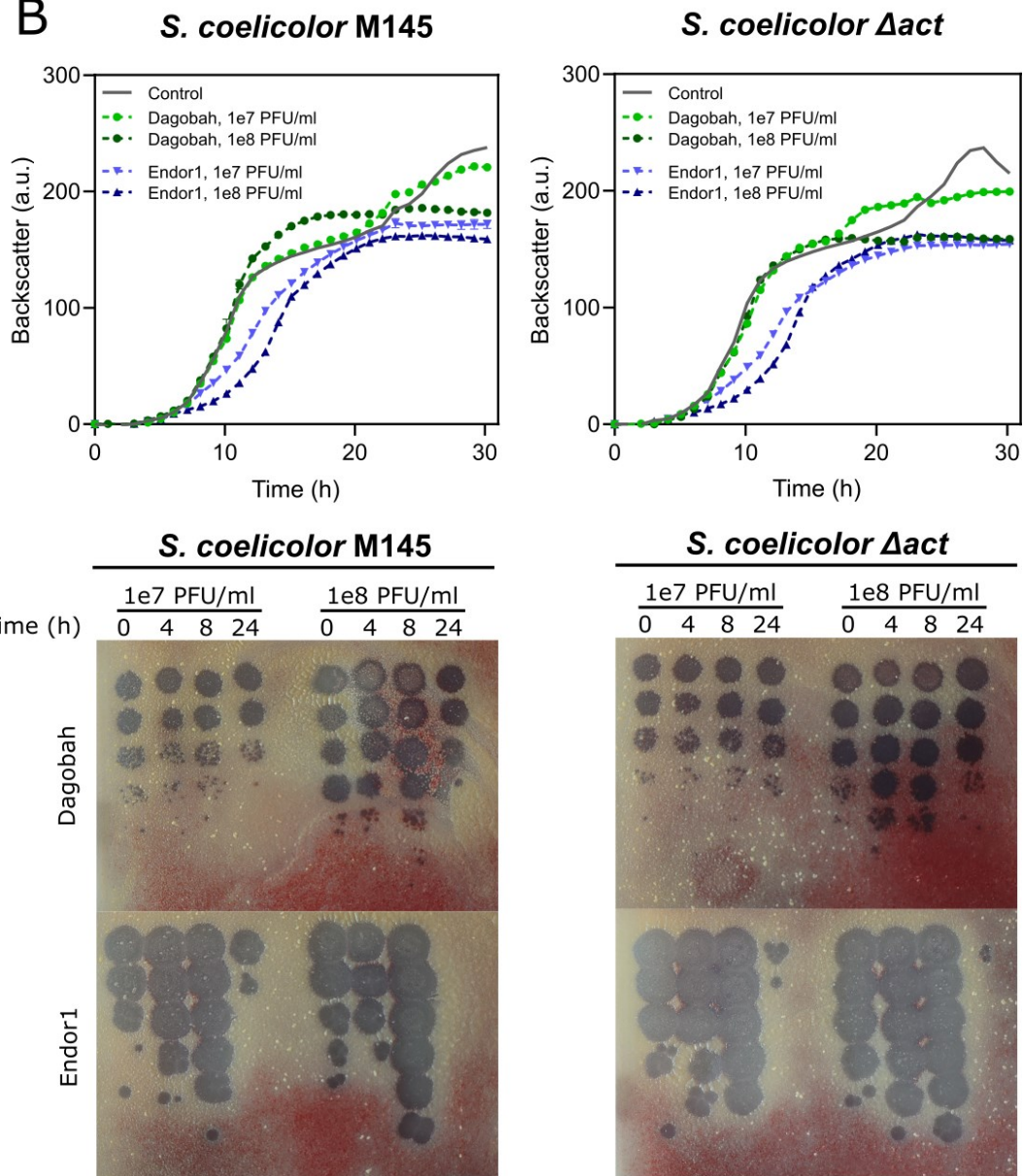


Figure 3 | **Deletion of the actinorhodin or undecylprodigiosin does not lead to increased sensitivity to phage infection.** (A) Comparison of plaque counts obtained after spotting a serial dilution of the phages Dagobah, Endor1 and Endor2 on actinorhodin and undecylprodigiosin single mutants (Δact and Δred) and double mutant ($\Delta act \Delta red$) (B) Infection curves performed by infection either *S. coelicolor* M145 and Δact with Dagobah or Endor1. Backscatter was measured over time (top), in parallel to phage titers (bottom).

Spent medium of S. coelicolor WT and actinorhodin and undecylprodigiosin mutants do not protect against phage infection

Synthesis of secondary metabolites generally involves complex and extensive pathways, and increase in actinorhodin in liquid cultures is for example spread over several dozen hours (Bystrykh et al., 1996). In contrast, most phages complete an infection cycle in less than an hour, and exponential propagation at the expense of their host can lyse cultures in a matter of a few hours. As result, the similar phage sensitivity observed between *S. coelicolor* WT and actinorhodin and undecylprodigiosin mutants could be due to this difference of chronology between the release of secondary metabolites and phage infection.

To account for this difference in timelines, we first grew WT *S. coelicolor*, actinorhodin and undecylprodigiosin deletion mutants. We then harvested the culture supernatants and stored the filtrates (hereafter called 'spent medium'). We challenged *S. coelicolor* with phages on plates in presence of spent medium (5% and 15% of the total volume) (**Figure 4A**). However, supplementation with spent medium nor from *S. coelicolor* WT neither from the mutants caused differences in plaque counts or morphology. The decreased plaque numbers of Dagobah as the fraction of spent medium increased was also seen when using fresh medium (GYM) instead of spent medium, indicating that this decreased plaque formation is probably caused by a dilution effect rather than by the compounds of the spent medium.

We then performed similar experiments in liquid cultures (**Figure 4B and 4C, Figure S5**). Here too, we did not observe differences in infection between cultures supplemented with the spent medium of the wild type and of the mutants. The growth delay seen with cultures supplemented with 15% spent medium from the undecylprodigiosin mutant was found both in uninfected and infected cultures, suggesting a toxic effect of this spent medium at high doses.

Altogether, the data obtained with both the direct infection of the mutants and the indirect use of spent medium suggest that actinorhodin and undecylprodigiosin do not provide direct protection against phage infection.

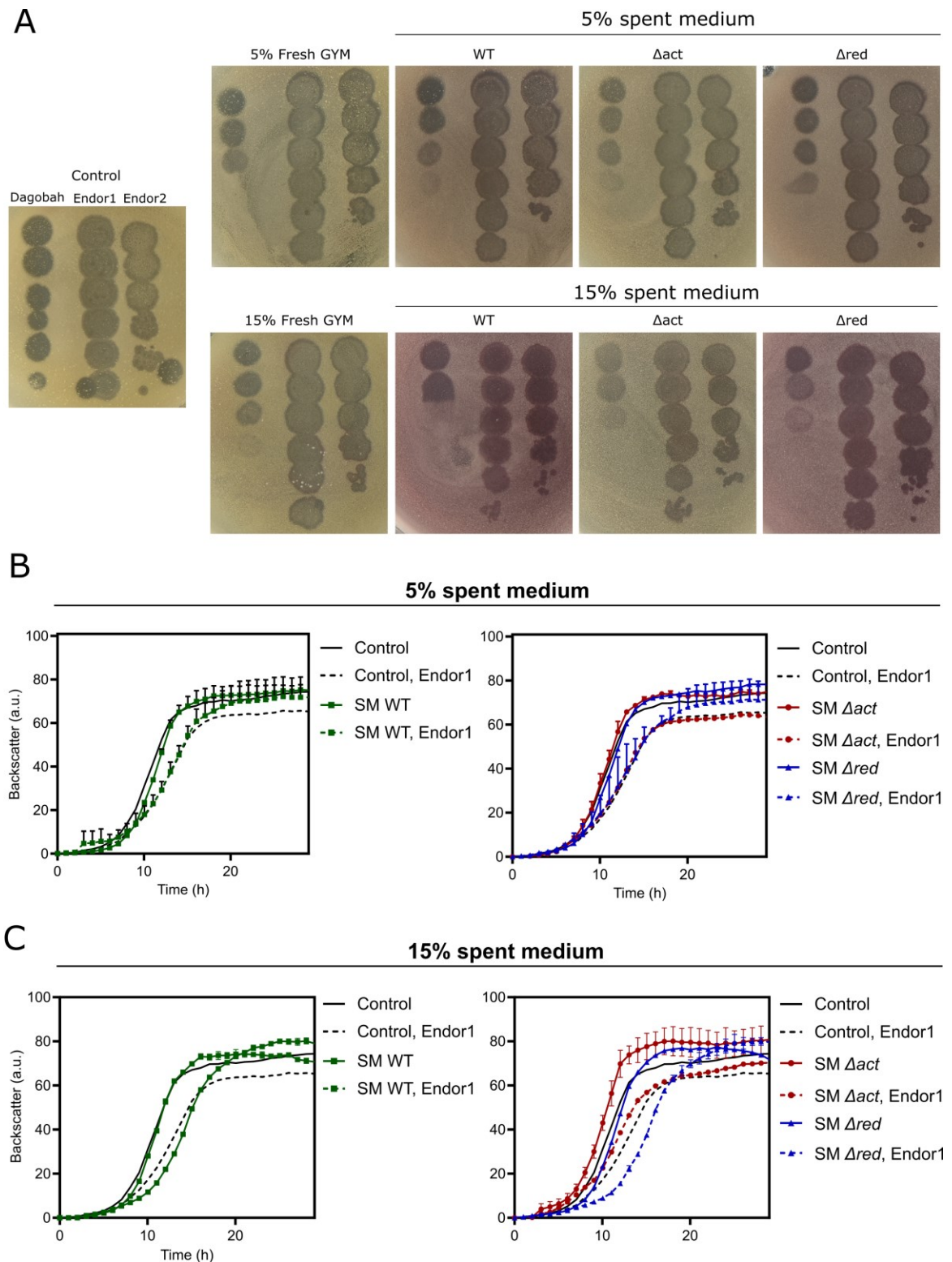


Figure 4 | **Supplementation with spent medium of *S. coelicolor* WT and the actinorhodin and undecylprodigiosin mutant does not impact phage infection.** (A) Spot assays performed by spotting the phages Dagobah, Endor1 and Endor2 on lawn of *S. coelicolor* M145. The plates were supplemented with spent medium from *S. coelicolor* M145, the actinorhodin (Δact) and undecylprodigiosin mutants (Δred) or fresh GYM (for the controls). (B) Infection curves performed by infecting *S. coelicolor* M145

with the phage Endor1 in presence of spent medium (SM) from *S. coelicolor* M145, the actinorhodin (Δact) and undecylprodigiosin mutants (Δred).

Production of actinorhodin and undecylprodigiosin could be triggered by cell death and not by phage infection in particular. To test this hypothesis, we checked the impact of multiple antibiotics on *S. coelicolor*. These antibiotics comprise several β -lactams inhibiting cell wall synthesis (amoxicillin, ampicillin, cefalothin, cefazolin and cefuroxin) and two unrelated antibiotics hindering translation (chloramphenicol and kanamycin). At the concentrations used here, kanamycin was the only antibiotic to cause visible growth inhibition of *S. coelicolor*, and the surrounding bacterial lawn showed reddish halos (**Figure S6**). Exposure of the plates to ammonia fumes caused a shift of the pigmentation of the halos to intense blue, which is characteristic of actinorhodin. Exposure to kanamycin hence causes a synthesis of actinorhodin by *S. coelicolor*, indicating that actinorhodin may be a stress-induced molecule rather than an antiphage agent.

Discussion

Here, we show that phage infection in *S. coelicolor* triggers the formation of colour halos surrounding phage plaques. Although measurements by LC-MS show some inconsistencies, these halos seem to contain actinorhodin and undecylprodigiosin. These two well-known secondary metabolites of *S. coelicolor* are secreted constitutively in *S. coelicolor*, yet their role related with phage infection remains unclear. Deletion mutants for these two BGCs did not exhibit increased sensitivity to the phages triggering the formation of the coloured halos. Similarly, supplementation of infected cultures with spent medium from either *S. coelicolor* WT or the mutants did not impact phage propagation. The release of actinorhodin in reaction to challenge with the antibiotic kanamycin suggests that secondary metabolite production following phage infection is a stress-response triggered by cell death. In accordance with this hypothesis, secretion of actinorhodin was also observed in reaction to predation by myxococcus (Lee et al., 2020; Pérez et al., 2011). Actinorhodin could therefore act as a signalling molecule to warn neighbours of incoming danger, in addition to serving as an antibiotic against certain Gram-positive competitors (Mak and Nodwell, 2017).

Some bacterial secondary metabolites were already shown to directly block phage amplification. They fall mostly in two well-known classes of secondary metabolites naturally produced by *Streptomyces*: anthracyclines and aminoglycosides (Kever et al., 2021; Kronheim et al., 2018). The mechanism of action behind their antiviral activity remains unclear, but both anthracyclines and aminoglycosides seem to block an early step of the phage life cycle, between genome injection and replication. However, the studies about the antiphage properties of these compounds were conducted only in

non-producer hosts, which leaves unanswered the question of their physiological significance in natural bacterial communities.

Awakening silent BGCs has been a major focus of the last decades. The methods employed cover a wide range of approaches, including among others media optimization and variation of culture conditions, pathway mutagenesis and rational genetic engineering (Hertweck, 2009; Manteca and Yagüe, 2019; Nguyen et al., 2020). Recently, microbial interactions proved to be a crucial addition to the repertoire of BGC elicitors (Netzker et al., 2018; Seyedsayamdost et al., 2012; Traxler et al., 2013). However, this approach has not been employed for phages yet. The present work was initiated by and focused on two pigmented metabolites, yet we suspect that the shift of secondary metabolism in response to phage infection may be a broad antiviral strategy encompassing a wide range of natural products.

The in-depth study of phage-induced secondary metabolite synthesis is dependent on analytical methods. Mass spectrometry imaging (MSI) allows the determination of the metabolic landscape of a sample while retaining its spatial structure. In-plaque MSI already provided important insights in the remodelling of lipidic metabolism in virus-infected algae (Schleyer et al., 2019). Yet, to this day it has not been applied to phages and could significantly advance our understanding of the bacterial metabolic response to phage infection.

References

- Bentley, S.D., Chater, K.F., Cerdeño-Tárraga, A.-M., Challis, G.L., Thomson, N.R., James, K.D., Harris, D.E., Quail, M.A., Kieser, H., Harper, D., et al. (2002). Complete genome sequence of the model actinomycete *Streptomyces coelicolor* A3(2). *Nature* *417*, 141–147.
- Bystrykh, L.V., Fernández-Moreno, M.A., Herrema, J.K., Malpartida, F., Hopwood, D.A., and Dijkhuizen, L. (1996). Production of actinorhodin-related “blue pigments” by *Streptomyces coelicolor* A3(2). *J. Bacteriol.* *178*, 2238–2244.
- Chater, K. (1999). David Hopwood and the emergence of *Streptomyces* genetics. *Int. Microbiol.* *2*, 61–68.
- Craney, A., Ahmed, S., and Nodwell, J. (2013). Towards a new science of secondary metabolism. *J. Antibiot* *66*, 387–400.

Publications and manuscripts

Domingo-Almenara, X., and Siuzdak, G. (2020). Metabolomics Data Processing Using XCMS. *Methods Mol Biol* 2104, 11–24.

Forsberg, E.M., Huan, T., Rinehart, D., Benton, H.P., Warth, B., Hilmers, B., and Siuzdak, G. (2018). Data processing, multi-omic pathway mapping, and metabolite activity analysis using XCMS Online. *Nat Protoc* 13, 633–651.

Gomez-Escribano, J.P., and Bibb, M.J. (2011). Engineering *Streptomyces coelicolor* for heterologous expression of secondary metabolite gene clusters. *Microb Biotechnol* 4, 207–215.

Hardy, A., Sharma, V., Keiver, L., and Frunzke, J. (2020). Genome Sequence and Characterization of Five Bacteriophages Infecting *Streptomyces coelicolor* and *Streptomyces venezuelae*: Alderaan, Coruscant, Dagobah, Endor1 and Endor2. *Viruses* 12, 1065.

Hertweck, C. (2009). Hidden biosynthetic treasures brought to light. *Nat Chem Biol* 5, 450–452.

Hopwood, D.A. (2006). Soil To Genomics: The *Streptomyces* Chromosome. *Annual Review of Genetics* 40, 1–23.

Hoskisson, P.A., and van Wezel, G.P. (2019). *Streptomyces coelicolor*. *Trends Microbiol* 27, 468–469.

Keiser, T., Bibb, M.J., Buttner, M.J., Chater, K.F., and Hopwood, D.A. (2000). *Practical Streptomyces Genetics* (Norwich: The John Innes Foundation).

Kensy, F., Zang, E., Faulhammer, C., Tan, R.-K., and Büchs, J. (2009). Validation of a high-throughput fermentation system based on online monitoring of biomass and fluorescence in continuously shaken microtiter plates. *Microb. Cell Fact.* 8, 31.

Keiver, L., Hardy, A., Luthe, T., Hünnefeld, M., Gätgens, C., Milke, L., Wiechert, J., Wittmann, J., Moraru, C., Marienhagen, J., et al. (2021). Aminoglycoside antibiotics inhibit phage infection by blocking an early step of the phage infection cycle.

Kronheim, S., Daniel-Ivad, M., Duan, Z., Hwang, S., Wong, A.I., Mantel, I., Nodwell, J.R., and Maxwell, K.L. (2018). A chemical defence against phage infection. *Nature* 564, 283.

Publications and manuscripts

- Lee, N., Kim, W., Chung, J., Lee, Y., Cho, S., Jang, K.-S., Kim, S.C., Palsson, B., and Cho, B.-K. (2020). Iron competition triggers antibiotic biosynthesis in *Streptomyces coelicolor* during coculture with *Myxococcus xanthus*. *The ISME Journal*.
- Mak, S., and Nodwell, J.R. (2017). Actinorhodin is a redox-active antibiotic with a complex mode of action against Gram-positive cells: Molecular action of actinorhodin. *Molecular Microbiology* *106*, 597–613.
- Manteca, Á., and Yagüe, P. (2019). *Streptomyces* as a Source of Antimicrobials: Novel Approaches to Activate Cryptic Secondary Metabolite Pathways (IntechOpen).
- Netzker, T., Flak, M., Krespach, M.K., Stroe, M.C., Weber, J., Schroeckh, V., and Brakhage, A.A. (2018). Microbial interactions trigger the production of antibiotics. *Curr Opin Microbiol* *45*, 117–123.
- Nguyen, C.T., Dhakal, D., Pham, V.T.T., Nguyen, H.T., and Sohng, J.-K. (2020). Recent Advances in Strategies for Activation and Discovery/Characterization of Cryptic Biosynthetic Gene Clusters in *Streptomyces*. *Microorganisms* *8*, 616.
- Pérez, J., Muñoz-Dorado, J., Braña, A.F., Shimkets, L.J., Sevillano, L., and Santamaría, R.I. (2011). *Myxococcus xanthus* induces actinorhodin overproduction and aerial mycelium formation by *Streptomyces coelicolor*. *Microbial Biotechnology* *4*, 175–183.
- Rudd, B.A.M., and Hopwood, D.A. (1979). Genetics of Actinorhodin Biosynthesis by *Streptomyces coelicolor* A3(2). *Microbiology* *114*, 35–43.
- Schleyer, G., Shahaf, N., Ziv, C., Dong, Y., Meoded, R.A., Helfrich, E.J.N., Schatz, D., Rosenwasser, S., Rogachev, I., Aharoni, A., et al. (2019). In plaque-mass spectrometry imaging of a bloom-forming alga during viral infection reveals a metabolic shift towards odd-chain fatty acid lipids. *Nature Microbiology* *1*.
- Seyedsayamdost, M.R., Traxler, M.F., Clardy, J., and Kolter, R. (2012). Old meets new: using interspecies interactions to detect secondary metabolite production in actinomycetes. *Methods Enzymol* *517*, 89–109.

Publications and manuscripts

Tenconi, E., Traxler, M.F., Hoebreck, C., van Wezel, G.P., and Rigali, S. (2018). Production of Prodiginines Is Part of a Programmed Cell Death Process in *Streptomyces coelicolor*. *Front. Microbiol.* **9**.

Tenconi, E., Traxler, M., Tellatin, D., van Wezel, G.P., and Rigali, S. (2020). Prodiginines Postpone the Onset of Sporulation in *Streptomyces coelicolor*. *Antibiotics* **9**, 847.

Traxler, M.F., Watrous, J.D., Alexandrov, T., Dorrestein, P.C., and Kolter, R. (2013). Interspecies interactions stimulate diversification of the *Streptomyces coelicolor* secreted metabolome. *MBio* **4**.

4 Appendix

4.1 Supplementary Information to “2.2.4 Phage-induced natural product synthesis in *Streptomyces*”

Table 1 | **Summary information about all *Streptomyces* phages present in the laboratory collections.** Information is grouped between description of the bacterial host, host range and diverse genomic features. a: Bacterial host used for isolation

Phage	Host ^a		Morphology (TEM)	Host Range		Genomic Data								
	Name	Species		Strain	Species	Strains	Sequenced?	Published?	Size (kb)	GC content (%)	Lifestyle	PhagesDB cluster (if applicable)	Genomic ends	Genome composition
Alderaan	<i>S. venezuelae</i>	ATCC10712	Siphophage	<i>S. lividans</i>		Yes	Yes	34	72.1	Most likely virulent	BC3	Circularly permuted	linear dsDNA	
Coruscant	<i>S. venezuelae</i>	ATCC10712	Siphophage	-		Yes	Yes	133 (12 kb DTR)	48.4	Virulent	BE1	Long direct terminal repeats	linear dsDNA	
SvenA = Chymera	<i>S. venezuelae</i>	ATCC10712	Siphophage			Yes	No	34	71.4	Temperate	Singleton	3' Sticky overhangs	linear dsDNA	Identical to a prophage of Sven, only 2 SNPs with Chymera
SV1	<i>S. venezuelae</i>	ATCC10712	Siphophage			Yes	Yes	37	72.7	Temperate	BC1	Circularly permuted	linear dsDNA	
VWB (for now as DNA only)	<i>S. venezuelae</i>	ATCC10712	Siphophage			Yes	Yes	49	71.1	Temperate	BA	Unknown	linear dsDNA	Gift of Lieve Van Mellaert

Appendix

Imma1	<i>S. venezuelae</i>	ΔbldD		<i>S. venezuelae</i>	WT									
Dagobah	<i>S. coelicolor</i>	M145	Siphophage	<i>S. lividans</i>		Yes	Yes	47 (1kb DTR)	68.9	Temperate	Singleton	Short direct terminal repeats	linear dsDNA	
Endor1	<i>S. coelicolor</i>	M145	Siphophage	<i>S. scabiei, S. platensis, S. xanthochromogenes, S. cyaneofuscatus</i>		Yes	Yes	49	65.8	Temperate	BD3	Circularly permuted	linear dsDNA	
Endor2	<i>S. coelicolor</i>	M145	Siphophage	<i>S. platensis, S. xanthochromogenes, S. olivaceus S. cyaneofuscatus</i>		Yes	Yes	48	65.1	Temperate	BD3	Circularly permuted	linear dsDNA	
Sco4	<i>S. coelicolor</i>	M145	Siphophage			Yes	No			Temperate	BD		linear dsDNA	99% similarity with Endor1
Scol	<i>S. coelicolor</i>	M145	Siphophage			Yes	No			Temperate	BD		linear dsDNA	88% identity with phage Saftant (other member of the BD cluster)
Scoll	<i>S. coelicolor</i>	M145	Siphophage			Yes	No			Temperate	BD		linear dsDNA	98% identical with Endor2

Appendix

ScoV	<i>S. coelicolor</i>	M145	Siphophage			Yes	No			Temperate	BD		linear dsDNA	99% identity with phage Joe (other member of the BD cluster)
ScoVI	<i>S. coelicolor</i>	M145	Siphophage			Yes	No			Temperate	BD		linear dsDNA	
phiIMSco	<i>S. coelicolor</i>	M145	Siphophage			Yes	No						linear dsDNA	Needs to be resequenced
phiIM1	<i>S. griseus</i>	DSM 40236	Siphophage			Yes	No						linear dsDNA	Needs to be resequenced
phi A.Streptomycini III	<i>S. griseus</i>	DSM 40236		<i>S. olivaceus</i>		Yes	No	55	69					
P26	<i>S. griseus</i>	DSM 40236		<i>S. olivaceus</i>		Yes	No	56	69					
phiIMSka	<i>S. kasugaensis</i>	DSM 40819	Siphophage			Yes	No						linear dsDNA	Needs to be resequenced, isolated from the same soil sample than phiIMSco
S7	<i>S. olivaceus</i>	DSM 41536				Yes	No	58	67					
phi8238	<i>S. olivaceus</i>	DSM 41536				Yes	No	39	61					
phiSoli1	<i>S. olivaceus</i>	DSM 41536												
phiSoli2	<i>S. olivaceus</i>	DSM 41536												

Appendix

Table 2 | Comparison for selected features of phage-infected samples to uninfected controls using LC-MS in *S. coelicolor* WT. 'Up' ('down') refer to increased (decreased, respectively) abundance of the given metabolite in the phage-infected sample in comparison to the control. Data measured in collaboration with David Widdick and Andrew Truman (John Innes Centre, UK).

Family	Compounds	Exact masses	<i>m/z</i> observed	WT control vs Dagobah		WT control vs Endor1		WT control vs Endor2	
				fold-change	p-value	fold-change	p-value	fold-change	p-value
Actinorhodin derivatives	Actinorhodin	633.125	-	-	-	-	-	-	-
	Kalafungin	315.051	-	-	-	-	-	-	-
	γ-Actinorhodin	629.0937	629.0955	1.5 DOWN	0.49936	1.1 DOWN	0.86819	1.4 DOWN	0.50581
	Actinorhodic acid	665.1148	665.1012	1.9 DOWN	0.39893	2.0 DOWN	0.41484	-	-
	ε-Actinorhodin	647.1042	647.1077	1.1 DOWN	0.94114	8.7 DOWN	0.10537	1.2 DOWN	0.77606
	Deshydroxy-actinorhodic acid	649.1199	649.1223	4.9 UP	0.22588	-	-	2.7 UP	0.36099
Desferrioxamines	Desferrioxamine B	561.3612	561.3691	1.4 DOWN	0.60464	1.0 DOWN	0.94080	1.6 DOWN	0.51458
	Desferrioxamine E	601.3561	601.3636	1.6 DOWN	0.45561	1.4 DOWN	0.61271	1.8 DOWN	0.38150
	Peak group 12	-	770.4614	15.6 UP	0.07795				
		-	385.2333	29.9 UP	0.08831				
		-	768.4459	27.5 UP	0.09357				
		-	769.4477	33.1 UP	0.09462				
		-	384.7298	17.3 UP	0.12119				
	Peak group 17	-	797.4832	41.7 UP	0.08285				
		-	796.4789	41.9 UP	0.08952				
		-	398.7444	24.2 UP	0.09226				
	Peak group 25	-	392.2399	23.9 UP	0.08270				
		-	783.4704	24.8 UP	0.08997				
		-	782.4625	17.2 UP	0.09557				
-		391.7378	21.0 UP	0.09854					

Appendix

Table 3 | Comparison of undecylprodigiosin abundance between phage-infected samples and uninfected controls using LC-MS in a *S. coelicolor* actinorhodin mutant (Δact). 'Up' ('down') refer to increased (decreased, respectively) abundance of the given metabolite in the phage-infected sample in comparison to the control. Data measured in collaboration with David Widdick and Andrew Truman (John Innes Centre, UK).

Compounds	Exact mass	<i>m/z</i> observed	Δact control vs Dagobah		Δact control vs Endor1		Δact control vs Endor2	
			fold-change	p-value	fold-change	p-value	fold-change	p-value
Undecylprodigiosin	394.2853	394.2884	27.4 UP	0.09158	29.9 UP	0.11003	22.9 UP	0.11005

Phage-induced secondary metabolite production in *Streptomyces*: beyond actinorhodin and undecylprodigiosin

Naturally, phage-induced natural product synthesis in *Streptomyces* is much broader than actinorhodin and undecylprodigiosin and we extended our investigations to other secondary metabolites.

Desferrioxamines are hydroxamate siderophores conserved in *Streptomyces* and are produced by *S. coelicolor* under a wide range of conditions (Barona-Gómez et al., 2004). In *S. coelicolor*, the two main desferrioxamines are desferrioxamines B and E, and desferrioxamine synthesis is directed by a four-gene operon (*desA–D*). We used the LC-MS dataset primarily generated to assess production of actinorhodin and undecylprodigiosin on plates (cf. 2.2.4 Phage-induced natural product synthesis in *Streptomyces*) and examined desferrioxamine abundance in the different samples. Desferrioxamine B and E were found in high abundance in the samples, but no difference was observed between the controls and phage-infected samples. Interestingly, the Dagobah samples, when compared with controls, showed several peak groups (i.e., peaks that shared the same retention time) whose intensity was clearly higher, with fold-changes comprised between 20 and 50-fold (Appendix 4.1, Table 2). Comparison of the mass-to-charge ratio of these peaks with those of a network analysis performed following LC-MS/MS (Andrew Truman, personal communication) suggested that these peaks correspond to desferrioxamine derivatives distinct from desferrioxamines B and E, desferrioxamines being known to be detected under various forms depending on the lengths of the acyl chains and metal ions bound. The same peak groups were either not found or found at much lower intensity in the samples infected by Endor1 and Endor2, suggesting a specificity of the bacterial response to phage infection.

To deepen our understanding of the relationship between phage infection and desferrioxamines, we used a *S. coelicolor* mutant defective in the production of desferrioxamine B and E, obtained by the disruption of the *desD* gene (Barona-Gómez et al., 2004). The first obvious difference in phenotype when comparing the desferrioxamine-deficient mutant with *S. coelicolor* wild-type is the difference in pigmentation (Appendix 4.1, **Figure 1A**), a lack of desferrioxamines being known to impede secondary metabolite production (Tierrafría et al., 2011; Yamanaka et al., 2005). Interestingly, the phage Dagobah did not form plaques on the desferrioxamine-deficient mutant, and the plaques formed by Endor1 and Endor2, although comparable in numbers, were more turbid and substantially smaller. Considering that when using the same medium (GYM medium), Dagobah - unlike Endor1 and Endor2 - triggered a strong release of desferrioxamines (cf. 2.2.4 Phage-induced natural product synthesis in *Streptomyces* and Appendix 4.1, Table 2), this inability of Dagobah to plaque on the desferrioxamine-

deficient mutant suggests that desferrioxamines could be needed for successful phage infection. However, these differences showed some medium specificity: when switching to a different medium (CTT medium), the plaque counts of Dagobah were restored and similar to those of the wild type, despite a smaller plaque size (Appendix 4.1, **figure 1B**). Plaques formed by Endor1 and Endor2 were smaller comparatively to those of the wild type on CTT medium too. Next, we attempted to rescue the phenotype of the desferrioxamine mutant by adding to the plates increasing amounts of desferrioxamine B, which is purified from *Streptomyces pilosus*. Supplementation with up to 1 mM of desferrioxamine B had no effect on the plaque count and phenotype (Appendix 4.1, **Figure 1C**). This lack of complementation could be explained by the fact that desferrioxamine E (or other desferrioxamine derivatives) are needed, or that the concentrations used here were not sufficient. We then tested the impact of supplementation with ferrous iron Fe(II) on phage infection in the desferrioxamine-deficient *S. coelicolor* mutant.

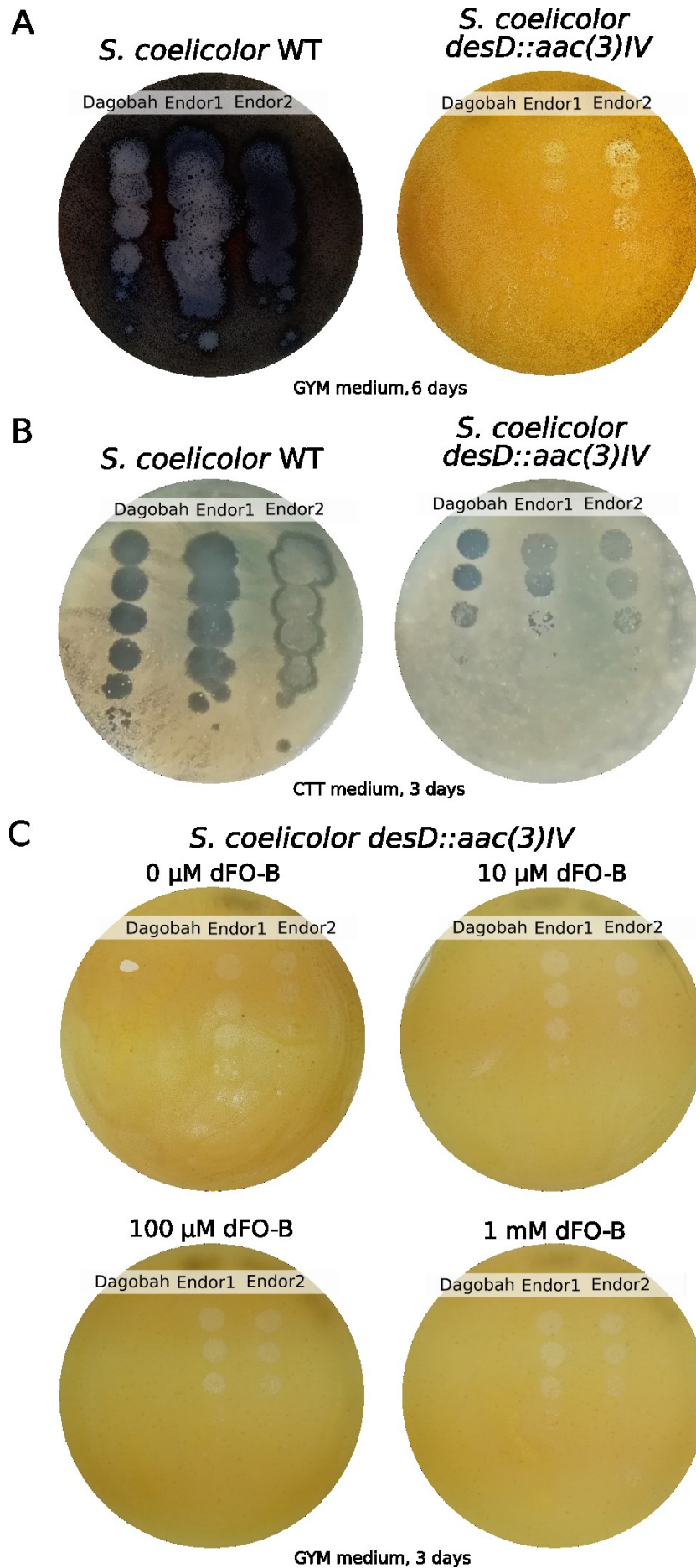


Figure 1 | **Impact of desferrioxamines on phage infection in *S. coelicolor*.** (A) and (B) Comparison of plaque phenotype and plaque counts between *S. coelicolor* WT and a mutant whose *desD* gene is disrupted by an apramycin resistance cassette (*aac(3)IV*) grown on GYM medium (A) and CTT medium (B). (C) Influence of the supplementation with increasing amounts of desferrioxamine B (dFO-B) on phage infection in a *S. coelicolor* desferrioxamine-deficient mutant. The *desD* mutant was obtained from Gregory Challis (University of Warwick, UK).

Addition of up to 250 μM FeSO_4 did not show an impact on plaque phenotype and counts (Appendix 4.1, **Figure 2A**). Similarly, further modulation of the iron content by supplementation of either ferric iron Fe(III) or of a chelating agent (2,2'-bipyridyl) showed only minor effects (Appendix 4.1, **Figure 2B**).

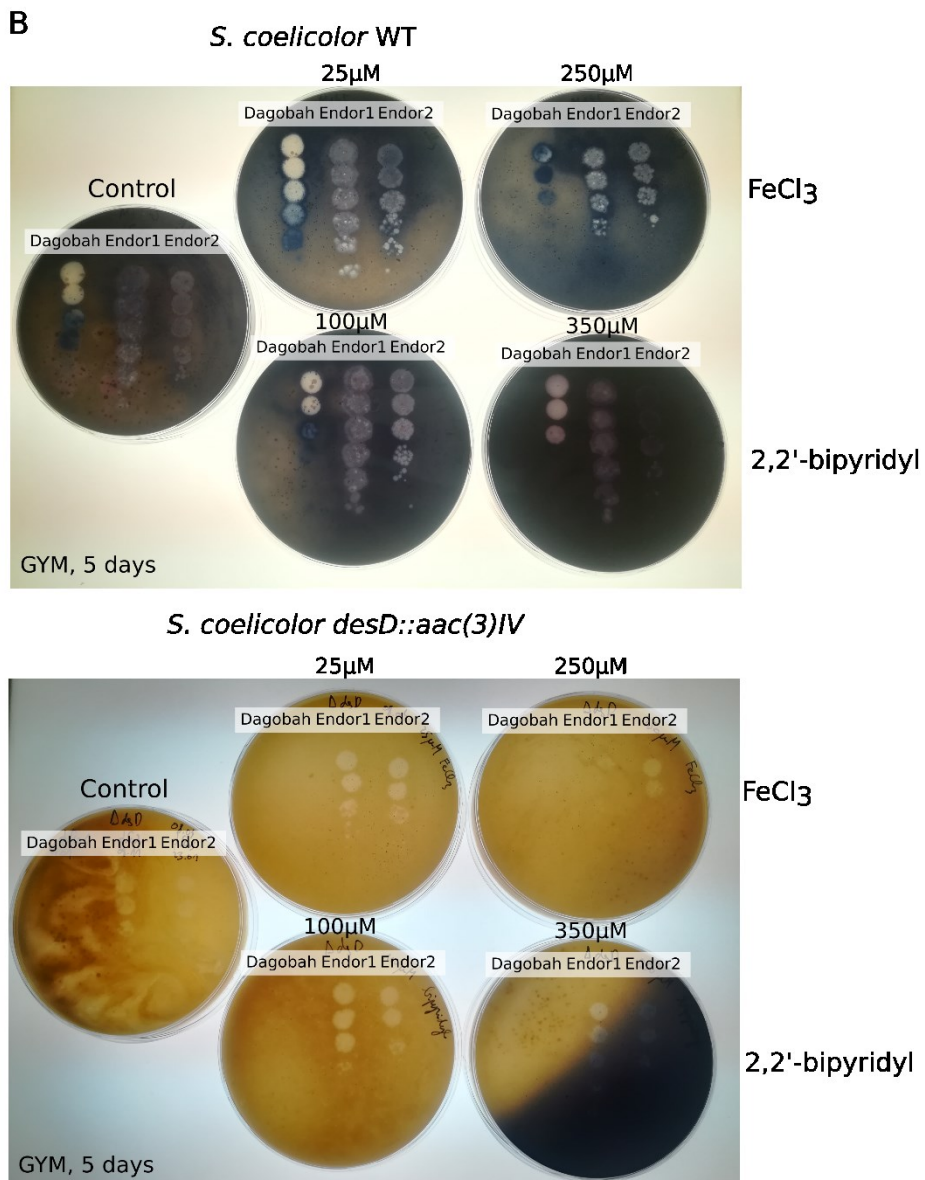
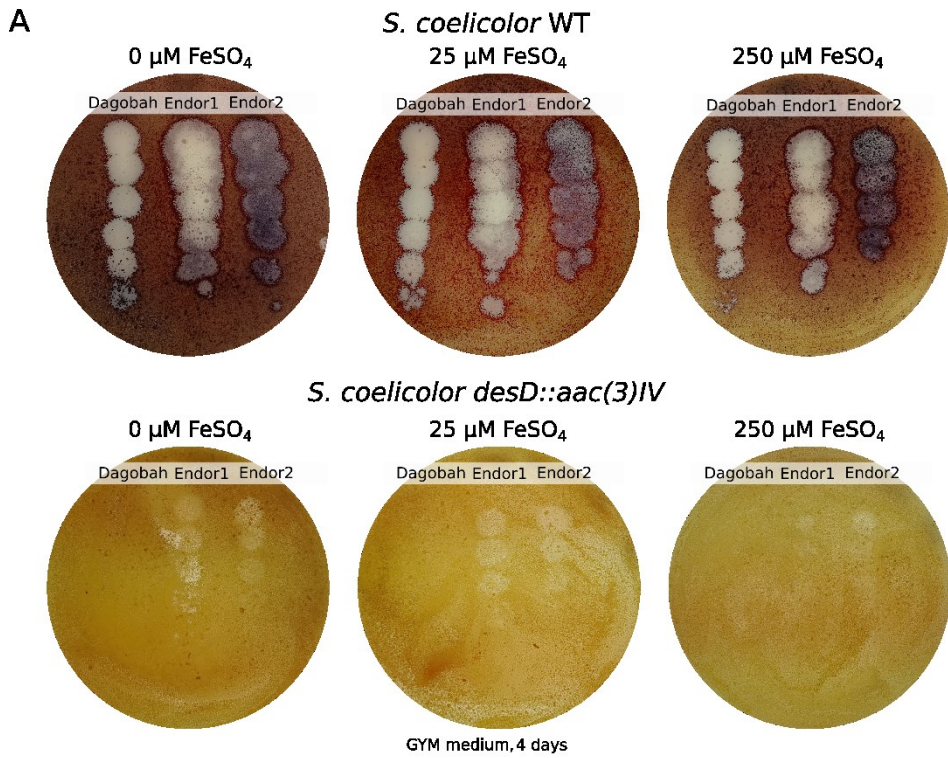


Figure 2 | **Influence of iron content on phage infection in *S. coelicolor*.** Influence of the supplementation with increasing amounts of ferrous iron Fe(II) (A) or ferric iron Fe(III) and the iron chelator 2,2'-bipyridyl (B) on phage infection in *S. coelicolor* WT and a *S. coelicolor* desferrioxamine-deficient mutant. The *desD* mutant was obtained from Gregory Challis (University of Warwick, UK).

Finally, we would like to report some rather preliminary and exploratory work about phage-triggered natural product synthesis in *S. venezuelae*. 'Soft-agar free assays' performed with our two *S. venezuelae* phages revealed brown halos diffusing from phage-infected colonies (Appendix 4.1, **Figure 3**). The identity of the molecule(s) responsible for these halos is not clear yet, but melanin is a prime candidate. *S. venezuelae* encodes two BGCs directing the synthesis of melanin (Gomez-Escribano et al., 2021) and melanin is a secondary metabolite commonly produced among *Streptomyces*. It remains to be demonstrated if the release of melanin in reaction to phage infection is a common strategy and what function does melanin fulfil in this context.

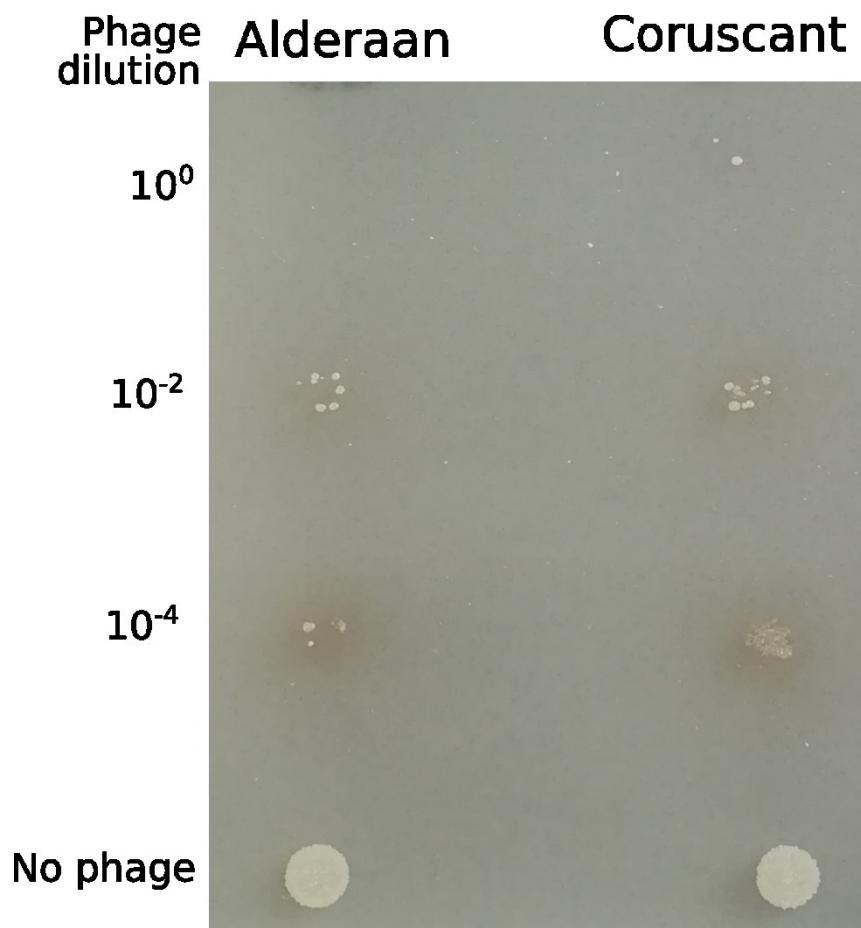


Figure 3 | **Phage infection triggers the release of a brown diffusible pigment in *S. venezuelae*.** *S. venezuelae* was infected with the phages Alderaan and Coruscant in a 'soft-agar free assay'.

A promising strategy which could provide insights into the response to phage infection at the metabolite level is MALDI imaging. This technique consists in the use of matrix-assisted laser desorption ionization (MALDI) on a solid sample while conserving the spatial structure of the sample. In other words, MALDI imaging allows the determination of analytes present in every point of the sample, with the limit imposed by the spatial resolution of the device. Use of this technique with colonies of *S. venezuelae* infected by the phage Alderaan revealed metabolites which were strongly enriched in the phage-infected colonies compared to the controls (Appendix 4.1, **Figure 4**). The following step of metabolite identification is not trivial and comprises prediction of the expected masses of known BGCs encoded by this strain as well as purification of the suspected compounds from large scale cultures, if possible.

In conclusion, we have showed that desferrioxamines were released by *S. coelicolor* in reaction to phage infection. Interestingly, when using the same growth medium, the phage triggering this release could not infect a desferrioxamine mutant. This observation suggests that desferrioxamine synthesis is needed for this phage to complete its infection cycle. This dependency could be indirect, with desferrioxamines ensuring a sufficient iron uptake and steady metabolic state under low-iron conditions. More generally, the release of desferrioxamines consecutive to phage infection can also be seen as a strategy for the *Streptomyces* population as a whole to secure iron released following the lysis of phage-infected cells.

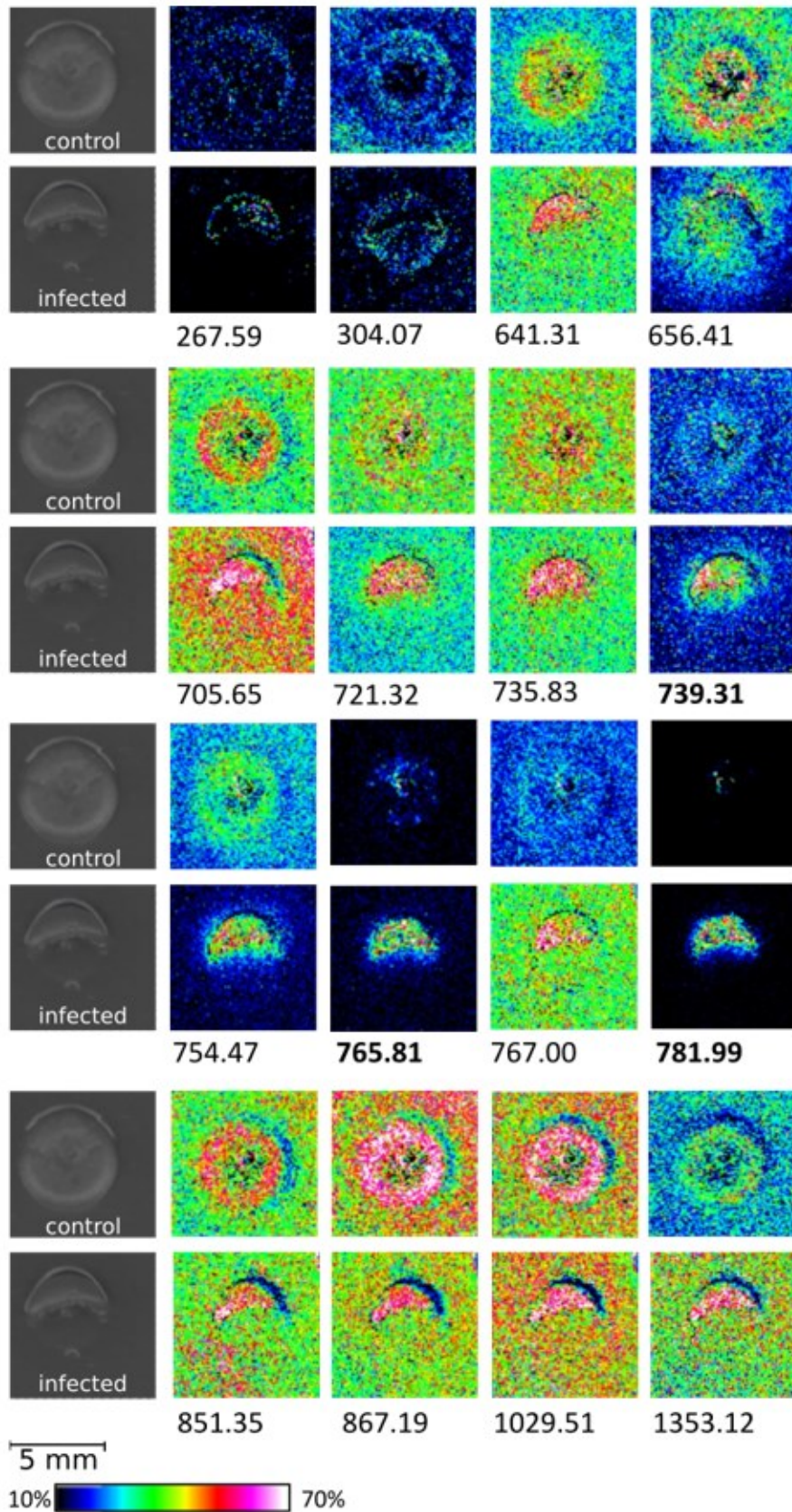


Figure 4 | **Selected extracted ion chromatograms of *S. venezuelae* samples analysed by MALDI Imaging.** *S. venezuelae* was infected with the phage Alderaan in 'soft-agar free assays'. The intensities were normalized after the respective total ion chromatograms. m/z values whose intensities are

notably higher in the phage-infected samples compared to the controls are highlighted in bold. Data obtained in collaboration with Silke Probst and Jörn Piel (ETH Zürich, Switzerland)

References

Barona-Gómez, F., Wong, U., Giannakopoulos, A.E., Derrick, P.J., and Challis, G.L. (2004). Identification of a Cluster of Genes that Directs Desferrioxamine Biosynthesis in *Streptomyces coelicolor* M145. *J. Am. Chem. Soc.* *126*, 16282–16283.

Gomez-Escribano, J.P., Holmes, N.A., Schlimpert, S., Bibb, M.J., Chandra, G., Wilkinson, B., Buttner, M.J., and Bibb, M.J. (2021). *Streptomyces venezuelae* NRRL B-65442: genome sequence of a model strain used to study morphological differentiation in filamentous actinobacteria. *Journal of Industrial Microbiology and Biotechnology* *48*, kuab035.

Tierrafría, V.H., Ramos-Aboites, H.E., Gosset, G., and Barona-Gómez, F. (2011). Disruption of the siderophore-binding *desE* receptor gene in *Streptomyces coelicolor* A3(2) results in impaired growth in spite of multiple iron-siderophore transport systems: Ferrioxamine-binding proteins of *Streptomyces*. *Microbial Biotechnology* *4*, 275–285.

Yamanaka, K., Oikawa, H., Ogawa, H., Hosono, K., Shinmachi, F., Takano, H., Sakuda, S., Beppu, T., and Ueda, K. (2005). Desferrioxamine E produced by *Streptomyces griseus* stimulates growth and development of *Streptomyces tanashiensis*. *Microbiology*, *151*, 2899–2905.

4.2 Supplementary information to “Genome Sequence and Characterization of Five Bacteriophages Infecting *Streptomyces coelicolor* and *Streptomyces venezuelae*: Alderaan, Coruscant, Dagobah, Endor1 and Endor2”

Article

Genome sequence and characterization of five bacteriophages infecting *Streptomyces coelicolor* and *Streptomyces venezuelae*: Alderaan, Coruscant, Dagobah, Endor1 and Endor2

Aël Hardy, Vikas Sharma, Larissa Kever and Julia Frunzke*

Institute of Bio- und Geosciences, IBG-1: Biotechnology, Forschungszentrum Jülich, 52425 Jülich, Germany

* Correspondence: j.frunzke@fz-juelich.de; Tel.: +49 2461 615430

Supplementary data

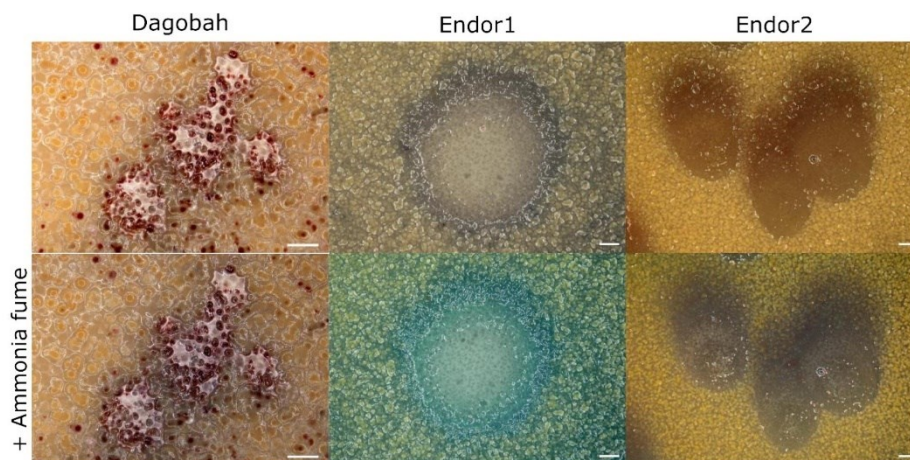


Figure S1. Close-ups of phage plaques imaged using a Nikon SMZ18 stereomicroscope, before (upper row) and after (lower row) exposure to ammonia fumes. *S. coelicolor* M145 was infected by phages using GYM double agar overlays. The plates were incubated at 30°C overnight and then kept at room temperature for two (Dagobah and Endor2) or three days (Endor1). The ammonia fume test was performed as follows: the plates were inverted and exposed to ammonia fumes for 15 min by placing 5 ml of 20% ammonium hydroxide solution on the inner surface of the lid. Scale bar: 1 mm.

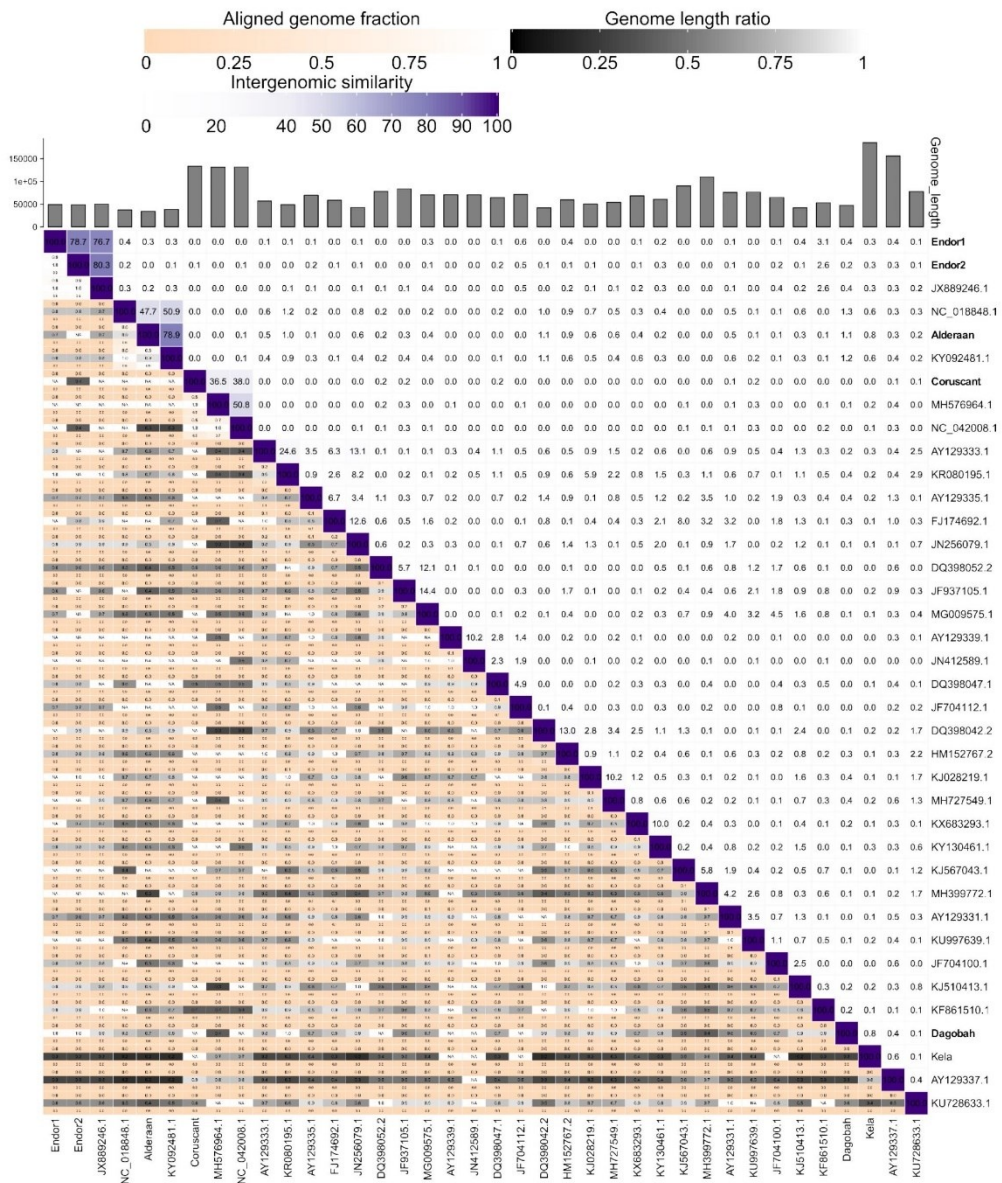


Figure S2. VIRIDC generated heatmap showing the intergenomic similarities of the newly sequenced phages with reference phages. For each phage pair, the fraction of aligned genome, the genome length ratio and the intergenomic similarities are displayed. The parameters used were the default ones.

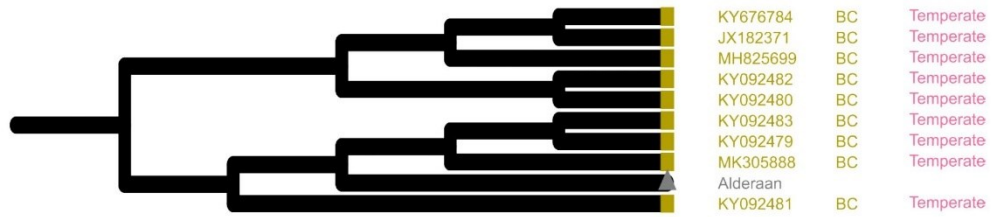


Figure S3. Subclade dendrogram with *Streptomyces* phage Alderaan and its closely related actinophages(enlargement from Figure 5). The phage lifestyles shown are those indicated on PhagesDB.

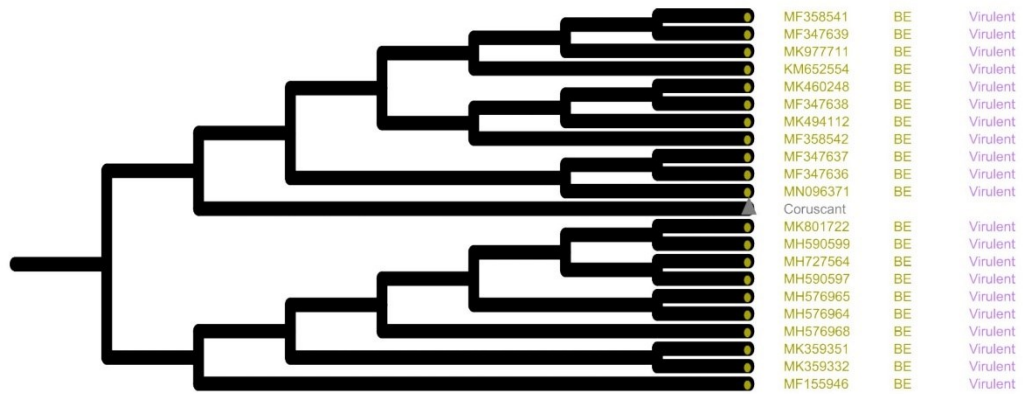


Figure S4. Subclade dendrogram with *Streptomyces* phage Coruscant and its closely related actinophages (enlargement from Figure 5). The phage lifestyles shown are those indicated on PhagesDB.

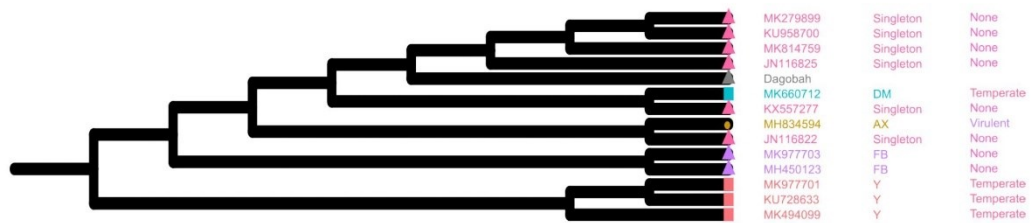


Figure S5. Subclade dendrogram with *Streptomyces* phage Dagobah and its closely related actinophages (enlargement from Figure 5). The phage lifestyles shown are those indicated on PhagesDB. “None” corresponds to phages with no lifestyle prediction on PhagesDB.

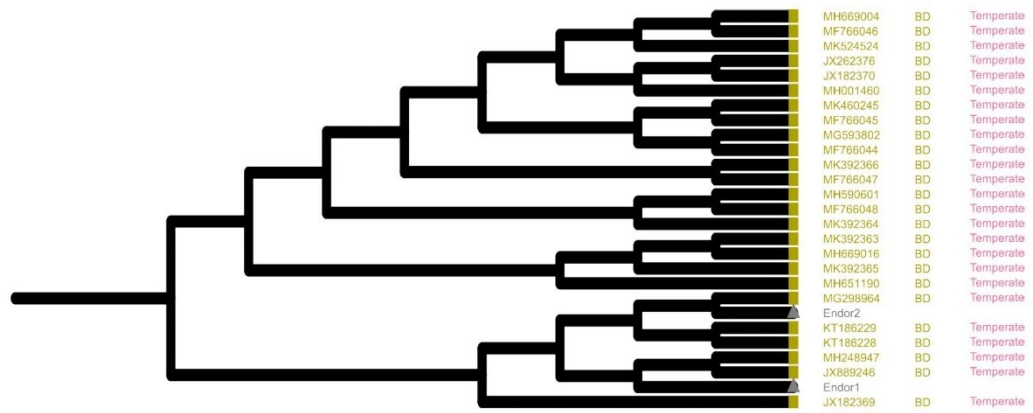


Figure S6. Subclade dendrogram with *Streptomyces* phages Endor1 and Endor2 and their closely related actinophages (enlargement from Figure 5). The phage lifestyles shown are those indicated on PhagesDB.

4.3 Supplementary information to “Aminoglycoside antibiotics inhibit phage infection by blocking an early step of the phage infection cycle”

Supplementary information to

Aminoglycoside antibiotics inhibit phage infection by blocking an early step of the infection cycle

Running title: Aminoglycosides inhibit phage infection

Larissa Kever^{1#}, Aël Hardy^{1#}, Tom Luthé¹, Max Hünnefeld¹, Cornelia Gätgens¹, Lars Milke¹,
Johanna Wiechert¹, Johannes Wittmann², Cristina Moraru³, Jan Marienhagen^{1,4} and Julia
Frunzke^{1*}

¹Institute of Bio- und Geosciences, IBG-1: Biotechnology, Forschungszentrum Jülich, 52425
Jülich, Germany

²Leibniz Institute DSMZ—German Collection of Microorganisms and Cell Cultures,
Inhoffenstraße 7B, 38124 Braunschweig, Germany

³Institute for Chemistry and Biology of the Marine Environment (ICBM), Carl-von-Ossietzky-
University Oldenburg, Oldenburg, Germany

⁴Institute of Biotechnology, RWTH Aachen University, Aachen, Germany

Authors contributed equally to this work.

*Corresponding author:

Julia Frunzke; Email: j.frunzke@fz-juelich.de; Phone: +49 2461 615430

Tables

Table S1 | Aminoglycoside-modifying enzymes used in this study

Table S2 | Bacterial strains used in this study.

Table S3 | Phages used in this study

Table S4 | Plasmids used in this study

Table S5 | Oligonucleotides used in this study

Table S6 | Polynucleotides used for phage targeting direct-geneFISH

Figures

Supplementary Figure S1 | Dose-dependent effect of apramycin on the *Streptomyces* phage Alderaan.

Supplementary Figure S2 | Effect of aminoglycosides on *E. coli* phage λ .

Supplementary Figure S3 | Synchronized infection of *Streptomyces venezuelae* with phage Alderaan under apramycin pressure.

Supplementary Figure S4 | Investigations of the mechanism of action of apramycin.

Supplementary Figure S5 | Pre-incubation of phage Alderaan with apramycin.

Supplementary Figure S6 | Distribution of fluorescence intensities from phage targeting direct-geneFISH.

Videos

Video S1: Apramycin prevents cell lysis during infection of *S. venezuelae* with phage Alderaan.

Tables

Supplementary Table S1: Aminoglycoside-modifying enzymes used in this study

Antibiotic	Gene	Annotation	Protein sequence	Modification
Apramycin	<i>aac(3)IV</i>	Aminoglycoside N(3)-acetyltransferase	VQYEWKRAELIGQLNLGVTGGVLLVHSSFR SVRPLEDGPLGLIEALRAALGPGGTLVMP SWSGLDDEPFDPATSPVTPDLGVVSDTFW RPLNVKRSAPHPFAAAAGPQAEQIISDPL PLPPHSPASPVARVHELDDGQVLLLVG HDANTLLHLAELMAKVYPYGVPRHCTI LQDQGLVRRVDYLENDHCCE RFALADR WLKEKSLQKEGPGVGHAFARLIRS DIVATALGQLGRDPLIFLHPPEAGCE ECCDAARQ SIG	Acetylation of 3-amino group of the deoxystreptamine ring
Hygromycin	<i>aph(7'')-Ia</i>	Aminoglycoside O-phosphotransferase APH(7'')-Ia,	VTQESLLLLDRIDSDDSYASLRNDQEF WEPLARRALEELGLPVPPVLRVPGEST NPNVLVGEPPDVIKLFGHEWCGPESL ASESEAYAVLADAPVPVPRLLGRGEL RPGTGAWPWVYLVMSRMTGTT WRS AMDGTTDRNALLALARELGRVLRGRL HRRVPLTGNTVLTPHSEVFPPELLR RERRAATVEDHRGWGYLSPRLLDR LEDWLPDVTLLAGREPRFVHGD LHGNTNIFVDLAATEVTGIVDFTD VYAGDSRYSLVQLHLNAFRGDREI LAALLDGAQWKRTEDFARELLAFT FLHDFEVFEETPLDLSGFTDPEE LAQFLWGPPDTAPGA	Phosphorylation of hydroxyl group at position 7''
Kanamycin	<i>aph(3'')-Ia</i>	Aminoglycoside 3'-phosphotransferase	MSHIQRETSRPRLNNSMDADLYGK WARDNVVGQSGATIYRLYGKPDAP ELFLKHGKGSVANVDTDEMVR LNWLTEFMPLPTIKHFIRTPDD AWLLTTAIPGKTAQVLEEYDPS GENIVDALAVFLRRLHSIPVCN PCFNSDRVFRLAQAQSRM NNGLYDASDFDDERNGWPVEQ VWKEMHKL LFPSPDSVVT HGDVSLDNLIFDEGKLGICID VGRVGIADRYQDLAILWNC LGEFSPSLQKRLFQK YGID NPD MNKLQFHMLLDEFF	Phosphorylation of hydroxyl group at position 3'
Spectinomycin/ Streptomycin	<i>aadA</i>	Aminoglycoside (3'') (9) adenylyltransferase	MREAVIAEVSTQLSEVVGVI ERHLEPTLLAVHLYGSAVDGGL KPHSDIDLLVTVRLDETTRRA LINDLLETASPGESEILRAVE VTIVVHDDIIPWRYPAKRELQ FGEWQRNDILAGIFEPATID IDLAILLTKAREHSVALVGPAA EELFDPVPEQDLFEALNETL TLWNSPPDWAGDERNVVLT LSRIWYS AVTGKIAPKDVA ADWAMERLPAQYQPVILEA RQAYLGQEEEDRLASRADQ LEEFVHYVKGEITK VVGK	O-adenylation at positions 3'' and 9

Supplementary Table S2: Bacterial strains used in this study

Strains	Genotype	Reference
<i>C. glutamicum</i> MB001	ATCC 13032 strain with deletion of prophages ΔCGP1 (cg1507-cg1524), ΔCGP2 (cg1746-cg1752) und ΔCGP3 (cg1890-cg2071)	1
<i>C. glutamicum</i> MB001 – pEKEx2a	MB001 carrying the plasmid pEKEx2a, Kan ^R	This study
<i>C. glutamicum</i> MB001 – pEKEx2b	MB001 carrying the plasmid pEKEx2b, Hyg ^R	This study
<i>C. glutamicum</i> MB001 – pEKEx2d	MB001 carrying the plasmid pEKEx2d, Apr ^R	This study
<i>C. glutamicum</i> MB001 – pEKEx2e	MB001 carrying the plasmid pEKEx2e, Sp ^R /Sm ^R	This study
<i>Escherichia coli</i> DH5α	<i>supE44 ΔlacU169 (f80lacZDM15) hsdR17 recA1 endA1 gyrA96 thi-1 relA1</i>	Invitrogen
<i>Escherichia coli</i> ET12567/pUZ8002	<i>dam-13::Tn9 dcm-6 hsdM hsdR</i> , carrying plasmid pUZ8002	2
<i>Escherichia coli</i> BL21 (DE3)	F ⁻ <i>ompT hsdS_B(r_B⁻ m_B⁻) gal dcm λ(DE3)</i>	3
<i>Escherichia coli</i> DSM 613	Wild-type strain	4
<i>E. coli</i> DSM 613 – pEKEx2a	<i>E. coli</i> DSM 613 carrying the plasmid pEKEx2a, Kan ^R	This study
<i>E. coli</i> DSM 613 – pEKEx2b	<i>E. coli</i> DSM 613 carrying the plasmid pEKEx2b, Hyg ^R	This study
<i>E. coli</i> DSM 613 – pEKEx2d	<i>E. coli</i> DSM 613 carrying the plasmid pEKEx2d, Apr ^R	This study
<i>E. coli</i> DSM 613 – pEKEx2e	<i>E. coli</i> DSM 613 carrying the plasmid pEKEx2e, Sp ^R /Sm ^R	This study
<i>Escherichia coli</i> DSM 5695	F ⁺ <i>met str T1^s T6^s lambda⁻</i>	5
<i>E. coli</i> DSM 5695 – pEKEx2a	<i>E. coli</i> DSM 5695 carrying the plasmid pEKEx2a, Kan ^R	This study
<i>E. coli</i> DSM 5695 – pEKEx2b	<i>E. coli</i> DSM 5695 carrying the plasmid pEKEx2b, Hyg ^R	This study
<i>E. coli</i> DSM 5695 – pEKEx2d	<i>E. coli</i> DSM 5695 carrying the plasmid pEKEx2d, Apr ^R	This study
<i>E. coli</i> DSM 5695 – pEKEx2e	<i>E. coli</i> DSM 5695 carrying the plasmid pEKEx2e, Sp ^R /Sm ^R	This study
<i>Escherichia coli</i> DSM 4230	F ⁻ <i>hsdR514 (rk⁻ mk⁻) supE44 supF58 Δ(lacIZY)6 galk2 galT22 metB1 trpR55 lambda⁻</i>	6
<i>E. coli</i> DSM 4230 – pEKEx2a	<i>E. coli</i> DSM 4230 carrying the plasmid pEKEx2a, Kan ^R	This study
<i>E. coli</i> DSM 4230 – pEKEx2b	<i>E. coli</i> DSM 4230 carrying the plasmid pEKEx2b, Hyg ^R	This study
<i>E. coli</i> DSM 4230 – pEKEx2d	<i>E. coli</i> DSM 4230 carrying the plasmid pEKEx2d, Apr ^R	This study

Appendix

<i>E. coli</i> DSM 4230 – pEKEx2e	<i>E. coli</i> DSM 4230 carrying the plasmid pEKEx2e, Sp ^R /Sm ^R	This study
<i>Escherichia coli</i> JW3996	<i>E. coli</i> BW25113 $\Delta lamB$	7
<i>Streptomyces venezuelae</i> ATCC 10712	Wild-type strain	8
<i>S. venezuelae</i> ATCC 10712 – pIJLK01	<i>S. venezuelae</i> ATCC 10712 carrying the integrative plasmid pIJLK01, Hyg ^R	This study
<i>S. venezuelae</i> ATCC 10712 – pIJLK04	<i>S. venezuelae</i> ATCC 10712 carrying the integrative plasmid pIJLK04, Apr ^R	This study
<i>S. venezuelae</i> ATCC 10712 – pIJLK05	<i>S. venezuelae</i> ATCC 10712 carrying the integrative plasmid pIJLK05, Sp ^R /Sm ^R	This study
<i>Streptomyces coelicolor</i> M145	<i>S. coelicolor</i> A3(2) lacking plasmids SCP1 and SCP2	9
<i>S. coelicolor</i> M145– pIJLK01	<i>S. coelicolor</i> M145 carrying the integrative plasmid pIJLK01, Hyg ^R	This study
<i>S. coelicolor</i> M145– pIJLK04	<i>S. coelicolor</i> M145 carrying the integrative plasmid pIJLK04, Apr ^R	This study
<i>S. coelicolor</i> M145– pIJLK05	<i>S. coelicolor</i> M145 carrying the integrative plasmid pIJLK05, Sp ^R /Sm ^R	This study

Supplementary Table S3: Phages used in this study

Phage	Host organism	Lifestyle	Family	Genome	State of injected genome ^{13,14}	Reference
Alderaan	<i>S. venezuelae</i> ATCC 10712	Virulent	<i>Siphoviridae</i>	dsDNA	Linear with terminal redundancy	15
Coruscant	<i>S. venezuelae</i> ATCC 10712	Virulent	<i>Siphoviridae</i>	dsDNA	Linear with terminal repeats	15
Dagobah	<i>S. coelicolor</i> M145	Temperate	<i>Siphoviridae</i>	dsDNA	Linear with terminal repeats	15
Endor1	<i>S. coelicolor</i> M145	Temperate	<i>Siphoviridae</i>	dsDNA	Linear with terminal redundancy	15
Endor2	<i>S. coelicolor</i> M145	Temperate	<i>Siphoviridae</i>	dsDNA	Linear with terminal redundancy	15
CL31	<i>C. glutamicum</i> MB001	Temperate	<i>Siphoviridae</i>	dsDNA	Linear with cohesive ends	16
Spe2	<i>C. glutamicum</i> ATCC 13032	Virulent	<i>Siphoviridae</i>	dsDNA	Unknown	This study, DSM110582
T4	<i>E. coli</i> B (DSM613)	Virulent	<i>Myoviridae</i>	dsDNA	Linear with terminal redundancy	DSM4505
T5	<i>E. coli</i> B (DSM613)	Virulent	<i>Siphoviridae</i>	dsDNA	Linear with terminal redundancy	DSM16353
T6	<i>E. coli</i> B (DSM613)	Virulent	<i>Myoviridae</i>	dsDNA	Linear with terminal repeats	DSM4622
T7	<i>E. coli</i> B (DSM613)	Virulent	<i>Podoviridae</i>	dsDNA	Linear with terminal repeats	DSM4623
M13	<i>E. coli</i> W1485 (DSM5695)	Chronic infection	<i>Inoviridae</i>	ssDNA	Circular (+) strand	DSM13976
fd	<i>E. coli</i> W1485 (DSM5695)	Chronic infection	<i>Inoviridae</i>	ssDNA	Circular (+) strand	DSM4498
MS2	<i>E. coli</i> W1485 (DSM5695)	Virulent	<i>Leviviridae</i>	ssRNA	Linear, bound to the maturation protein ¹⁷	DSM13767
Lambda (λ)	<i>E. coli</i> LE392 (DSM4230)	Temperate	<i>Siphoviridae</i>	dsDNA	Linear with cohesive ends	DSM4499

Supplementary Table S4: Plasmids used in this study

Plasmids	Characteristics						Reference
pIJ10257	Hyg ^R ; Cloning vector for the conjugal transfer of DNA from <i>E. coli</i> to <i>Streptomyces spp.</i> ; (constitutive promoter <i>ermE*</i> ; Integration at the Φ BT1 attachment site)						18
pEKEx2	Kan ^R ; <i>C. glutamicum</i> / <i>E. coli</i> shuttle vector for regulated gene expression; P_{tac} , <i>lacI^q</i> , pBL1 <i>oriV_{C.g.}</i> , pUC18 <i>oriV_{E.c.}</i>						19
pIJ773	pBluescript II SK(+)-based plasmid containing the apramycin resistance cassette flanked by FRT (FLP recognition target) recombination sites						20
pCDFduet-1	Sp ^R /Sm ^R ; <i>E. coli</i> vector for coexpression of two target genes; P_{T7} , <i>lacI</i> , CloDF13 ori, T7 terminator						Novagen
pUZ8002	Kan ^R ; RK2 derivative with nontransmissible oriT						21
pAN6	Kan ^R ; <i>E. coli</i> vector for regulated gene expression; derivative of pEKEx2 (P_{tac} , <i>lacI^q</i> , pBL1 <i>oriV_{C.g.}</i> , pUC18 <i>oriV_{E.c.}</i>)						22
Plasmids	Characteristics	Template	Primer	Vector	Restriction enzyme	Sequencing primer	Reference
pIJLK01	Hyg ^R ; Derivative of pIJ10257 with additional restrictions sites Bst1107I (upstream) and StuI (downstream) of the <i>aph(7'')-la</i> gene allowing exchanging of the antibiotic cassette	pIJ10257	1 + 2 + 4 3 5 + 6	pIJ10257	KpnI; PvuII	25 - 28	This study
pIJLK04	Apr ^R ; Derivative of pIJLK01 with <i>aph(7'')-la</i> exchanged for <i>aac(3)IV</i> (apramycin resistance gene)	pIJ773	7 + 8	pIJLK01	Bst1107I; StuI	28	This study
pIJLK05	Sp ^R /Sm ^R ; Derivative of pIJLK01 with <i>aph(7'')-la</i> exchanged for <i>aadA</i> (spectinomycin/streptomycin resistance gene)	pCDFduet-1	9 + 10	pIJLK01	Bst1107I; StuI	28	This study

Appendix

pEKEEx2a	Kan ^R ; Derivative of pEKEEx2 with additional restrictions sites Bst1107I (upstream) and NotI (downstream) of the <i>aphA1</i> gene allowing exchanging of the antibiotic cassette	pEKEEx2	11 + 12 13 + 14 15 + 16	pEKEEx2	SapI; StuI	29 - 32	This study
pEKEEx2b	Hyg ^R ; Derivative of pEKEEx2a with <i>aphA1</i> exchanged for <i>aph(7'')-Ia</i> (hygromycin resistance gene)	pIJ10257	17 + 18	pEKEEx2a	Bst1107I; NotI	31 + 32	This study
pEKEEx2d	Apr ^R ; Derivative of pEKEEx2a with <i>aphA1</i> exchanged for <i>aac(3)IV</i> (apramycin resistance gene)	pIJ773	19 + 20	pEKEEx2a	Bst1107I; NotI	31 + 32	This study
pEKEEx2e	Sp ^R /Sm ^R ; Derivative of pEKEEx2a with <i>aphA1</i> exchanged for <i>aadA</i> (spectinomycin/streptomycin resistance gene)	pCDFduet-1	21 + 22	pEKEEx2a	Bst1107I; NotI	31 + 32	This study
pAN6_aac(3)IV_Cstrep	Kan ^R ; Derivative of pAN6 with <i>aac(3)IV</i> fused to a C-terminal Strep-tag	pIJ773	23 + 24	pAN6_CStrep	NdeI; NheI	33 + 34	This study

Supplementary Table S5: Oligonucleotides used in this study

No.	Oligonucleotide name	Sequence (5' - 3')
Construction of plasmids		
1	pIJ10257_RE1_1_fw	TGCTCGGGTCGGGCTGGTACCAGTGAGCGTTTTTCAACCTCAG
2	pIJ10257_RE1_1_rv	GATTCTTGTGTACAGTATACAGCGGACCTCTATTACAGGG
3	pIJ10257_RE1_2_fw	AATAGAGGTCCGCTGTATACGTGACACAAGAATCCCTGTTACTTCTCG
4	pIJ10257_RE2_2_rv	CGGGCGGCCCGGGGCGAGGCCTTCAGGCGCCGGGGG
5	pIJ10257_RE2_3_fw	CCCCCGGCCTGAAGCCTCGCCCCGGGCCG
6	pIJ10257_RE2_3_rv	GAAACCTGTCGTGCCAGCTGCATTAATGAATCGGCCAACGCGC
7	pIJLK04_aac(3)IV_fw	TGAATAGAGGTCCGCTGTATACGTGCAATACGAATGGCGAAAAG
8	pIJLK04_aac(3)IV_rv	GGCGCCCCGGGGCGAGGCCTTCAGCCAATCGACTGGCG
9	pIJLK05_aadA_fw	TGAATAGAGGTCCGCTGTATACATGAGGGAAGCGGTGATCG
10	pIJLK05_aadA_rv	GCGGCCCGGGGCGAGGCCTTTATTTGCCGACTACCTTGGTGAT
11	pEKEx2_RE1_1_fw	GCGGTTTTCGTATTGGGCGCTCT
12	pEKEx2_RE1_1_rv	ATGGCTCATGTATACAACACCCCTTGTATTACTGTTTATGTAAGCAGAC
13	pEKEx2_RE1_2_fw	GGGGTGTGTATACATGAGCCATATTCAACGGGAAACGTCT
14	pEKEx2_RE2_2_rv	TTCTGAGCGCCGCTTAGAAAACTCATCGAGCATCAAATGAAAC
15	pEKEx2_RE2_3_fw	TTTCTAAGCGCCGCTCAGAATTGGTTAATTGGTTGTAACA
16	pEKEx2_RE2_3_rv	CGTGAAGAAGGTGTTGCTGACTC
17	pEKEx2b_hygR_fw	ATACAAGGGGTGTTGTATACGTGACACAAGAATCCCTGTTACTTCTC
18	pEKEx2b_hygR_rv	AATTAACCAATTCTGAGCGGCCGCTCAGGCGCCGGGGG
19	pEKEx2d_aac(3)IV_fw	ATACAAGGGGTGTTGTATACGTGCAATACGAATGGCGAAAAG
20	pEKEx2d_aac(3)IV_rv	ACCAATTCTGAGCGGCCGCTCAGCCAATCGACTGGCGAG
21	pEKEx2e_aadA_fw	ACAAGGGGTGTTGTATACATGAGGGAAGCGGTGATCG
22	pEKEx2e_aadA_rv	ACCAATTCTGAGCGGCCGCTTATTTGCCGACTACCTTGGTGATC
23	pAN6_aac(3)IV_Cstrep_fw	CCTCGAGAAGGAGATATACATATGATGTCATCAGCGGTGGAG
24	pAN6_aac(3)IV_Cstrep_rv	TGTGGGTGGGACCAGCTAGCGCCAATCGACTGGCGAGC
Sequencing primer		
25	pIJLK01_seq_fw_1	GATCAACCGCGACTAGCATC
26	pIJLK01_seq_fw_2	CCGGTGATCAAGCTGTTC
27	pIJLK01_seq_fw_3	TTTCTGCGGTAATCTGCTG
28	pIJLK0x_seq_fw_4	CGTAGAGATTGGCGATCCC
29	pEKEx2a_seq_fw	TTCCAGTCGGGAAACCTGTC
30	pEKEx2a_seq_rv	TCGCGAGCCCATTTATACCC
31	pEKEx2x_seq_fw	GGAAAGCCACGTTGTGTCTC
32	pEKEx2x_seq_rv	GCCTCGTGAAGAAGGTGTTG
33	pAN6_seq_Cstrep_fw	CGGCGTTTCACTTCTGAGTTCGGC
34	pAN6_seq_Cstrep_rv	GATATGACCATGATTACGCC
qPCR primer		
35	qPCR_atpD_Sv_fw	TGTTTCGAGACCGGCCTGAAG
36	qPCR_atpD_Sv_rv	AGACACCGTCGTGCAGCTTG
37	qPCR_Alderaan_HQ601_00028_fw	CTCGGCTATCCGATCATCC
38	qPCR_Alderaan_HQ601_00028_rv	TTGGTTGCGGTTGATGGAC

Supplementary Table S6: Polynucleotides used for phage targeting direct-geneFISH

No.	Sequence (5' - 3')
Gene probes for phage targeting direct-geneFISH with Alderaan infecting <i>S. venezuelae</i>	
1	ACGGCGATCAGCACCCAGGACAGGACGACGTCTTTGTGTGCGACCCACCATGGCGGTCTCGGTCTCGGCTCTTCCATCAACT TTCCCCAGTTCGGCAACAGTCGACATCGTATGGAGAGAGGGGGTGAAGCCCGTCCCATTCACCCCGGCATGGTCGAGCCC CTCGCCGAACGCACCCGCGATCTCTACGCCGCCGCCG
2	TACGCGGACGCCGAGGACGCTGTAACGGCTACCTCTGAACAAGAAGGCCAAGGCGGACGGCATCAACCCGGCCGCCCT GTTGAGCGGCCAGCCGATCGCGTACGCCGAGCGTCGGACGAGCTGAAAGAGTGGTGGGCCGAACACGGTCGCTAA CGCAGGCGGAGTTCATCGAGCAGGTACCCGCAAGGCTCA
3	CGCCGACAGCAACGGCCGTCACGAGCAGTCACCAACTACGACGTGCGCACGGCCTCCCCACCACCCGTAAGGAGGTCC GCCCATGGCGGGTAACAGCAGGTCCATCGACGCGCGGATGGCTCTCGAGGTCAAGGACACCGACGCCAGCACCGAGA CGTGGCTCCGATCGCCGGTCTCAACTCTGGTCTACT
4	CGGCGGTACGAGGAGGACGTATGCAGCGCGGCCCTCCATCACCTGGAGGGTCAAGTACCGCATCGACAAGACGACCA AGGCCCGGACGTGGGACAGCGTACATCGATGAGGAATGGACGCCGCTCTCGGCATCGACTCGCACAAACAGATCCGCT ACCGGCACGAGACGCAGTCCGATGGGCGATCTGGGACG
5	CGTAGACGTGCGCAAGACCTCTGGACACGTTCCGCGAGTATCCGACGGAGTTCGTCAGCTCGGCCTCGACGCCGAGAC GGCGATGGGGTCTCTCCAGGGACTCCAAGCGGTGCGCGGACGCCGATACGGTTCGCGGACGCGTTGAAGGAATTCA CGCTCATGGCTCAGGGCATGGGCGAGTCAACTGCGGAGT
6	GCCGTGTGGGCCGGGGCCATCGTCGTCGGTCAAGTGGTCTCATGGCCACACAGGCCCTCATGCAGGCCCGCCGATGGCC GCCGCTGGTCTCATCGCCATGGGCCGATTGGCTGCTCATCGCTGCCGTGGTGGTCTCGTCTGCTCTGATCATCAAGTATT GGGATGACATCGTCGACGCCACCACGAAGGCGTGGGA
7	GGCCCGCGGACTACGTCGAGATGACATTTTCAGCGGCGCCGCTGTCCGGCATTCCGTCAGCTACAGCCGGGCGTC GTTGGTCTGGCAGGGCCCGCTGAGCGGCATGTACCGGCTGTTCTGTGCGACCTGCGATCCGACCAAGTCTCGACATCC TTCCCGCGCAGGGCATCAAGTGCAGGACTACATCGG
8	CCGCGACGTTGACTCGTACCTCGCGCACCGGCTACTCAAGGACGGGTGGACCGGGAACGGGGTTCGACCAACTCGACATCG CCCGTCAGATCGTACTGGTCCAGTCGACCGAGGGCGGCAACATCGGCATCGAACTGGACTGGTTCGAGACATCCGGA GTGCTCCGCGACCGGGCTACTCCGCTACGACCTGTAC
9	GTCGTGCGGACGTGCTCGACCAACTCGCCAACGTCGAGAACGGGTTTCAGTGGCGGTACGTACGTACCGCATGCGTCC GGCCCGCGTGAAGAGCTTGCAGCTCGGCTATCCGATCATCCGGAGCAGCGTACCGAGTTGGTCTCTCTCCCGGGCC CGGTATCGACTACCGGATGCCGAGGACGGCACCT
10	GCGCCACCGCGCAGCTTCAGTTCGCGTGAACGGAACCATCGTGGCGACCGGCACGGCGGGTCAACCGCTCCTTGCCACCT TCGCCATCCCGTGTACGCGTTCGGCATGAACGCCGAGTTCGAGCTACAGGCCCGGTGTCCAGCGGCACCGGAACCGCCT ACGCCAGACCCGCTACCTGTACGGTTCAGTCTAA
11	GGCGGGTGTCTGGCGGGTGTCTGGCACGGTCTGTCGGTGGCGCTCATCGGCTGCTCTCTCTTGGGGGCGTGTCCGGA ATGGTCCACCTTGACACCCCGTCCGGACGTATCTGCCCAAGCGAGGACAGTTGAGACGTCTCTCGTACGGTTCGAAT AAGGCCAAAAGTCCGGGACAGGGGGTTGACAGTGA
12	AACCGCGCGGACGCTGCACGGGCGCTGGGAGTGGATGAGGAAATGATCTGGCCGAAGGCGGTGACAGGACCGGTAAGG TCGGCGGACCGGGAGATCTCCGCACTTACCATACCGCTCGGCGTCCCTCCAACGTGTGGGCGGACCTCGCTGCCG GCGCCGAGCAGAGTGTCTCGCCGGGTATACGAATA
13	GCGAGGTGACCCGGCAGCGGAGGTAATCGAAGGCGTTCGCTGTCGGTTCCACGCGCATTCCGATCACGCTCGATGAGT TGCGCGGCTCGGTCGGTTCGAGGGTGTGAGGCCCGGCTGAGCGCTGCCGAGGATGCCGTAATCACGTGAGCTGTGCG GTATTCCGATTCGACGAGGAGGCCCTCGTAACGCCTCAT

Appendix

14	TGCGGGCGGCACGTTGACGGCGGGATGTTGACCGCTTCGCAGAGCACGCCGAAGAGCTGTGGGAGCGGGCCGTGCCCGTG ACGTCGTAGACGACGAACGGCCCCGCTCCAGACAGGGACGCGGGGCCGTGCGTTTTCCGACAGTCAAGCAACCATCCG TATCGCTCCCTTTAGGTCCACTGTCGTGGGGTGTGGA
15	GACGCGAGTGTCTGTGACTGCTTCGCCCTGAGGAGCCGGCCGACGGTCGAGGCGCTGATGCCGCTATCTGCGGCAAAGCG GGAGCGCCCCCGCTGCGTAGGCCGGTGACGTGATCCGCGTCTACGAGTTCCTGGGAGAGCCATGCGGCGAACGCCGA GCGCGTCGCGTGGTCTGTTTTCTGCCATGGCAGAAA
16	CCGCGGGCGAGAAGGGCACGCACACCGTGTCCGGATGCTGTACCGCATCTACGGCCCGCCGGCGACTGCCTCGCCGTC ACCATCCCGGGCGAGGCCATGGACACGGCCGACAAGAGCACCACAAGGCGATGTCGGCCGCGCTCAAGTACATGCTCTTT CAGGTGTTTATGATCCCCGTGGACGCCCGCAGCATCGA
17	GGTGTATCCCGCCCGCTTACCCCGGAGGACGGCACCTAGCCCCCTCGATAGGGGGAGCCGGATCAGCCCCACATCCGCT ATCTTTCTGTCTGACAGATACATGCTGTGAGACAGAACCGCGAGCGCGCGCTCAGCACGTAGAGCAGGAGGACCGC CCCGTGAACACCCCGAGCGCTTCGCCGCAAGGTGCA
Gene probes for phage targeting direct-geneFISH with λ infecting <i>E. coli</i>	
1	AGCAGTATCTTAAATTTGGCGACAAAGAGACGCCGTTTGGCCTCAAATGGACGCCGGATGACCCCTCCAGCGTGTTTTATCT CTGCGAGCATAAATGCCTGCGTATCCGCCAGCAGGAGCTGGACTTTACTGATGCCCGTTATATCTGCGAAAAGACCGGGATC TGGACCCGTGATGGCATTCTCTGTTTTCTGTCATCCGGTGAAGAGATTGAGCCACCTGACAGTGTGACCTTTCACATCTGGAC AGCGTACAGCCGTTACCACCTGGGTGCAGATTGCAAAGACTGGATGAAAA
2	GCAGGACAACGTATTCGATGTGTTATCTGAAAGTACTGATGAACGGTGCGGTGATTATGATGGCGGGCGAACGAGGGC GTACAGGTGTTCTCCCGTATTGTTGACATGCCAGCGGGTGGGGAAACGTGATCCTGACGTTACGCTTACGTCCACACGGC ATTGGCAGATATCCGCGTATACGTTTCCAGCGATGTGCAGGTTATGGTGATTAAGAAACAGGCGCTGGGCATCAGCG TGGTCTGAGTGTGTTACAGAGGTTCTCCGGGAACGGGCGTTTTATTATAAAACAGT
3	AGATTATTATGGGCGCCACGACGATGAACAGACGCTGCTGCGTGTGGATGAGCCATCAATAAAACCTATACCCGCCGGA ATGGTGCAGAAATGTCGATATCCCGTATCTGCTGGGATACTGGCGGGATTGACCCGACCATTTGTGATGAACGCTCGAAAA AACATGGGCTGTTCCGGGTGATCCCATTAAGGGGCATCCGCTACGGAAAGCCGGTGGCCAGCATGCCACGTAAGCGAA ACAAAAACGGGTTTACCTTACCAGAAATCGGTACGGATACCGGAAAGAGCAGATT
4	CAATTTTGTCCACTCCCTGCCTCTGTCATCACGATACTGTGATGCCATGGTGTCCGACTTATGCCCGAGAAGATGTTGAGCA AATTATCGCTTATCTGCTTCTCATAGAGTCTTGACAGAACTGCGCAACTCGTAAAGGTAGGCGGATCCCTTCGAAGG AAAGACCTGATGCTTTTCTGCGCGCATAAAATACCTTGATACTGTCCGGATGAAAGCGGTTGCGCAGCAGTAGATGCAAT TATGTTTTCTCCGCAAGAATCTTTGCATTTATCAAGTGTTCCTTCATTG
5	TGCTCGACATAAAGATATCCATCTACGATATCAGACCACTTCATTTGCATAAATCACCACCTCGTTGCCGGTAAACAACGC CAGTTCATTGCAAGTCTGAGCCAACATGGTGATGATTCTGCTGCTTGATAAATTTTTCAGGATTCTGTCAGCCGTAAGTCTTG ATCTCTTACCTCTGATTTTCTGCGCAGTGGCAGCGACATGTTTTGTTTATATGGCCTTACGCTATTGCTCTCGGAAT GCATCGCTCAGTGTGATCTGATTAACCTGGCTGACGCCGCTTGCCTCG
6	AACTCAATGTTGGCCTGTATAGCTTCAGTGATTGCGATTGCTGCTGCTGCTAATCCAACTCTTTACCCGCTCTTGGGTCC CTGTAGCAGTAATATCCATTGTTTCTTATATAAAGTTAGGGGGTAAATCCCGCGCTCATGACTTCGCTTCTTCCATTCT GATCCTTCAAAGGCCACCTGTTACTGGTCGATTTAAGTCAACCTTACCCTGATTGTTGGAACAGATACTCTTCCATC CTTAACCGAGGTGGGAATATCCTGCATTTCCGAACCCATCGACGAAC
7	TGTTTCAAGGCTTCTTGGACGTGCTGGCGTGCCTTCCACTCCTGAAGTGTCAAGTACATCGCAAAGTCTCCGCAATTACAG CAAGAAAAACCGCCATCAGGCGGCTTGGTGTCTTTTCAAGTCTTCAATTGGAATTTGTTACGTCTGCATGTGCTATCTGC GCCATATCATCCAGTGGTCTGAGCAGTCTGATGTTCTCCGCTTCCGATAACTCTGTTGAATGGCTCTCATTCCATTCTCT GTGACTCGGAAGTGCATTTATCATCTCCATAAAACAAAACCCGCCGTAGC
8	ACTCAACCCGATGTTTGGTACGGTTCATCTGACACTACAGACTCTGGCATCGCTGTGAAGACGACGCGAAATTCAGCAT TTTACAAGCGTTATCTTTTACAAAACCGATCTCACTCTCTTTGATGCGAATGCCAGCGTCAGACATCATATGCAGATACTCA CCTGCATCTGAACCCATTGACCTCAACCCGTAATAGCGATGCGTAATGATGTCGATAGTTACTAACGGGTCTTGTTCGAT TAACTGCCGAGAACTCTTCCAGGTACCAGTGCAGTGTGATAACAGG

Appendix

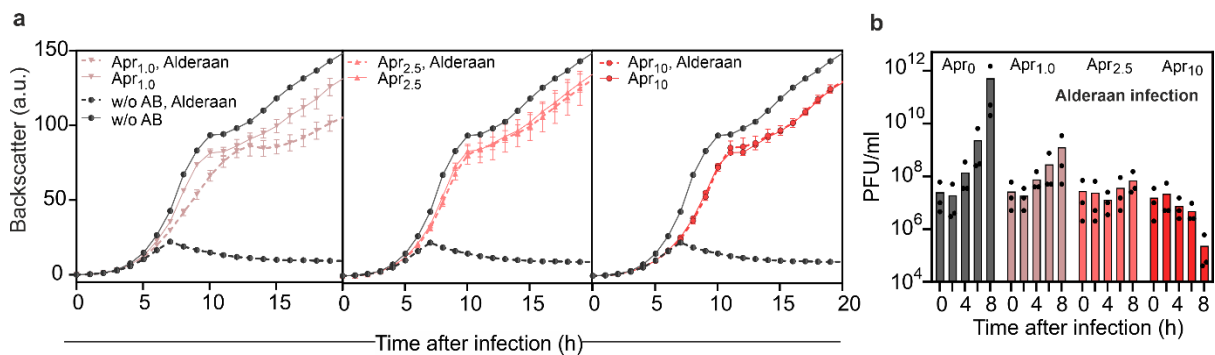
9	GTTTCATCCAGCAGTTCAGCACAATCGATGGTGTACCAATTCATGGAAAAGGCTGCGTCAAATCCCCAGTCGTCATGCATT GCCTGCTCTGCCGCTTACGCAGTGCCTGAGAGTTAATTCGCTCACTCGAACCTCTCTGTTTACTGATAAGTTCCAGATCCT CCTGGCAAATGACAAAGTCCGACAACCCTGAACGACCAGGCGTCTTCGTTTCATCTATCGGATCGCCACTCACAAATGA GTGGCAGATATAGCCTGGTGGTTCAGGCGGCGCATTTTTATTGCTGTGT
10	TGAGGGTGAATGCGAATAATAAAAAAGGAGCCTGTAGCTCCCTGATGATTTTGCTTTTCATGTTTCATGTTCCCTTAAAGACGC CGTTTAACATGCCGATTGCCAGGCTTAAATGAGTCGGTGTGAATCCCATCAGCGTTACGTTTTCGCGGTGCTTCTTCAGTACG CTACGGCAAATGTCATCGACGTTTTATCCGGAACACTGCTGTCTGGCTTTTTTTGATTCAGAATTAGCCTGACGGGCAATGC TGCGAAGGGCGTTTTCTGCTGAGGTGTCATTGAACAAGTCCATGTCGGC
11	AGGTAACGGGCATTTTCAGTTCAAGGCCGTTGCCGTCCTGCATAAACCATCGGGAGAGCAGGCGGTACGCATACTTTCGT CGCGATAGATGATCGGGGATTTCAGTAACATTCACGCCGGAAGTGAATCAAACAGGGTCTGGCGTCTGTTCTCGTACTGTT TCCCCAGGCCAGTGTCTTAGCGTTAACTTCCGGAGCCACACCGGTGCAAACCTCAGCAAGCAGGGTGTGAAGTAGGACAT TTTCATGTCAGGCCACTTCTTTCCGGAGCGGGTTTTGCTATCACGTTGTGAACCT
12	TGATGACGCCGAGCCGTAATTTGTGCCACGCATCATCCCCCTGTTTCGACAGCTCTCATATCGATCCCGGTACGCTGCAGGATA ATGTCCGGTGTGATGCTGCCACCTTCTGCTCTGCGGCTTCTGTTTCAGGAATCCAAGAGCTTTTACTGTTTCGGCCTGTGTCA GTTCTGACGATGCAGGAATGTCGCGGCGAAATATCTGGGAACAGAGCGGCAATAAGTCGTATCCCATGTTTTATCCAGGG CGATCAGCAGAGTGTTAATCTCTGTCATGGTTTCATCGTTAACGGAGTGAT
13	TCGCGTTCCGGCTGACGTTCTGCAGTGTATGCAGTATTTTCGACAATGCGCTCGGCTTCATCCTTGTATAGATACCAGCAAA TCCGAAGGCCAGACGGGCACACTGAATCATGGCTTTATGACGTAAACATCCGTTTGGGATGCGACTGCCACGGCCCCGTGATT TCTCTGCCTTCGCGAGTTTTGAATGGTTCGCGGCGGCATTATCCATCCATTCCGTAACGCAGATCGGATGATTACGGTCCCT GCGGTAATCCGGCATGTACAGGATTATTGTCCTGCTCAAAGTCCATGCCA
14	TCAAACCTGCTGTTTTTTCATTGATGATGCGGGACCAGCCATCAACGCCACCACCGGAACGATGCCATTCTGCTTATCAGGAA AGGCGTAAATTTCTTTCGTCACGGATTAAGGCCGTAAGGCTTGGCAACGATCAGTAATGCGATGAACTGCGCATCGCTGGC ATCACCTTTAAATGCCGTCTGGCGAAGAGTGGTGTGATCAGTTCCTGTGGGTGACAGAAATCCATGCCGACAGTTCAGCCAGC TTCCAGCCAGCGTTGCGAGTGCAGTACTATTGTTTTATACCTCTGAATCAA
15	TATCAACCTGGTGGTGTGAGCAATGGTTTTCAACCATGTACCGGATGTGTTCTGCCATGCGCTCCTGAAACTCAACATCGTCATCA AACGCACGGGTAAATGGATTTTTGCTGGCCCCGTTGGCCTTCAAATGATCGATGCATAGCGATTCAAACAGGTGCTGGGGC AGGCCTTTTTTCATGTCGCTGCCAGTTCTGCTCTTTCTTTCACGGGCGAGCTGCTGGTAGTGACGCGCCAGCTCTGAGC CTCAAGACGATCCTGAATGTAATAAGCGTTCATGGCTGAACCTCTGAAATAGC
16	GATAAAGCCAAGGCCAATATCTAAGTAAGTACTAGATAAGAGGAATCGATTTTCCCTTAATTTTCTGGCGTCCACTGCATGTTATG CCGCGTTCCGCAAGGCTTGTGTACCATGTGCGGTGATTCTTGGCGTCAATACGTTGCAAGTTGCTTTCAATCTGTTTGTGGTA TTCAGCCAGCACTGTAAGGTCTATCGGATTTAGTGCCTTCTACTCGTATTTCCGGTTTGCATTGAGCAGAGAGAATAGGG CGGTTAACTGGTTTTGCGCTTACCCCAACCAACAGGGGATTTGCTGCTTTCC
17	AGCCTGTTTCTCTGCGGACGTTTCGCGGCGGCGTGTGTTGTCATCCATCTGGATTCTCCTGTCAGTTAGCTTTGGTGGTGTGT GGCAGTTGTAGTCTGAACGAAAACCCCGCGATTGGCACATTGGCAGCTAATCCGGAATCGCACTTACGGCCAATGCTTC GTTTTGATCACACACCCAAAGCCTTCTGCTTTGAATGCTGCCCTTCTTCAGGGCTTAATTTTTAAGAGCGTACCTTCATGG TGTCAGTGGTCTGCTGATGTGCTCAGTATCACCGCCAGTGGTATTAT
18	TACTATGTTATGTTCTGAGGGGAGTGAATAATCCCTAATTCGATGAAGATTCTGCTCAATTGTTATCAGCTATGCGCCGAC CAGAACACCTTGGCGATCAGCCAAACGTCTCTCAGGCCACTGACTAGCGATAACTTTCCCAACGGAACAACCTCTATTG CATGGGATCATTGGGACTGTGGTTTTAGTGGTGTAAAAACACCTGACCGCTATCCCTGATCAGTTTCTGAAGGTAACCT ATCACCCCAAGTCTGGCTATGCAGAAATCACCTGGCTCAACAGCCTGCTC
19	TATTTGCATACATTCAATCAATTGTTATCTAAGGAAATACTTACATATGGTTCGTGCAAACAAACGCAACGAGGCTCTACGAA TCGAGAGTGCCTTGAACAAAATCGCAATGCTTGAACACTGAGAAGACAGCGGAAGCTGTGGGCGTTGATAAGTGCAGACA TCAGCAGGTGGAAGAGGGACTGGATTCAAAGTCTCAATGCTGCTTGTGTTCTTGAATGGGGGCTGTTGACGACGACA TGCTCGATTGGCGGACAAGTTGCTGCGATTCTACCAATAAAAAACGCCCGC
20	TCAAGCAGCAAGGCGGCATGTTTGGACCAAATAAAAAACATCTCAGAATGGTGCATCCCTCAAACGAGGGGAAAATCCCCTA AAACGAGGGATAAAAACATCCCTCAAATGGGGGATTGCTATCCCTCAAACAGGGGGACAAAAGACACTATTACAAAAG AAAAAGAAAAGATTATTCGTACAGAAATCTGGCGAATCCTGACAGCCAGAAAACGACCTTTCTGTGGTGAACCCGG ATGCTGCAATTCAGAGCGGCAGCAAGTGGGGGACAGCAGAAGACCTGACCGCCGAG

Appendix

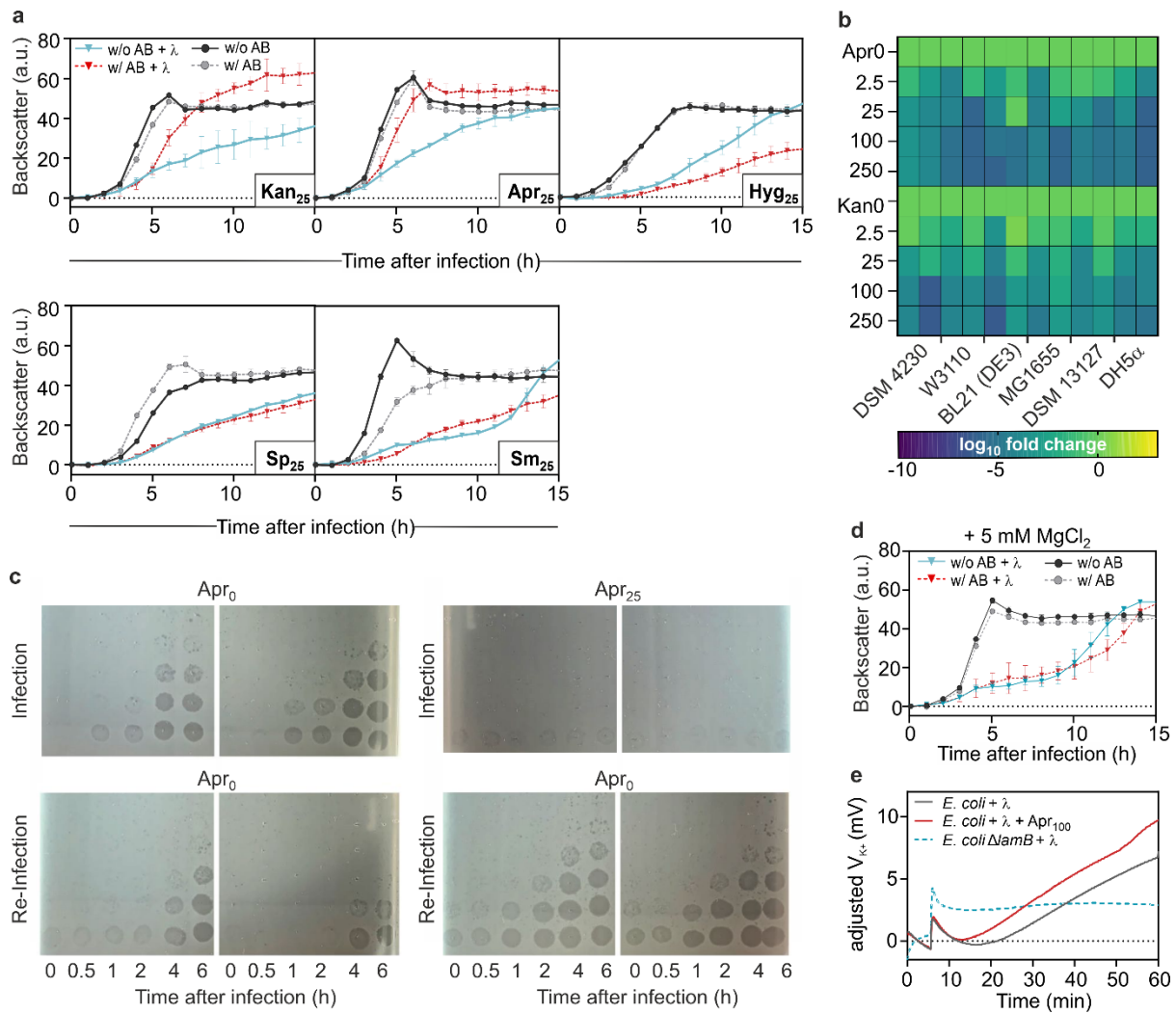
21	ATAAGTGGACCCAACCTCGAAATCAACCGTAACAAGCAACAGGCAGGCGTGACAGCCAGCAAACCAAACTCGACCTGACAA ACACAGACTGGATTTACGGGGTGGATCTATGAAAAACATCGCCGCACAGATGGTAACTTTGACCGTGAGCAGATGCGTCCG GATCGCCAACAACATGCCGGAACAGTACGACGAAAAGCCGAGGTACAGCAGGTAGCCGAGATCATCAACGGTGTGTTCA GCCAGTTACTGGCAACTTTCCCGGCGAGCCTGGCTAACCGTGACCAGAACGAAGTGAA
22	TGGCGGTATATGGAGTTAAAAGATGACCATCTACATTACTGAGCTAATAACAGGCCTGCTGGTAATCGCAGGCCTTTTTATTT GGGGGAGAGGGAAGTCATGAAAAAATAACCTTTGAAATTCGATCTCCAGCACATCAGCAAAACGCTATTACGCAGTACA GCAAATCCTTCAGACCCAACCAACCAATCGTAGTAACCATTAGGAAACGCAACCGCAGCTTAGACCAAAACAGGAAGCTA TGGGCTGCTTAGGTGACGTCTCTCGTACAGTTGAATGGCATGGTCGCTGGCTG
23	GATGCAGAAAGCTGGAAGTGTGTGTTTACCGCAGCATTAAAGCAGCAGGATGTTGTTCTAACCTTGCCGGGAATGGCTTT GTGGTAATAGGCCAGTCAACCAGCAGGATGCGTGTAGGCGAATTTGCGGAGCTATTAGAGCTTATACAGGCATTGCGTACA GAGCGTGGCGTTAAGTGGTCAGACGAAGCAGACTGGCTCTGGAGTGGAAAGCGAGATGGGGAGACAGGGCTGCATGAT AAATGTCGTTAGTTTCTCCGGTGGCAGGACGTCAGCATATTTGCTCTGGCTAATGGAGC
24	CCATTTCCGGGCGAGGGAATTACACCACGTGGATTGGCATCAGAGCTGATGAACCGAAGCGGCTAAAGCCAAAGCCTGGAAT CAGATATCTTGCTGAACTGTCAGACTTTGAGAAGGAAGATATCCTCGCATGGTGGAAAGCAACAACCTTCGATTTGCAAATA CCGGAACATCTCGGTAACGTCATATTCTGCATTAATAAATCAACGCAAAAAATCGGACTTGCTGCAAAGATGAGGAGGGA TTGCAGCGTGTTTAATGAGGTCATCACGGGATCCCATGTGCGTGACGGACATCG
25	GGAAACGCCAAAGGAGATTATGTACCGAGGAAGAATGTCGCTGGACGGTATCGCGAAAATGTATTCAGAAAATGATTATCA AGCCCTGTATCAGGACATGGTACGAGCTAAAAGATTGCATACCGGCTCTGTTCTGAGTCATGCGAAAATTTGGAGGGCAG CTTGATTTGACTTCGGGAGGGAAGCTGCATGATGCGATGTTATCGGTGCGGTGAATGCAAAGAAGATAACCGCTTCCGAC CAAAATCAACCTTACTGGAATCGATGGTGTCTCCGGTGTGAAAGAACCAACAGGG
26	GTGTTACCACTACCGCAGGAAAAGGAGACGTGTGGCGAGACAGCAGCAAGTATCACCGACATAATCTGCGAAAACCTGC AAATACCTTCCAACGAAACGCACCAGAAATAAACCAGCAATCCCAAAAGAATCTGACGTAAAAACCTTCAACTACACGG CTCACCTGTGGGATATCCGGTGGCTAAGACGTCGTGCGAGGAAAACAAGGTGATTGACCAAAATCGAAGTTACGAACAAGA AAGCGTCGAGCGAGCTTAACTGCGCTAACTGCGGTGAGAAGCTGCATGTGCTGGA
27	GCGCAGAACTGATGAGCGATCCGAATAGCTCGATGCACGAGGAAGAAGATGATGGCTAAACCAGCGCGAAGACGATGTAA AAACGATGAATGCCGGGAATGGTTTACCCTGCATTCGCTAATCAGTGGTGGTCTCTCCAGAGTGTGGAACCAAGATAGC ACTCGAACGACGAAGTAAAGAACCGGAAAAAGCGGAAAAAGCAGCAGAGAAGAAACGACGACGAGAGGAGCAGAAAACA GAAAGATAAATTAAGATTGAAAACTCGCTTAAAGCCCCGCACTTACTGGATTAACAA
28	CCAACAAGCCGTAAACGCCTTCATCAGAGAAAGAGACCGCGACTTACCATGTATCTCGTGCGGAACGCTCACGTCTGCTCAG TGGGATGCCGGACATTACCGGACAACCTGCTGCGGCACCTCAACTCCGATTTAATGAACGCAATATTACAAGCAATGCGTGG TGTGCAACCAGCACAAAAGCGGAAATCTCGTTCGGTATCGCGTGAAGTATTAGCCGCATCGGGCAGGAAGCAGTAGACG AAATCGAATCAACCATAACCGCCATCGCTGGACTATCGAAGAGTGCAAGGCGAT
29	TGTTATCTGCCACGCCGATTATCCCTTTGACGAATACGAGTTTGAAAGCCAGTTGATCATCAGCAGGTAATCTGGAACCGC GAACGAATCAGCAACTCAGAAAACGGGATCGTGAAAGAAATCAAAGGCGCGGACAGTTCATCTTTGGTCATACGCCAGCA GTGAAACCACTCAAGTTTGCCAACCAATGTATATCGATACCGGCGCAGTGTCTGCGGAAACCTAACATTGATTAGGTAC AGGGAGAAGGCGCATGAGACTCGAAAGCGTAGCTAAATTTCACTCGCAAAAAGC
30	CAGAGATTGCCATGGTACAGGCCGTGCGGTTGATATTGCCAAAACAGAGCTGTGGGGGAGAGTTGTGCGAGAAAGAGTGCG GAAGATGCAAAGCGTCCGCTATTCAAGGATGCCAGCAAGCGCAGCATATCGCGCTGTGACGATGCTAATCCCAAACCTTA CCCAACCCACTGGTCACGCACTGTTAAGCCGCTGTATGACGCTCTGGTGGTGAATGCCACAAAGAAGAGTCAATCGCAGA CAACATTTGAATGCGGTCACACGTTAGCAGCATGATTGCCACGGATGGCAACATAT
31	TGAATAAAATTGGGTAATTTGACTCAACGATGGGTTAATTCGCTCGTTGTGGTAGTGAGATGAAAAGAGGCGGCGCTTAC TACCGATTCGCTAGTTGGTCACTTCGACGTATCGTCTGGAACCTCAACCATCGCAGGCAGAGAGGTCTGCAAAATGCAAT CCCGAAACAGTTCGACAGTAATAGTTAGAGCTGCATAACGGTTTCCGGATTTTTATATCTGCACAACAGGTAAGAGCATT GAGTCGATAATCGTGAAGAGTCGGCGAGCCTGGTTAGCCAGTGCTCTTTCCGTTG
32	TGCTGAATTAAGCGAATACCGGAAGCAGAACCGGATCACAAATGCGTACAGGCGTCATCGCCGCCAGCAACAGCACAAAC CCAACTGAGCCGTAGCCACTGTCTGTCTGAATTCATTAGTAATAGTTACGCTGCGCCTTTTACACATGACCTTCGTGAAA GCGGGTGGCAGGAGGTGCGGCTAACAACTCCTGCCGTTTTGCCGTGCATATCGGTACGAAACAAATCTGATTACTAAACA CAGTAGCCTGGATTTGTTCTATCAGTAATCGACCTTATTCCTAATTAATAGAG

33	CAAATCCCCTTATTGGGGGTAAGACATGAAGATGCCAGAAAACATGACCTGTTGGCCGCCATTCTCGCGGCAAAGGAACA AGGCATCGGGGCAATCCTTGCCTTTCGTTGCAATGGCGTACCTTCGCGGCAGATATAATGGCGGTGCGTTTACAAAAACAGTAATC GACGCAACGATGTGCGCCATTATCGCCTGGTTCATTCGTGACCTTCTCGACTTCGCGGACTAAGTAGCAATCTCGCTTATAT AACGAGCGTGTATCGGCTACATCGGTACTGACTCGATTGGTTTCGCTTATCAA
34	ATCATGGTTATGACGTCATTGTAGGCGGAGAGCTATTTACTGATTACTCCGATCACCTCGCAAATTGTCACGCTAAACCCA AAACTCAAATCAACAGGCGCCGGACGCTACCAGCTTCTTTCCCGTTGGTGGGATGCCTACCGAAGCAGCTTGGCCTGAAAG ACTTCTCTCCGAAAAGTCAGGACGCTGTGGCATTGCAGCAGATTAAGGAGCGTGGCGCTTTACCTATGATTGATCGTGGTGA TATCCGTCAGGCAATCGACCGTTGCAGCAATATCTGGGCTTCACTGCCGGGCG
35	GATAAAACAAAAGCCACCGTGTGCGTCACTGGTATGACCATCACCGTGAACGGCGTTGCTGCAGGCAAGGTCAACATTCCG GTTGATCCGGTAATGGTGAATTTGCTGCGTTGCAGAAATTACCGTACCGCCAGTTAATCCGGAGAGTCAGCGATGTTCC TGAAAACCGAATCATTGAACATAACGGTGTGACCGTCACTGCTTCTGAACTGTCAGCCCTGCAGCGCATTGAGCATCTCGC CCTGATGAAACGGCAGGAGCAACAGGGCGAGTCAGACAGCAACCGGAAGTTACT

Figures

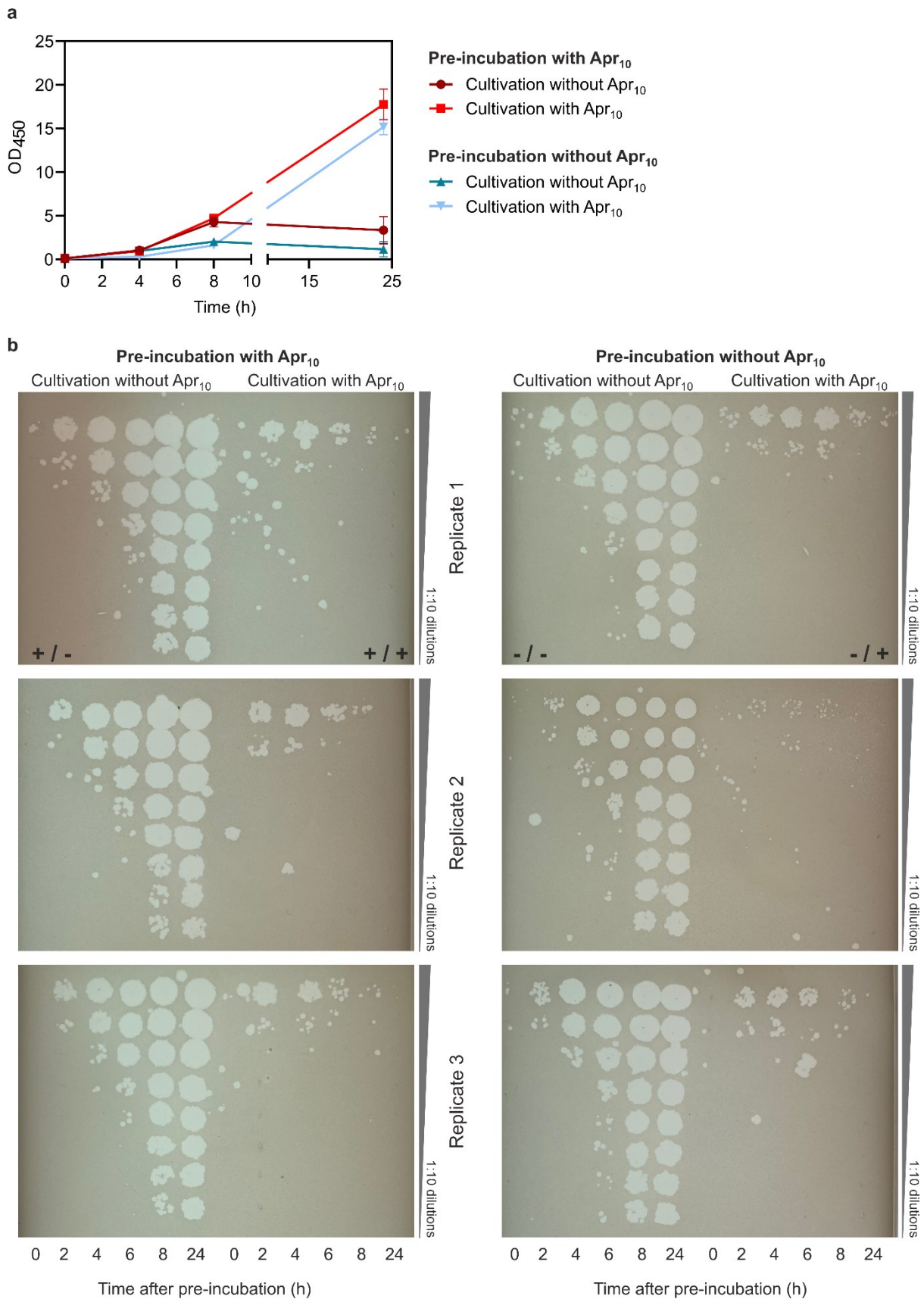


Supplementary Figure S1 | Dose-dependent effect of apramycin on the *Streptomyces* phage Alderaan. **a**, Growth of *Streptomyces venezuelae* ATCC 10712 pJLK04 infected with the phage Alderaan showing the dose-dependent effects of apramycin on infection (n = 3 independent biological replicates; error bars represent s.d., AB = antibiotic). **b**, Corresponding phage titers over time in presence of increasing concentrations of apramycin (0, 1, 2.5 and 10 µg/ml). Data represent an average of three independent biological replicates.



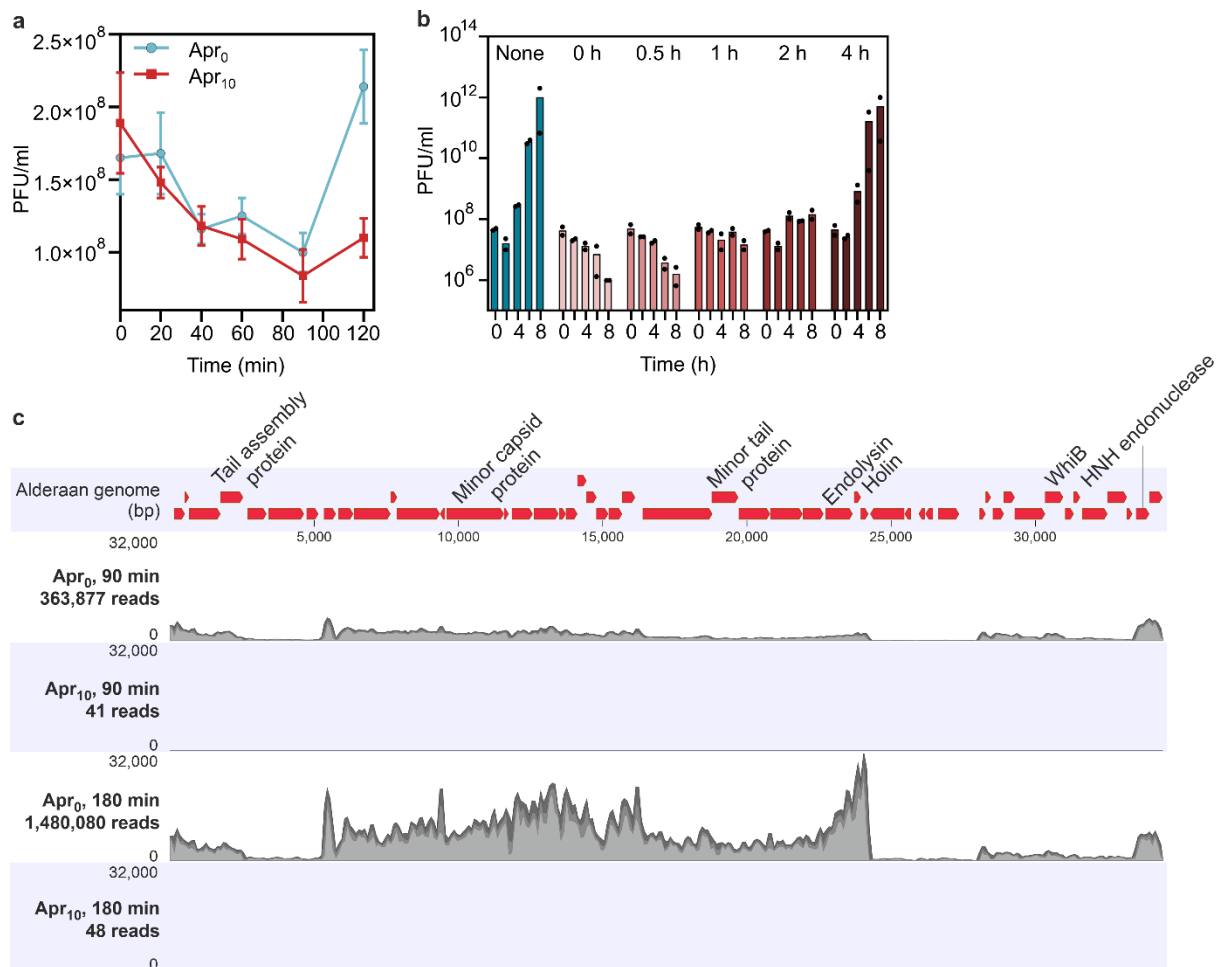
Supplementary Figure S2 | Effect of aminoglycosides on *E. coli* phage λ . **a**, Infection curves of *E. coli* DSM 4230 infected with phage λ in presence of different aminoglycosides ($n = 3$ independent biological replicates; error bars represent s. d.). **b**, Heat map showing the \log_{10} -fold change in plaque formation by λ on different *E. coli* strains in the presence of aminoglycosides relative to the aminoglycoside-free control. **c**, Re-infection of cultures previously treated with apramycin (Apr₂₅, upper row, right), shows efficient infection of *E. coli* DSM 4230 by phage λ in the absence of apramycin (Apr₂₅, lower row, right). **d**, Addition of MgCl₂ counteracts the effect of apramycin on infection of *E. coli* DSM 4230 by λ . **e**, Potassium efflux assays performed with *E. coli* DSM 4230 wild type and the *E. coli* JW3996 $\Delta lamB$ strain (lacking the λ receptor). λ was added after 5.5 minutes.

Appendix



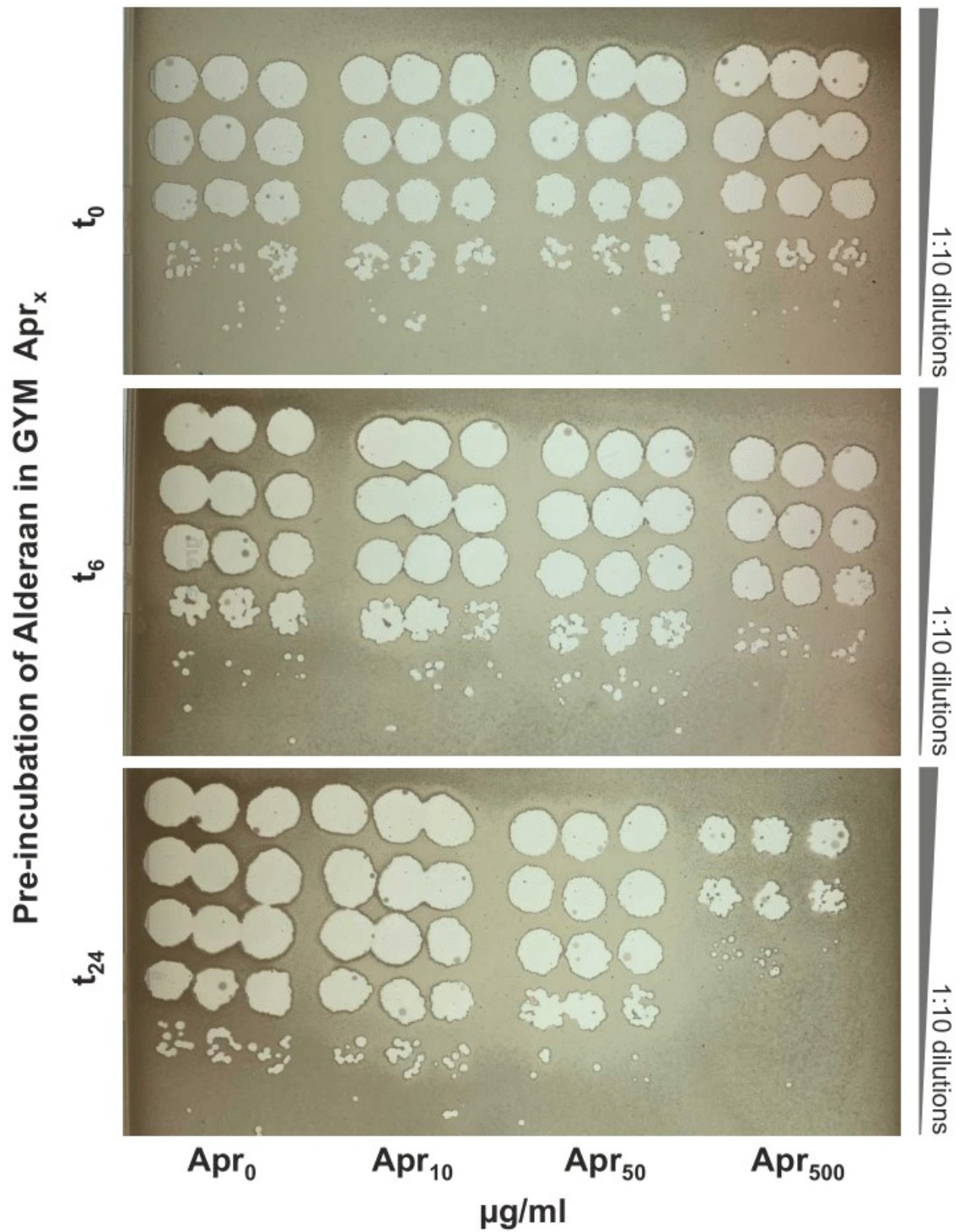
Supplementary Figure S3 | Synchronized infection of *Streptomyces venezuelae* with phage Alderaan under apramycin pressure. *Streptomyces venezuelae* ATCC 10712 pJLK04 was

inoculated to an OD₄₅₀ of 1 and pre-incubated with 10⁸ PFU/ml for 15 min at room temperature with gentle shaking. After four washing steps with GYM medium to remove unadsorbed phages, cultures were diluted to a final starting OD₄₅₀ of 0.1. Pre-incubation with phages and further cultivation was performed with and without apramycin (10 µg/ml) as indicated. **a**, Growth of *Streptomyces venezuelae* infected with phage Alderaan (n = 3 independent biological replicates). **b**, Corresponding plaque assays showing comparable phage amplification during the main cultivations performed in absence of apramycin, independent of the presence of apramycin in the pre-incubation step.

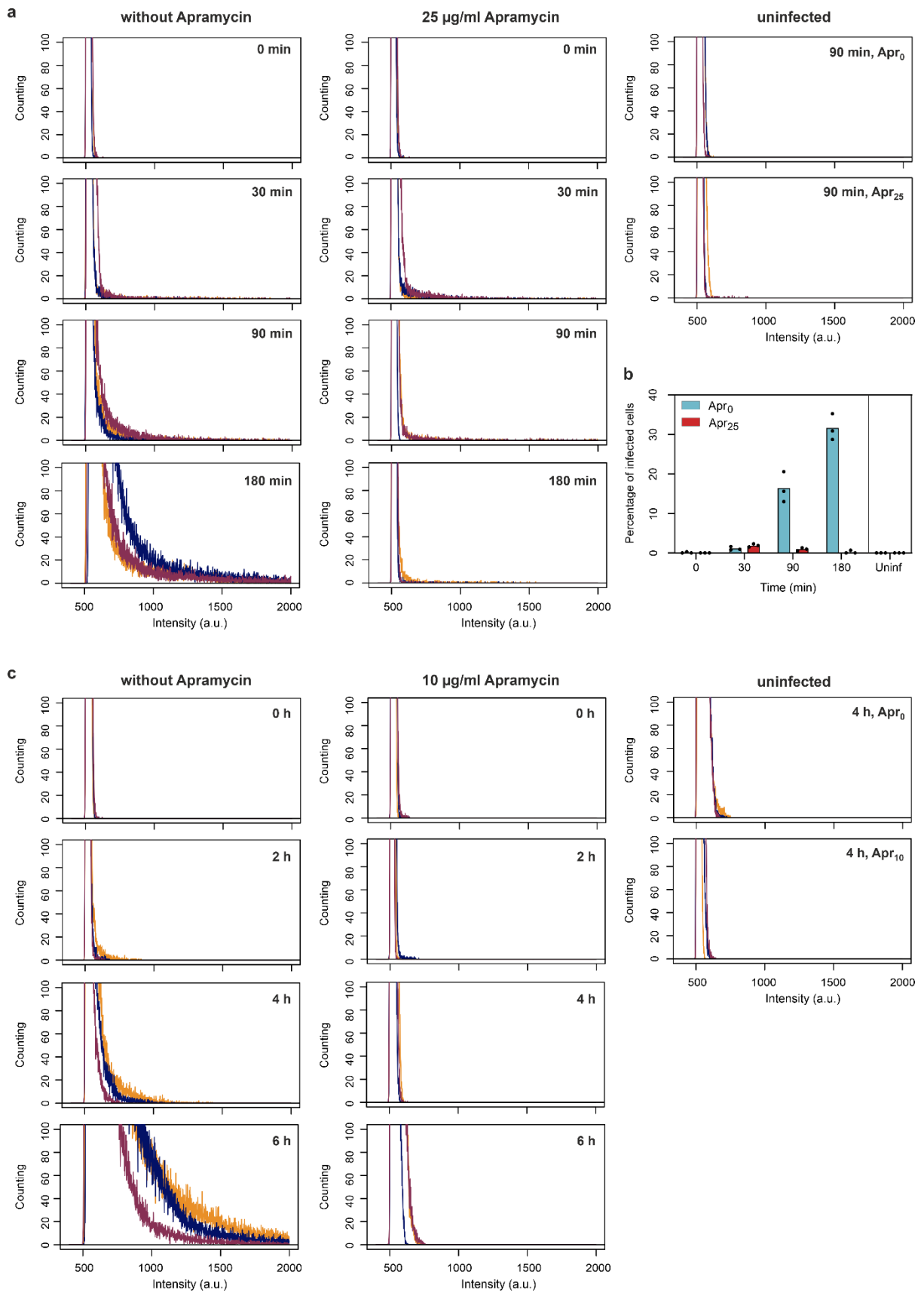


Supplementary Figure S4 | Investigations of the mechanism of action of apramycin.

a, Effect of apramycin on phage adsorption of phage Alderaan to *S. venezuelae* ATCC 10712 pJLK04. Shown is the time-resolved quantification of extracellular Alderaan DNA via qPCR using a gene coding for the minor tail protein (HQ601_00028, oligonucleotide sequences are provided in Supplementary File 5). Culture supernatants were pre-treated with 100 U/ml DNase to exclusively quantify phage DNA deriving from intact phage particles. A DNase-treated phage stock with known phage titer was used to infer phage titers (in PFU/ml) from DNA quantification. Data represent mean values of two independent biological replicates measured as technical duplicates. **b**, Impact of apramycin (10 µg/ml) when added at the different indicated time points post phage infection. For each sample, phage titers were measured over time. Data represent an average of two independent biological replicates. **c**, Enlargement of **Fig. 4c** showing the RNA-seq coverage of the Alderaan genome in presence or absence of apramycin. Genome organization of Alderaan is displayed in the upper part.



Supplementary Figure S5 | Pre-incubation of phage Alderaan with apramycin. Alderaan phages were pre-incubated in GYM medium containing the indicated apramycin concentrations at 30 °C and 900 rpm before spotting on a bacterial lawn of *Streptomyces venezuelae* ATCC 10712 pIJLK04.



Supplementary Figure S6 | Distribution of fluorescence intensities from phage targeting direct-geneFISH. a and c, Quantification of Alexa647 fluorescence in (a) *E. coli* cells infected with λ and (c) *S. venezuelae* cells infected with Alderaan, shown as density plot of pixel counts relative to their fluorescence intensity. For each panel, profiles of the three biological replicates are shown. **b,** Determination of the percentage of *E. coli* cells infected with λ over time (n=3 independent biological replicates; 'Uninf': uninfected).

Videos

Video S1: Apramycin prevents cell lysis during infection of *S. venezuelae* with phage Alderaan. Time-lapse video of *S. venezuelae* ATCC 10712 carrying the pIJLK04 plasmid, which was cultivated in a microfluidics system and challenged with Alderaan (10^8 PFU/ml; flow rate 200 nl/min) in presence and absence of 5 or 10 μ g/ml apramycin.

The video is provided as a separate file:

- Video S1_Svenezueale_Alderaan_apramycin effect

References

- 1 Baumgart, M. *et al.* Construction of a prophage-free variant of *Corynebacterium glutamicum* ATCC 13032 for use as a platform strain for basic research and industrial biotechnology. *Appl Environ Microbiol* **79**, 6006-6015, doi:10.1128/AEM.01634-13 (2013).
- 2 MacNeil, D. J. *et al.* Analysis of *Streptomyces avermitilis* genes required for avermectin biosynthesis utilizing a novel integration vector. *Gene* **111**, 61-68, doi:10.1016/0378-1119(92)90603-M (1992).
- 3 Studier, F. W. & Moffatt, B. A. Use of Bacteriophage T7 RNA Polymerase to Direct Selective High-level Expression of Cloned Genes *J Mol Biol* **189**, 113-130, doi:10.1016/0022-2836(86)90385-2 (1986).
- 4 Luria, S. E., Delbrück, M. & Anderson, T. F. Electron microscope studies of bacterial viruses. *Journal of Bacteriology* **46**, 57-77, doi:10.1128/JB.46.1.57-77.1943 (1943).

- 5 Lederberg, E. M. & Lederberg, J. Genetic Studies of Lysogenicity in *Escherichia Coli*. *Genetics* **38**, 51-64 (1953).
- 6 Murray, N. E., Brammar, W. J. & Murray, K. Lambdoid Phages that Simplify the Recovery of in vitro Recombinants. *Mol Gen Genet.* **150**, 53-61, doi:10.1007/BF02425325. (1977).
- 7 Baba, T. *et al.* Construction of *Escherichia coli* K-12 in-frame, single-gene knockout mutants: the Keio collection. *Mol Syst Biol* **2**, 2006 0008, doi:10.1038/msb4100050 (2006).
- 8 Ehrlich, J., Gottlieb, D., Burkholder, P. R., Anderson, L. E. & Pridham, T. G. *Streptomyces venezuelae*, n. sp., the source of chloromycetin. *Journal of Bacteriology* **56**, 467-477, doi:10.1128/jb.56.4.467-477.1948 (1948).
- 9 Kieser, T., Bibb, M., Buttner, M., Chater, K. & Hopwood, D. A. *Practical Streptomyces Genetics: A Laboratory Manual*. (John Innes Foundation, Norwich, United Kingdom, 2000).
- 10 Higgins, C. E. & Kastner, R. E. Nebramycin, a new broad-spectrum antibiotic complex. II. Description of *Streptomyces tenebrarius*. *Antimicrobial agents and chemotherapy* **7**, 324-331 (1967).
- 11 Lv, M. *et al.* Characterization of a C3 Deoxygenation Pathway Reveals a Key Branch Point in Aminoglycoside Biosynthesis. *Journal of the American Chemical Society* **138**, 6427-6435, doi:10.1021/jacs.6b02221 (2016).
- 12 Zhang, Q., Chi, H. T., Wu, L., Deng, Z. & Yu, Y. Two Cryptic Self-Resistance Mechanisms in *Streptomyces tenebrarius* Reveal Insights into the Biosynthesis of Apramycin. *Angewandte Chemie (International ed. in English)* **60**, 8990-8996, doi:10.1002/anie.202100687 (2021).
- 13 Kronheim, S. *et al.* A chemical defence against phage infection. *Nature* **564**, 283-286, doi:10.1038/s41586-018-0767-x (2018).
- 14 Casjens, S. R. & Gilcrease, E. B. Determining DNA packaging strategy by analysis of the termini of the chromosomes in tailed-bacteriophage virions. *Methods in molecular biology (Clifton, N.J.)* **502**, 91-111, doi:10.1007/978-1-60327-565-1_7 (2009).
- 15 Hardy, A., Sharma, V., Keever, L. & Frunzke, J. Genome sequence and characterization of five bacteriophages infecting *Streptomyces coelicolor* and *Streptomyces venezuelae*: Alderaan, Coruscant, Dagobah, Endor1 and Endor2. *Viruses* **12**, 1065, doi:10.3390/v12101065 (2020).
- 16 Hünnefeld, M. *et al.* Genome Sequence of the Bacteriophage CL31 and Interaction with the Host Strain *Corynebacterium glutamicum* ATCC 13032. *Viruses* **13**, 495, doi:10.3390/v13030495 (2021).
- 17 Harb, L. *et al.* ssRNA phage penetration triggers detachment of the F-pilus. *Proc Natl Acad Sci U S A* **117**, 25751-25758, doi:10.1073/pnas.2011901117 (2020).
- 18 Hong, H. J., Hutchings, M. I., Hill, L. M. & Buttner, M. J. The role of the novel Fem protein VanK in vancomycin resistance in *Streptomyces coelicolor*. *J Biol Chem* **280**, 13055-13061, doi:10.1074/jbc.M413801200 (2005).
- 19 Eikmanns, B. J., Kleinertz, E., Liehl, W. & Sahm, H. A family of *Corynebacterium glutamicum/Escherichia coli* shuttle vectors for cloning, controlled gene expression, and promoter probing. *Gene* **102**, 93-98, doi:10.1016/0378-1119(91)90545-M (1991).
- 20 Gust, B., Challis, G. L., Fowler, K., Kieser, T. & Chater, K. F. PCR-targeted *Streptomyces* gene replacement identifies a protein domain needed for biosynthesis of the sesquiterpene soil odor geosmin. *PNAS* **100**, 1541-1546, doi:10.1073/pnas.0337542100. (2003).
- 21 Paget, M. S. B., Chamberlin, L., Atrih, A., Foster, S. J. & Buttner, M. J. Evidence that the Extracytoplasmic Function Sigma Factor sigmaE Is Required for Normal Cell Wall Structure in *Streptomyces coelicolor* A3(2). *Journal of Bacteriology* **181**, 204-211, doi:10.1128/JB.181.1.204-211.1999 (1999).
- 22 Frunzke, J., Engels, V., Hasenbein, S., Gätgens, C. & Bott, M. Co-ordinated regulation of gluconate catabolism and glucose uptake in *Corynebacterium glutamicum* by two functionally equivalent transcriptional regulators, GntR1 and GntR2. *Mol Microbiol* **67**, 305-322, doi:10.1111/j.1365-2958.2007.06020.x (2008).

4.4 Supplementary information to "Antiphage molecules produced by bacteria – beyond protein-mediated defenses"

Table 1 | **List of small molecules with known antiphage properties.** It includes the phages inhibited and the proposed mechanism of action (when available)

Class	Compound	Phages affected	Bacterial host	Phage family	Genome	Proposed molecular mechanism	Reference	Remarks
<u>Anthracyclines</u>	Rutilantin	phages infecting staphylococci, enterococci, <i>Bacillus cereus</i> , <i>Barillus megatherium</i> , <i>Escherichia coli</i> , <i>Salmonella paratyphi</i> and <i>Vibrio cholerae</i>					(Asheshov and Gordon, 1961)	
	Aclacinomycin (Aklavin) A and analogues	φX174	<i>E. coli</i>	<i>Microviridae</i>	circular ssDNA		(Morita et al., 1979)	Inactivation of free particles
		λ	<i>E. coli</i>	<i>Siphoviridae</i>	linear dsDNA		(Tanaka et al., 1983)	
		Various phages infecting both Gram + and Gram -						(Strelitz et al., 1956)
	Daunorubicin (Daunomycin)	φX174	<i>E. coli</i>	<i>Microviridae</i>	circular ssDNA		(Morita et al., 1979)	Inactivation of free particles

Appendix

	λ	<i>E. coli</i>	<i>Siphoviridae</i>	linear dsDNA	Inhibition of an early step of the infection cycle, after DNA injection but before DNA replication	(Kronheim et al., 2018)	
	T1	<i>E. coli</i>	<i>Siphoviridae</i>	linear dsDNA		(Parisi and Soller, 1964)	
	T3	<i>E. coli</i>	<i>Autographiviridae</i>	linear dsDNA			
	T4	<i>E. coli</i>	<i>Myoviridae</i>	linear dsDNA	Daunomycin does not inactivate free particles nor does it affect adsorption, DNA injection and lysis, but causes a decrease in DNA synthesis		
	T5	<i>E. coli</i>	<i>Siphoviridae</i>	linear dsDNA		(Kronheim et al., 2018)	
	T6	<i>E. coli</i>	<i>Myoviridae</i>	linear dsDNA		(Kronheim et al., 2018; Parisi and Soller, 1964)	
	T7	<i>E. coli</i>	<i>Autographiviridae</i>	linear dsDNA		(Kronheim et al., 2018)	
	JBD26	<i>P. aeruginosa</i>	<i>Siphoviridae</i>	linear dsDNA			
	JBD30	<i>P. aeruginosa</i>	<i>Siphoviridae</i>	linear dsDNA			
	ϕ Scoe2	<i>S. coelicolor</i>	<i>Siphoviridae</i>	linear dsDNA			

Appendix

		φScoe25	<i>S. coelicolor</i>	<i>Siphoviridae</i>	linear dsDNA			
	Doxorubicin (Adriamycin)	φX174	<i>E. coli</i>	<i>Microviridae</i>	circular ssDNA		(Morita et al., 1979)	Inactivation of free particles
		λ	<i>E. coli</i>	<i>Siphoviridae</i>	linear dsDNA		(Kronheim et al., 2018)	
		φScoe2	<i>S. coelicolor</i>	<i>Siphoviridae</i>	linear dsDNA			
		φScoe25	<i>S. coelicolor</i>	<i>Siphoviridae</i>	linear dsDNA			
		PBS1	<i>B. subtilis</i>	<i>Myoviridae</i>	linear dsDNA	Phage DNA is ejected but DNA uptake into the cell is incomplete	(Pritikin and Reiter, 1969)	Site of primary adsorption: flagellum (Raimondo et al., 1968)
		SP10	<i>B. subtilis</i>	<i>Myoviridae</i>	linear dsDNA			
		φScoe2	<i>S. coelicolor</i>	<i>Siphoviridae</i>	linear dsDNA		(Kronheim et al., 2018)	
		φScoe25	<i>S. coelicolor</i>	<i>Siphoviridae</i>	linear dsDNA			
	Cosmomycin D	φScoe2	<i>S. coelicolor</i>	<i>Siphoviridae</i>	linear dsDNA			
		φScoe25	<i>S. coelicolor</i>	<i>Siphoviridae</i>	linear dsDNA			
	Epirubicin	λ	<i>E. coli</i>	<i>Siphoviridae</i>	linear dsDNA		(Kronheim et al., 2018)	

Appendix

	Idarubicin	λ	<i>E. coli</i>	<i>Siphoviridae</i>	linear dsDNA			
	Mitoxantrone	λ	<i>E. coli</i>	<i>Siphoviridae</i>	linear dsDNA			
<u>Aminoglycosides</u>	Streptomycin	MS-2	<i>E. coli</i>	<i>Leviviridae</i>	linear ssRNA	Inhibition of one very early step of the replication cycle. The phage genome exists transiently after adsorption at a site accessible to streptomycin	(Brock, 1962)	
		P9	<i>Streptococcus faecium</i>	<i>Siphoviridae</i>	linear dsDNA	2 phases: - if streptomycin is added before injection: inhibition of the injection of phage DNA, where binding to phage DNA prevents unfolding necessary for injection (reversible by dilution) -if streptomycin is added after injection: rapid inactivation of the phage genome	(Brock and Wooley, 1963; Brock et al., 1963)	
		f2	<i>E. coli</i>	<i>Leviviridae</i>	linear ssRNA		(Schindler, 1964)	When streptomycin was present during the whole infection, effect seen for
		μ2	<i>E. coli</i>	<i>Leviviridae</i>	linear ssRNA			

Appendix

		fd	<i>E. coli</i>	<i>Inoviridae</i>	circular ssDNA			quite high concentrations (>200 µg/ml) => precipitation rather than inhibition?
		F-WJ-I	-	-	-		(Jones and Greenberg, 1978)	Correlation between resistance to chloroform and streptomycin: phages resistant to streptomycin are also resistant to chloroform
		Legendre	<i>M. smegmatis</i>	<i>Siphoviridae</i>	linear dsDNA			
		Clark	<i>M. smegmatis</i>	<i>Siphoviridae</i>	linear dsDNA			
		D29	<i>M. smegmatis</i>	<i>Siphoviridae</i>	linear dsDNA		(Jiang et al., 2020; Jones and Greenberg, 1978)	
		phAE159	<i>M. smegmatis</i>	phasmid (derived from TM4 phage)	circular dsDNA	Aminoglycosides block replication of phage DNA. Inhibition occurs after injection	(Jiang et al., 2020)	
	Kanamycin	D29	<i>M. smegmatis</i>	<i>Siphoviridae</i>	linear dsDNA			
		phAE159	<i>M. smegmatis</i>	phasmid (derived from TM4 phage)	circular dsDNA			

Appendix

		Spe2	<i>C. glutamicum</i>	<i>Siphoviridae</i>	linear dsDNA	(Kever et al., 2021)	
		λ	<i>E. coli</i>	<i>Siphoviridae</i>	linear dsDNA		
		T3	<i>E. coli</i>	<i>Autographiviridae</i>	linear dsDNA	(Zuo et al., 2021)	
		WSP	<i>E. coli</i>	-	-		
		BSP	<i>B. cereus</i>	-	-		
	Hygromycin	D29	<i>M. smegmatis</i>	<i>Siphoviridae</i>	linear dsDNA	(Jiang et al., 2020)	
		phAE159	<i>M. smegmatis</i>	phasmid (derived from TM4 phage)	circular dsDNA		
		Alderaan	<i>S. venezuelae</i>	<i>Siphoviridae</i>	linear dsDNA	(Kever et al., 2021)	
	Apramycin	Alderaan	<i>S. venezuelae</i>	<i>Siphoviridae</i>	linear dsDNA		Apramycin blocks the phage life cycle between injection

Appendix

		λ	<i>E. coli</i>	<i>Siphoviridae</i>	linear dsDNA	and replication of the phage genome		
	Neomycin	80	<i>S. aureus</i>	<i>Siphoviridae</i>	linear dsDNA		(Joy Harrison et al., 1959)	
		T3	<i>E. coli</i>	<i>Autographiviridae</i>	linear dsDNA		(Zuo et al., 2021)	
		WSP	<i>E. coli</i>	-	-			
		BSP	<i>B. cereus</i>	-	-			

<u>Known DNA-intercalating agents</u>							
Alkaloid	Ellipticine	λ	<i>E. coli</i>	<i>Siphoviridae</i>	linear dsDNA		(Kronheim et al., 2018)
Fluorochrome	Propidium iodide	λ	<i>E. coli</i>	<i>Siphoviridae</i>	linear dsDNA		
		ϕ Scoe2	<i>S. coelicolor</i>	<i>Siphoviridae</i>	linear dsDNA		
		ϕ Scoe25	<i>S. coelicolor</i>	<i>Siphoviridae</i>	linear dsDNA		
Acridine family compounds	Acriflavine	λ	<i>E. coli</i>	<i>Siphoviridae</i>	linear dsDNA		
		ϕ Scoe2	<i>S. coelicolor</i>	<i>Siphoviridae</i>	linear dsDNA		

Appendix

		φScoe25	<i>S. coelicolor</i>	<i>Siphoviridae</i>	linear dsDNA		
	Ethacridine lactate	λ	<i>E. coli</i>	<i>Siphoviridae</i>	linear dsDNA		
Polypeptide antibiotic	Actinomycin D	T2r	<i>E. coli</i>	<i>Myoviridae</i>	linear dsDNA	Actinomycin causes a decrease in encapsidated phage DNA, potentially by interfering with protein synthesis or DNA packaging	(Nakata et al., 1961)
		T4	<i>E. coli</i>	<i>Myoviridae</i>	linear dsDNA	Actinomycin strongly decrease the formation of phage progeny without interfering with the synthesis of RNA, DNA, or proteins	(Korn et al., 1965)
Other							
Di-benzimidazole	Ro 90-7501	λ	<i>E. coli</i>	<i>Siphoviridae</i>	linear dsDNA		(Kronheim et al., 2018)
Quaternary ammonium	Dequalinium chloride	λ	<i>E. coli</i>	<i>Siphoviridae</i>	linear dsDNA		
?	"Phagostatin"	T3	<i>E. coli</i>	<i>Autographiviridae</i>	linear dsDNA	Phagostatin inhibits lysis of infected cells	(Higo, 1958)
Cyclopentenone	Sarkomycin	f2	<i>E. coli</i>	<i>Leviviridae</i>	linear ssRNA		(Koenuma et al., 1974)
Naphthocoumarin	Chrysomycin	Diverse phages					(Strelitz et al., 1955b)
?	"Phagocidin"	T3	<i>E. coli</i>	<i>Autographiviridae</i>	linear dsDNA	Phagocidin inactivates free T3 but does not interfere with intracellular growth	(Higo, 1956; Higo and Hinuma, 1956)

Appendix

Pyrrolobenzodiazepine	Tomaymycin	T1	<i>E. coli</i>	<i>Siphoviridae</i>	linear dsDNA	(Arima et al., 1972)	
		T3	<i>E. coli</i>	<i>Autographiviridae</i>	linear dsDNA		
		M2	<i>B. subtilis</i>	<i>Podoviridae</i>	linear dsDNA		
		SP10	<i>B. subtilis</i>	<i>Myoviridae</i>	linear dsDNA		
Heterocyclic anthracene	Nybomycin	15/60 phages tested				(Strelitz et al., 1955a)	
?	"Phagolessin A58"	T1	<i>E. coli</i>	<i>Siphoviridae</i>	linear dsDNA	Inactivation of free phage particles	(Hall and Asheshov, 1953)
		T3	<i>E. coli</i>	<i>Autographiviridae</i>	linear dsDNA		
		T7	<i>E. coli</i>	<i>Autographiviridae</i>	linear dsDNA		

References

- Arima, K., Kohsaka, M., and Tamura, G. (1972). Studies on tomaymycin, a new antibiotic. I Isolation and properties of tomaymycin. *The Journal of Antibiotics* 8.
- Asheshov, I., and Gordon, J. (1961). Rutilantin: an antibiotic substance with antiphage activity. *Biochem J* 81, 101–104. <https://doi.org/10.1042/bj0810101>.
- Brock, T.D. (1962). The inhibition of an RNA bacteriophage by streptomycin, using host bacteria resistant to the antibiotic. *Biochem. Biophys. Res. Commun.* 9, 184–187. [https://doi.org/10.1016/0006-291x\(62\)90111-0](https://doi.org/10.1016/0006-291x(62)90111-0).
- Brock, T.D., and Wooley, S.O. (1963). Streptomycin as an Antiviral Agent: Mode of Action. *Science* 141, 1065–1067. <https://doi.org/10.1126/science.141.3585.1065>.

Appendix

- Brock, T.D., Mosser, J., and Peacher, B. (1963). The inhibition by streptomycin of certain streptococcus bacteriophages, using host bacteria resistant to the antibiotic. *J. Gen. Microbiol.* 33, 9–22. <https://doi.org/10.1099/00221287-33-1-9>.
- Hall, E.A., and Asheshov, I.N. (1953). A study of the action of phagolessin A58 on the T phages. *J Gen Physiol* 37, 217–230. <https://doi.org/10.1085/jgp.37.2.217>.
- Higo, N. (1956). Studies on antiviral antibiotics from *Streptomyces*. II. Phagocidin, a new antiviral antibiotic. *J Antibiot (Tokyo)* 9, 152–156.
- Higo, N. (1958). Studies on Antiviral Antibiotics Produced by *Streptomyces* XI. Effect of phagostin on the multiplication of bacteriophage T3. *Japanese Journal of Microbiology* 2, 203–215. <https://doi.org/10.1111/j.1348-0421.1958.tb00072.x>.
- Higo, N., and Hinuma, Y. (1956). Studies on antiviral antibiotics from *Streptomyces*. III. Mode of action of phagocidin on bacterial virus. *J Antibiot (Tokyo)* 9, 157–163. .
- Jiang, Z., Wei, J., Liang, Y., Peng, N., and Li, Y. (2020). Aminoglycoside Antibiotics Inhibit Mycobacteriophage Infection. *Antibiotics* 9, 714. <https://doi.org/10.3390/antibiotics9100714>.
- Jones, W.D., and Greenberg, J. (1978). Resistance relationships in *Mycobacterium smegmatis* ATCC 607 to phages sensitive or resistant to both chloroform and streptomycin sulphate. *J. Gen. Virol.* 39, 555–557. <https://doi.org/10.1099/0022-1317-39-3-555>.
- Joy Harrison, K., Beavon, J., and Griffin, E. (1959). The effect of neomycin on phage-typing of staphylococci. *The Lancet* 273, 908–910. [https://doi.org/10.1016/S0140-6736\(59\)91309-1](https://doi.org/10.1016/S0140-6736(59)91309-1).
- Kever, L., Hardy, A., Luthe, T., Hünnefeld, M., Gätgens, C., Milke, L., Wiechert, J., Wittmann, J., Moraru, C., Marienhagen, J., et al. (2021). Aminoglycoside antibiotics inhibit phage infection by blocking an early step of the phage infection cycle.
- Koenuma, M., Kinashi, H., and Otake, N. (1974). An improved screening method for antiphage antibiotics and isolation of sarkomycin and its relatives. *J. Antibiot.* 27, 801–804. <https://doi.org/10.7164/antibiotics.27.801>.
- Korn, D., Protass, J.J., and Leive, L. (1965). A novel effect of actinomycin D in preventing bacteriophage T4 maturation in *Escherichia coli*. *Biochemical and Biophysical Research Communications* 19, 473–481. [https://doi.org/10.1016/0006-291X\(65\)90149-X](https://doi.org/10.1016/0006-291X(65)90149-X).
- Kronheim, S., Daniel-Ivad, M., Duan, Z., Hwang, S., Wong, A.I., Mantel, I., Nodwell, J.R., and Maxwell, K.L. (2018). A chemical defence against phage infection. *Nature* 564, 283. <https://doi.org/10.1038/s41586-018-0767-x>.

Appendix

Morita, J., Tanaka, A., Komano, T., and Oki, T. (1979). Inactivation of Phage ϕ X174 by Anthracycline Antibiotics, Aclacinomycin A, Doxorubicin and Daunorubicin. *Agricultural and Biological Chemistry* 43, 2629–2631. <https://doi.org/10.1080/00021369.1979.10863874>.

Nakata, A., Sekiguchi, M., and Kawamata, J. (1961). Inhibition of Multiplication of Bacteriophage by Actinomycin. *Nature* 189, 246–247. <https://doi.org/10.1038/189246b0>.

Parisi, B., and Soller, A. (1964). Studies on Antiphage Activity of Daunomycin. *Giornale Di Microbiologia* 12, 183–194. .

Pritikin, W.B., and Reiter, H. (1969). Abortive Infection of *Bacillus subtilis* Bacteriophage PBS1 in the Presence of Actinomycin D. *Journal of Virology* 3, 578–585. <https://doi.org/10.1128/JVI.3.6.578-585.1969>.

Raimondo, L.M., Lundh, N.P., and Martinez, R.J. (1968). Primary adsorption site of phage PBS1: the flagellum of *Bacillus subtilis*. *J Virol* 2, 256–264. <https://doi.org/10.1128/JVI.2.3.256-264.1968>.

Schindler, J. (1964). Inhibition of reproduction of the f2 bacteriophage by streptomycin. *Folia Microbiol* 9, 269–276. <https://doi.org/10.1007/BF02873305>.

Strelitz, F., Flon, H., and Asheshov, I.N. (1955a). Nybomycin, a new antibiotic with antiphage and antibacterial properties. *Proc Natl Acad Sci U S A* 41, 620–624. .

Strelitz, F., Flon, H., and Asheshov, I.N. (1955b). Chrysomycin: a new antibiotic substance for bacterial viruses. *J Bacteriol* 69, 280–283. .

Strelitz, F., Flon, H., Weiss, U., and Asheshov, I.N. (1956). Aklavin, an antibiotic substance with antiphage activity. *J Bacteriol* 72, 90–94. <https://doi.org/10.1128/JB.72.1.90-94.1956>.

Tanaka, A., Sen, K., Morita, J., and Komano, T. (1983). Phage inactivation by aclacinomycin A and its analogues. *J. Antibiot.* 36, 1242–1244. <https://doi.org/10.7164/antibiotics.36.1242>.

Zuo, P., Yu, P., and Alvarez, P.J.J. (2021). Aminoglycosides Antagonize Bacteriophage Proliferation, Attenuating Phage Suppression of Bacterial Growth, Biofilm Formation, and Antibiotic Resistance. *Appl Environ Microbiol* 87, e00468-21. <https://doi.org/10.1128/AEM.00468-21>.

4.5 Supplementary information to “Phage-triggered synthesis of actinorhodin and undecylprodigiosin in *Streptomyces coelicolor*”

Tables

Table S1 | Bacterial strains used in this study.

Table S2 | Phages used in this study

Figures

Figure S1 | Effect of exposure to ammonia fumes of phage-infected *S. coelicolor* plates

Figure S2 | Chemical structures of actinorhodin and structurally related compounds produced by *S. coelicolor*

Figure S3 | Extracted ion chromatograms for undecylprodigiosin (exact mass: 394.2853) in samples of *S. coelicolor* Δact analysed by LC-MS

Figure S4 | Plaque phenotype with *S. coelicolor* WT and the actinorhodin (Δact) and undecylprodigiosin (Δred) mutants

Figure S5 | Evolution of Endor1 phage titers over time after infection of *S. coelicolor* M145 in the presence of spent medium

Figure S6 | Effect of exposure to ammonia fumes on *S. coelicolor* M600 challenged with antibiotics.

Tables

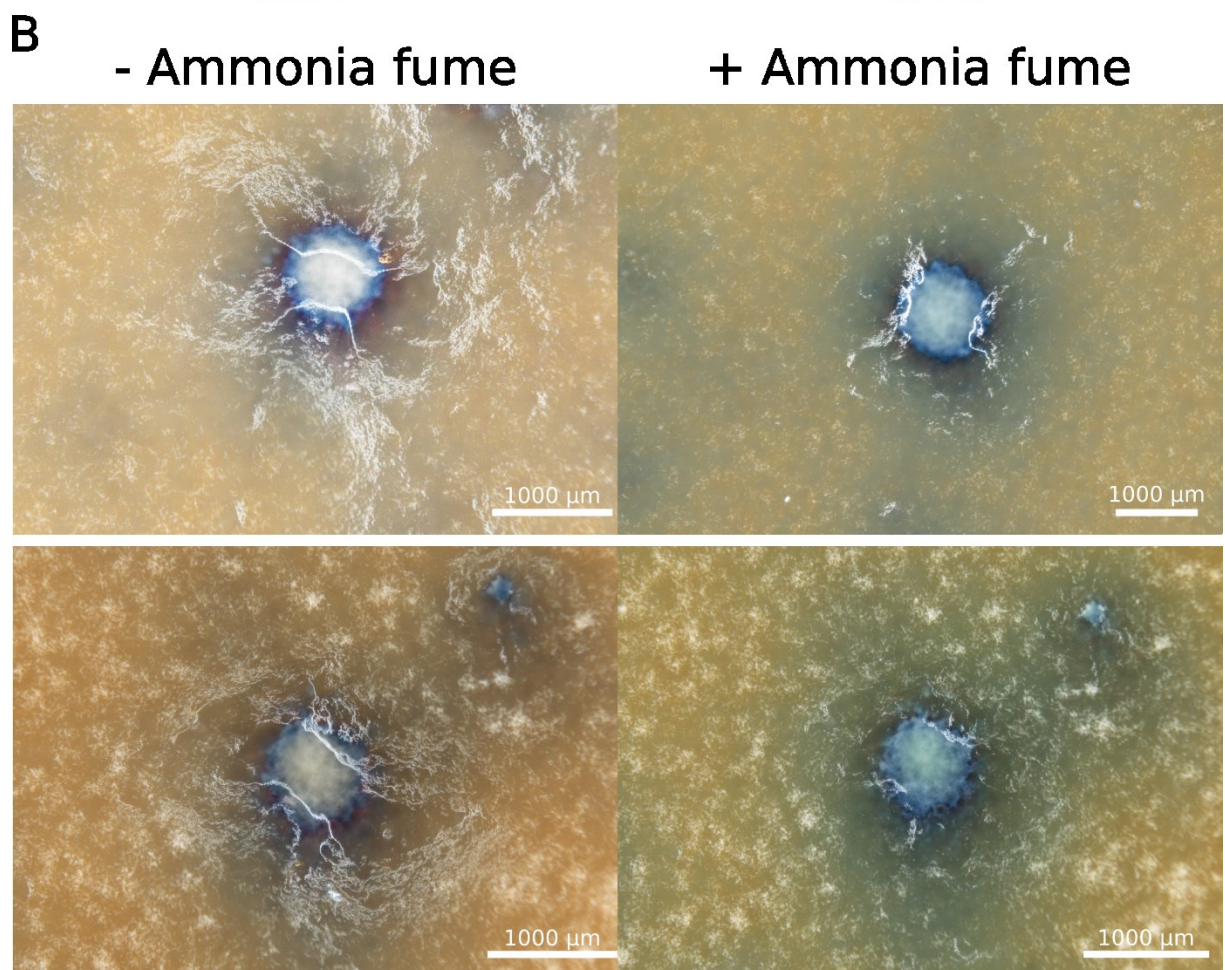
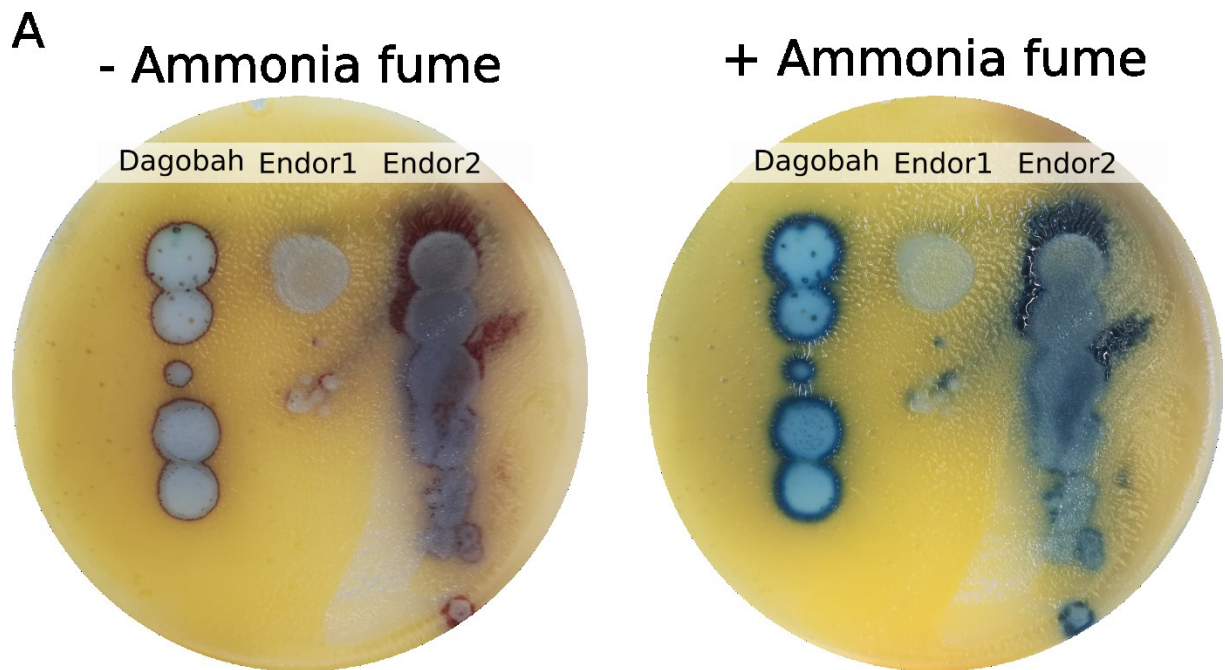
Supplementary Table S1: Bacterial strains used in this study

Strains	Genotype	Reference
<i>Streptomyces coelicolor</i> M145	<i>S. coelicolor</i> A3(2) lacking plasmids SCP1 and SCP2 and having short direct terminal repeats	1,2
<i>Streptomyces coelicolor</i> M600	<i>S. coelicolor</i> A3(2) lacking plasmids SCP1 and SCP2 and having long direct terminal repeats	2
<i>Streptomyces coelicolor</i> Δact	<i>S. coelicolor</i> M145 carrying a 17-kb deletion in the actinorhodin cluster	3
<i>Streptomyces coelicolor</i> Δred	<i>S. coelicolor</i> M145 carrying a 220-bp deletion in the <i>redD</i> gene	4
<i>Streptomyces coelicolor</i> $\Delta act \Delta red$	<i>S. coelicolor</i> M145 carrying a 17-kb deletion in the actinorhodin cluster and a 27-kb deletion in the undecylprodigiosin cluster	3

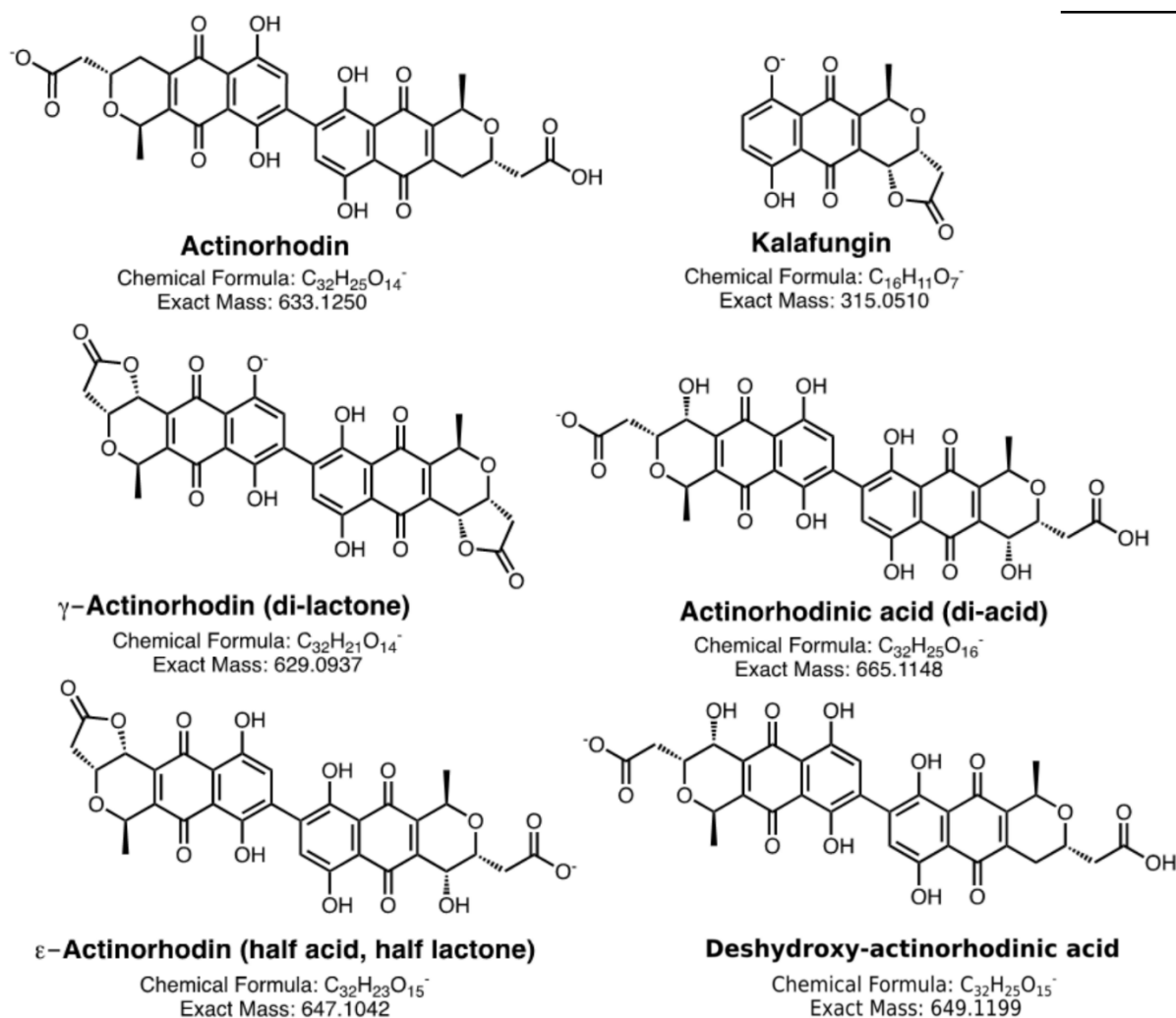
Supplementary Table S2: Phages used in this study

Phage	Host organism	Lifestyle	Family	Genome	State of injected genome ^{13,14}	Reference
Dagobah	<i>S. coelicolor</i> M145	Temperate	<i>Siphoviridae</i>	dsDNA	Linear with terminal repeats	5
Endor1	<i>S. coelicolor</i> M145	Temperate	<i>Siphoviridae</i>	dsDNA	Linear with terminal redundancy	5
Endor2	<i>S. coelicolor</i> M145	Temperate	<i>Siphoviridae</i>	dsDNA	Linear with terminal redundancy	5

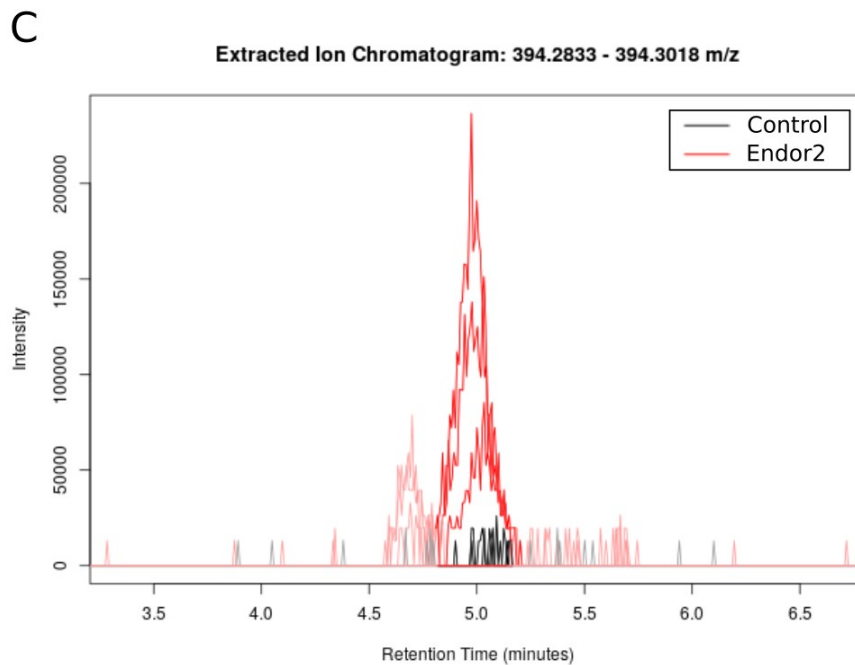
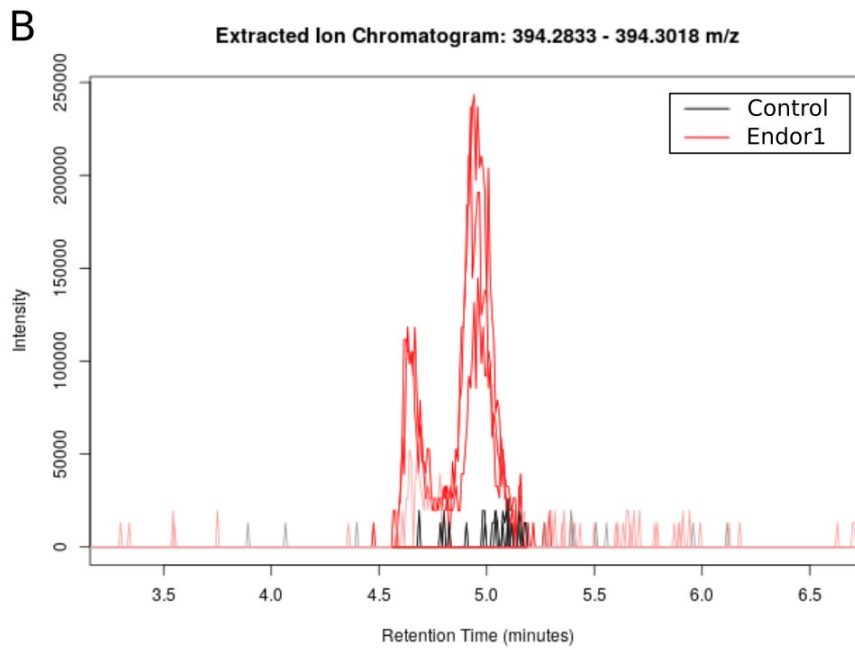
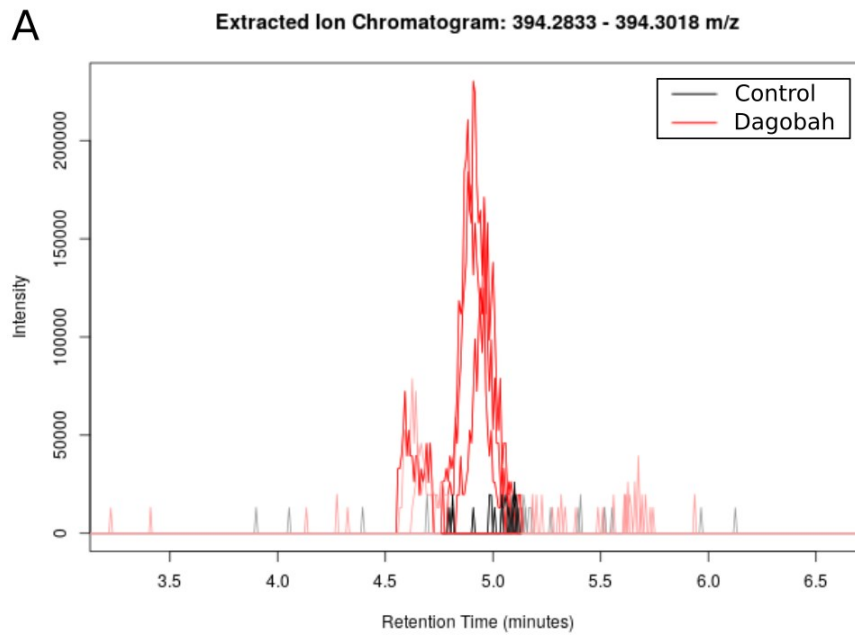
Figures



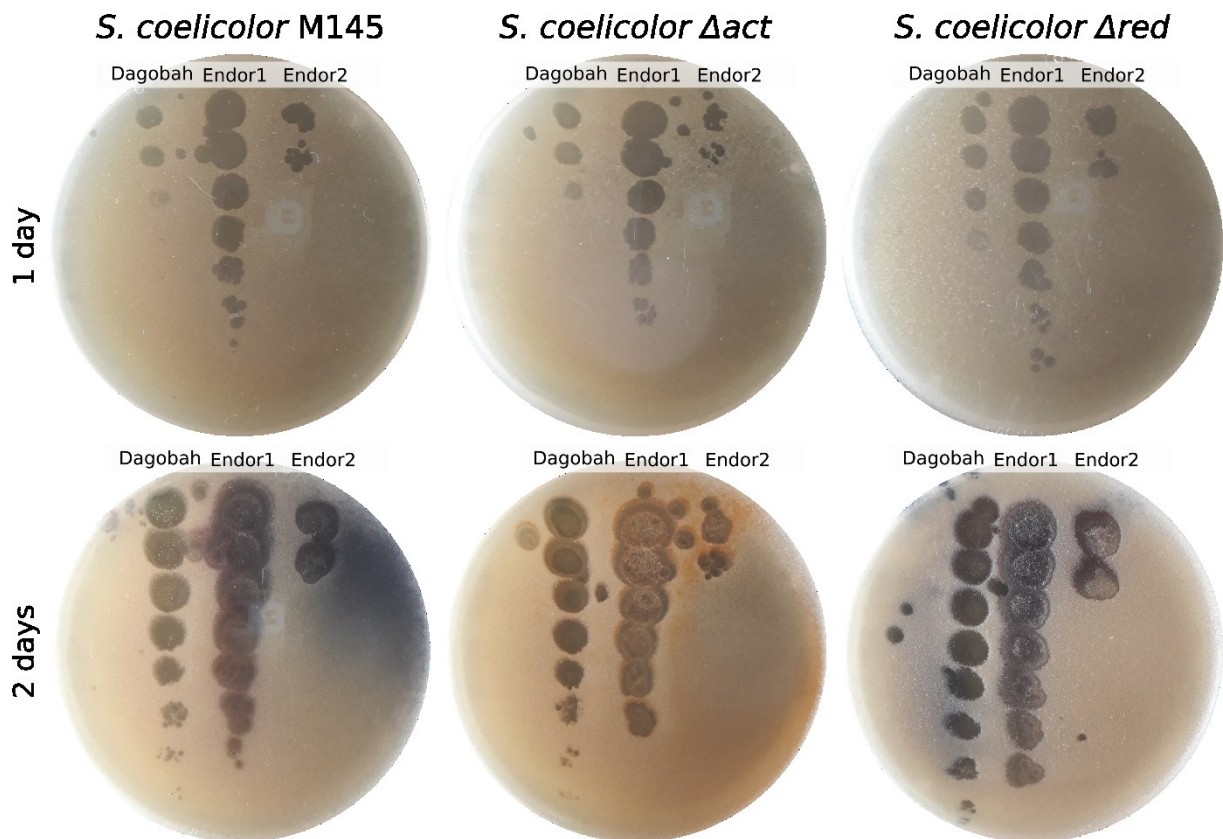
Supplementary Figure S1 | Effect of exposure to ammonia fumes of phage-infected *S. coelicolor* plates. (A) The phages Dagobah, Endor1 and Endor2 were spotted on a lawn of *S. coelicolor* M600. The plates were incubated overnight at 30°C and then at room temperature for 4 additional days. (B) Single plaques of Dagobah formed on *S. coelicolor* M600 were imaged using a stereomicroscope Nikon SMZ18. The plates were incubated overnight at 30°C and then at room temperature for 2 additional days.



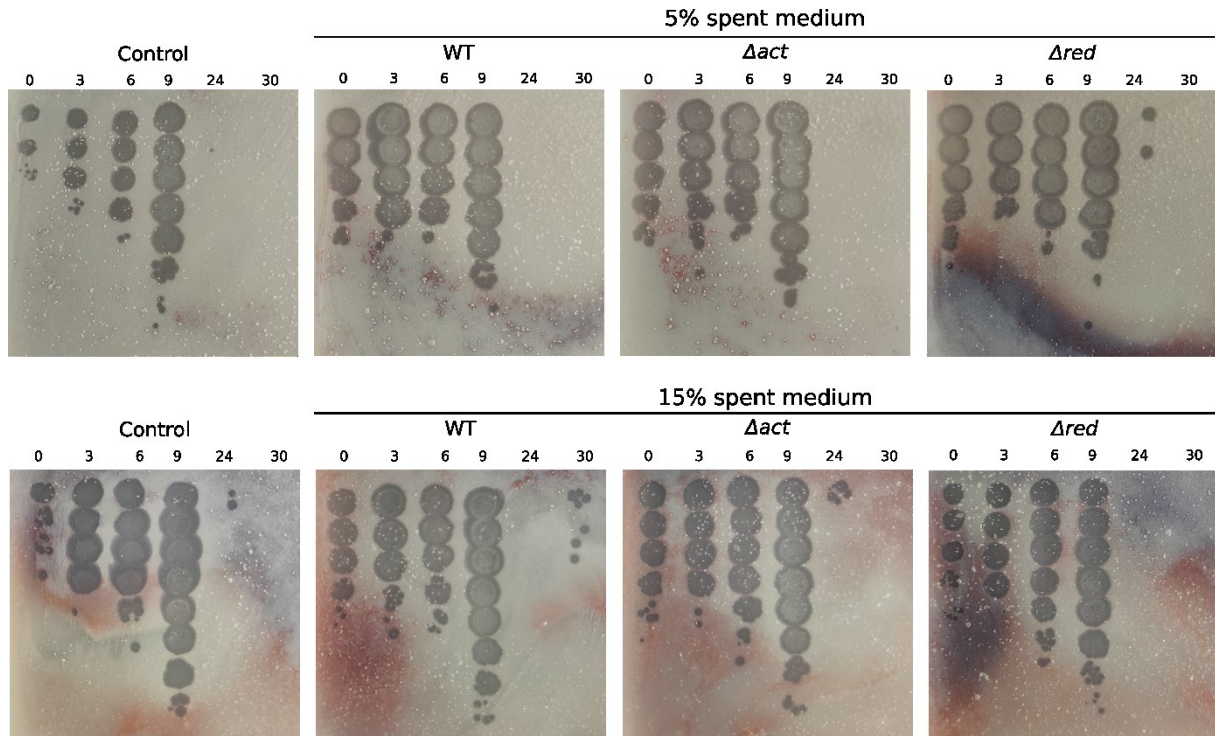
Supplementary Figure S2 | Chemical structures of actinorhodin and structurally related compounds produced by *S. coelicolor*. All masses are shown as negative mode masses ($(M-H)^-$).



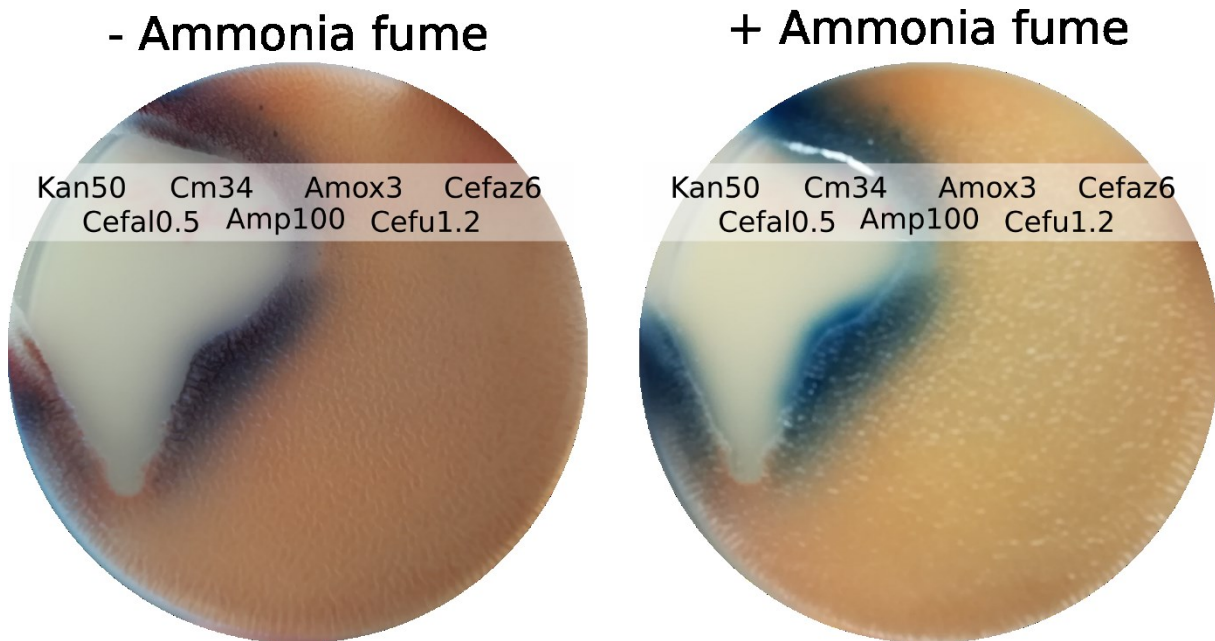
Supplementary Figure S3 | Extracted ion chromatograms for undecylprodigiosin (exact mass: 394.2853) in samples of *S. coelicolor* Δact analysed by LC-MS. *S. coelicolor* Δact was infected with the phages Dagobah (A), Endor1 (B) and Endor2 (C).



Supplementary Figure S4 | Plaque phenotype with *S. coelicolor* WT and the actinorhodin (Δact) and undecylprodigiosin (Δred) mutants.



Supplementary Figure S5 | Evolution of Endor1 phage titers over time after infection of *S. coelicolor* M145 in the presence of spent medium. Titer determination with a supplementation of 5% and 15% spent medium correspond to the infection curves show in panels B and C of Figure 4, respectively.



Supplementary Figure S6 | Effect of exposure to ammonia fumes on *S. coelicolor* M600 challenged with antibiotics. A 10-fold serial dilution of antibiotics was spotted on a lawn of *S. coelicolor* M600.

The concentration indicated is in mg/ml. Kan: kanamycin, Cefal: cefalothin, Cm: chloramphenicol, Amp: ampicillin, Amox: amoxicillin, Cefu: cefuroxin, Cefa: cefazolin

References

1. Bentley, S. D. *et al.* Complete genome sequence of the model actinomycete *Streptomyces coelicolor* A3(2). *Nature* **417**, 141–147 (2002).
2. Weaver, D. *et al.* Genome plasticity in *Streptomyces*: identification of 1 Mb TIRs in the *S. coelicolor* A3(2) chromosome: Identification of 1 Mb TIRs in *S. coelicolor* A3(2). *Molecular Microbiology* **51**, 1535–1550 (2004).
3. Gomez-Escribano, J. P. & Bibb, M. J. Chapter Fourteen - *Streptomyces coelicolor* as an Expression Host for Heterologous Gene Clusters. in *Methods in Enzymology* (ed. Hopwood, D. A.) vol. 517 279–300 (Academic Press, 2012).
4. Floriano, B. & Bibb, M. *afsR* is a pleiotropic but conditionally required regulatory gene for antibiotic production in *Streptomyces coelicolor* A3(2). *Molecular Microbiology* **21**, 385–396 (1996).
5. Hardy, A., Sharma, V., Kever, L. & Frunzke, J. Genome Sequence and Characterization of Five Bacteriophages Infecting *Streptomyces coelicolor* and *Streptomyces venezuelae*: Alderaan, Coruscant, Dagobah, Endor1 and Endor2. *Viruses* **12**, 1065 (2020).

5 Acknowledgments

First and foremost, I would like to expression my special thanks to Prof. Dr. Julia Frunzke for giving me the opportunity to complete my PhD under her supervision. From day one until the final sprint to complete this thesis, I am very thankful for the exciting projects she proposed to me, her constant and unflinching help and support as well as her strong interest in both my scientific and personal development. Her supervision style is to my eyes very close to a perfect equilibrium, providing me guidance and help every time I needed it, but also letting me space and time to develop and pursue my own ideas.

Furthermore, I would like to thank Prof. Dr. Georg Groth for agreeing to be my mentor.

A special thanks go to all current and former members of the AG Frunzke, and in particular Dr. Eva Davoudi, Sebastian Erdrich, Cornelia Gätgens, Dr. Max Hünnefeld, Larissa Kever, Aileen Krüger, Sophia Lorke, Tom Luthe, Bente Rackow, Dr. Vikas Sharma, Dr. Robert Stella, Ulrike Viets and Dr. Johanna Wiechert. Thank you all for all the support in the lab, the phantastic discussions, the pleasant lunch breaks, and the overall excellent working atmosphere you are creating every day. Beyond scientific aspects, going to the lab everyday was a pleasure largely thanks to you; you can be sure I will fondly remember my time among you. I may not forget my ‘proofreading gang’ for the time they spent reading this thesis and providing me with valuable input.

I also want to thank heartfully my closest friends—Gabrielle, Jean-Eudes, Jeanne, Martin, Nadiia and Sophie—for being part of my life. Despite the distance and the too rare meetups, they always supported me, and did their best for me to relax when I needed it the most. Spending time with them—be it in person or on late night phone calls—was key for my well-being throughout this PhD, and I am very grateful for that.

Last but not least, I would like to thank my brother and my parents, their encouragements were crucial despite the hundreds or the thousands of kilometres which separated us.

Erklärung

Hiermit versichere ich an Eides Statt, dass die Dissertation von mir selbständig und ohne unzulässige fremde Hilfe unter Beachtung der „Grundsätze zur Sicherung guter wissenschaftlicher Praxis an der Heinrich-Heine-Universität Düsseldorf“ erstellt worden ist. Die Dissertation wurde in der vorgelegten oder in ähnlicher Form noch bei keiner anderen Institution eingereicht. Ich habe bisher keine erfolglosen Promotionsversuche unternommen.

Aël Hardy